Supplementary Information

Saturation mutagenesis of twenty disease-associated regulatory elements at single base-pair resolution

Martin Kircher[1,2,3,^,*], Chenling Xiong[4,5,^], Beth Martin[1,^], Max Schubach[2,3,^], Fumitaka Inoue[4,5], Robert J.A. Bell[6], Joseph F. Costello[6], Jay Shendure[1,7,*], Nadav Ahituv[4,5,*]

1 Department of Genome Sciences, University of Washington, Seattle WA, USA

2 Berlin Institute of Health (BIH), Berlin, Germany

3 Charité – Universitätsmedizin Berlin, Berlin, Germany

4 Department of Bioengineering and Therapeutic Sciences, University of California San Francisco, San Francisco, CA, USA

5 Institute for Human Genetics, University of California San Francisco, San Francisco, CA, USA

6 Department of Neurosurgery, University of California San Francisco, San Francisco, CA, USA

7 Brotman Baty Institute for Precision Medicine, Seattle WA, USA

^ These authors contributed equally

* Please direct correspondence to Nadav.Ahituv@ucsf.edu, shendure@uw.edu or martin.kircher@bihealth.de

Supplementary Note 1

All graphs showing inferred variant effects for SNVs from promoters or enhancers with available annotation data are shown in Supplementary Figure 8 or Supplementary Figure 9, respectively.

All correlations between replicates are shown in Supplementary Table 7. An overview of the promoter elements is in Supplementary Table 1 and Supplementary Table 2 contains all enhancer elements.

All MPRA results for disease-associated promoter or enhancer mutations referenced in the text are provided in Supplementary Table 10 or Supplementary Table 11, respectively.

Promoters (in alphabetical order)

Factor IX (F9)

Hemophilia B Leyden is an X-linked bleeding disorder characterized by low plasma levels of blood coagulation Factor IX (F9) during childhood. Single point mutations in the F9 promoter at positions NM_000133.3:c.-55G>C, c.-50T>G, c.-49T>A, c.-35G>A/C, c.-34A>T, c.-22 T>C and c.-17A>G/C have been found to be associated with this disease (Supplementary Table 10)[1,2]. The hepatocyte nuclear factor 4 alpha (HNF4A) is thought to bind to this promoter at positions -63 to -39 to activate F9[1,2] and both c.-55G>C and c.-49T>A are thought to reduce promoter activity due to aberrant HNF4A binding. In our MPRA results, carried out in HepG2 cells, we did not observe a significant reduction of promoter activity due to mutations in the HNF4A binding region (-63 to -39). We believe that this is mostly due to low barcode coverage at this region. However, we did observe that variants (c.-51T>A, c.-51T>C, c.-50T>A, c.-49T>A) in the core CTTTG sequence of the HNF4A motif (JASPAR ID MA0114.2) led to reduced promoter activity. We also found another region, positions -235 to -222, where mutations led to a significant reduction in promoter activity. Analysis of ENCODE motifs[3] of this region suggests that it is associated with Ets-related factors. In addition to the repressing variants, we observed activating variants in F9, several of which increase the transcription level up to 200%. These include mutations c.-25T>A and c.-25T>G, which are located in another annotated HNF4A motif, with both variants leading to a stronger motif. Overall, our results showed a high correlation between replicates (0.88 Pearson correlation; Supplementary Table 7).

FOXE1

A SNP, rs1867277 (NM_004473.3:c.-283G>A), in the promoter of the Forkhead Box E1 (*FOXE1*) gene was found to be associated with papillary thyroid cancer susceptibility[4]. The cancer-associated allele is thought to recruit the upstream transcription factor (USF) 1 and 2. Transfection studies in HeLa cells co-transfected with USF1 and USF2 showed

that the cancer-associated allele (A) led to a significant increase in promoter activity (~8 fold versus empty vector) compared to the unassociated allele (~3.5 fold versus empty vector)[4]. Our MPRA for this promoter was carried out in HeLa cells along with the co-transfection of USF1 and USF2. We did not observe a significant effect on promoter activity for rs1867277 (Supplementary Table 10). Overall, we only observed that 6 out of 1923 variants with a minimum of 10 associated tags showed a significant effect (p-value < 10^{-5}) on promoter activity, but with low expression effects. Our three technical replicates also had the lowest correlation of all MPRA experiments (0.16 Pearson correlation; Supplementary Table 7), precluding our ability to provide definitively interpretable results for this promoter.

GP1BB

Bernard–Soulier syndrome (BSS) is a rare autosomal recessive bleeding disorder characterized by defects of the GPIb-IX-V complex, a platelet receptor for von Willebrand factor (VWF). Most of the mutations identified in the genes encoding for the GP1BB (GPIbα), GP1BB (GPIbβ), and GP9 (GPIX) subunits prevent expression of the complex at the platelet membrane or its interaction with VWF. A mutation at the *GP1BB* promoter, NM_000407.4:c.-160C>G, is thought to disrupt the second GATA consensus binding site, and was shown to decrease promoter activity by 84% (Supplementary Table 10)[5]. In our MPRA, which was carried out in HEL 92.1.7 cell lines (erythroblasts originating from human bone marrow), we also observed a reduction in promoter activity for this mutation (52% promoter activity compared to baseline). We also saw a significant reduction across the whole GATA binding site. Several additional regions led to reduced promoter activity. For example, chr22:19,710,886-19,710,900 (GRCh37), which is annotated by JASPAR to have binding sites for Ets-related factors[6], showed significant reduction of promoter activity due to various mutations. Additional regions such as chr22:19,710,912-19,710,923, chr22:19,710,940-19,710,949 or chr22:19,711,001-19,711,032 (all GRCh37) also encompassed several mutations that led to significant reduction in promoter activity. Overall, we observed a good correlation (0.88 Pearson correlation; Supplementary Table 7) between replicates for this MPRA.

HBB

Mutations in the the Hemoglobin Subunit Beta (*HBB*) gene cause beta thalassemias (β^0 or β^+), characterized by reduced hemoglobin levels that lead to lower oxygen levels in the body. The severity of the disease depends on the nature of the mutation. There are 31 clinical variants in the *HBB* promoter that were reported as disease causing, based on the Leiden Open Variation Database (https://lovd.bx.psu.edu/home.php?select_db=HBB)[7]. In our MPRA, which was carried out in in HEL 92.1.7 cells (erythroblasts originating from human bone marrow), 17 out of 31 clinical variants were found to have a significant effect on promoter activity (p-value <

10^{-5}) (Supplementary Table 10). We observed several blocks where mutations led to reduction in activity, possibly due to transcription factor binding sites. For example, in positions c.-142 to c.-136 there is a known binding site for the erythroid Krüppel factor (EKLF), a zinc-finger transcription factor that plays a critical role in erythropoiesis and regulation of β-globin switching[8]. We observed a decrease in expression of about 12%-19% for previously reported nucleotide variants within this binding site (Supplementary Table 10). In contrast, the promoter mutation NM_000518.4:c.-18C>G, which has been previously shown to decrease steady state levels of mRNA to 85.2%[9] and is thought to disrupt the binding and transactivation of EKLF (causing mild β+ thalassemia[8]), did not show a significant effect in our study (Supplementary Table 10). We identified 12 promoter activating variants (showing greater than 20% upregulation in promoter activity), for example variant c.-99C>G showed an 128% increase in activity (Supplementary Table 10) and could potentially have a strong effect on *HBB* expression. Overall, we observed a good correlation between technical replicates (0.77 Pearson correlation; Supplementary Table 7). There could be several reasons why some of our MPRA results don't completely match previous results for these clinically associated variants. Our p-value minimum threshold might be too stringent to allow us to characterize these mutations (e.g. if we use a p-value threshold of 0.01, 23 out of the 31 variants show a significant effect on promoter activity), the clinical association might be incorrect and/or experimental differences could be contributing to these differences.

HBG1

The Hemoglobin Subunit Gamma 1 gene (*HBG1*) is a component of fetal hemoglobin, which is later replaced by adult hemoglobin at birth. Fourteen mutations in the promoter of this gene (NM_000559.2:c.-264C>T, c.-255C>T, c.-255C>G, c.-251T>C, c.-250C>T, c.-249C>T, c.-248C>G, c.-228T>C, c.-211C>T, c.-170G>A, c.-167C>T, c.-167C>G, c.-167C>A, c.-167A>C) have been identified in patients with hereditary persistence of fetal hemoglobin (HPFH; OMIM 142200; Supplementary Table 10). Work carried out in human erythroleukemia cells (K562 and HEL) has identified several proteins that may bind to the *HBG1* promoter and either activate or repress its activity[10]. For example, gamma CAAT is thought to bind to duplicated CCAAT box sequences (c.-168 to c.-164, c.-141 to c.-137) and activate activity. The c.-170G>A mutation is thought to increase the affinity of interaction between gamma CAAT and its cognate site. Two proteins, gamma CAC1 and gamma CAC2, bind a CACCC sequence located c.-197 to c.-194 from the TSS. Gamma OBP, binds an octamer sequence ATGCAAAT located c.-235 to c.-228 from the TSS. c.-228T>C mutates the eighth base of this octamer leading to a reduction of Gamma OBP binding and upregulation of *HBG1* expression, suggesting that OBP may act as a repressor in this context. The Sp1 transcription factor (SP1) is thought to function as a transcriptional activator, binding to positions c.-266 to c.-244. The c.-255C>G mutation is predicted to enhance SPl binding activity (5 to 10 fold-higher affinity for SP1) while c.-

255C>T decreases the similarity to the SP1 recognition site and is associated with a more moderate increase in *HBG1* expression[10,11].

We carried out MPRA on the *HBG1* promoter in HEL 92.1.7 cells (erythroblasts originating from human bone marrow) obtaining high reproducibility between technical replicates (0.92 Pearson correlation; Supplementary Table 7). We detected multiple blocks where mutations lead to reduced promoter activity, suggesting they serve as binding sites for activating transcription factors. We saw a significant repressive activity for mutations within the CAAT, CCAAT and CACCC blocks. However, we did not observe a continuous block of significant variants in our MPRA for the ATGCAAAT octamer sequence (c.-235 to c.-228) and the SP1 element (c.-266 to c.-244). Two blocks, one unannotated as a GAAAATAA sequence from c.-84 to c.-77 and the other is the CCAAT box from c.-141 to c.-137, showed a strong correlation with PhastCons vertebrate conservation scores.

As for individual mutations, we observed a significant change in promoter activity (p-value $< 10^{-5}$) for 6 (c.-255C>T, c.-251T>C, c.-228T>C, c.-211C>T, c.-167C>T, c.-167C>A) of the 14 disease-associated mutations (Supplementary Table 10). For example, c.-228T>C showed a strong increase in expression of over 50% and c.-167C>T led to a 65% reduction in promoter activity. Similar to *HBB*, these results could be due to: 1) Our p-value minimum threshold being too stringent (if we use a p-value threshold of 0.01, 8 out of the 14 variants show a significant effect on promoter activity); 2) The clinical association might be incorrect; 3) Experimental differences could all be contributing to these differences 4) Another limitation of our results for this promoter could be due to its regulation being driven by a complex pattern of repressor and activator binding which are temporally expressed.

HNF4A P2 promoter

Mutations in the Hepatocyte Nuclear Factor 4 Alpha (*HNF4A*) gene lead to maturity-onset diabetes of the young (MODY), a monogenic autosomal dominant subtype of early-onset diabetes mellitus caused by defective insulin secretion of pancreatic beta cells[12,13]. *HNF4A* has two characterized promoters, P1 and P2. We focused on the distant upstream P2 promoter, which is 46 kb 5' to the P1 promoter and is thought to be the major promoter regulating *HNF4A* pancreatic beta and hepatic cell expression[12]. Mutations in this promoter (NM_175914.4:c.-136A>G, c.-146T>C, c.-169C>T, c.-181G>A, c.-192C>G) have been associated with MODY[80,81] and are thought to affect the binding of various transcription factors and reduce promoter activity. Transfection assays with various mutations have identified functional binding sites for *HNF1A*, *HNF1B*, pancreatic and duodenal homeobox 1 (PDX1) and other transcription factors known to be associated with MODY[12]. They also showed that mutations c.-136A>G and c.-169C>T lead to reduced promoter activity compared to the wild-type sequence in HEK293 cells[12,13].

We carried out MPRA in HEK293T cells and observed an average Pearson correlation of 0.89 across replicates (Supplemental Table 7). Out of the five MODY-associated

mutations, we only observed a significant effect for c.-192C>G, which increased promoter activity by 20% (Supplementary Table 10). For c.-146T>C we observed a marginal reduction in activity (4%). Of interest were two variants, c.-6T>G and c.-138T>C, which increased activity up to 200% and might create strong new TF binding sites. Only c.-138T>C showed an overlap with motifs in ENCODE[3] (ONECUT1/2/3), with this variant causing a disruption in the binding site (position 7 of the MA0756.1 JASPAR[6] motif; compare with Supplementary Figure 8).

MSMB

A SNP, rs10993994, in the promoter (-57 bp from TSS) of the Microseminoprotein Beta (*MSMB*) gene was found to be associated with prostate cancer risk in two separate GWAS[14,15] and showed differential reporter activity[16,17]. The risk allele, T, of this SNP reduced promoter activity to 30% and 13% compared to the unassociated allele in HEK293T human embryonic kidney cells and prostate cancer cell lines (LNCaP), respectively[18,19]. We carried out MPRA for this promoter in HEK293T cells line, and observed a good correlation between replicates (0.88 Pearson correlation; Supplementary Table 7). For rs10993994, we obtained a 15% increase in promoter activity for the risk allele (T) instead of reduction in promoter activity as observed in LNCaP cells (Supplementary Table 10). This is likely due to the difference in cell lines used. The *MSMB* promoter has two potential androgen response element half sites (TGTTCT) located -113 to -118 bp 5' to the TSS and another is 23 bp upstream of SNP rs10993994[18] (chr10:51,549,467-51,549,472; GRCh37), which are likely to only get activated in LNCap cells but not in HEK293T cells. We observe multiple blocks that showed significant effects on promoter activity, which align with ENCODE motifs and conservation at the 3' half, but not on the other half (Supplementary Figure 8).

PKLR

Three different single nucleotide mutations (NM_000298.5:c.-324T>A, c.-83G>C, c.-72A>G) and a polymorphic deletion c.-248delT in the promoter of the Pyruvate Kinase L/R (*PKLR*) gene have been found in patients with pyruvate kinase (PK) deficiency[20,21], which leads to anemia. Functional analysis for both rat and human *PKLR* promoters revealed four conserved motifs (CAC/SP1, PKR-RE, GATA1) within the first 250 bp upstream region[21]. Both c.-72A>G and c.-83G>C significantly reduced promoter activity. c.-72A>G has been attributed to disruption of the consensus binding motif for GATA-1 at c.-69 to c.-74. c.-83G>C was shown to be a part of a core binding motif (CTCTG) of a novel regulatory element (PKR-RE1) in the erythroid-specific promoter of *PKLR*, in close proximity to a regulatory GATA-1 binding site. c.-324T>A did not show an effect on promoter activity, c.-248delT turned out to be a non-functional polymorphism[20,21].

We carried out MPRA for this promoter using two different post-transfection time points (24 and 48 hours) in K562 cells and observed a good correlation between replicates (0.86

and 0.91 Pearson correlation for 24hr and 48hr respectively; Supplementary Table 7). We observed a significant reduction in promoter activity for two of the disease causing mutations, c.-72A>G (24h=-1.77, 48h=-2.40) and c.-83G>C (24h=-1.25, 48h=-2.19). For c.-324T>A and c.-248delT we did not observe a significant effect which is consistent with the previous functional study[20,21]. Around 15% of all tested variants showed a significant effect, with the majority of these variants being located either near the 3' or 5' end, suggesting that these two regions are important for *PKLR* promoter activity. All positions at the GATA1 conserved site from c.-73 to c.-70 had significant repressing variants in both experiments. The same repressing effects can be seen for the two conserved CAC/SP1 sequences (c.-119 to c.-114 and c.-107 to c.-103) and the PKR-RE motif (c.-87 to c.-83). In general, annotated motifs align well with the significant variant effects on *PKLR* (Supplementary Figure 8). This experiment had one of the highest correlation for JASPAR motifs (Supplementary Table 12, 13), compared to all tested promoter elements.

Enhancers (in alphabetical order)

BCL11A

B cell CLL/lymphoma 11A (*BCL11A*) is a transcription factor that regulates hemoglobin switching and has a characterized erythroid enhancer where common genetic variation has been associated with fetal hemoglobin (HbF) levels[22]. Saturation mutagenesis of the *BCL11A* enhancer via CRISPR-Cas9 guide RNA libraries uncovered key functional regions in this enhancer and implicated DNase hypersensitive site (DHS) +58 to have the most significant effect on *BCL11A* expression and HbF levels[23]. We thus used DHS +58 for our MPRA, which was carried out in the HEL92.1.7 erythroblast cell line. For the *BCL11A* experiments, we did not observe high correlations between replicates (0.38 Pearson correlation; Supplementary Table 7), possibly due to low fold activation by this enhancer in our assay/cell line (2.5 fold compared to empty vector) and a high mutation rate from the error-prone PCR step (creating an average of 6 variants per construct and very few wild-type sequences; factors that negatively impact model fit). Only 3% of the tested variants had a significant effect (p-value < 10^{-5}). The average $\log_2$ expression effect of all variants was only 0.064 (4.5%) and 0.21 (16%) for the subset of significant variants. The low activation we observed for this enhancer could be due to the use of different cells lines. HEL92.1.7 is an established erythoblast cell line collected from bone marrow. HUDEP-2[24], which was used for the CRISPR-Cas9 assays, are human erythroid progenitors derived from the umbilical cord and are thought to be more similar to adult erythroid cells. It could also be due to differences in experimental methodologies, i.e. endogenous mutations via CRISPR-Cas9 that assay phenotypic changes versus MPRAs that test the ability of the sequence to drive regulatory activity.

IRF4

A SNP, rs12203592, within an intron of the gene encoding the Interferon Regulatory Factor 4 (*IRF4*), a transcription factor involved in pigmentation, is strongly associated with sensitivity of skin to sun exposure, freckles, blue eyes and brown hair color[25]. IRF4 is activated by the melanocyte master regulator melanocyte inducing transcription factor (MITF) along with the transcription factor AP-2 alpha (TFAP2A). The pigmentation-associated allele, rs12203592-T, is thought to disrupt a TFAP2A binding site and was shown to reduce enhancer activity[25]. We carried out saturation-based MPRA for this enhancer in human melanoma SK-MEL-28 cells and observed strong correlations between technical replicates (0.99 Pearson correlation; Supplementary Table 7). The rs12203592-T allele led to a significant reduction in enhancer activity, 36% compared to wild-type (Supplementary Table 11). Overall, we observed that 37% of the variants had a significant effect on enhancer activity. Conservation seems to be an informative measurement for activity and *IRF4* has one of the best agreement between different annotations and absolute expression effects (see Results and Supplementary Table 12, 13).

IRF6

A SNP, rs642961, in an Interferon Regulatory Factor (IRF6) associated-enhancer was shown to confer an 18% attributable risk for isolated cleft lip[26]. This variant is part of a common haplotype, rs76145088 (G>A), rs642961 (G>A) and rs77542756 (A>G) and the AAG associated-haplotype is thought to disrupt AP-2α binding sites and increase enhancer activity compared to the unassociated haplotypes in human foreskin keratinocyte HFK cells[26]. However, this difference did not reach statistical significance. Saturation based MPRA for this IRF6 enhancer was done in the human keratinocyte HaCaT cells and obtained a strong correlation between technical replicates (0.96 Pearson correlation; Supplementary Table 7). We observed that around 19% of all variants show a significant effect on enhancer activity. We did not observe a significant effect on enhancer activity for rs642961 and rs77542756 by themselves (Supplementary Table 11). However, the region where rs642961 and rs77542756 were located (chr1:209,989,152-209,989,314; GRCh37) had several activating mutations. For SNP rs76145088 our MPRA detected a significant repression by 18% (Supplementary Table 11). We could not detect an enrichment of significant variants at the AP-2α binding sites and because of the design of our MPRA, the associated-haplotype AAG is not covered. IRF6 had several conserved sites, but most of them do not align with blocks of significant expression effects (Supplementary Figure 9), leading to low correlation of conservation and functional scores (Supplementary Table 12, 13). Of note, although rs642961 shows minor effects on reporter gene expression in cell culture, it is possible that it has significantly larger or even opposing effects on IRF6 expression in vivo in its native chromosomal context and/or in the presence of trans-acting variants[26].

MYC rs6983267 and rs11986220

Activation of the MYC proto-oncogene, bHLH transcription factor (*MYC*) gene is a hallmark of cancer initiation and maintenance. Several GWAS reported association between the G-allele of rs6983267 and increased risk for various types of cancers such as colorectal and prostate cancer[27–29]. Studies have also shown that a region including rs6983267 has enhancer activity and interacts with the proto-oncogene *MYC* during early stages of colorectal cancer development[30,31]. rs11986220 resides ~100 kb away from rs6983267, and is associated with prostate cancer risk independent of rs6983267[32]. rs11986220 resides within a FOXA1 binding site, and the prostate cancer risk allele (A) is thought to facilitate both stronger FOXA1 binding and androgen responsiveness[32]. To study the individual variant effects of these SNPs and their surrounding sequences, we generated saturation mutagenesis libraries of 600 bp around rs6983267 and 464 bp around rs11986220. We tested the MYC rs6983267 MPRA library in human embryonic kidney cells, HEK293T, adding 20mM LiCl to activate the Wnt pathway and the MYC rs11986220 in human prostate adenocarcinoma LNCaP cells grown in a medium with 100nM Dihydrotestosterone to stimulate androgen activity.

For MYC rs6983267, we observed a strong correlation between replicates (0.75 Pearson correlation; Supplementary Table 7). We did not see a change in activity (p-value of coefficient 0.05; $\log_2$ expression effect -0.08 / 95% activity) due to the cancer-associated rs6983267 allele (T) (Supplementary Table 11). We observed a stretch of nucleotides that led to a reduction in enhancer activity at chr8:128,413,089-128,413,107 (GRCh37). This region correlates with an annotated CTCF binding site as determined by ERB v90[33]. Of note, two variants, chr8:128,413,279C>G and chr8:128,413,289G>T (GRCh37) led to a strong increase in enhancer activity by 86% and 84%.

For MYC rs11986220, we did not obtain a good correlation between replicates (0.31 Pearson correlation; Supplementary Table 7). rs11986220 showed a 14% repressing activity, but was not statistically significant (Supplementary Table 11). In total, only 11 out of 1685 variants had an expression effect on enhancer activity at a significance level of 10^{-5}.

RET

A common non-coding variant, rs2435357, within an enhancer in intron 1 of the gene Rearranged During Transfection Proto-oncogene (*RET*) is significantly associated with Hirschsprung disease (HSCR) susceptibility[34]. The disease-associated variant leads to a significant reduction in reporter activity (6-8 fold) compared to the unassociated allele in Neuro-2a cells[34]. Saturation mutagenesis based MPRA was carried out for this enhancer in Neuro-2a cells, with the library cloned into the pGL3 vector, similar to the experiment that originally tested this enhancer[34]. Overall, we observed a reasonable correlation between technical replicates (0.71 Pearson correlation; Supplementary Table 7). We did not detect a significant effect on enhancer activity for rs2435357 (Supplementary Table

11). However, this SNP is located within a sequence block that has multiple variants with significant activating and repressing effects (chr10:43,582,096-43,582,232; GRCh37). Both rs2506005 and rs2506004, which reside 76 bp upstream and 217 bp downstream of rs2435357 respectively, and are in linkage disequilibrium with this SNP, also showed no significant effect on enhancer activity. A region located towards the 3'-end of the sequence (chr10:43,582,390-43,582,526; GRCh37) is enriched in variants that led to differential enhancer activity.

TCF7L2

GWAS for type-2 diabetes (T2D) found a significant association with SNP rs7903146, located within an intron of the gene Transcription Factor 7 Like 2 (*TCF7L2*). The rs7903146 risk T allele is associated with impaired insulin secretion, incretin effects and enhanced rate of hepatic glucose production[35]. Luciferase assays of both alleles in mouse pancreatic beta MIN6 cells exhibited significant allele-specific differences with the T allele leading to a three fold stronger enhancer activity compared to the non-risk allele (Supplementary Table 11)[102]. We carried out mutation saturation based MPRA for this enhancer in MIN6 cells, which covered over 99% of all mutations in the tested region (Supplementary Table 3) and obtained high variant effect correlations between replicates (0.76 Pearson correlation; Supplementary Table 7). Functional and conservation scores do not correlate well with the observed variant effects, but we observed some correlation with JASPAR motifs (Supplementary Table 12, 13). We do observe a significant effect on enhancer activity for rs7903146, even though only a 19% expression increase.

UC88

Ultraconserved elements (UCEs) are sequences greater than 200 bp in length that are identical between human, mouse and rat[36]. Half of the UCEs were shown to be functional enhancers in developing mouse embryos, the majority of which are active in the central nervous system[37]. UC88 is located on chr2:162,094,920-162,095,508 (GRCh37) and was shown to be a robust forebrain enhancer at mouse embryonic day E11.5 (hs416; VISTA enhancer browser[38]). UC88 was tested for enhancer activity in mouse neuroblastoma Neuro-2a cells and showed significant enhancer activity (9.3 fold compared to empty vector). Mutation saturation based MPRA was performed on UC88 in Neuro-2a cells. Replicates had a lower replicate correlation (0.64 average Pearson coefficient); however, this increased to 0.9 for significant variants (using a lenient p-value threshold of < 0.01) (Supplementary Table 7). This limited our interpretability to 10% (196 out of 1964, p-value < 0.01) of all measured variants in UC88, not allowing us to see clear patterns regarding known motifs or other annotations (Supplementary Figure 9). Overall, we obtained a low correlation of functional, conservation and motif scores (Supplementary Table 12, 13).

ZFAND3

A Type 2 Diabetes GWAS found an associated with rs58692659, which is ~10 kb upstream to the zinc finger AN1-type containing 3 (*ZFAND3*) gene[39]. The rs58692659 SNP maps to an open chromatin region, identified previously by both islet FAIRE-seq and ChIP-seq for H2A.Z, and is thought to be bound by several beta cell transcription factors, including PDX1, FOXA2, NKX2.2 NKX6.1 and NEUROD1. Further TFBS analyses and EMSA suggest that the T allele alters the binding of NEUROD1[39]. Luciferase assays showed reduced enhancer activity (~5 fold) for the rs58692659 risk allele (T) compared to the C allele in mouse MIN6 beta cells[39]. We carried out mutation saturation based MPRA on this enhancer in MIN6 cells and obtained high variant effect correlations between replicates (0.89 Pearson correlation; Supplementary Table 7). For rs58692659, we observed a significant reduction in enhancer activity (70% residual activity) for the disease-associated allele (T) which is consistent with the previous reported luciferase results. Furthermore, we found that rs58692659 resides in a region (chr6:37,775,451-37,775,758; GRCh37) that with numerous mutations that lead to either a reduction or increase in enhancer activity (Supplementary Table 11). This region is highly conserved in vertebrates and contains predicted binding sites for the islet-enriched transcription factors RFX4, MAX and NHLH1[39] as annotated by JASPAR 2018[6]. Due to the high correlation of conservation, the tested functional scores result in high correlations as well (Spearman correlation ~0.4; Supplementary Table 12, 13).

ZRS

Mutations in the Sonic Hedgehog (*SHH*) limb enhancer, called the zone of polarizing activity regulatory sequence (ZRS), lead to a wide array of limb malformations[40]. These include polydactyly, triphalangeal thumb (TPT), syndactyly, tibial hypoplasia and Werner mesomelic syndrome (OMIM #188770)[41–46]. Several of these mutations were tested for enhancer activity using mouse transgenic assays, with the majority showing ectopic expression compared to the wild-type sequence[40]. *In vitro* assays were also done for a 1.7 kb version of this enhancer in NIH3T3 mouse fibroblasts which showed higher enhancer activity upon co-transfection of homeobox d13 (*Hoxd13*) and heart and neural crest derivatives expressed 2 (*Hand2*). As we were limited in length due to technical reasons, we first tested a 485 bp ZRS sequence that encompasses the majority of disease causing mutations in this *in vitro* system. We observed a significant fold change for co-transfections with Hoxd13 by itself (4.2 fold) or along with Hand2 (2.0 fold) compared to the empty vector. We thus set out to do saturation mutagenesis MPRA in NIH3T3 cells using both conditions (i.e. Hoxd13 or Hoxd13+Hand2).

We observed reasonable correlations between technical replicates (0.76 Pearson correlation for both Hoxd13 or Hoxd13+Hand2; Supplementary Table 7). Overall, we did not detect a high fraction of significant variant effects and those that were significant were distributed over the entire region with stronger effects towards the 3' end. For most

disease-causing mutations, we did not observe a significant effect, likely due to technical reasons. These could be due to this enhancer having important spatial and temporal activities in the developing limb that are likely not represented in an *in vitro* setting that uses a single cell type along with the co-transfection of additional factors. However, we did observe an effect for some known mutations. These include chr7:156,584,153T>C (GRCh37; ZRS417), which resulted in 16% and 9% increase with Hoxd13 and Hoxd13+Hand2 respectively (Supplementary Table 11), and is known to cause a more severe limb phenotype which includes polydactyly of the four extremities and bilateral tibial deficiency[44]. Another interesting mutation is chr7:156,584,285C>A (GRCh37; ZRS285) that led to 17% and 13% higher enhancer activity with Hoxd13 and Hoxd13+Hand2 respectively (Supplementary Table 11), and is known to cause polydactyly in Silkie chickens[47].

Supplementary Figures

Supplementary Figure 1

A

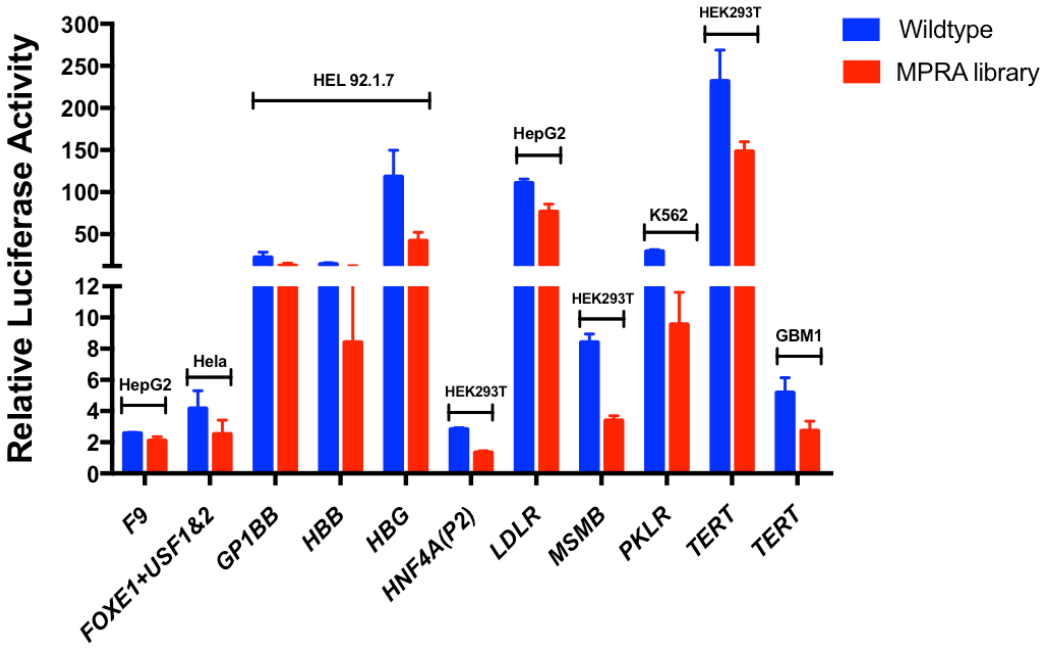

B

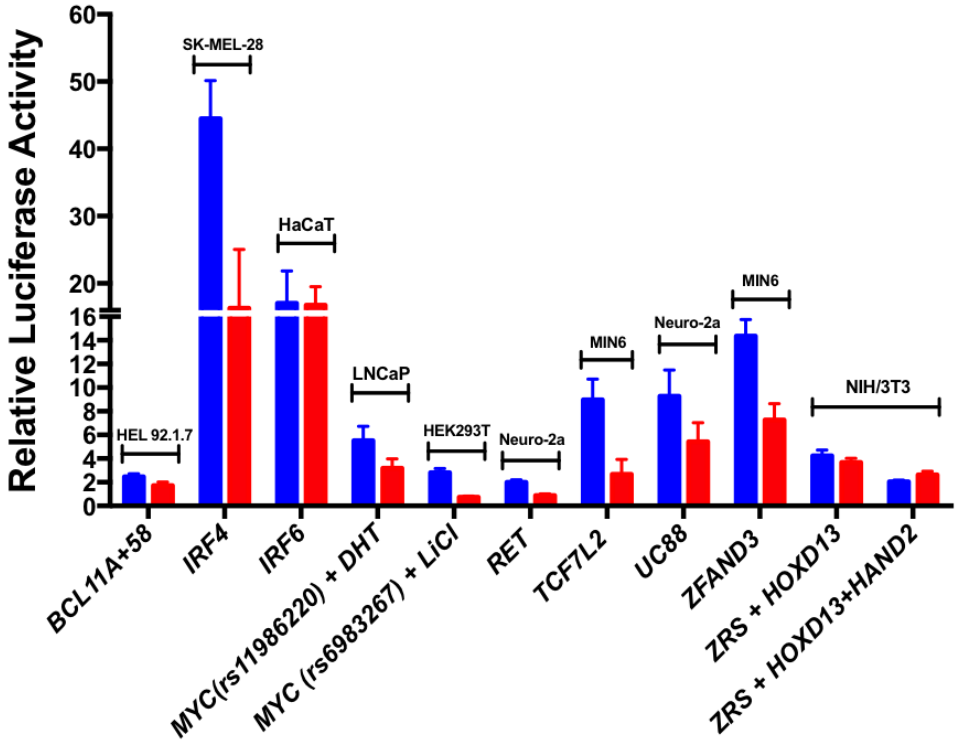

Promoter and enhancer luciferase assays. Bar charts representing the relative luciferase activity of the 10 selected promoters **(A)** and 10 selected enhancers **(B)** for either the wild-type (blue) or the saturation mutagenesis library (mutant library; red) normalized to the empty vector. In **(A)**, for *FOXE1*, 7.5ug of upstream transcription factor (USF) 1 and 2 were co-transfected along with the vector/library. All promoters activities were measured after 24hr transfection except for *PKLR* which was measured after 48hr. In **(B)**, for *ZRS,* 3.75ug *HOXD13* or *HOXD13* plus *HAND2,* were co-transfected along with the vector/library. For *MYC* (rs11986220), 10nM dihydrotestosterone (DHT) were also co-transfected. For *MYC* (rs6983267), 20mM of LiCl was added after 24hr to induce Wnt pathway activity and luciferase activity was measured at 32 hours. For all other enhancers, luciferase activity was measured 24 hours after transfection. All results are mean ± standard deviation of at least 3 independent experiments.

Supplementary Figure 2

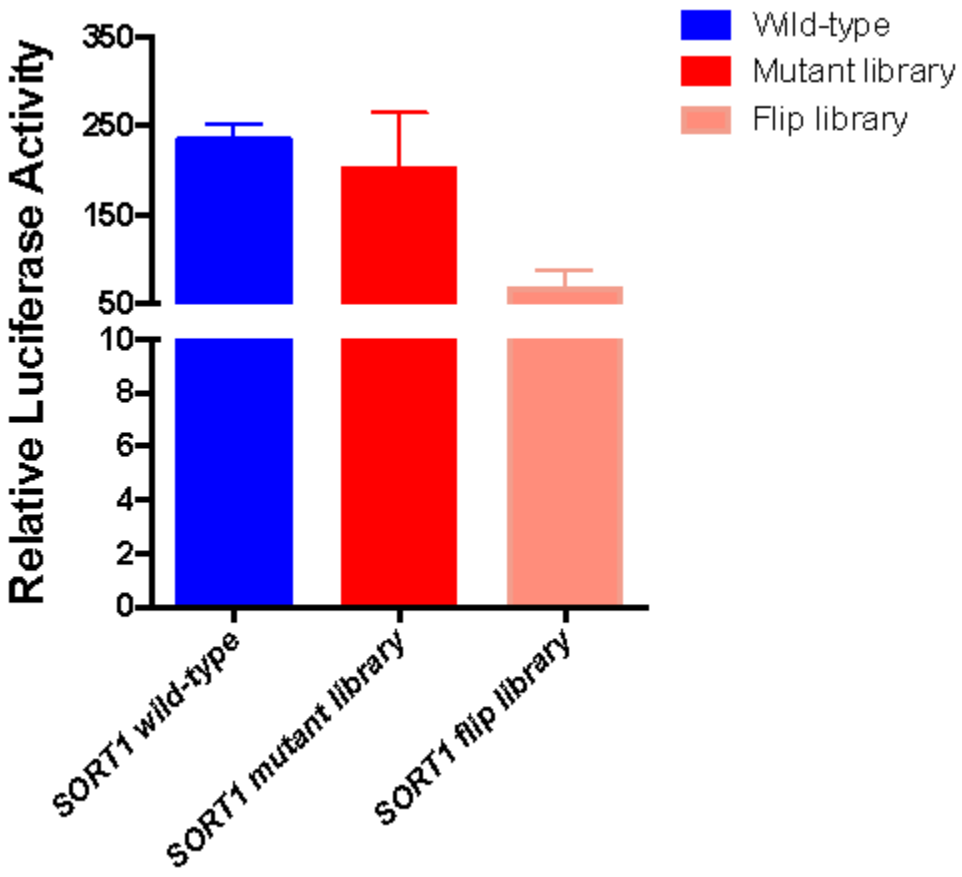

***SORT1* enhancer assays.** Bar charts representing the relative luciferase activity of the *SORT1* enhancer wild-type sequence (blue), mutant library (red) and flip library (light red). Luciferase levels were measured following 24 hour and results are plotted with mean ± standard deviation of at least 3 independent experiments.

Supplementary Figure 3

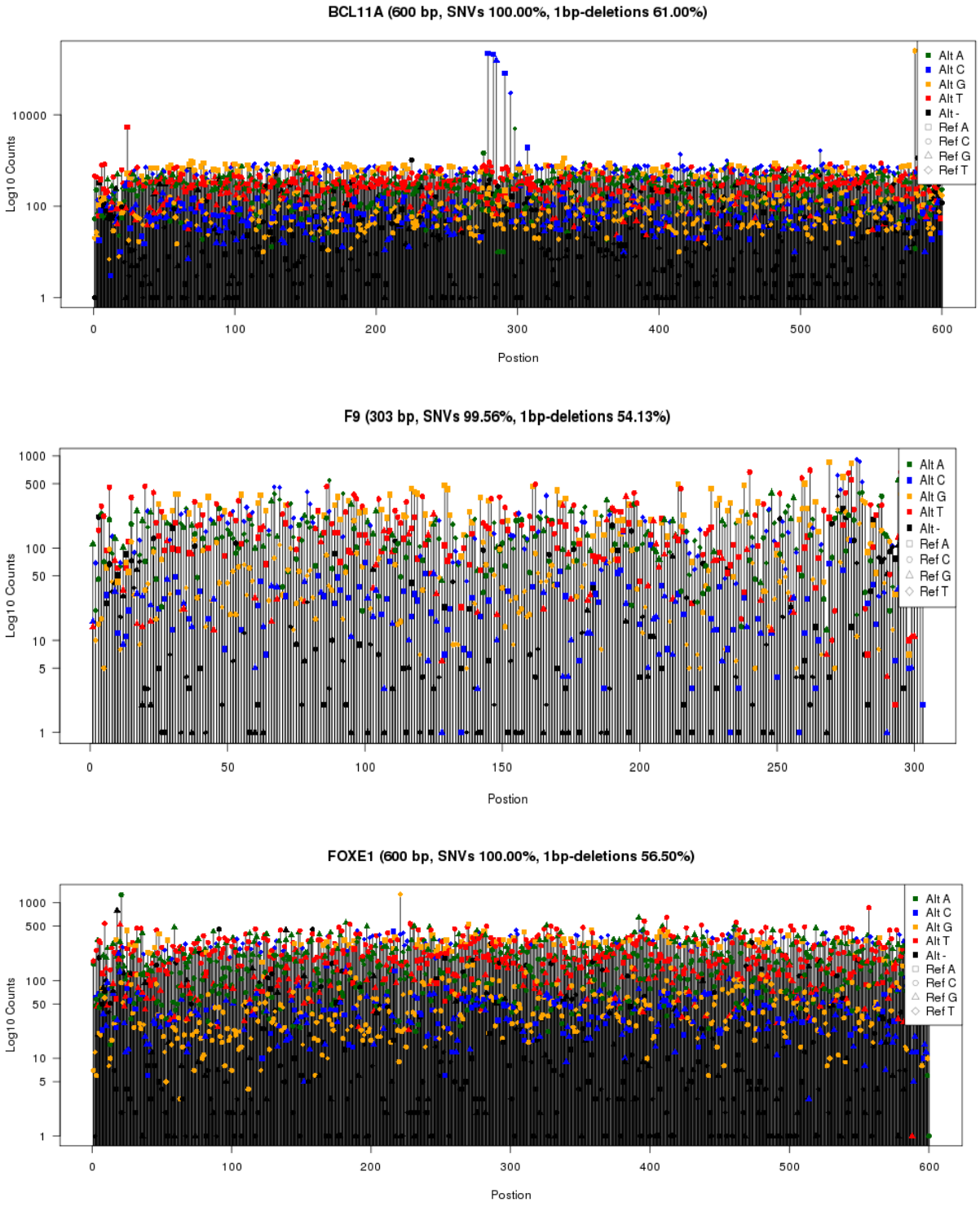

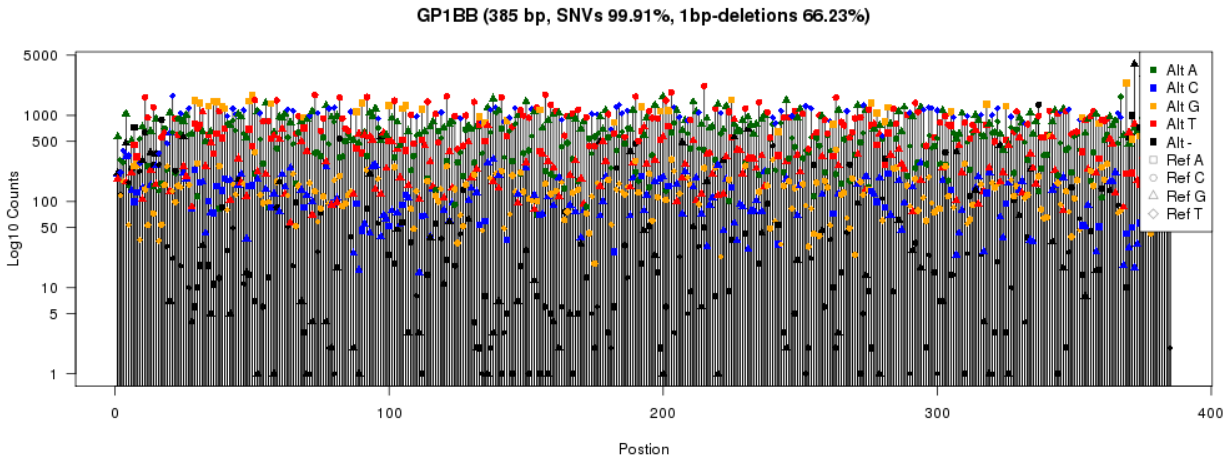
GP1BB (385 bp, SNVs 99.91%, 1bp-deletions 66.23%)
Log10 Counts
5000
1000
500
100
50
10
5
1
0
100
200
300
400
Postion
Alt A
Alt C
Alt G
Alt T
Alt -
Ref A
Ref C
Ref G
Ref T

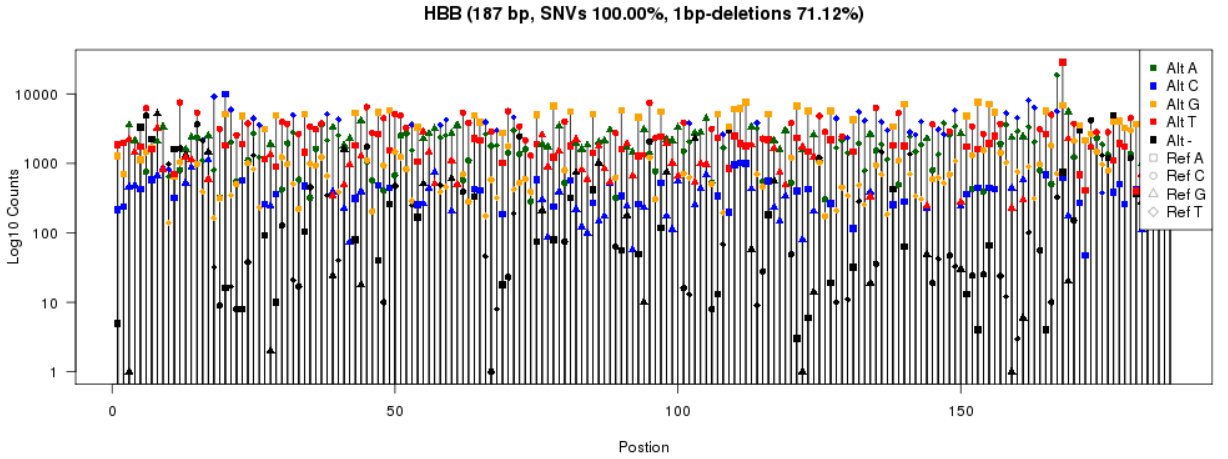
HBB (187 bp, SNVs 100.00%, 1bp-deletions 71.12%)
Log10 Counts
10000
1000
100
10
1
0
50
100
150
Postion
Alt A
Alt C
Alt G
Alt T
Alt -
Ref A
Ref C
Ref G
Ref T

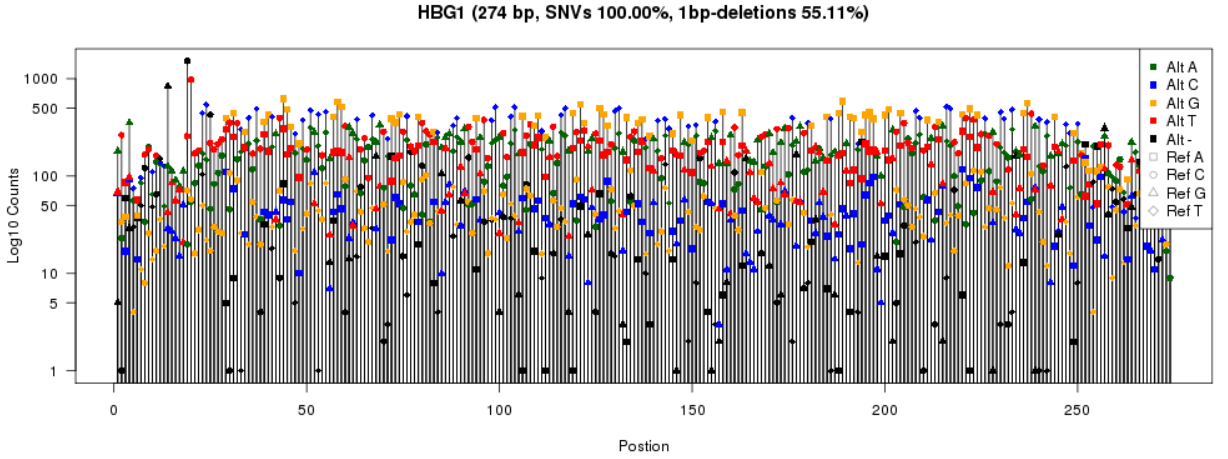
HBG1 (274 bp, SNVs 100.00%, 1bp-deletions 55.11%)
Log10 Counts
1000
500
100
50
10
5
1
0
50
100
150
200
250
Postion
Alt A
Alt C
Alt G
Alt T
Alt -
Ref A
Ref C
Ref G
Ref T

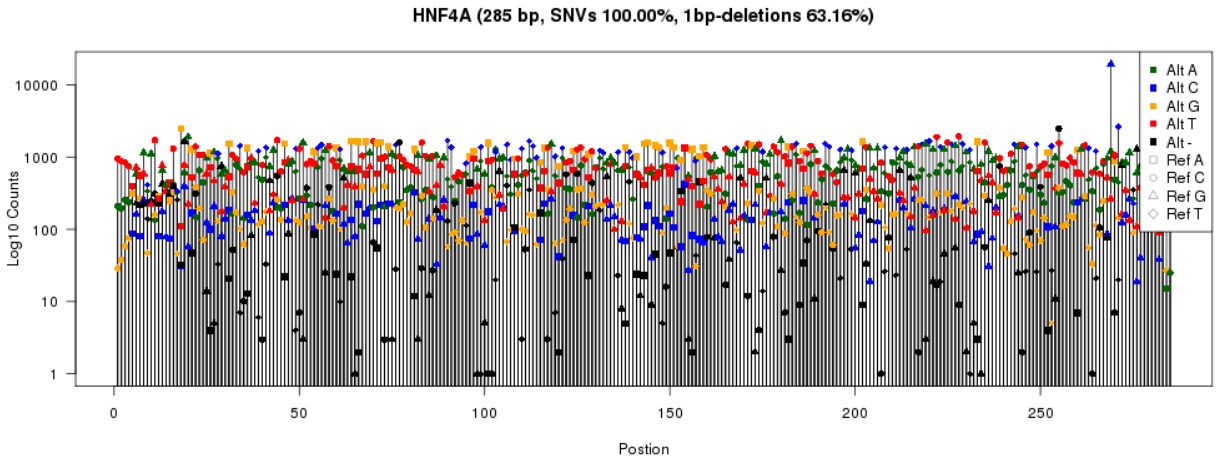
HNF4A (285 bp, SNVs 100.00%, 1bp-deletions 63.16%)
Log10 Counts
10000
1000
100
10
1
0
50
100
150
200
250
Postion
Alt A
Alt C
Alt G
Alt T
Alt -
Ref A
Ref C
Ref G
Ref T

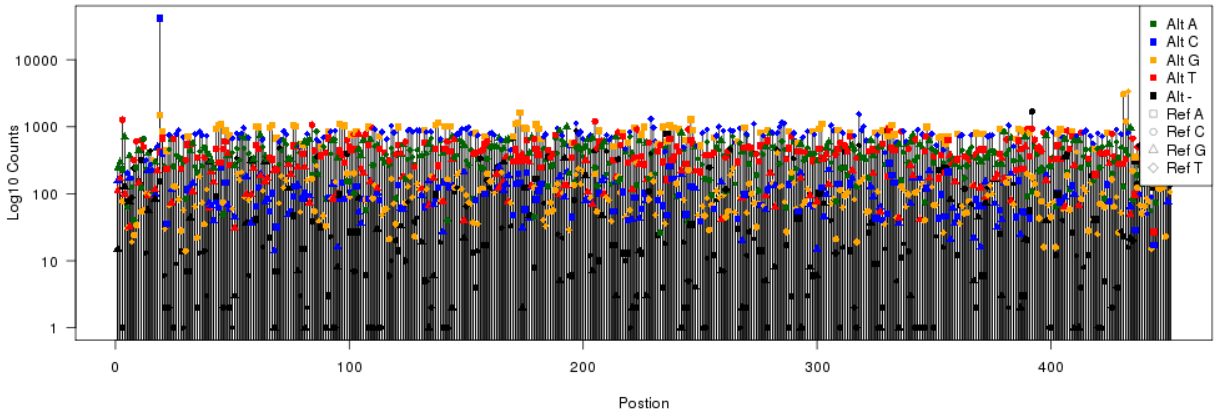
IRF4 (451 bp, SNVs 100.00%, 1bp-deletions 63.64%)
Log10 Counts
10000
1000
100
10
1
0
100
200
300
400
Postion
Alt A
Alt C
Alt G
Alt T
Alt -
Ref A
Ref C
Ref G
Ref T

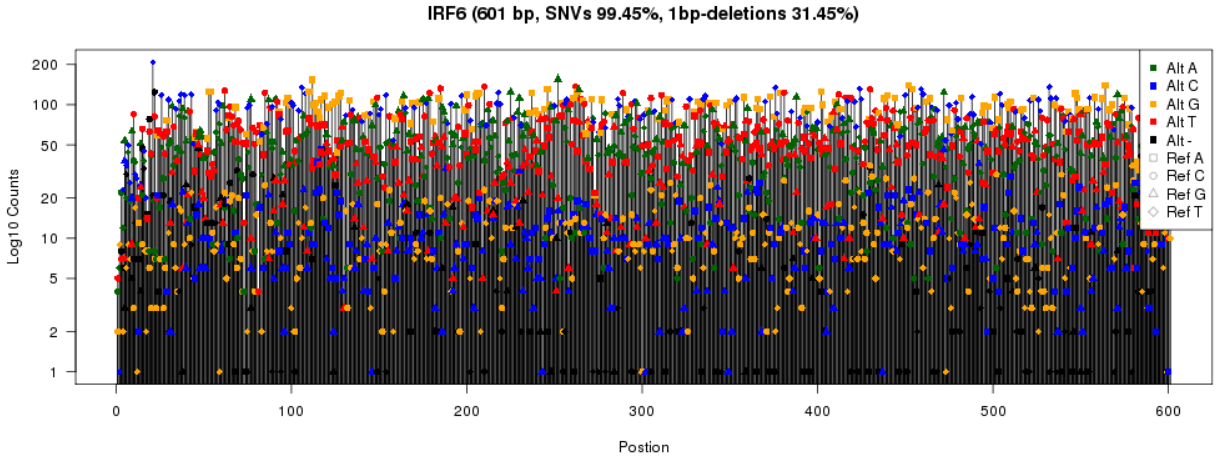
IRF6 (601 bp, SNVs 99.45%, 1bp-deletions 31.45%)
Log10 Counts
200
100
50
20
10
5
2
1
0
100
200
300
400
500
600
Postion
Alt A
Alt C
Alt G
Alt T
Alt -
Ref A
Ref C
Ref G
Ref T

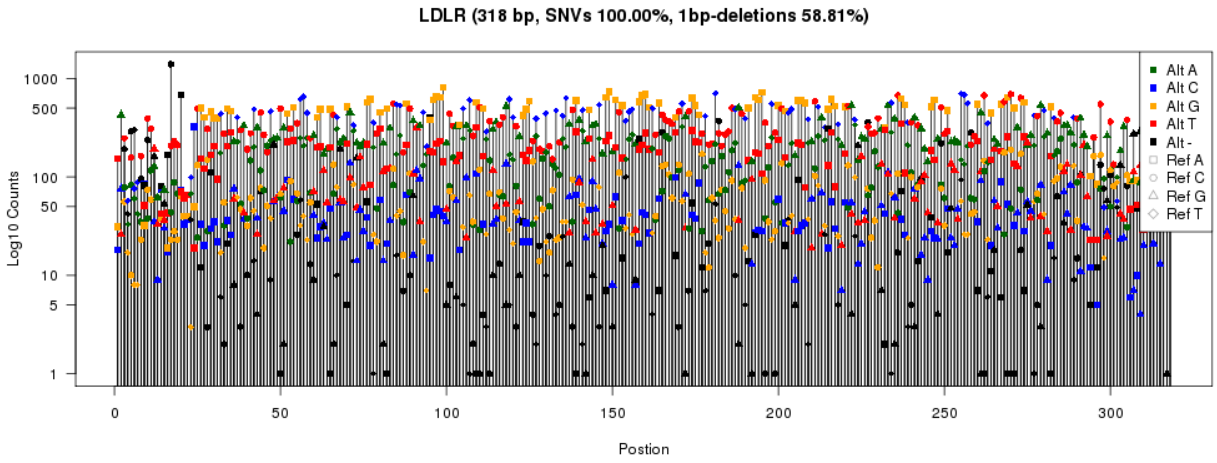
LDLR (318 bp, SNVs 100.00%, 1bp-deletions 58.81%)
Log10 Counts
1000
500
100
50
10
5
1
0
50
100
150
200
250
300
Postion
Alt A
Alt C
Alt G
Alt T
Alt -
Ref A
Ref C
Ref G
Ref T

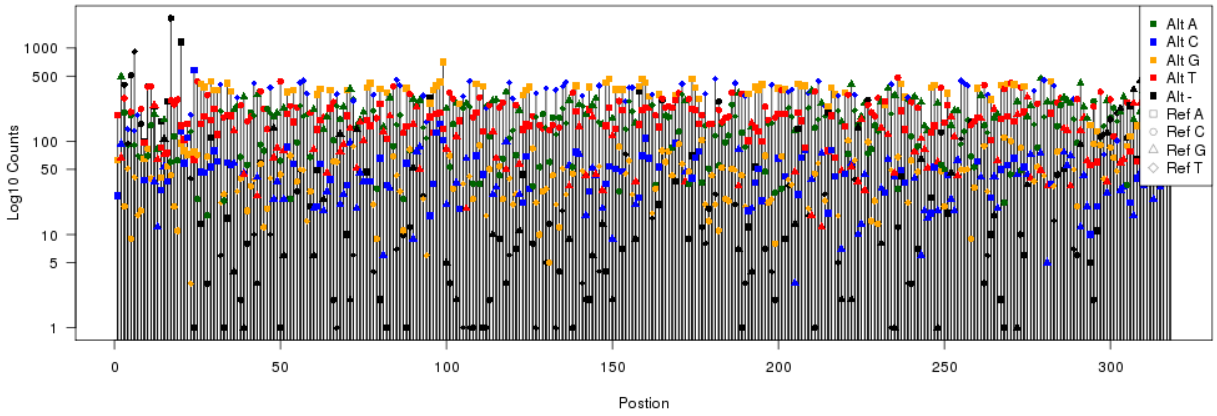
LDLR.2 (318 bp, SNVs 100.00%, 1bp-deletions 56.92%)
Log10 Counts
1000
500
100
50
10
5
1
0
50
100
150
200
250
300
Postion
Alt A
Alt C
Alt G
Alt T
Alt -
Ref A
Ref C
Ref G
Ref T

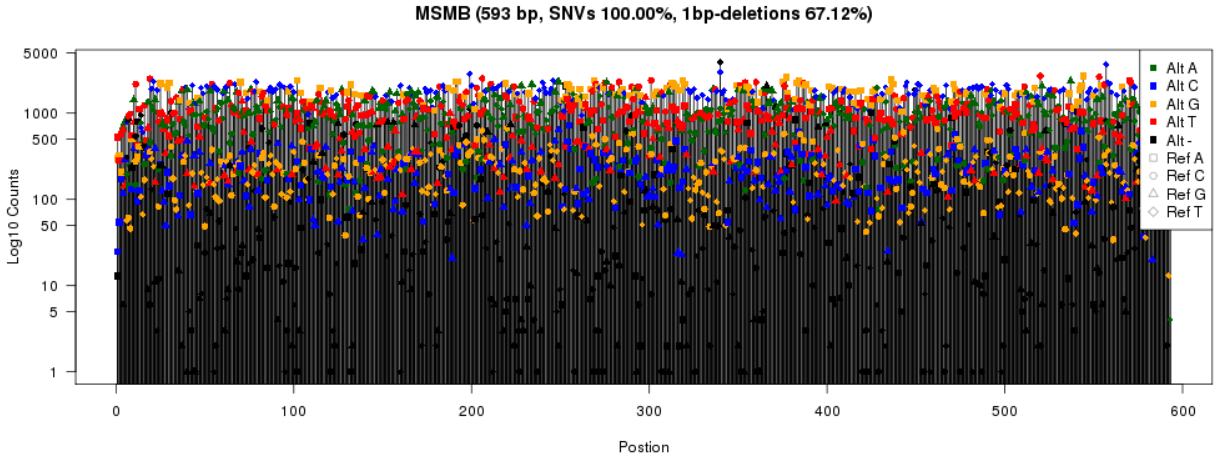
MSMB (593 bp, SNVs 100.00%, 1bp-deletions 67.12%)
Log10 Counts
5000
1000
500
100
50
10
5
1
0
100
200
300
400
500
600
Postion
Alt A
Alt C
Alt G
Alt T
Alt -
Ref A
Ref C
Ref G
Ref T

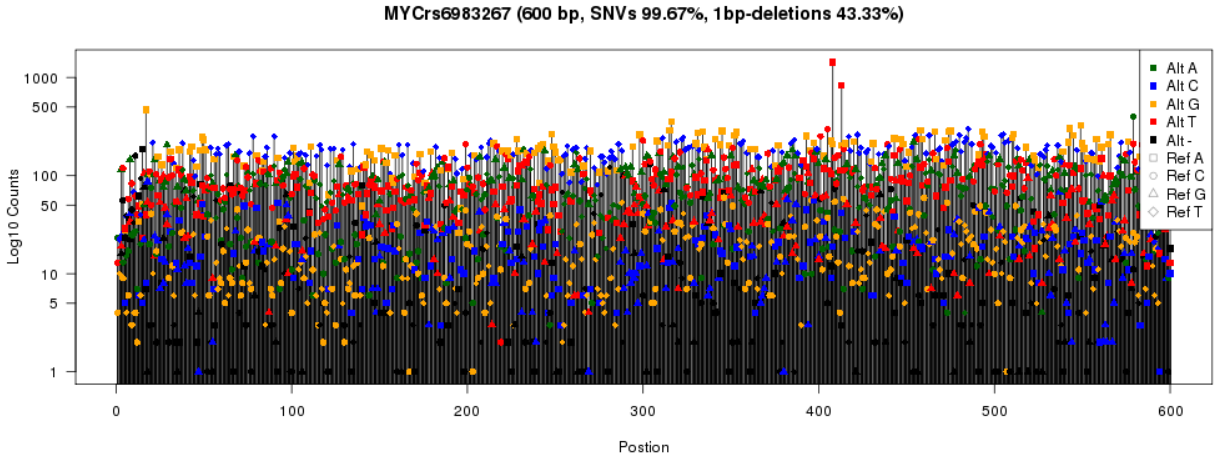
MYCrs6983267 (600 bp, SNVs 99.67%, 1bp-deletions 43.33%)
Log10 Counts
1000
500
100
50
10
5
1
0
100
200
300
400
500
600
Postion
Alt A
Alt C
Alt G
Alt T
Alt -
Ref A
Ref C
Ref G
Ref T

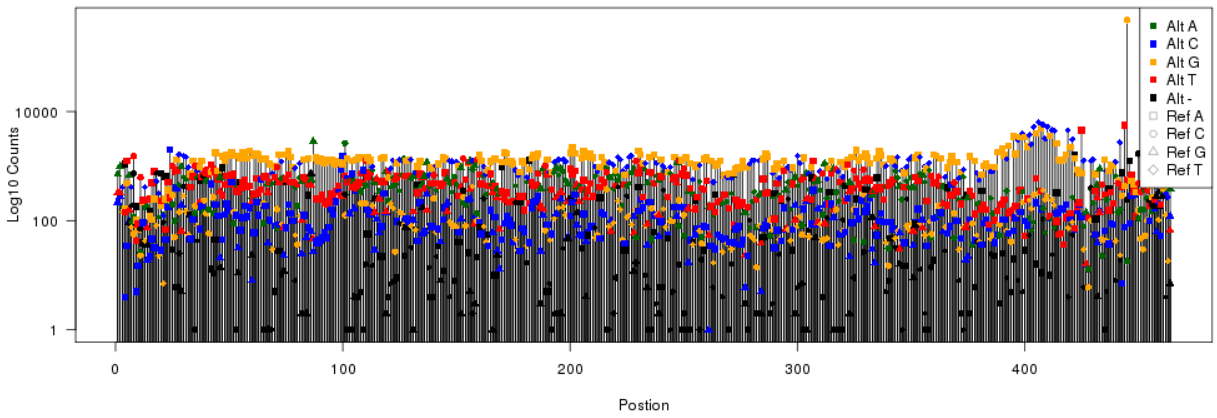
MYCrs11986220 (464 bp, SNVs 100.00%, 1bp-deletions 55.39%)
Log10 Counts
10000
100
1
0
100
200
300
400
Postion
Alt A
Alt C
Alt G
Alt T
Alt -
Ref A
Ref C
Ref G
Ref T

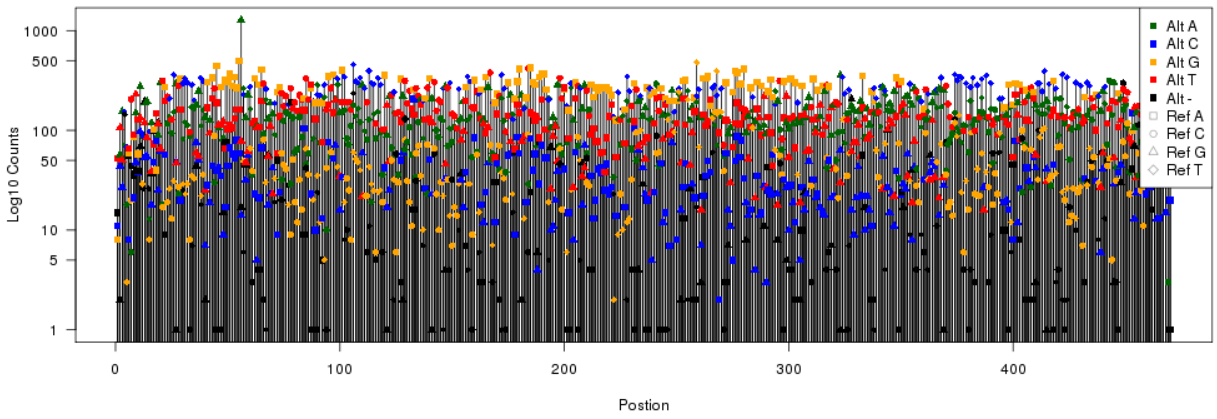
PKLR (470 bp, SNVs 99.93%, 1bp-deletions 45.74%)
Log10 Counts
1000
500
100
50
10
5
1
0
100
200
300
400
Postion
Alt A
Alt C
Alt G
Alt T
Alt -
Ref A
Ref C
Ref G
Ref T

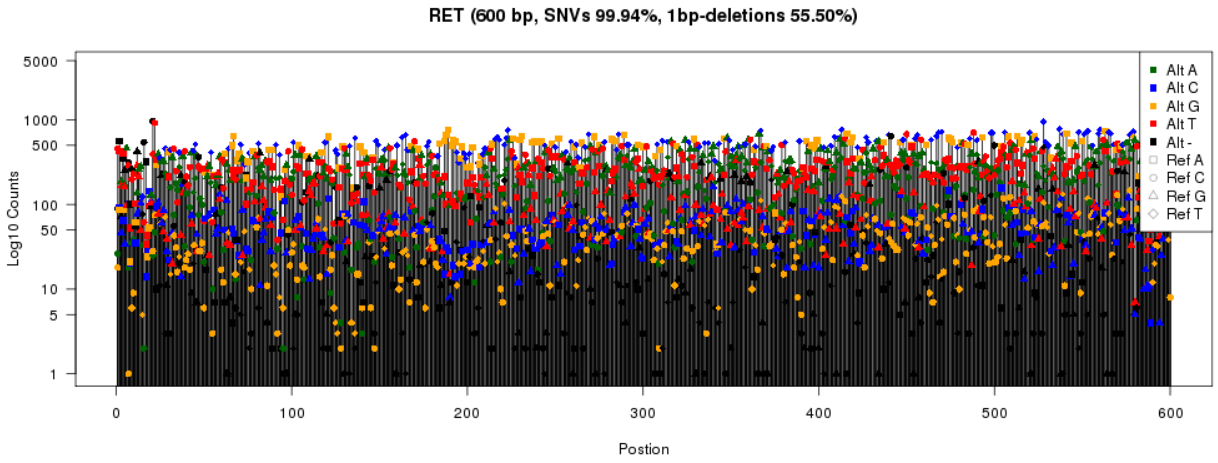
RET (600 bp, SNVs 99.94%, 1bp-deletions 55.50%)
Log10 Counts
5000
1000
500
100
50
10
5
1
0
100
200
300
400
500
600
Postion
Alt A
Alt C
Alt G
Alt T
Alt -
Ref A
Ref C
Ref G
Ref T

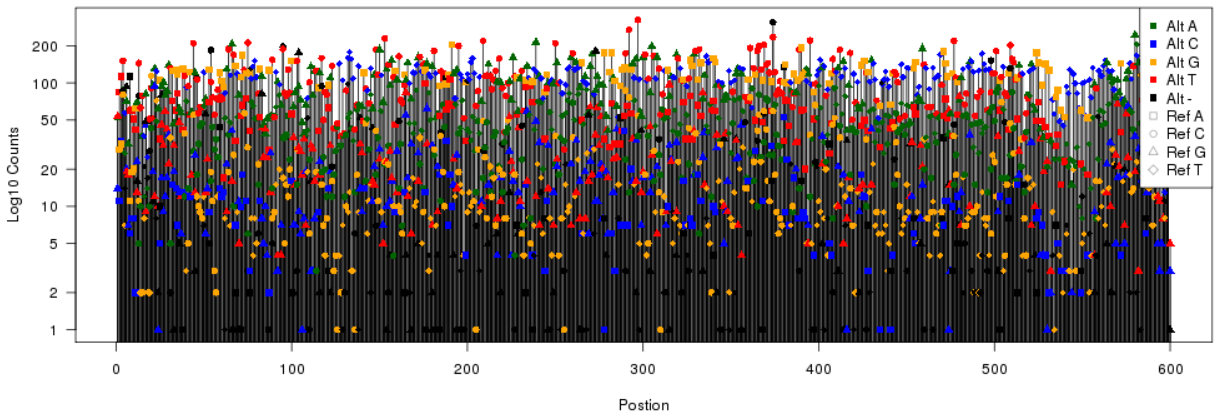
SORT1 (600 bp, SNVs 99.72%, 1bp-deletions 41.67%)
Log10 Counts
200
100
50
20
10
5
2
1
0
100
200
300
400
500
600
Postion
Alt A
Alt C
Alt G
Alt T
Alt -
Ref A
Ref C
Ref G
Ref T

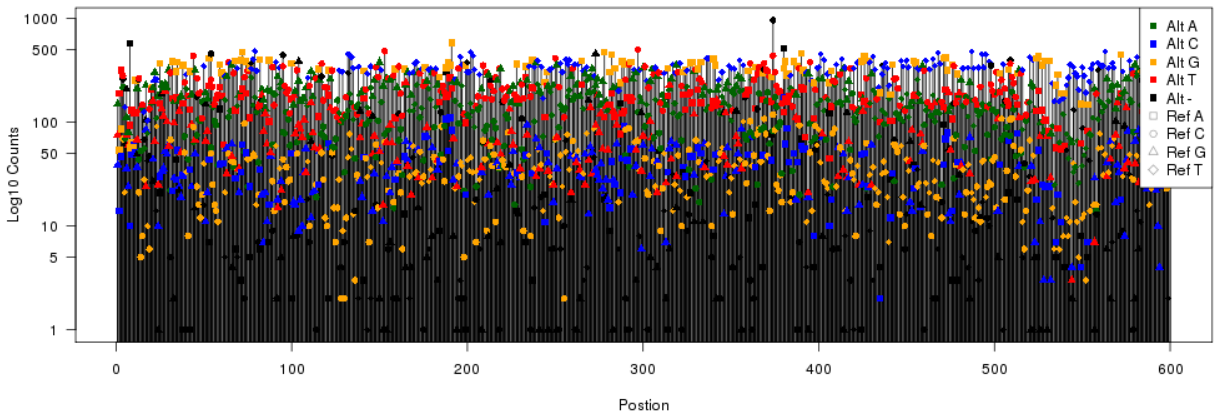
SORT1.2 (600 bp, SNVs 99.94%, 1bp-deletions 49.83%)
Log10 Counts
1000
500
100
50
10
5
1
0
100
200
300
400
500
600
Postion
Alt A
Alt C
Alt G
Alt T
Alt -
Ref A
Ref C
Ref G
Ref T

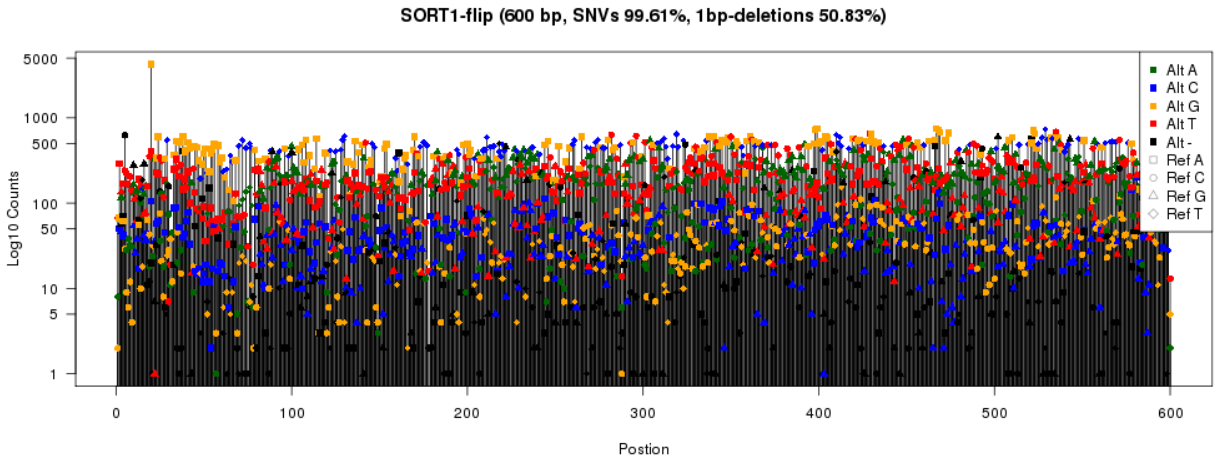
SORT1-flip (600 bp, SNVs 99.61%, 1bp-deletions 50.83%)
Log10 Counts
5000
1000
500
100
50
10
5
1
0
100
200
300
400
500
600
Postion
Alt A
Alt C
Alt G
Alt T
Alt -
Ref A
Ref C
Ref G
Ref T

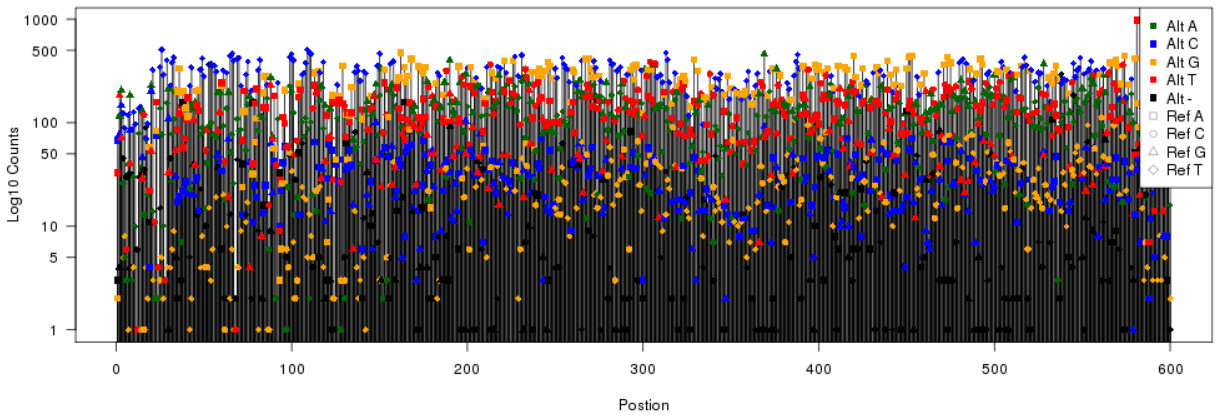
TCF7L2 (600 bp, SNVs 99.06%, 1bp-deletions 42.33%)
Log10 Counts
1000
500
100
50
10
5
1
0
100
200
300
400
500
600
Postion
Alt A
Alt C
Alt G
Alt T
Alt -
Ref A
Ref C
Ref G
Ref T

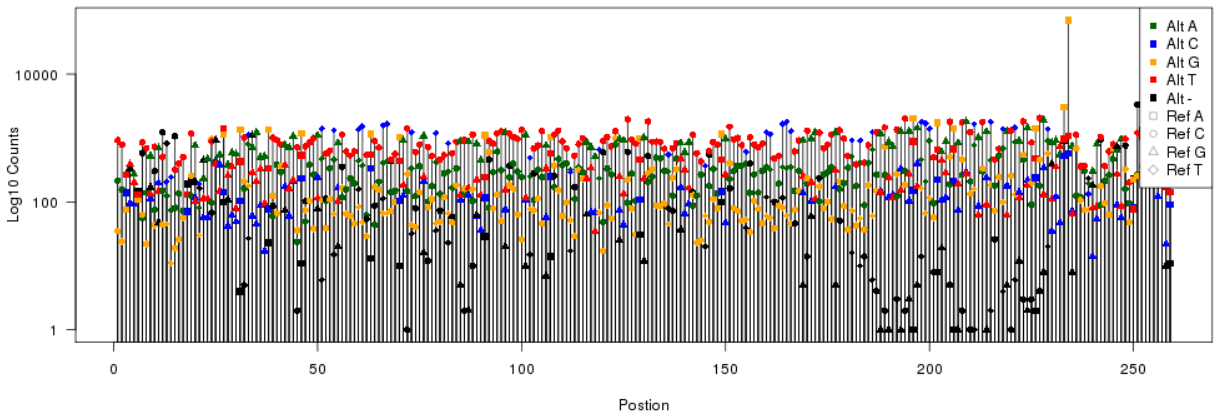
TERT (259 bp, SNVs 100.00%, 1bp-deletions 57.53%)
Log10 Counts
10000
100
1
0
50
100
150
200
250
Postion
Alt A
Alt C
Alt G
Alt T
Alt -
Ref A
Ref C
Ref G
Ref T

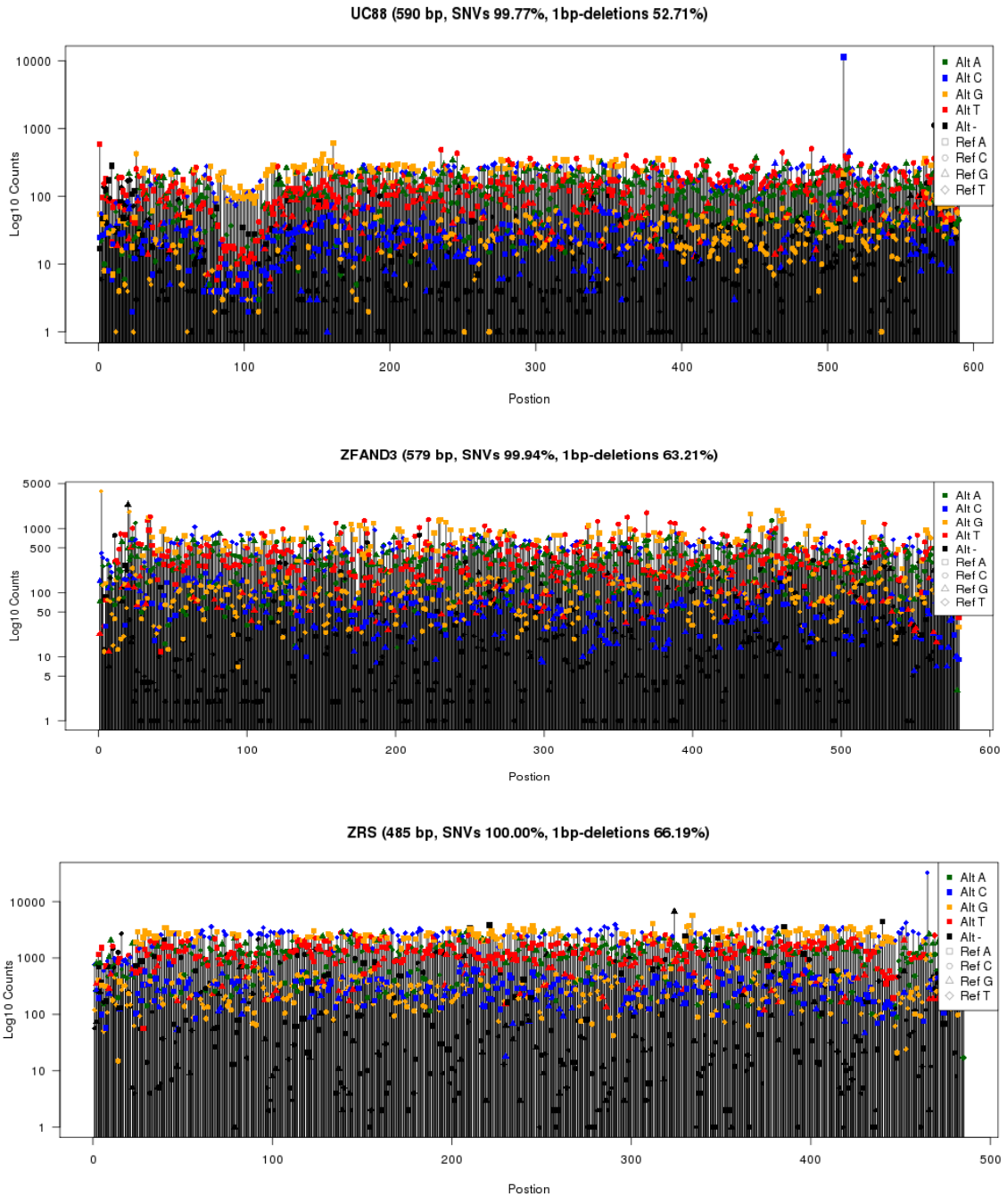

Tags assigned from saturation mutagenesis libraries. Plots for all 24 assignments described in Supplementary Table 3. Variant are sampled evenly across all the regions. The number of tags per variant follows previously characterized biases in error-prone PCR using Taq polymerase, with a preference of transitions over transversions and T-A preference among transversions. Insertions were rare, while short deletions occur at rates similar to those of the rare transversions. Shape denotes the reference and the color the alternative allele of the variant. The “-” in the legend stands for a 1 bp deletion.

Supplementary Figure 4

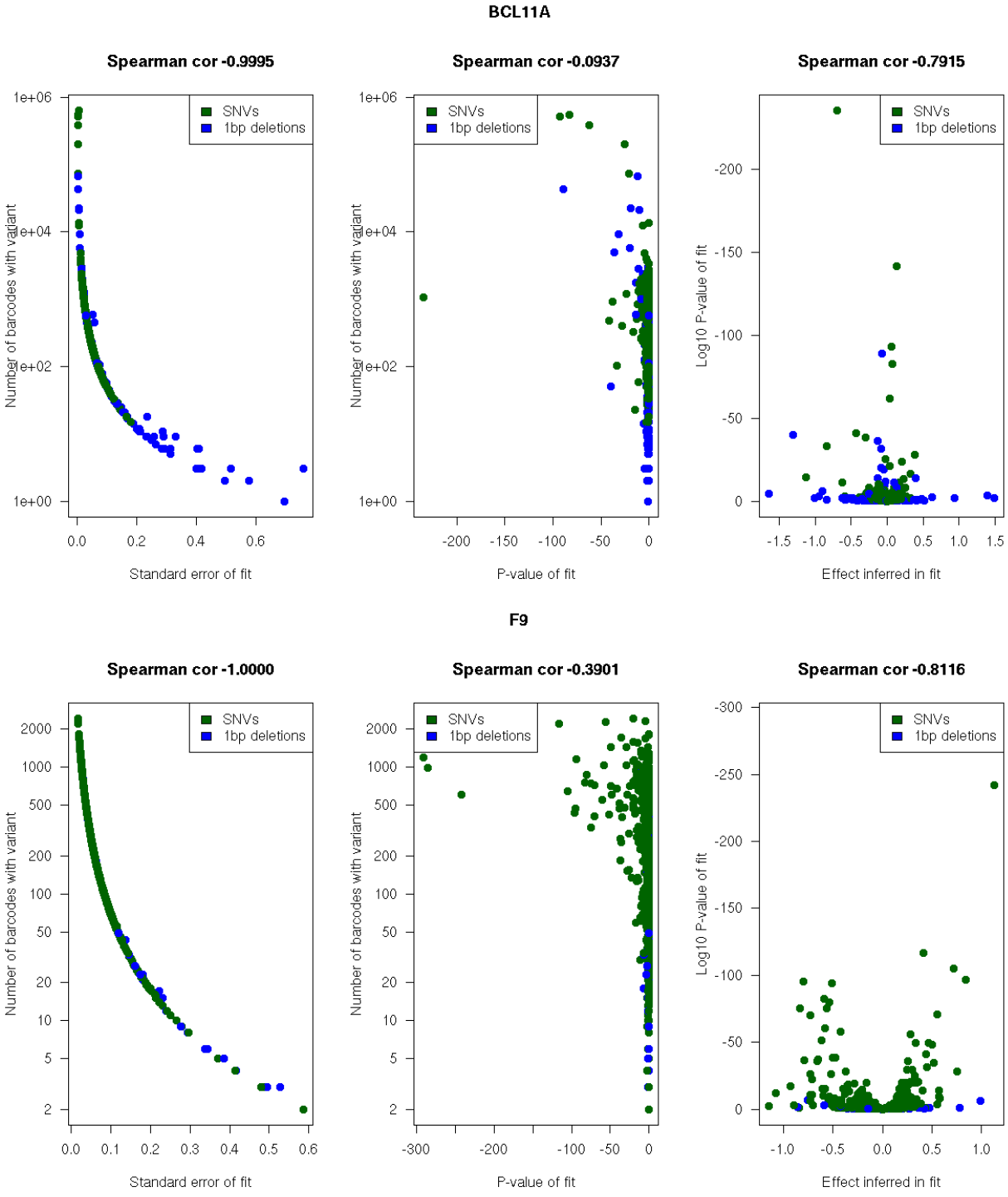

FOXE1

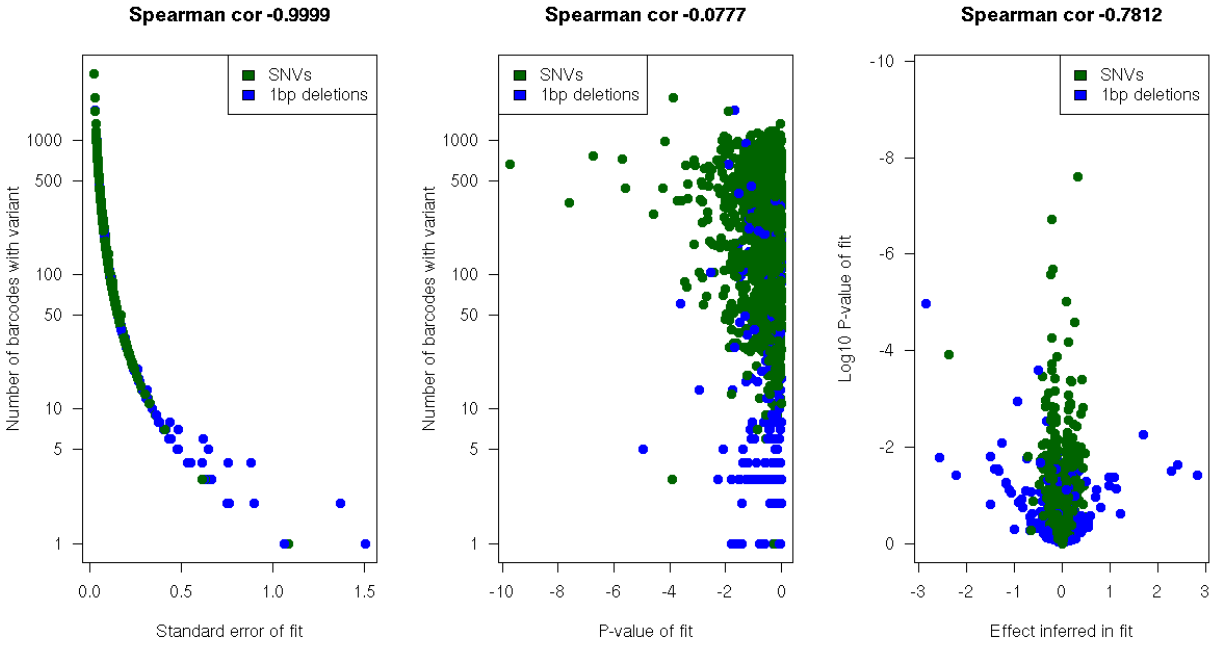
Spearman cor -0.9999
SNVs
1bp deletions
Number of barcodes with variant
Standard error of fit
Spearman cor -0.0777
P-value of fit
Spearman cor -0.7812
Log10 P-value of fit
Effect inferred in fit

GP1BB

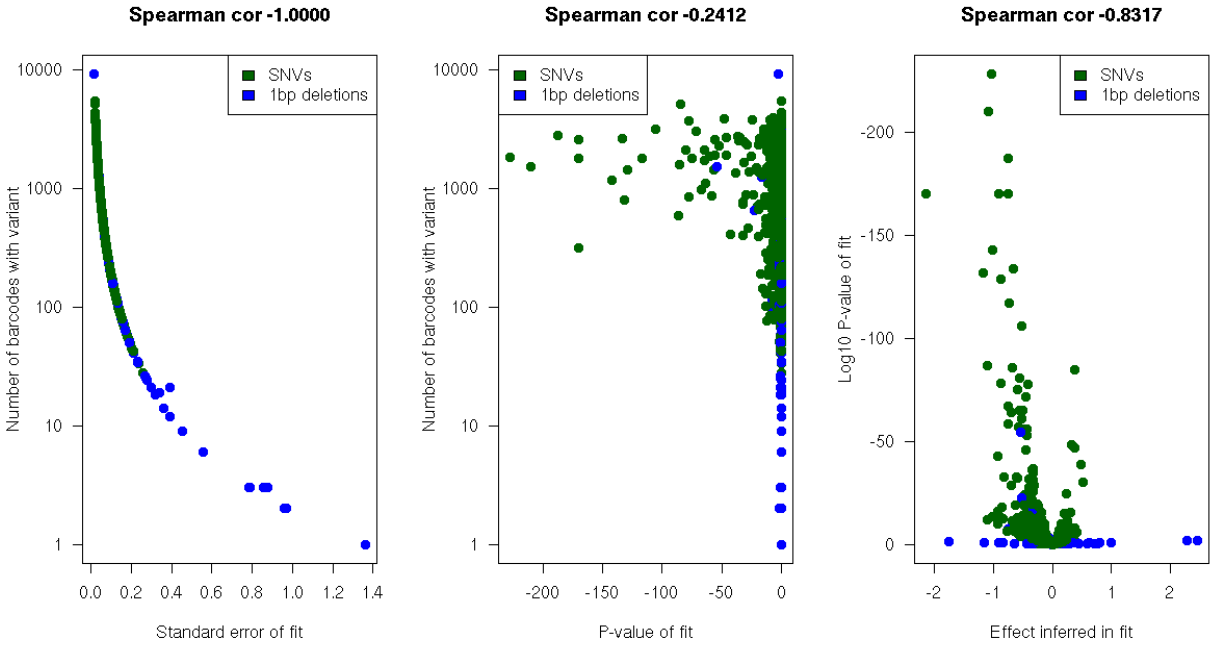
Spearman cor -1.0000
SNVs
1bp deletions
Number of barcodes with variant
Standard error of fit
Spearman cor -0.2412
P-value of fit
Spearman cor -0.8317
Log10 P-value of fit
Effect inferred in fit

HBB

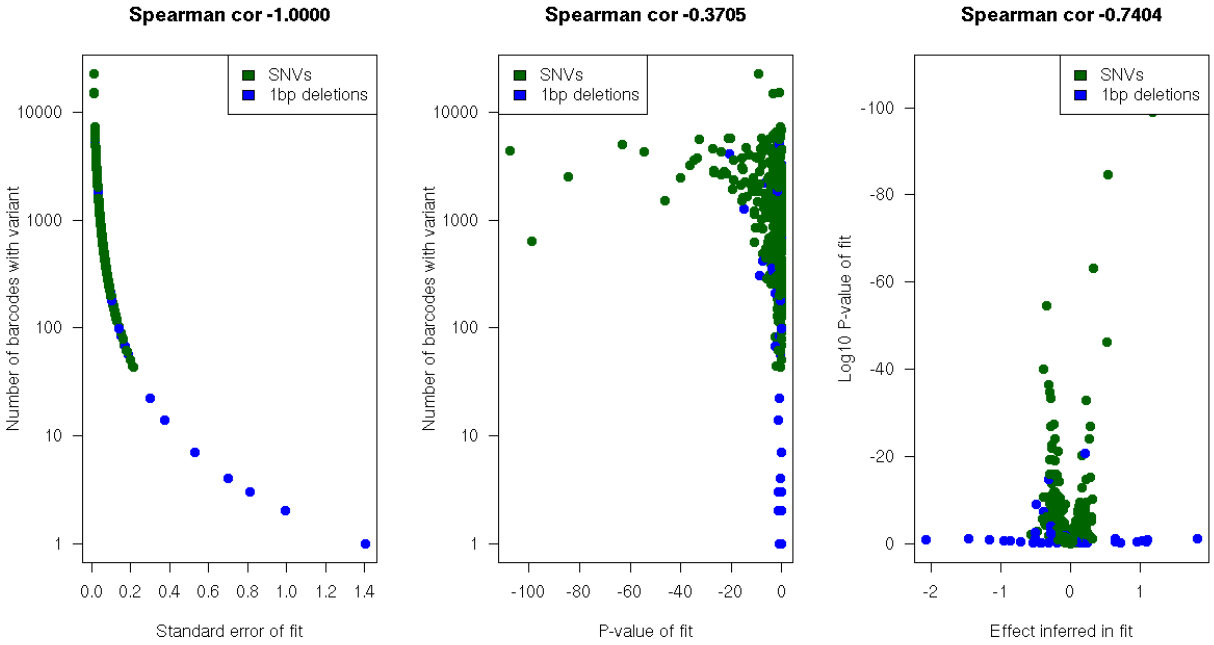
Spearman cor -1.0000
SNVs
1bp deletions
Number of barcodes with variant
Standard error of fit
Spearman cor -0.3705
P-value of fit
Spearman cor -0.7404
Log10 P-value of fit
Effect inferred in fit

HBG1

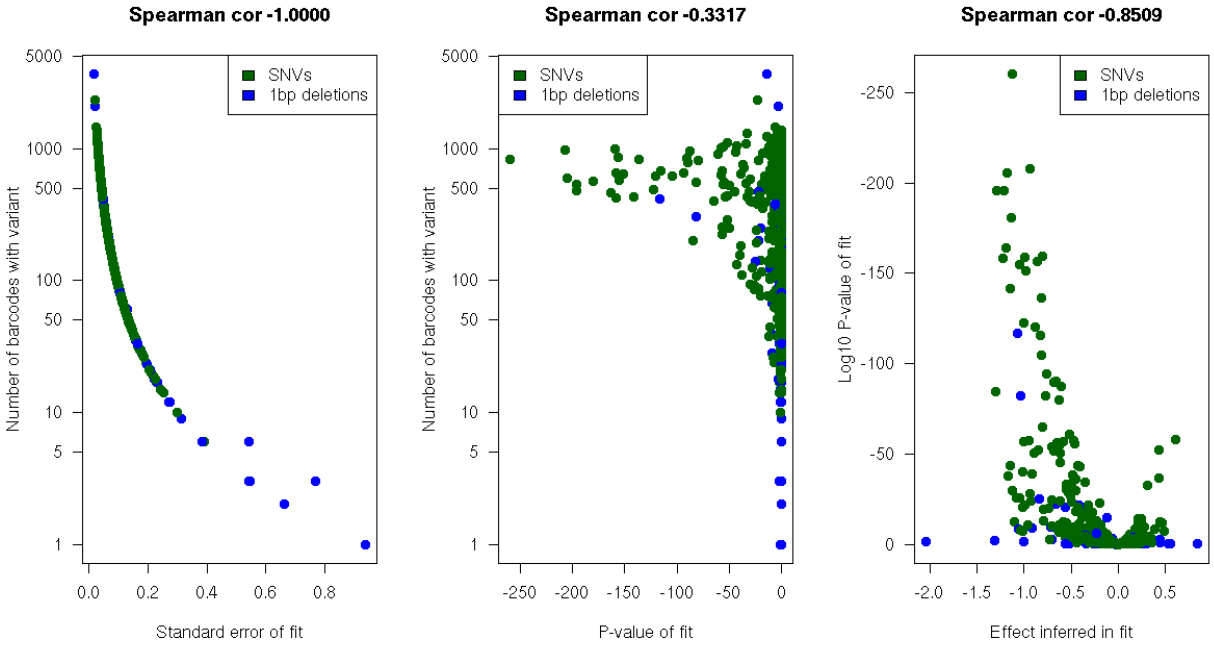
Spearman cor -1.0000
SNVs
1bp deletions
Number of barcodes with variant
Standard error of fit
Spearman cor -0.3317
P-value of fit
Spearman cor -0.8509
Log10 P-value of fit
Effect inferred in fit

HNF4A

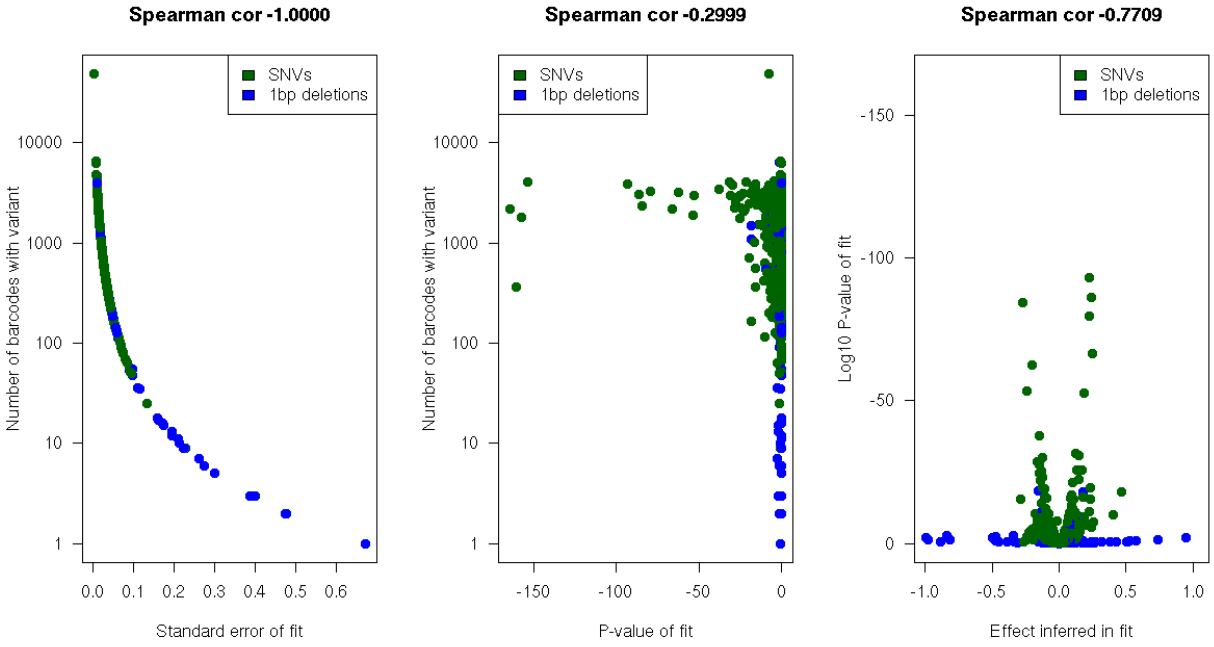
Spearman cor -1.0000
Spearman cor -0.2999
Spearman cor -0.7709
SNVs
1bp deletions
Number of barcodes with variant
Standard error of fit
P-value of fit
Log10 P-value of fit
Effect inferred in fit

IRF4

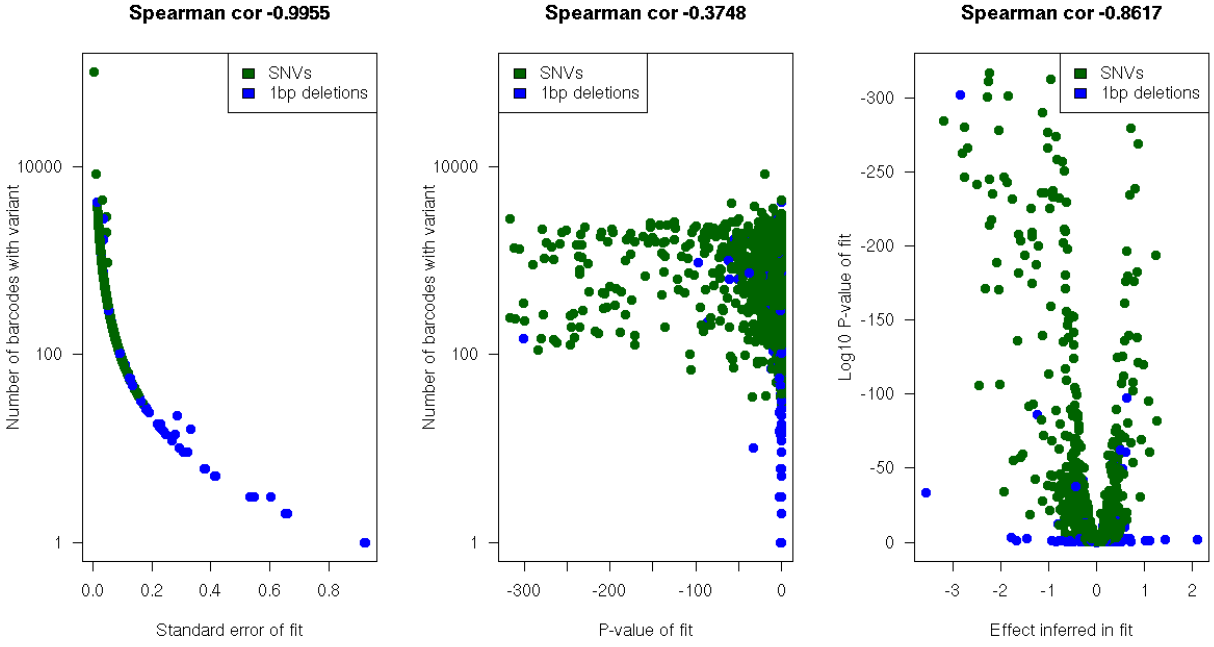
Spearman cor -0.9955
Spearman cor -0.3748
Spearman cor -0.8617
SNVs
1bp deletions
Number of barcodes with variant
Standard error of fit
P-value of fit
Log10 P-value of fit
Effect inferred in fit

IRF6

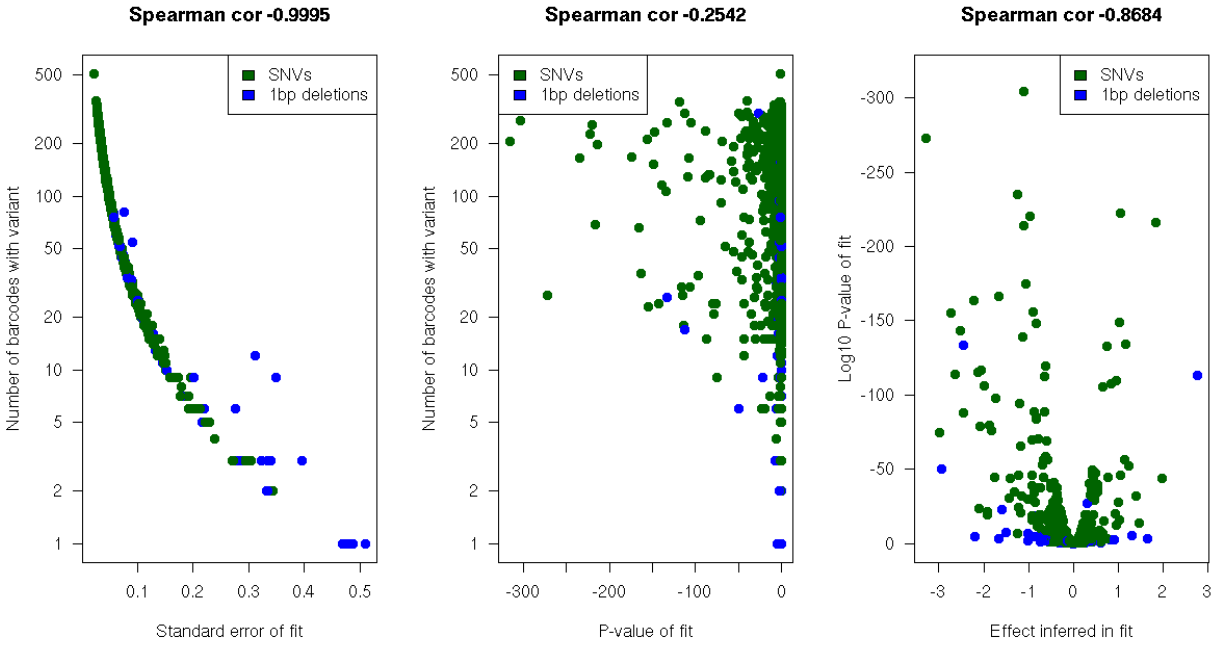
Spearman cor -0.9995
Spearman cor -0.2542
Spearman cor -0.8684
SNVs
1bp deletions
Number of barcodes with variant
Standard error of fit
P-value of fit
Log10 P-value of fit
Effect inferred in fit

LDLR.2

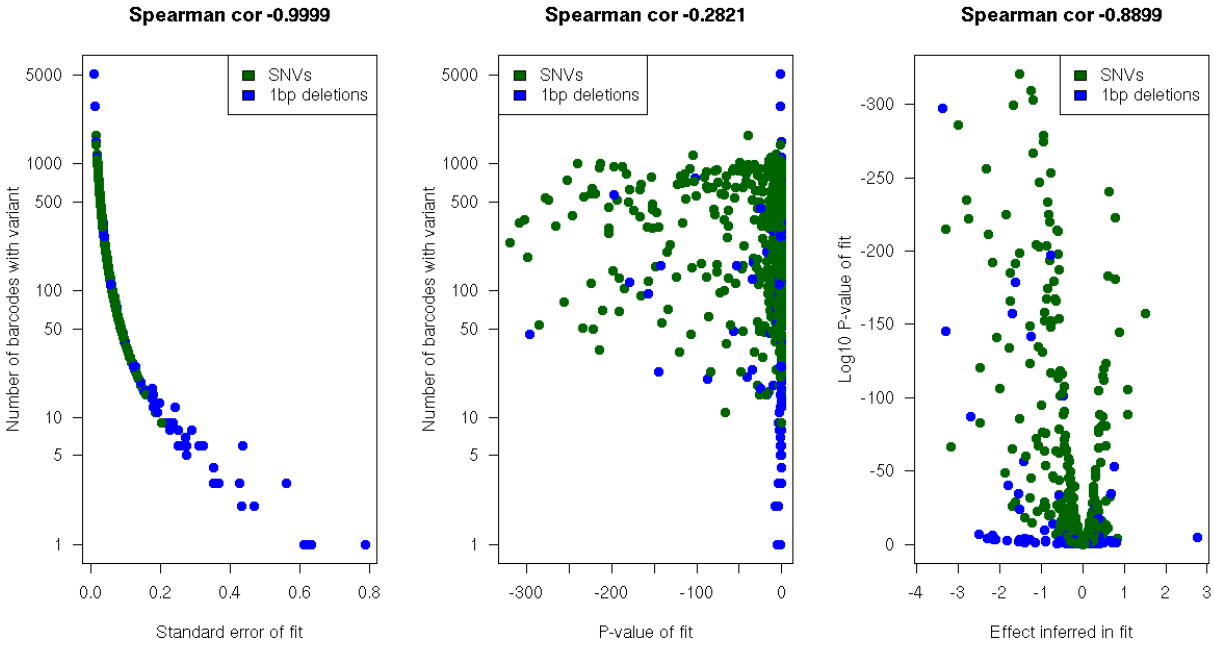
Spearman cor -0.9999
Spearman cor -0.2821
Spearman cor -0.8899
SNVs
1bp deletions
Number of barcodes with variant
Standard error of fit
P-value of fit
Log10 P-value of fit
Effect inferred in fit

LDLR

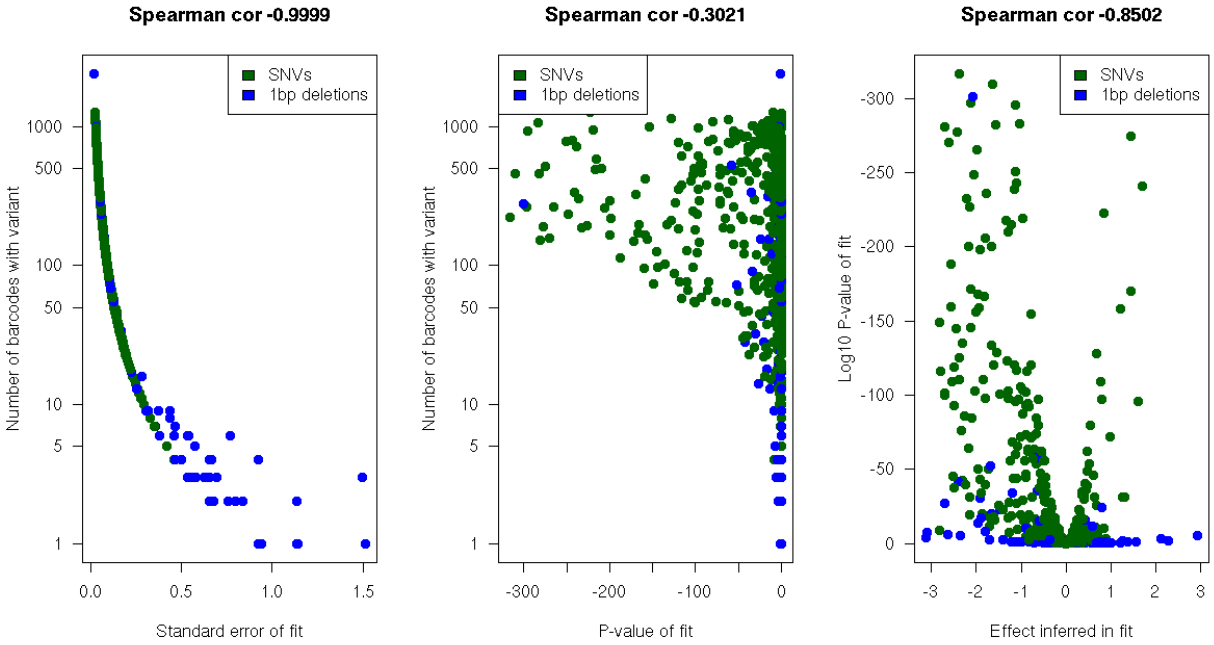
Spearman cor -0.9999
Spearman cor -0.3021
Spearman cor -0.8502
SNVs
1bp deletions
Number of barcodes with variant
Standard error of fit
P-value of fit
Log10 P-value of fit
Effect inferred in fit

MSMB

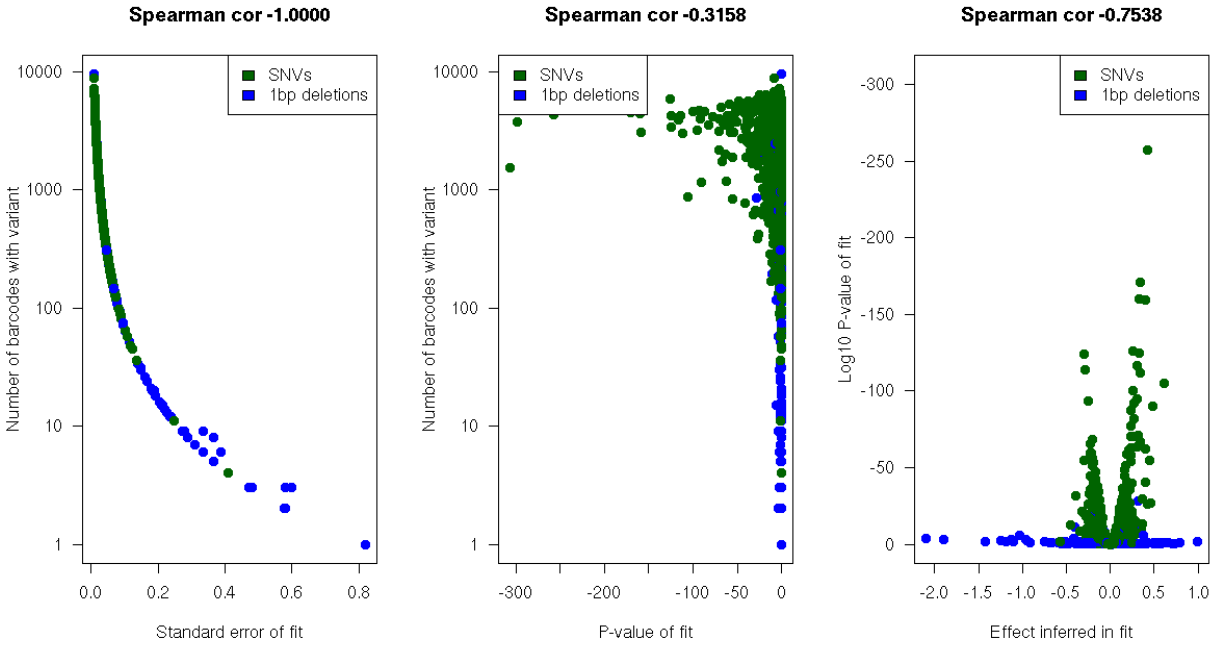
Spearman cor -1.0000
Spearman cor -0.3158
Spearman cor -0.7538
SNVs
1bp deletions
Number of barcodes with variant
Standard error of fit
P-value of fit
Log10 P-value of fit
Effect inferred in fit

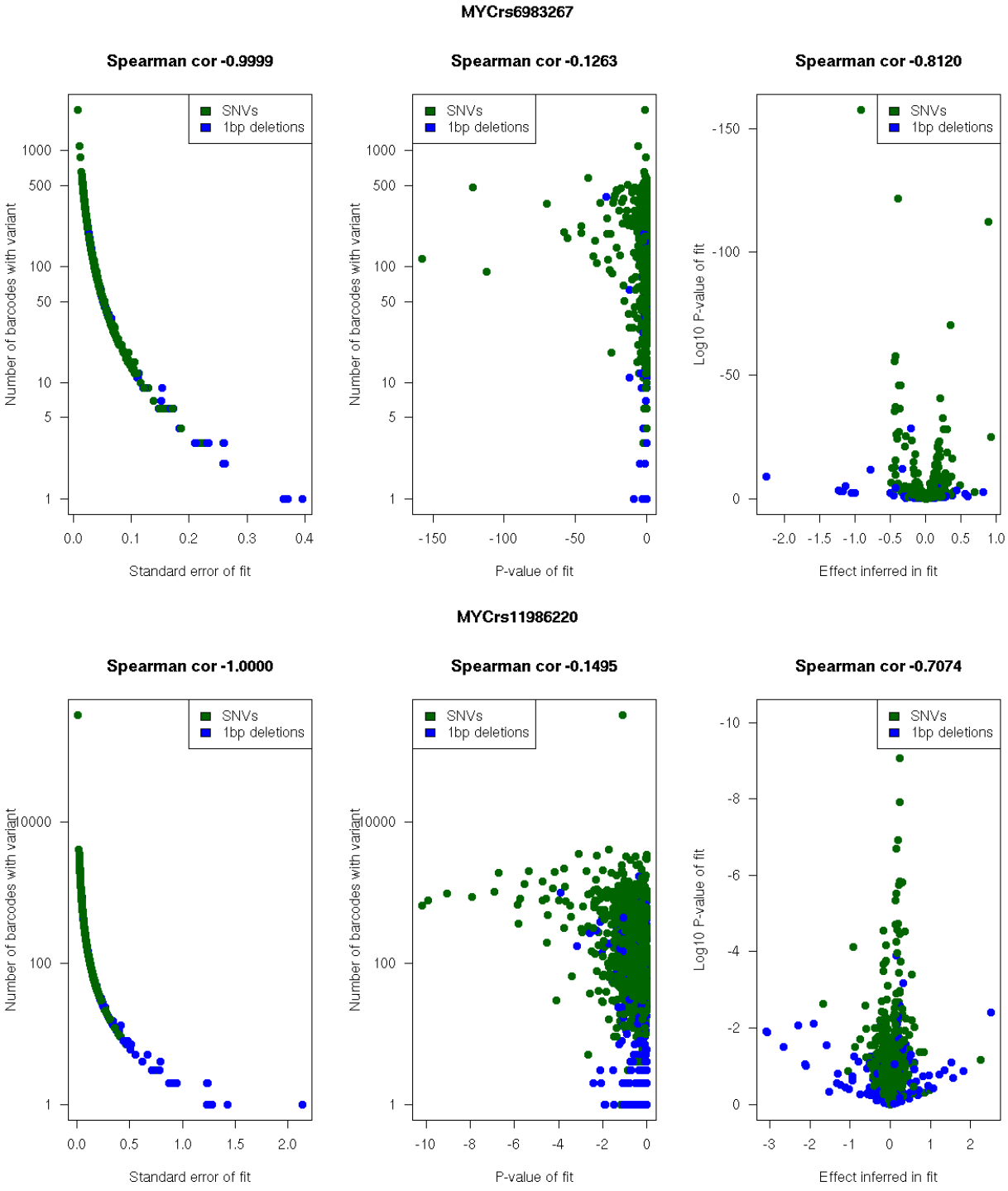
MYCrs6983267
Spearman cor -0.9999
Spearman cor -0.1263
Spearman cor -0.8120
SNVs
1bp deletions
Number of barcodes with variant
Standard error of fit
P-value of fit
Log10 P-value of fit
Effect inferred in fit
MYCrs11986220
Spearman cor -1.0000
Spearman cor -0.1495
Spearman cor -0.7074

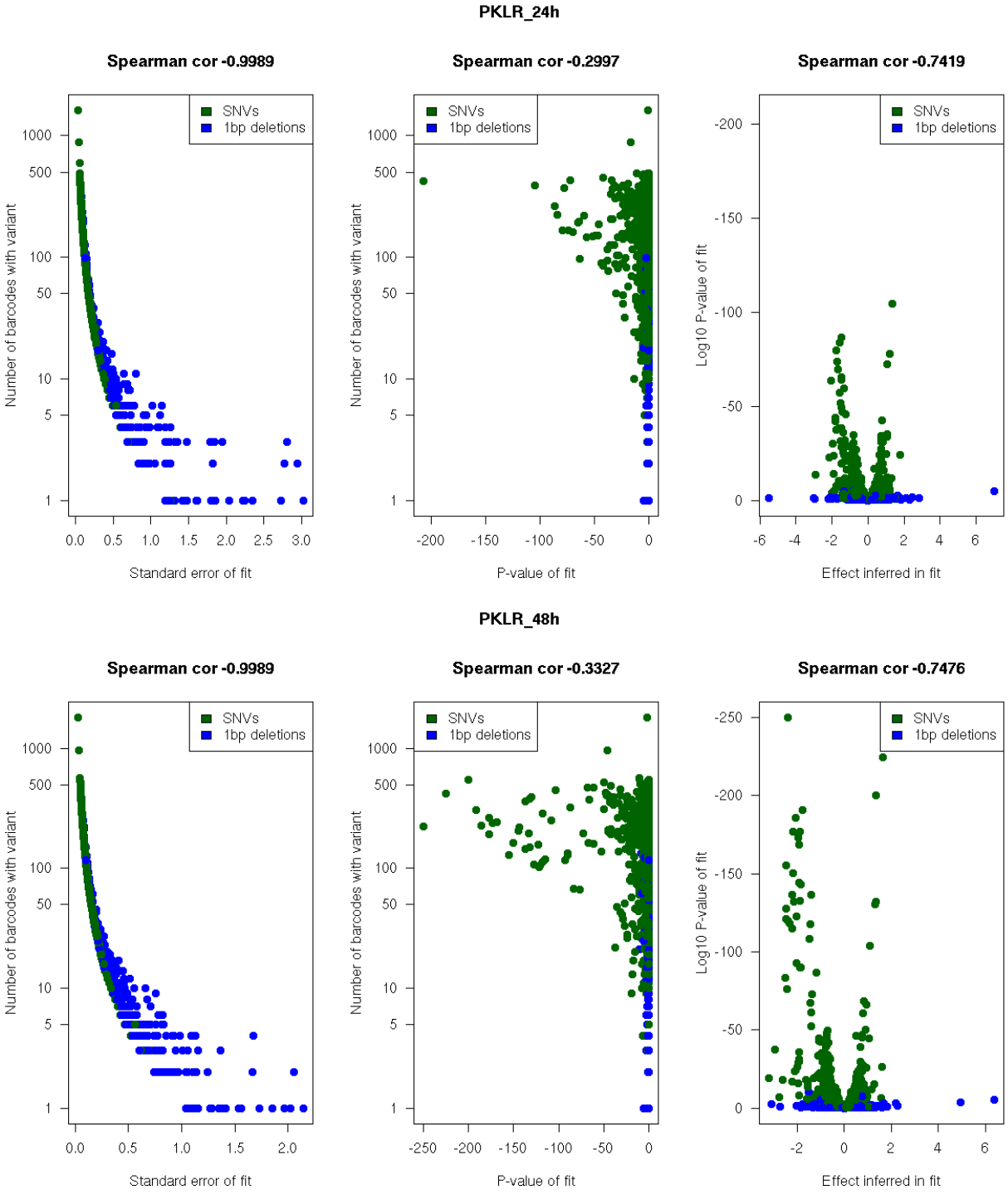
PKLR_24h
Spearman cor -0.9989
Spearman cor -0.2997
Spearman cor -0.7419
SNVs
1bp deletions
Number of barcodes with variant
Standard error of fit
P-value of fit
Log10 P-value of fit
Effect inferred in fit
PKLR_48h
Spearman cor -0.9989
Spearman cor -0.3327
Spearman cor -0.7476

RET

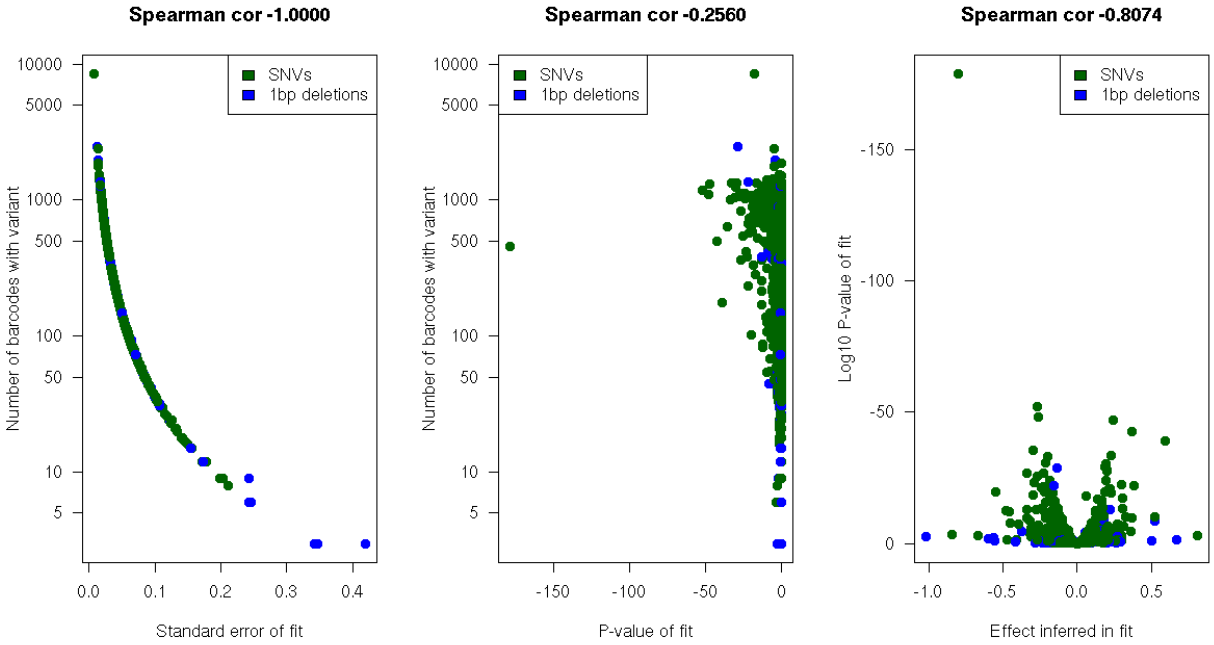
Spearman cor -1.0000
Spearman cor -0.2560
Spearman cor -0.8074
SNVs
1bp deletions
Number of barcodes with variant
Standard error of fit
P-value of fit
Log10 P-value of fit
Effect inferred in fit

SORT1.2

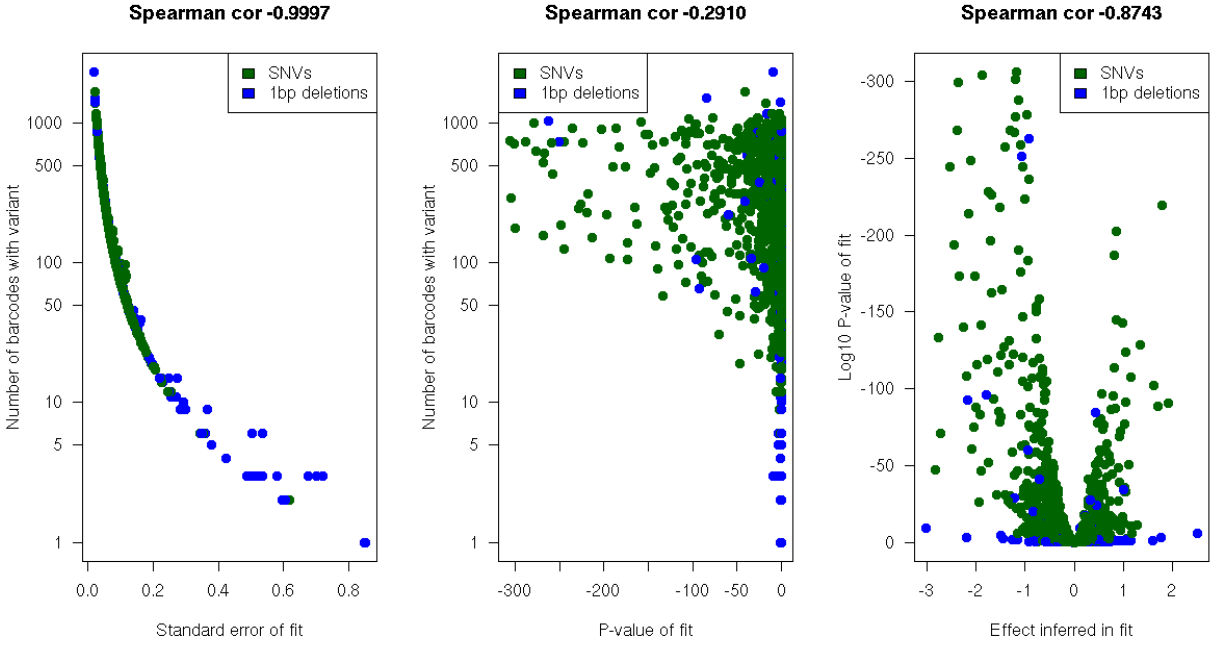
Spearman cor -0.9997
Spearman cor -0.2910
Spearman cor -0.8743
SNVs
1bp deletions
Number of barcodes with variant
Standard error of fit
P-value of fit
Log10 P-value of fit
Effect inferred in fit

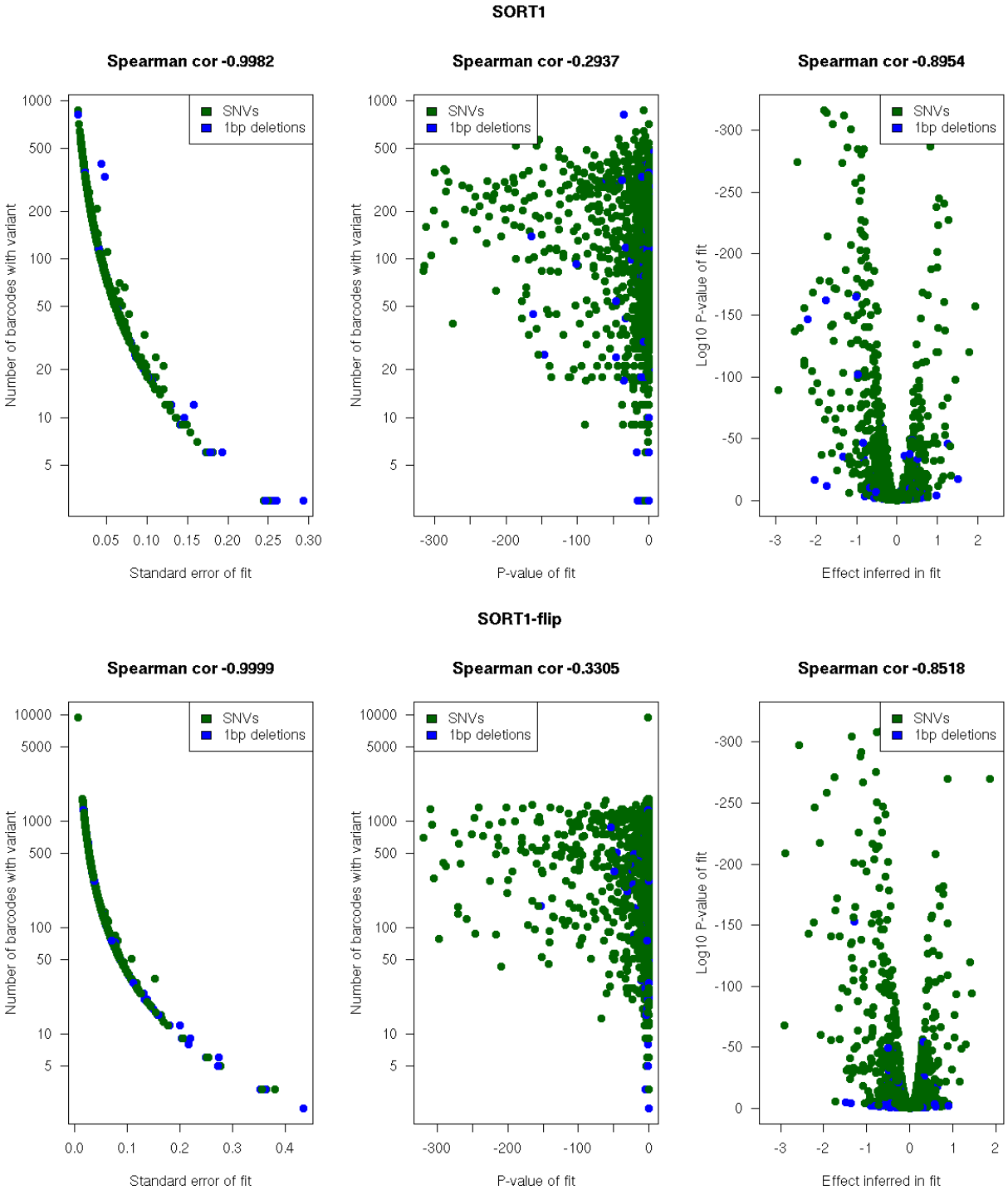
SORT1
Spearman cor -0.9982
Spearman cor -0.2937
Spearman cor -0.8954
SNVs
1bp deletions
Number of barcodes with variant
Standard error of fit
P-value of fit
Log10 P-value of fit
Effect inferred in fit
SORT1-flip
Spearman cor -0.9999
Spearman cor -0.3305
Spearman cor -0.8518

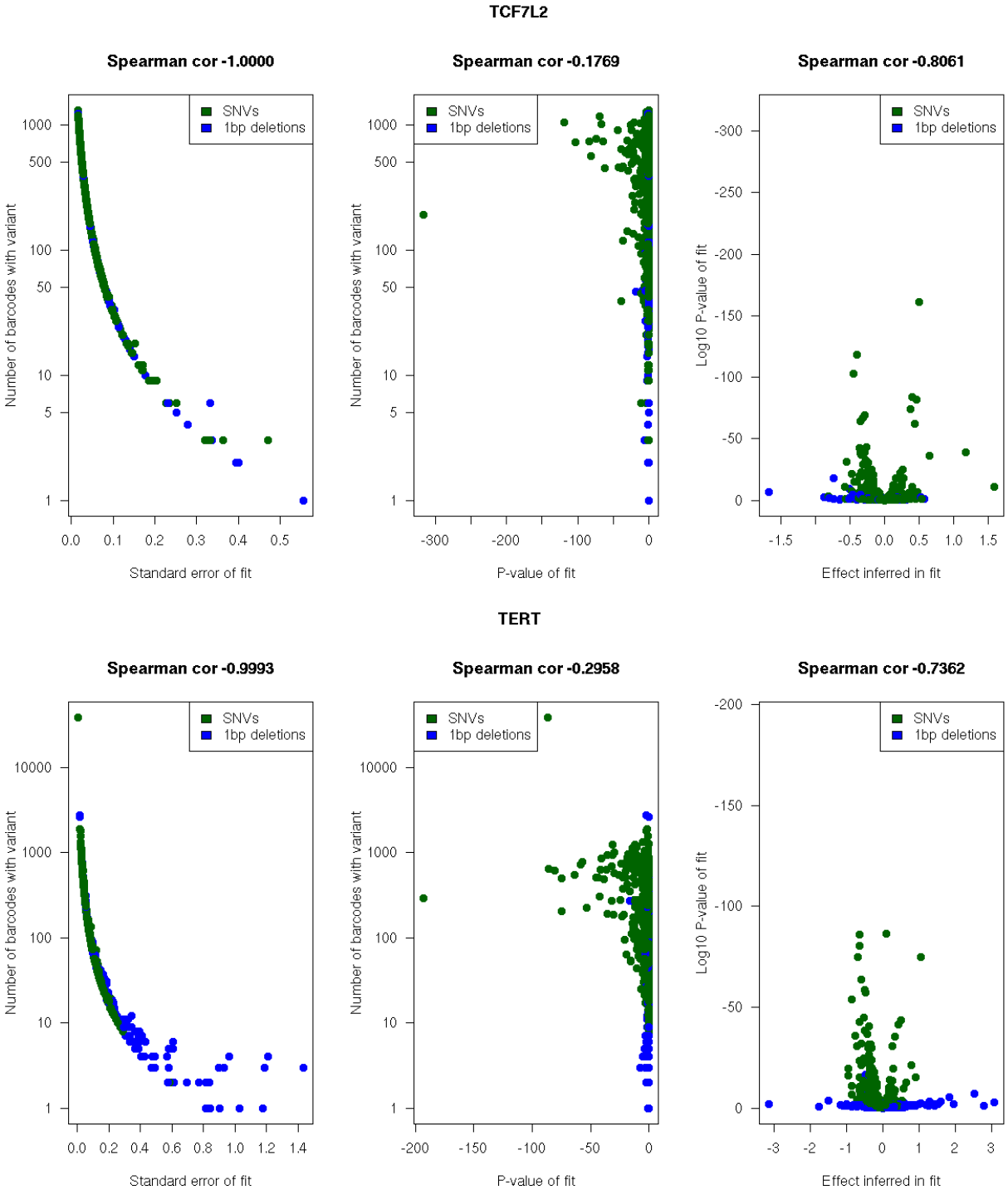
TCF7L2
Spearman cor -1.0000
Spearman cor -0.1769
Spearman cor -0.8061
SNVs
1bp deletions
Number of barcodes with variant
Standard error of fit
P-value of fit
Log10 P-value of fit
Effect inferred in fit
TERT
Spearman cor -0.9993
Spearman cor -0.2958
Spearman cor -0.7362

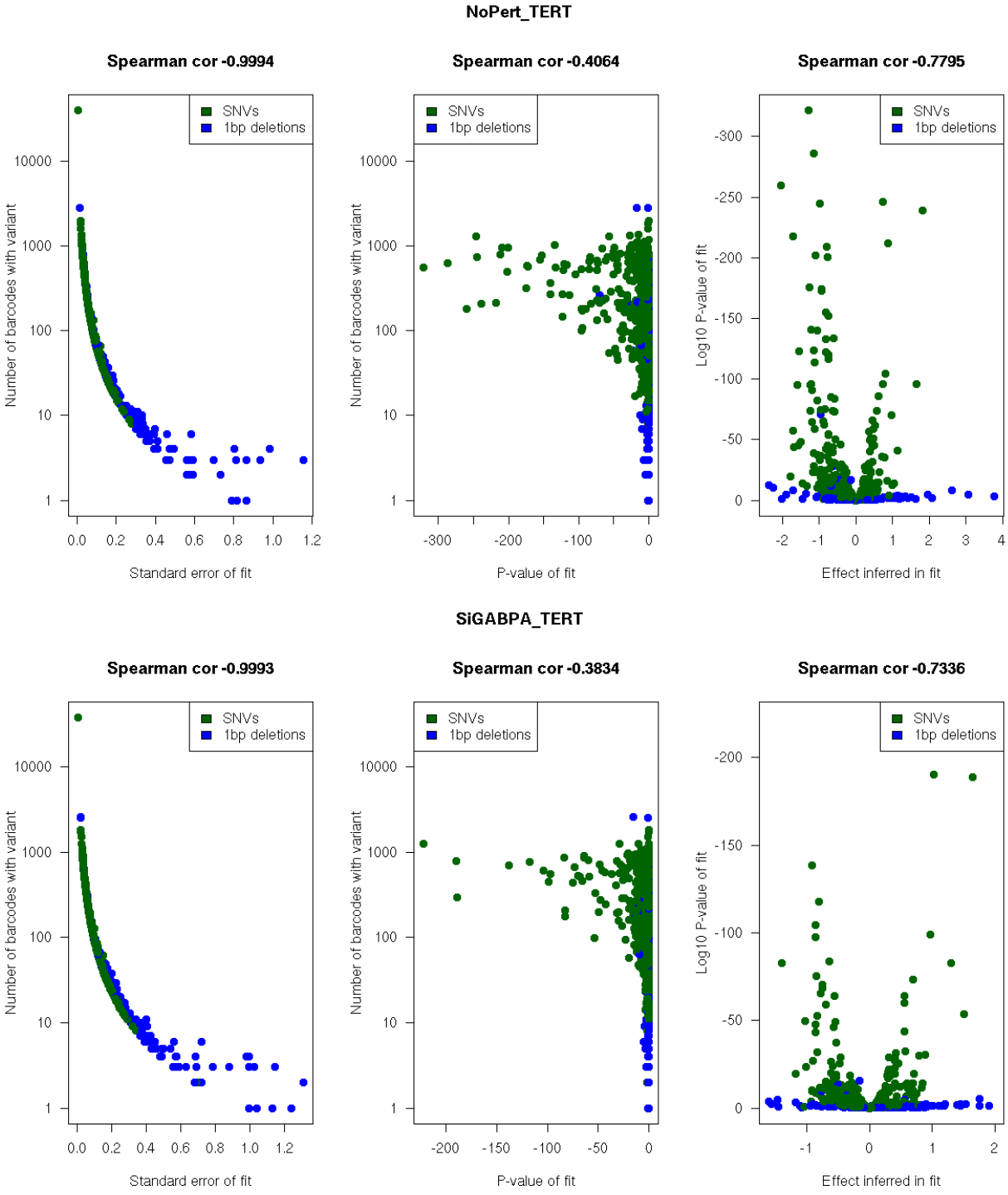
NoPert_TERT
Spearman cor -0.9994
Spearman cor -0.4064
Spearman cor -0.7795
SNVs
1bp deletions
Number of barcodes with variant
Standard error of fit
P-value of fit
Log10 P-value of fit
Effect inferred in fit
SiGABPA_TERT
Spearman cor -0.9993
Spearman cor -0.3834
Spearman cor -0.7336

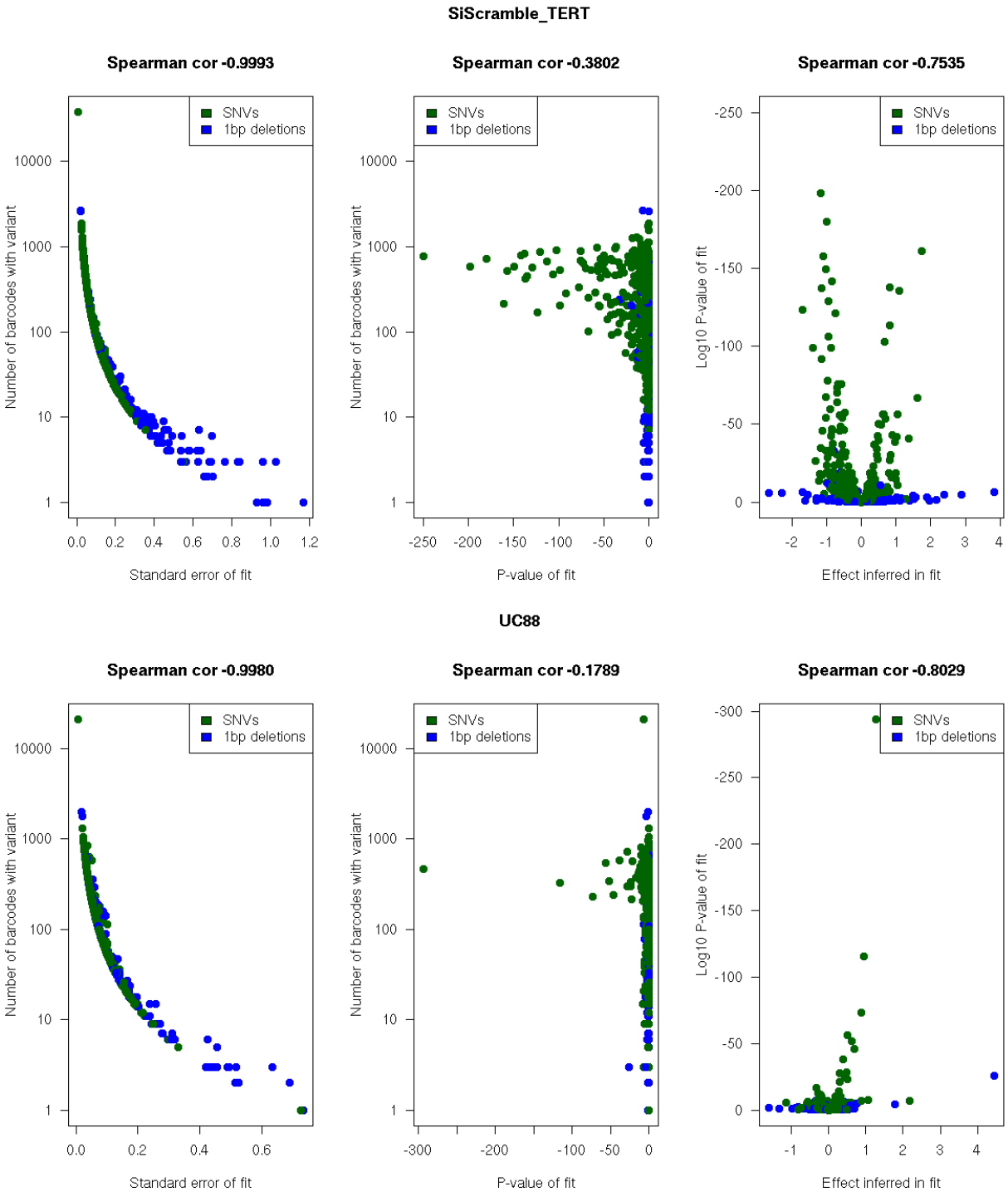
SiScramble_TERT
Spearman cor -0.9993
Spearman cor -0.3802
Spearman cor -0.7535
SNVs
1bp deletions
Number of barcodes with variant
Standard error of fit
P-value of fit
Log10 P-value of fit
Effect inferred in fit
UC88
Spearman cor -0.9980
Spearman cor -0.1789
Spearman cor -0.8029

ZFAND3

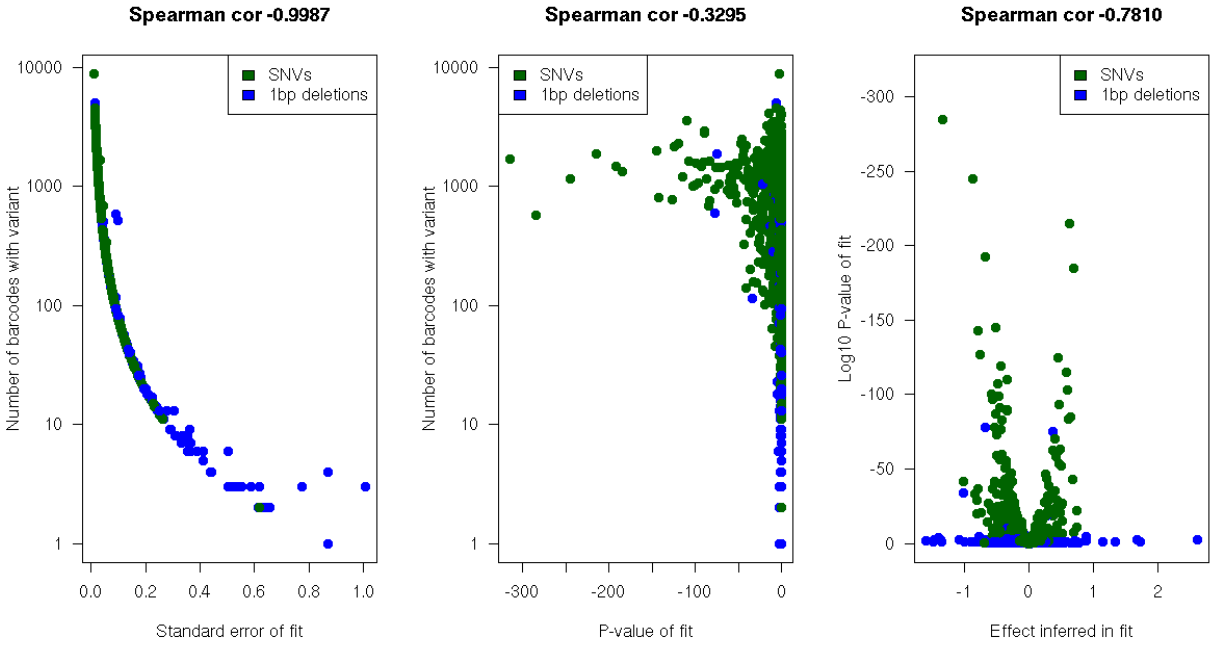

ZRSh13

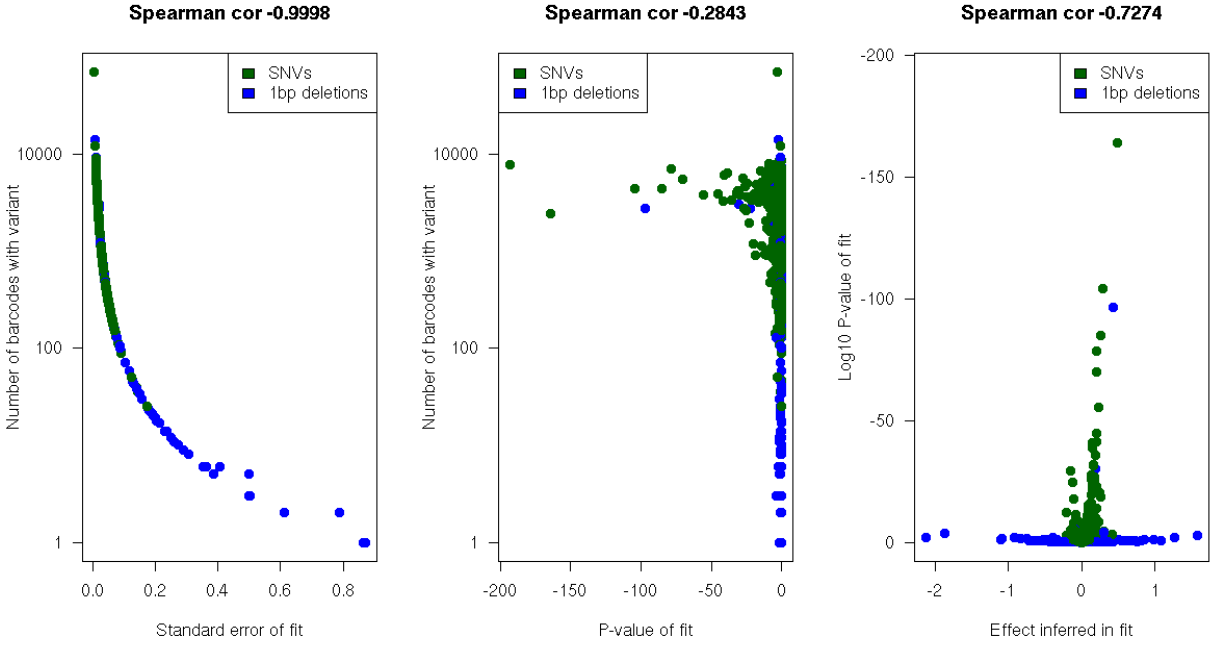

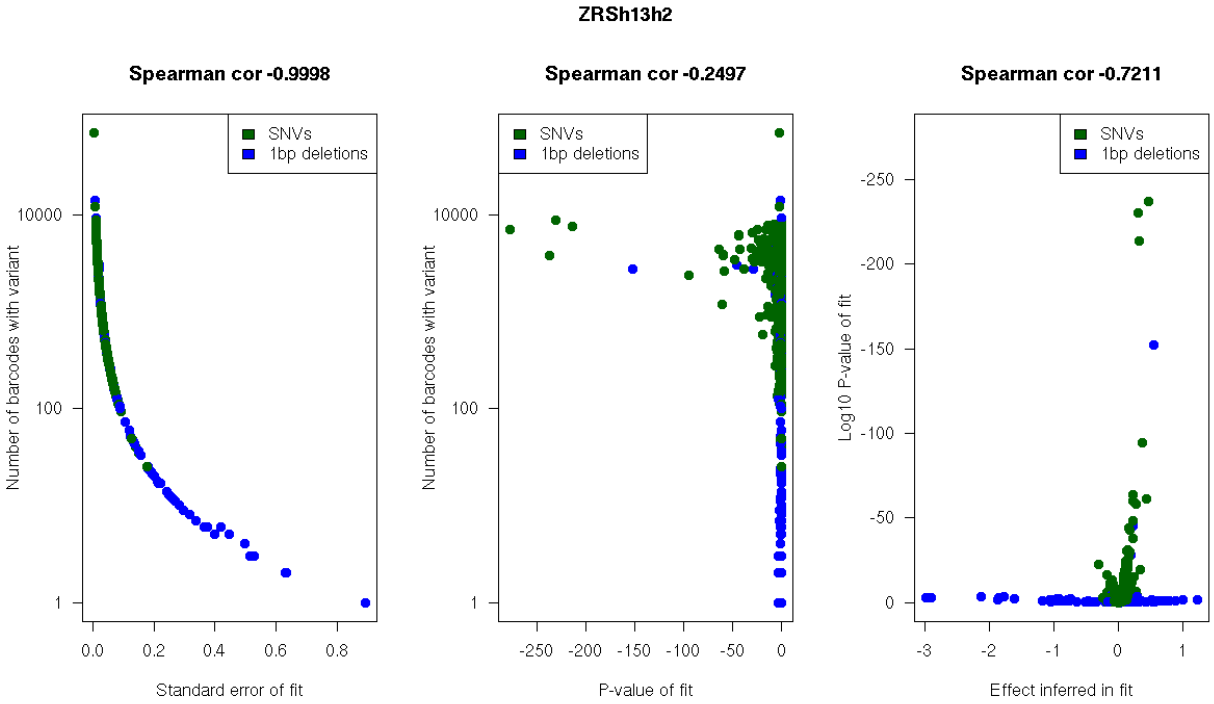

Quality of fit measures for variant effects determined by 29 linear regression models. For the 29 experiments (combining three technical replicates each), the left panel shows the standard error of the variant effect fit versus the number of tags/barcodes per variant, the middle panel shows the p-value (log_{10} transformed) from the fit variant effects versus the number tag/barcodes per variant and the right panel shows a volcano plot (inferred variant effect vs. the log_{10} transformed p-value).

Supplementary Figure 5

A

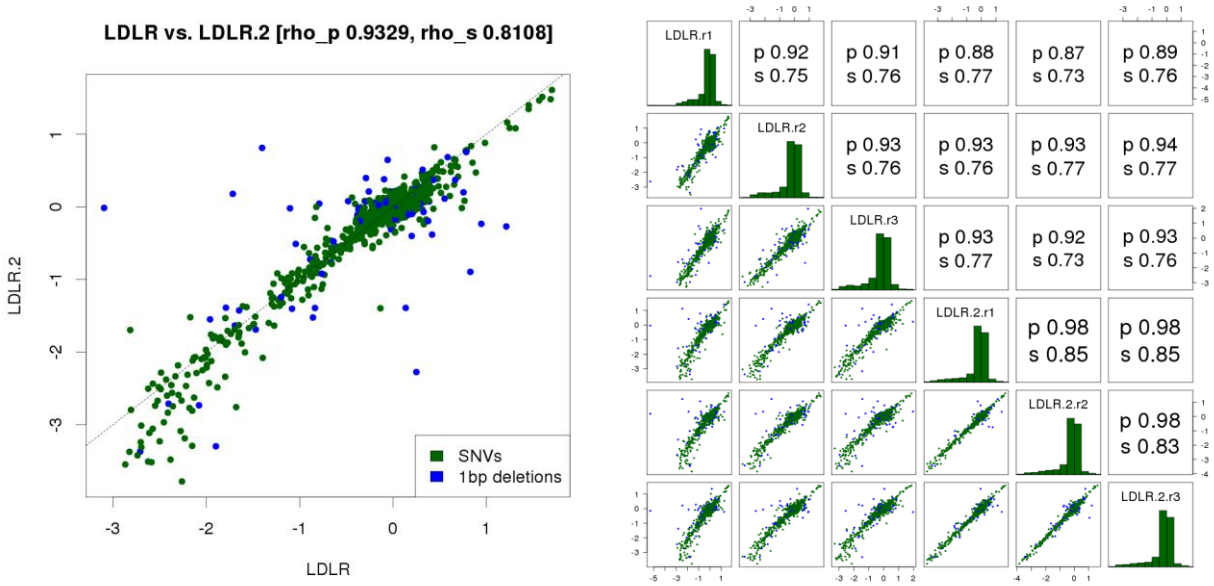

B

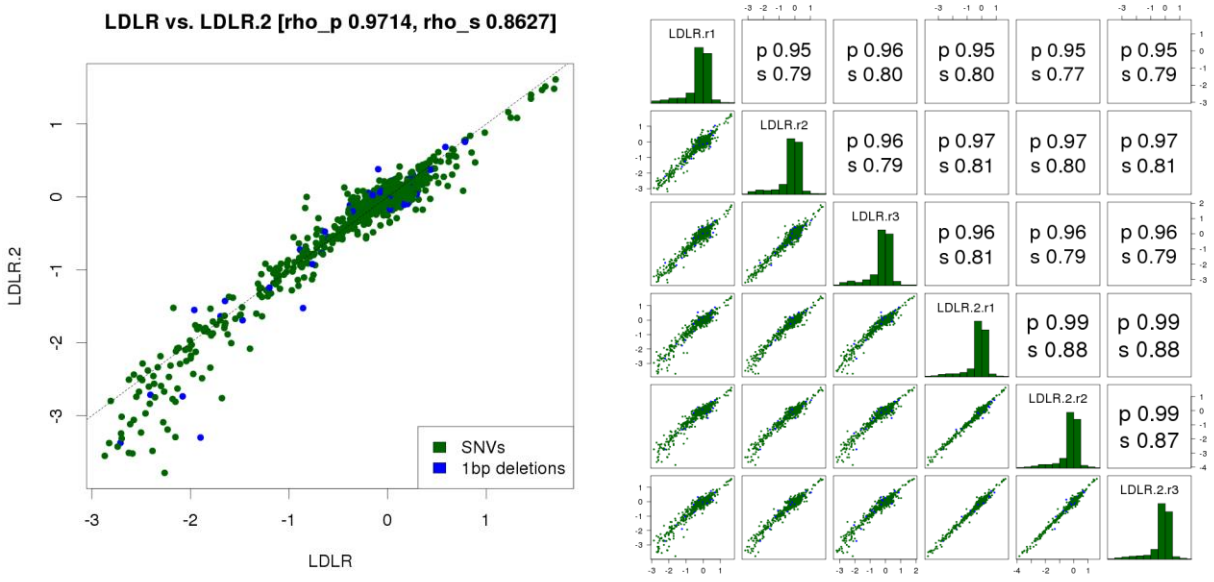

Biological replicate correlation for LDLR. Transfection and biological replicate correlation in LDLR experiments, before **(A)** and after **(B)** filtering for a minimum of 10 tags per variant.

Supplementary Figure 6

A

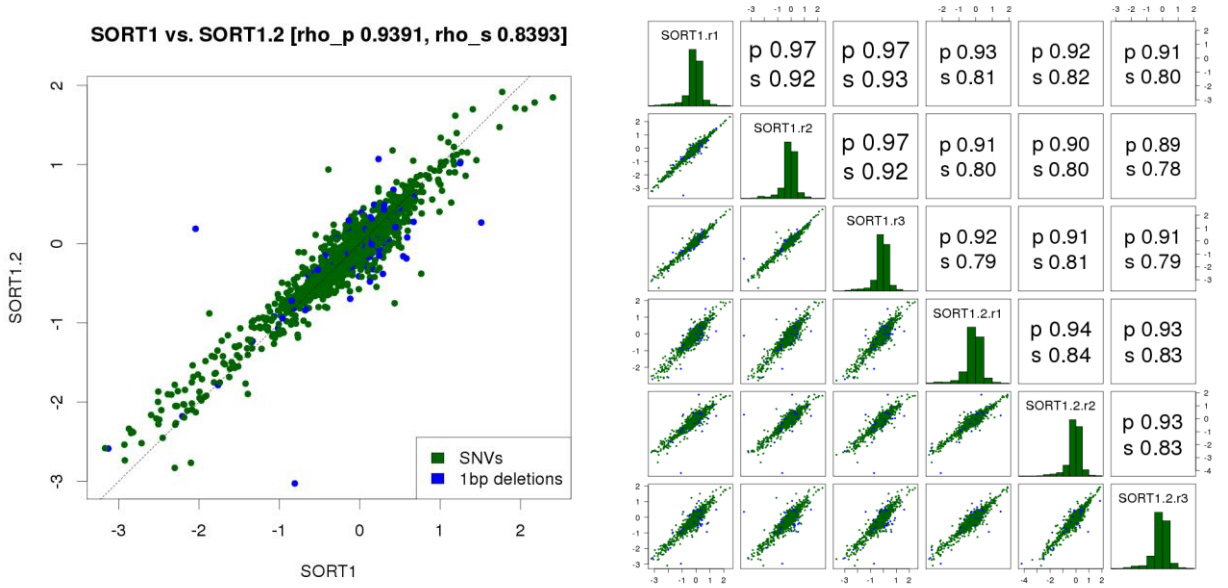

B

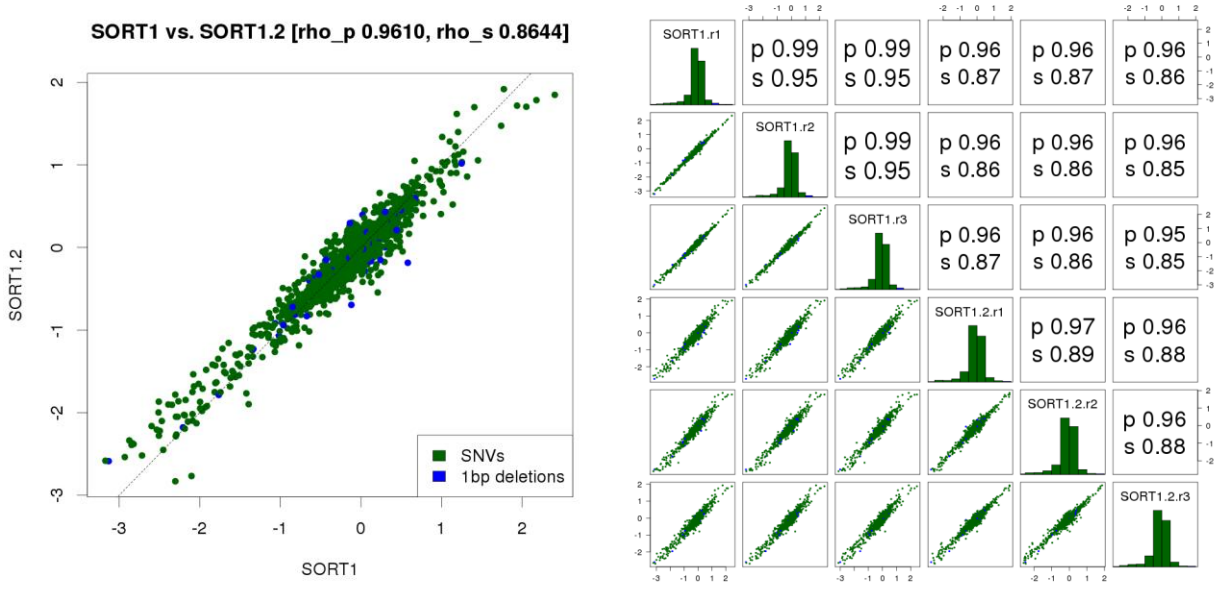

Biological replicate correlation for SORT1. Transfection and biological replicate correlation in SORT experiments, before **(A)** and after **(B)** filtering for a minimum of 10 tags per variant.

Supplementary Figure 7

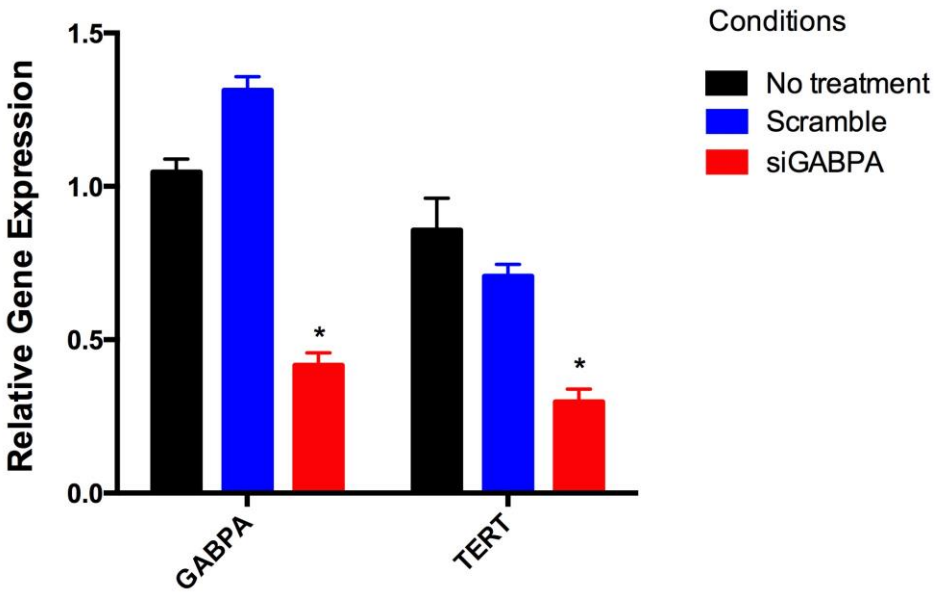

Quantitative RT-PCR validation results of TERT-GBM short-interfering RNA experiments. To measure siRNA knockdown efficiency, qPCR was performed using the Ambion Power SYBR Green Cells-to-Ct kit to measure mRNA abundance of *GABPA* and *TERT* with primer sequences previously used (see Methods). Relative expression levels were calculated using the deltaCT method against the housekeeping gene *GUSB*.

Supplementary Figure 8

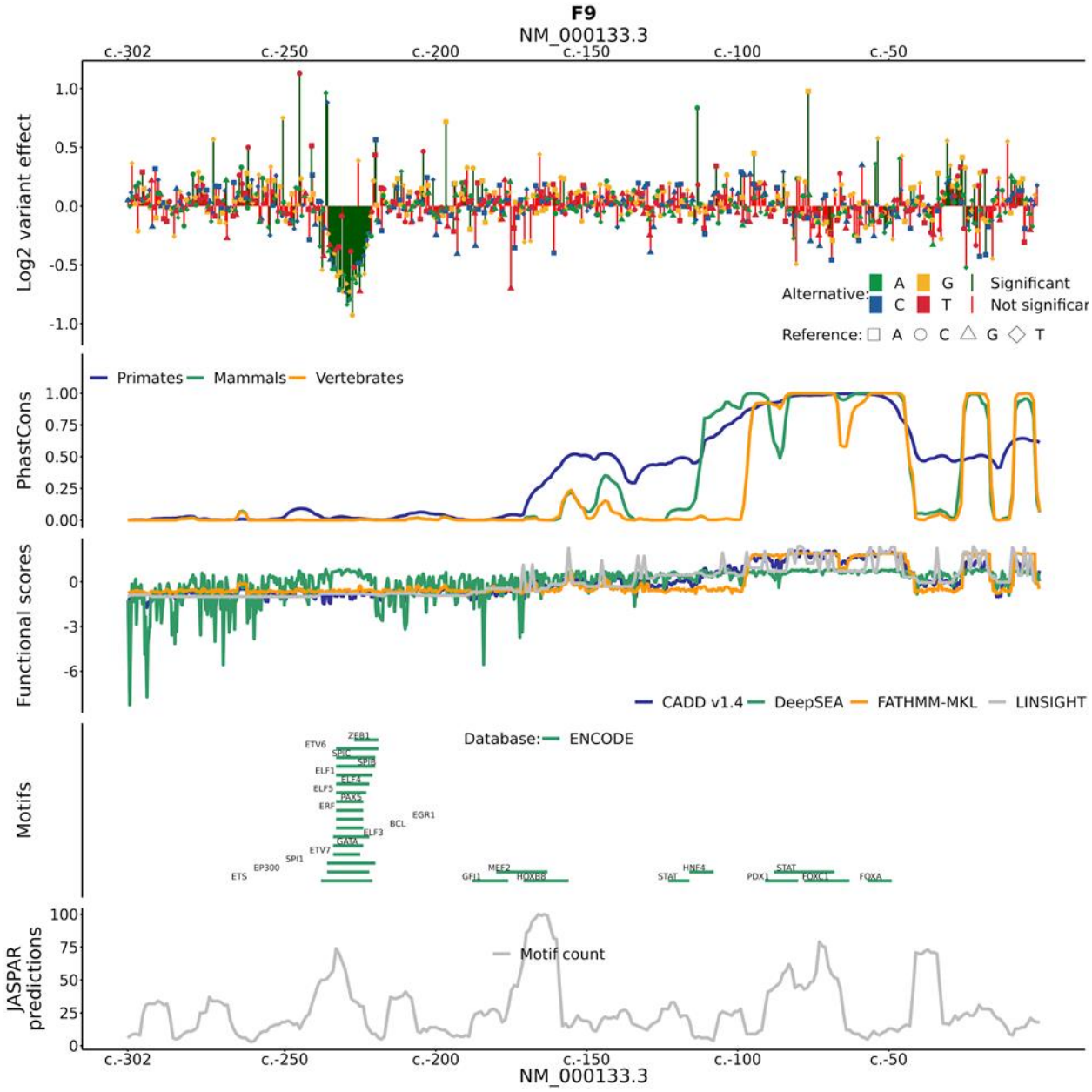

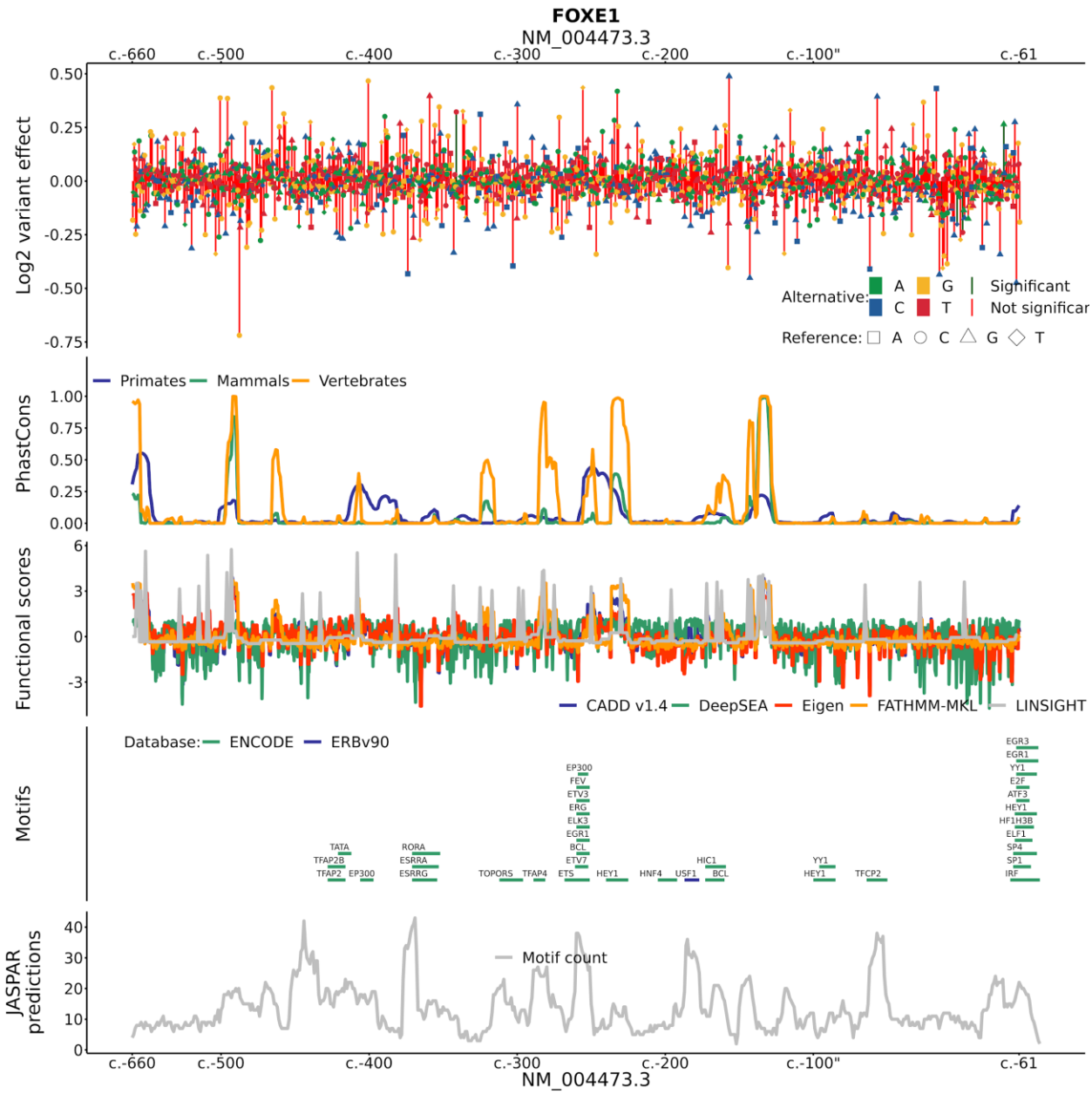
FOXE1
NM_004473.3
c.-660
c.-500
c.-400
c.-300
c.-200
c.-100"
c.-61
Log2 variant effect
0.50
0.25
0.00
-0.25
-0.50
-0.75
Alternative: A G Significant
C T Not significar
Reference: A C G T
PhastCons
Primates Mammals Vertebrates
1.00
0.75
0.50
0.25
0.00
Functional scores
6
3
0
-3
CADD v1.4 DeepSEA Eigen FATHMM-MKL LINSIGHT
Motifs
Database: ENCODE ERBv90
TATA
TFAP2B
TFAP2
EP300
RORA
ESRRA
ESRRG
TOPORS
TFAP4
EP300
FEV
ETV3
ERG
ELK3
EGR1
BCL
ETV7
ETS
HEY1
HNF4
USF1
HIC1
BCL
YY1
HEY1
TFCP2
EGR3
EGR1
YY1
E2F
ATF3
HEY1
HF1H3B
ELF1
SP4
SP1
IRF
JASPAR predictions
40
30
20
10
0
Motif count
c.-660
c.-500
c.-400
c.-300
c.-200
c.-100"
c.-61
NM_004473.3

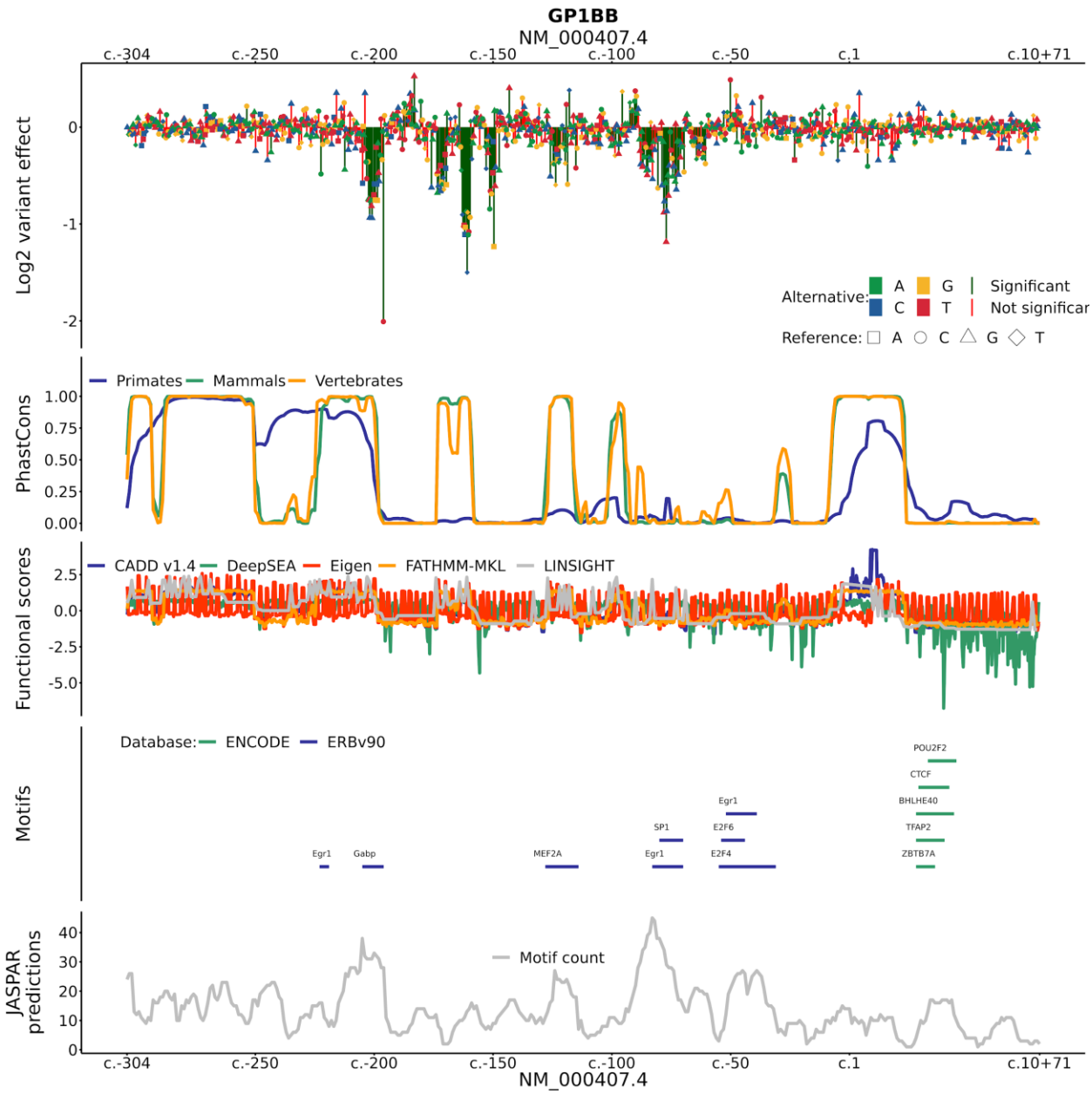
GP1BB
NM_000407.4
c.-304
c.-250
c.-200
c.-150
c.-100
c.-50
c.1
c.10+71
Log2 variant effect
0
-1
-2
Alternative:
A
C
G
T
Significant
Not significar
Reference: A C G T
PhastCons
Primates
Mammals
Vertebrates
1.00
0.75
0.50
0.25
0.00
Functional scores
CADD v1.4
DeepSEA
Eigen
FATHMM-MKL
LINSIGHT
2.5
0.0
-2.5
-5.0
Motifs
Database: ENCODE ERBv90
POU2F2
CTCF
BHLHE40
TFAP2
ZBTB7A
Egr1
SP1
E2F6
Egr1
Gabp
MEF2A
Egr1
E2F4
JASPAR predictions
Motif count
40
30
20
10
0
c.-304
c.-250
c.-200
c.-150
c.-100
c.-50
c.1
c.10+71
NM_000407.4

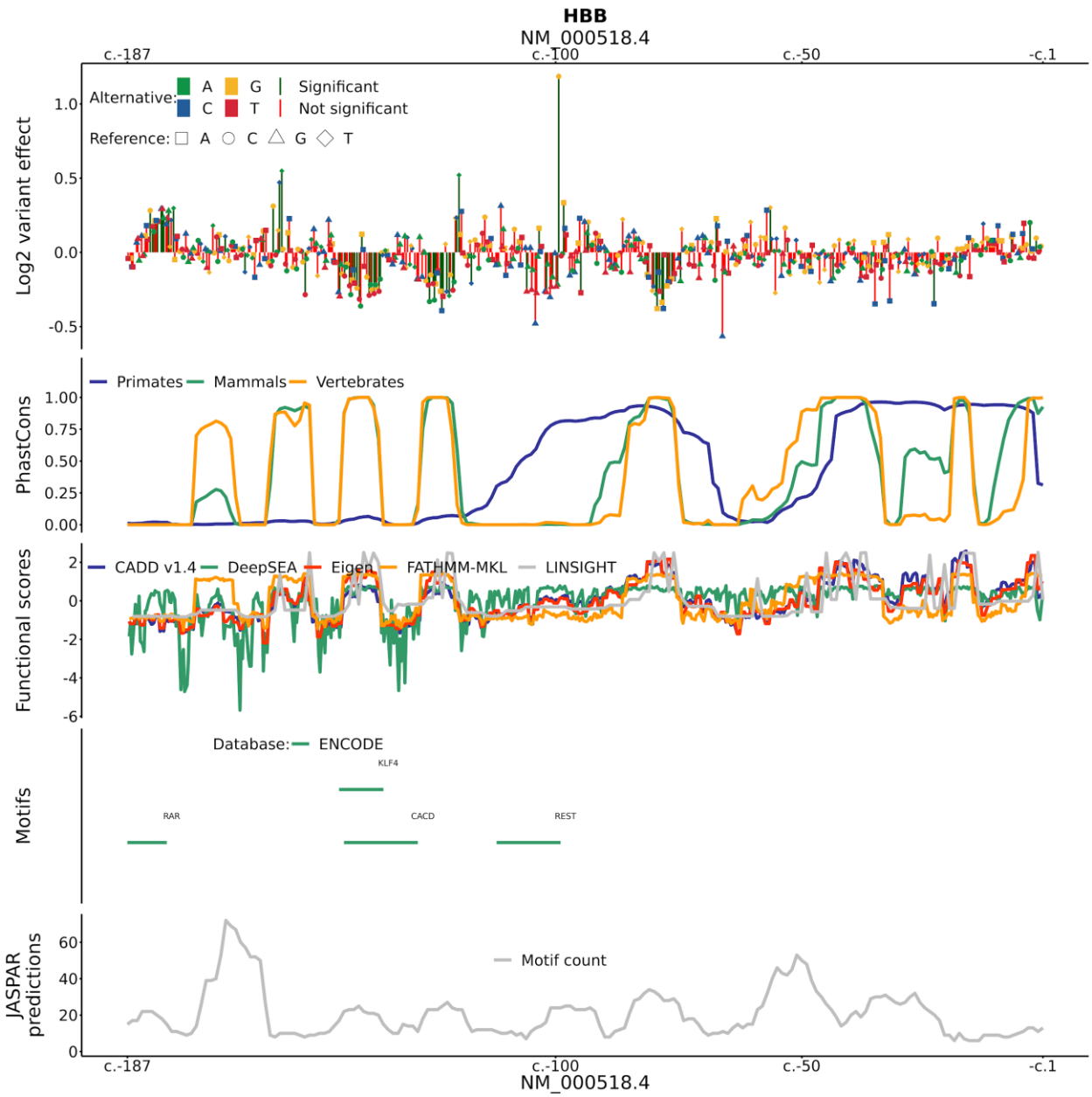
HBB
NM_000518.4
c.-187
c.-100
c.-50
-c.1
Alternative: A C G T
Significant
Not significant
Reference: A C G T
Log2 variant effect
1.0
0.5
0.0
-0.5
Primates
Mammals
Vertebrates
PhastCons
1.00
0.75
0.50
0.25
0.00
CADD v1.4
DeepSEA
Eigen
FATHMM-MKL
LINSIGHT
Functional scores
2
0
-2
-4
-6
Database: ENCODE
Motifs
KLF4
RAR
CACD
REST
Motif count
JASPAR predictions
60
40
20
0
c.-187
c.-100
c.-50
-c.1
NM_000518.4

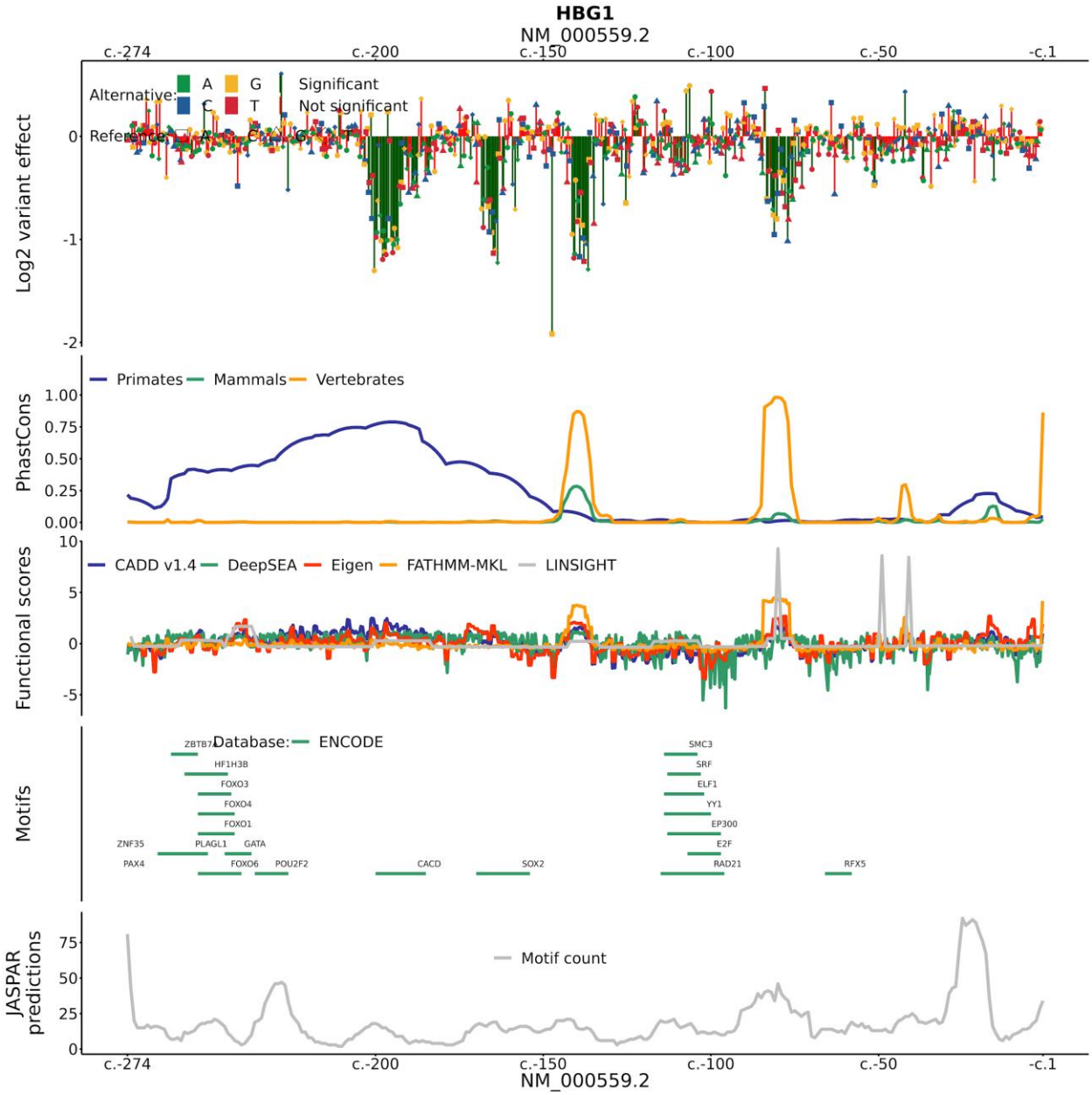
HBG1
NM_000559.2
c.-274
c.-200
c.-150
c.-100
c.-50
-c.1
Alternative:
A
C
G
T
Significant
Not significant
Reference:
Log2 variant effect
PhastCons
Primates
Mammals
Vertebrates
Functional scores
CADD v1.4
DeepSEA
Eigen
FATHMM-MKL
LINSIGHT
Motifs
Database:
ENCODE
ZBTB7A
HF1H3B
FOXO3
FOXO4
FOXO1
ZNF35
PLAGL1
GATA
PAX4
FOXO6
POU2F2
CACD
SOX2
SMC3
SRF
ELF1
YY1
EP300
E2F
RAD21
RFX5
JASPAR predictions
Motif count
NM_000559.2

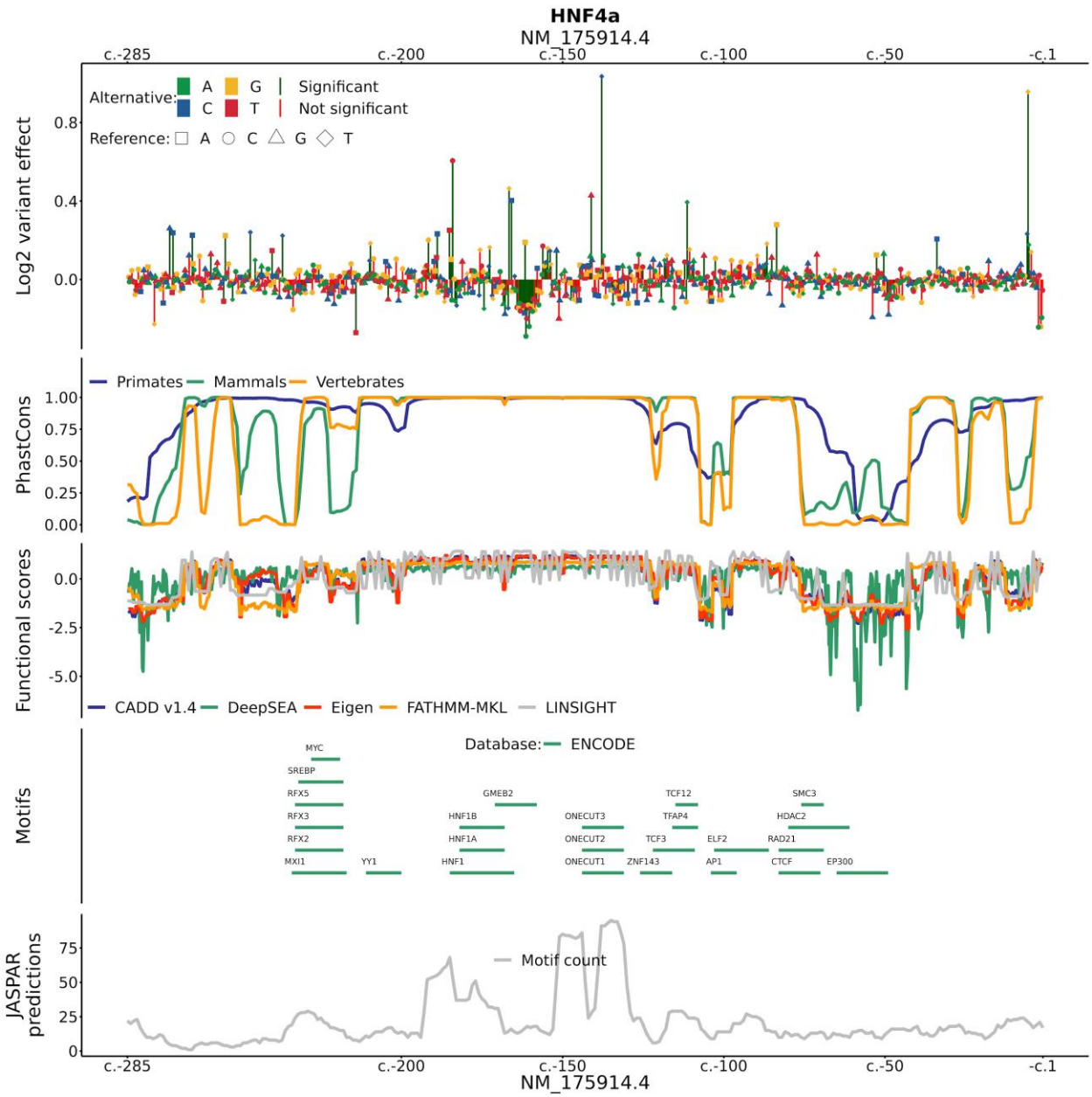
HNF4a
NM_175914.4
c.-285
c.-200
c.-150
c.-100
c.-50
-c.1
Alternative: A C G T Significant Not significant
Reference: A C G T
Log2 variant effect
0.8
0.4
0.0
Primates Mammals Vertebrates
PhastCons
1.00
0.75
0.50
0.25
0.00
Functional scores
0.0
-2.5
-5.0
CADD v1.4 DeepSEA Eigen FATHMM-MKL LINSIGHT
Motifs
Database: ENCODE
MYC
SREBP
RFX5
RFX3
RFX2
MXI1
YY1
GMEB2
HNF1B
HNF1A
HNF1
ONECUT3
ONECUT2
ONECUT1
TCF12
TFAP4
TCF3
ZNF143
ELF2
AP1
SMC3
HDAC2
RAD21
CTCF
EP300
JASPAR predictions
75
50
25
0
Motif count
c.-285
c.-200
c.-150
c.-100
c.-50
-c.1
NM_175914.4

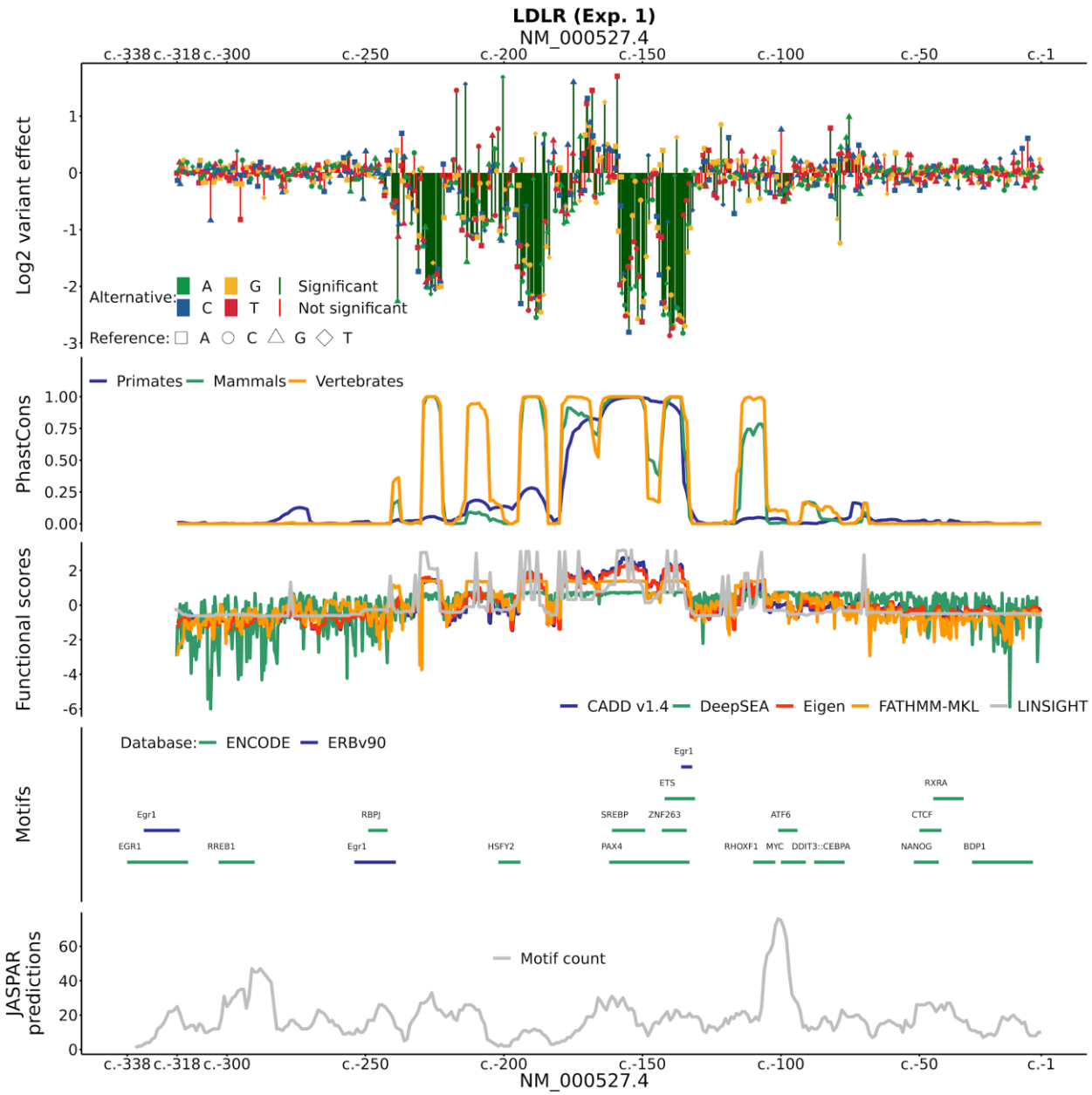
LDLR (Exp. 1)
NM_000527.4
c.-338 c.-318 c.-300 c.-250 c.-200 c.-150 c.-100 c.-50 c.-1
Log2 variant effect
Alternative: A G Significant
C T Not significant
Reference: A C G T
PhastCons
Primates Mammals Vertebrates
Functional scores
CADD v1.4 DeepSEA Eigen FATHMM-MKL LINSIGHT
Motifs
Database: ENCODE ERBv90
Egr1
EGR1 RREB1 RBPJ Egr1 HSFY2 ETS SREBP ZNF263 PAX4 ATF6 RHOXF1 MYC DDIT3::CEBPA RXRA CTCF NANOG BDP1
JASPAR predictions
Motif count
NM_000527.4

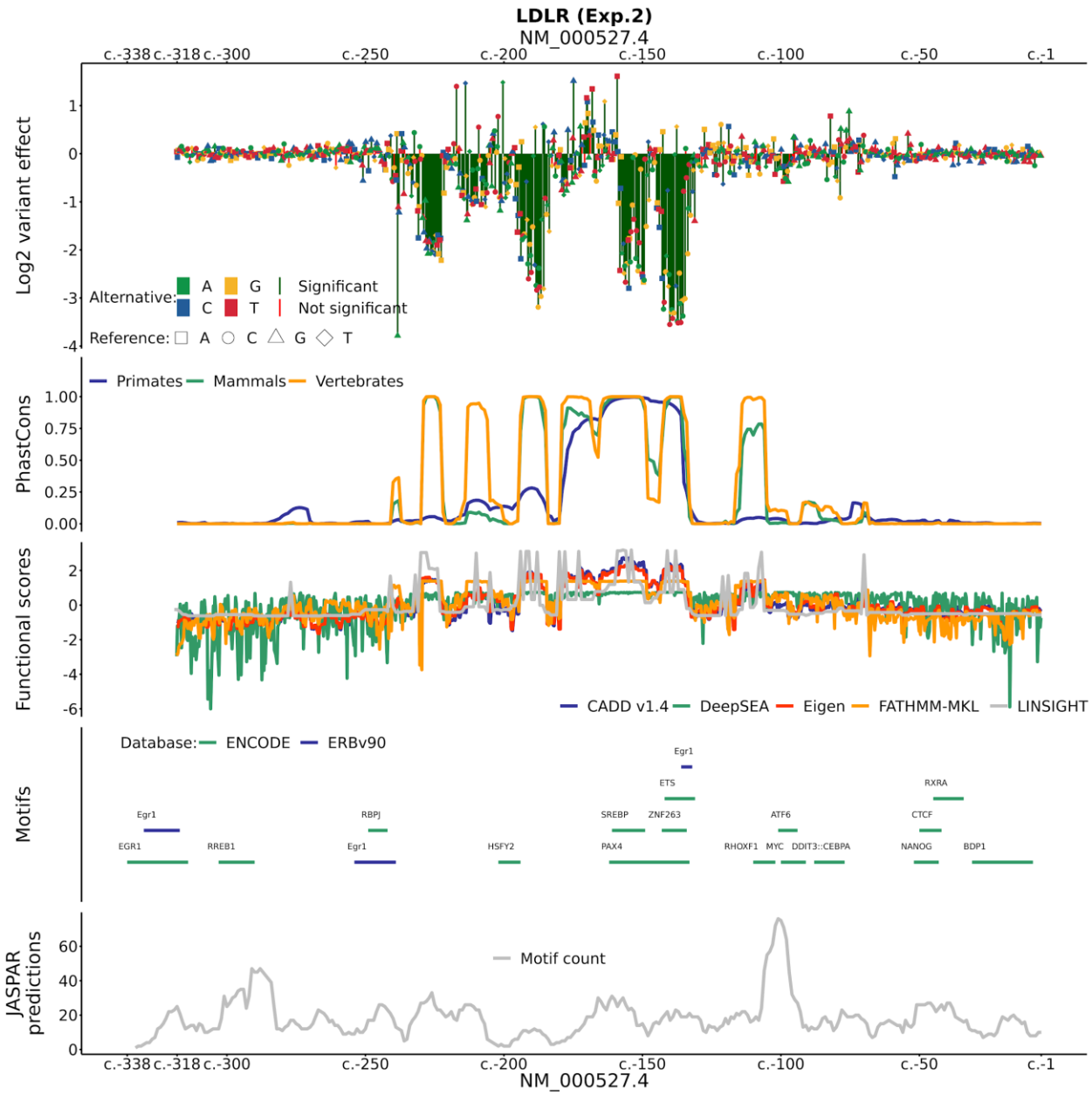
LDLR (Exp.2)
NM_000527.4
c.-338 c.-318 c.-300 c.-250 c.-200 c.-150 c.-100 c.-50 c.-1
Log2 variant effect
Alternative: A G Significant
C T Not significant
Reference: A C G T
PhastCons
Primates Mammals Vertebrates
Functional scores
CADD v1.4 DeepSEA Eigen FATHMM-MKL LINSIGHT
Motifs
Database: ENCODE ERBv90
Egr1
EGR1
RREB1
RBPJ
Egr1
HSFY2
ETS
SREBP
ZNF263
PAX4
ATF6
RHOXF1
MYC
DDIT3::CEBPA
RXRA
CTCF
NANOG
BDP1
JASPAR predictions
Motif count
NM_000527.4

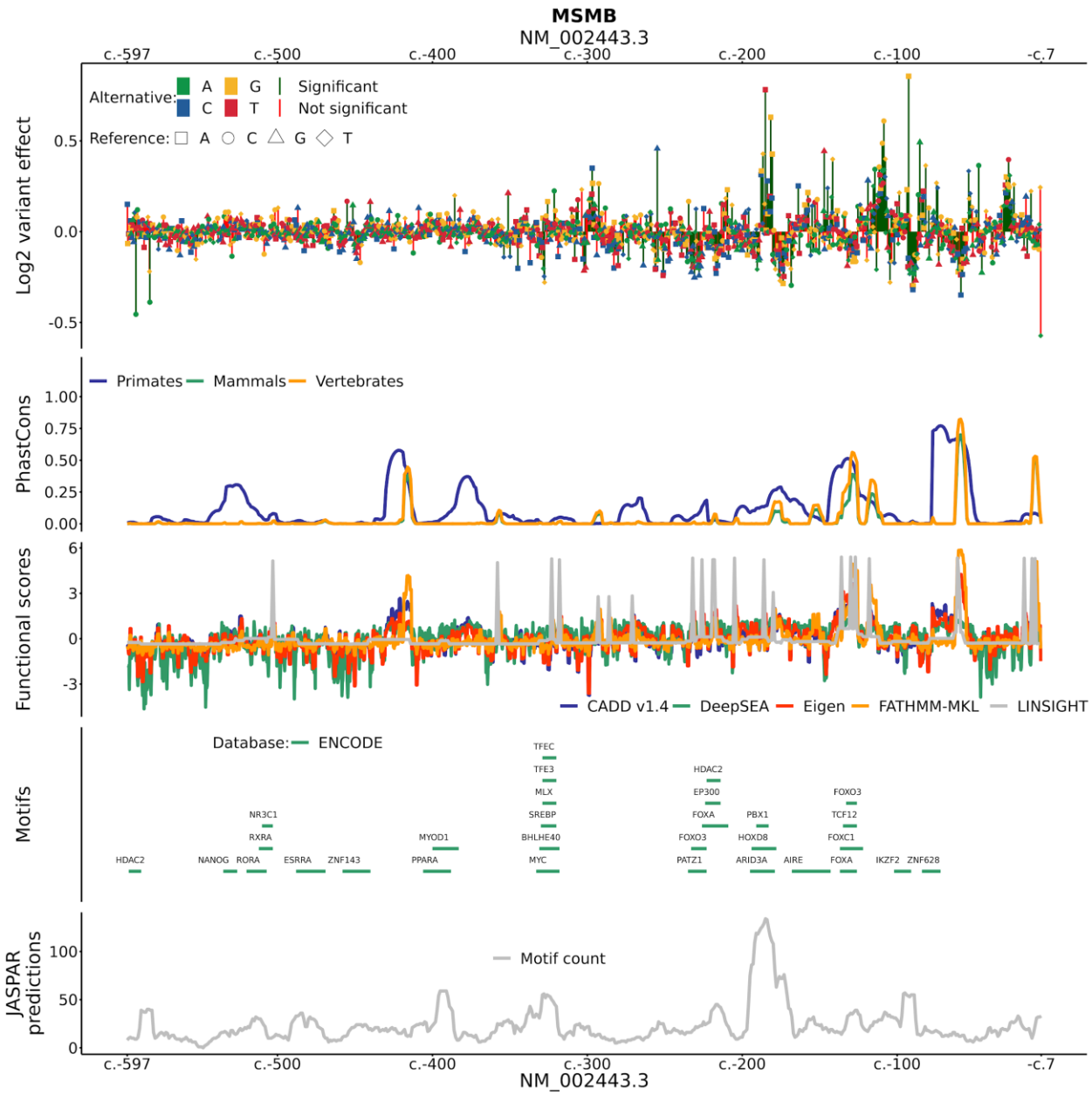
MSMB
NM_002443.3
c.-597
c.-500
c.-400
c.-300
c.-200
c.-100
-c.7
Alternative: A C G T
Significant
Not significant
Reference: A C G T
Log2 variant effect
0.5
0.0
-0.5
Primates
Mammals
Vertebrates
PhastCons
1.00
0.75
0.50
0.25
0.00
Functional scores
6
3
0
-3
CADD v1.4
DeepSEA
Eigen
FATHMM-MKL
LINSIGHT
Motifs
Database: ENCODE
HDAC2
NANOG
NR3C1
RORA
ESRRA
ZNF143
MYOD1
PPARA
TFEC
TFE3
MLX
SREBP
BHLHE40
MYC
HDAC2
EP300
FOXA
FOXO3
PATZ1
PBX1
HOXD8
ARID3A
AIRE
FOXO3
TCF12
FOXC1
FOXA
IKZF2
ZNF628
JASPAR predictions
100
50
0
Motif count
c.-597
c.-500
c.-400
c.-300
c.-200
c.-100
-c.7
NM_002443.3

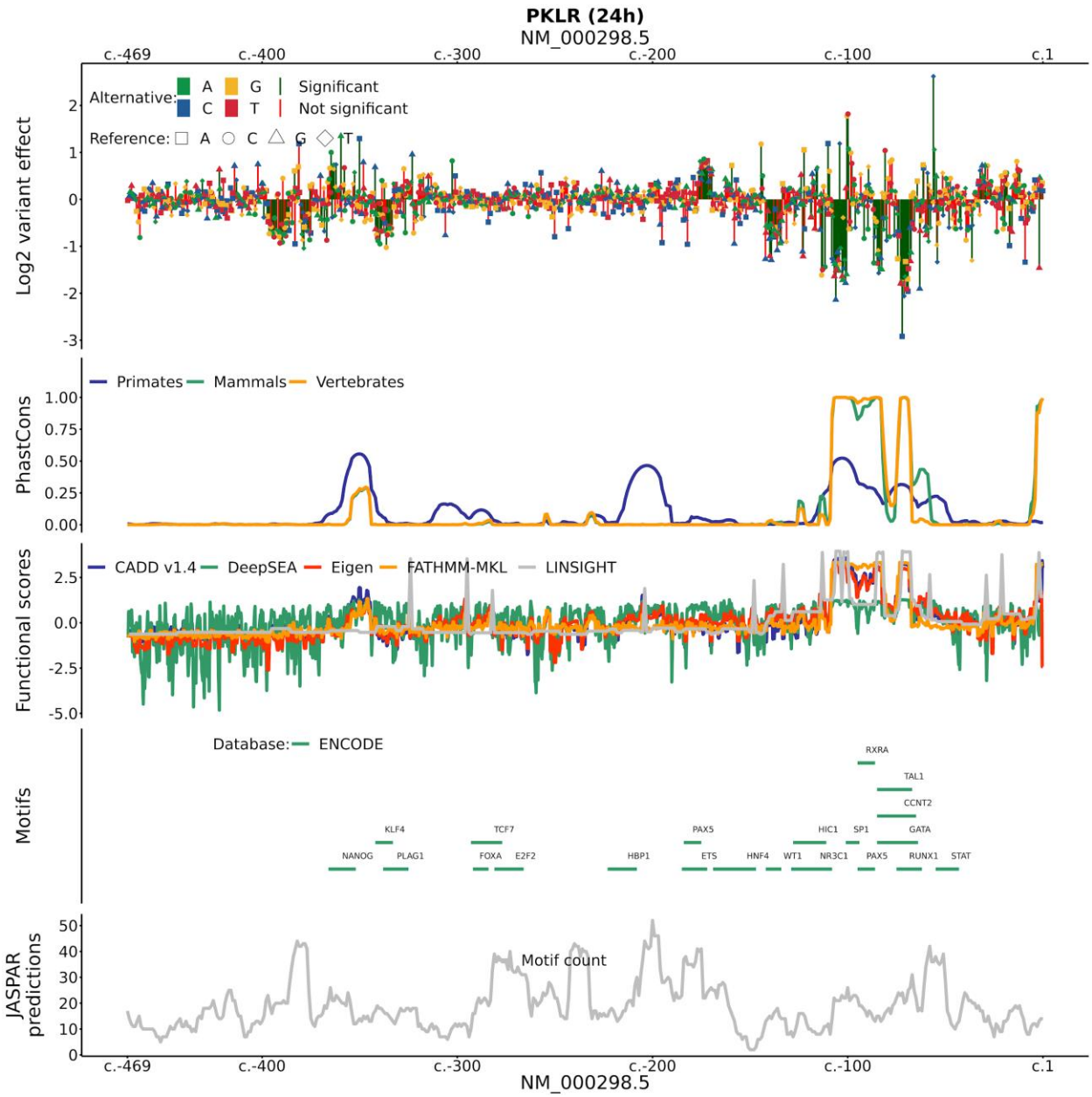
PKLR (24h)
NM_000298.5
c.-469
c.-400
c.-300
c.-200
c.-100
c.1
Alternative: A C G T
Significant
Not significant
Reference: A C G T
Log2 variant effect
PhastCons
Primates
Mammals
Vertebrates
Functional scores
CADD v1.4
DeepSEA
Eigen
FATHMM-MKL
LINSIGHT
Motifs
Database: ENCODE
RXRA
TAL1
CCNT2
KLF4
TCF7
PAX5
HIC1
SP1
GATA
NANOG
PLAG1
FOXA
E2F2
HBP1
ETS
HNF4
WT1
NR3C1
PAX5
RUNX1
STAT
JASPAR predictions
Motif count
NM_000298.5

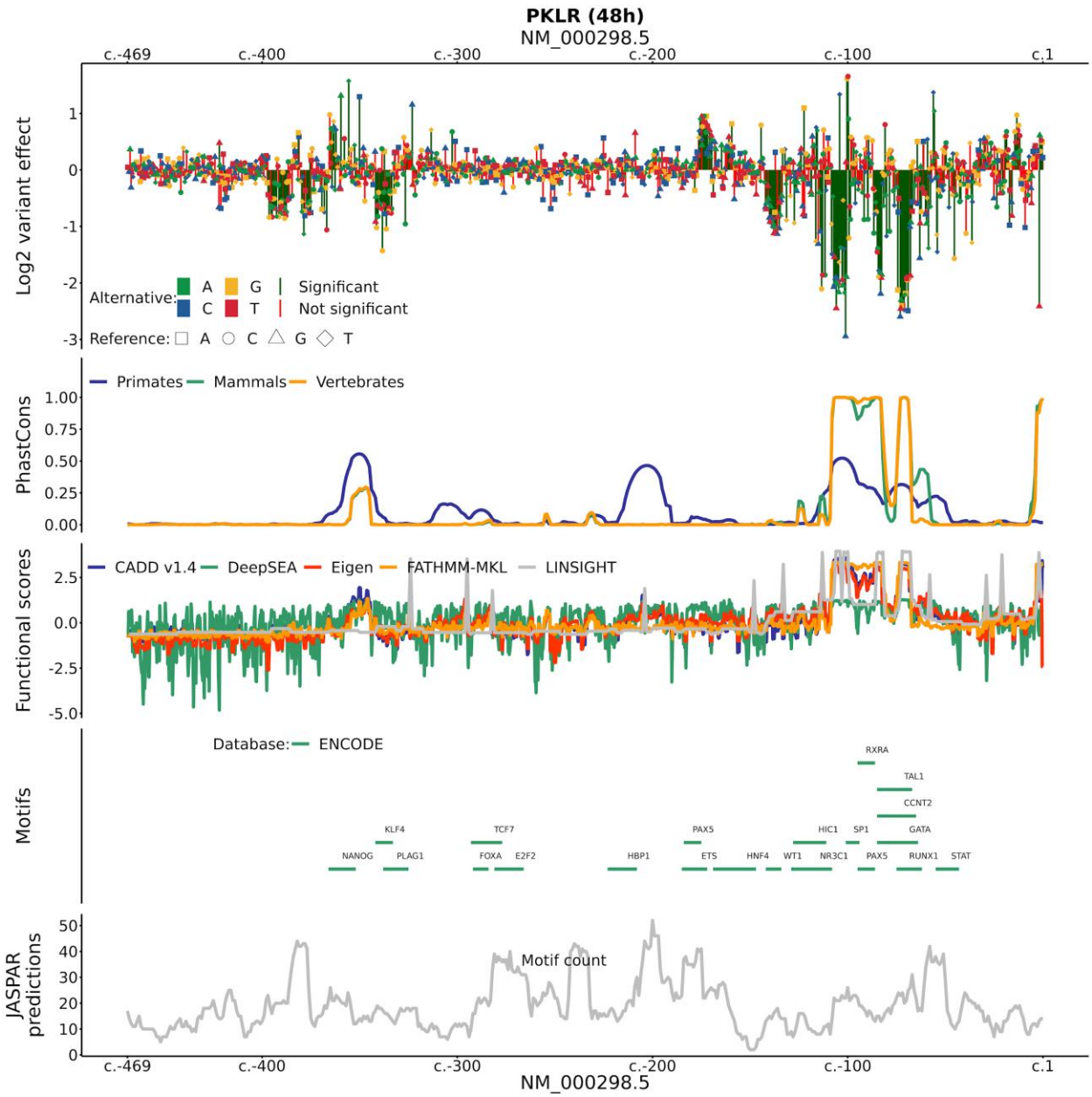
PKLR (48h)
NM_000298.5
c.-469
c.-400
c.-300
c.-200
c.-100
c.1
Log2 variant effect
Alternative:
A
C
G
T
Significant
Not significant
Reference: A C G T
PhastCons
Primates
Mammals
Vertebrates
Functional scores
CADD v1.4
DeepSEA
Eigen
FATHMM-MKL
LINSIGHT
Motifs
Database: ENCODE
RXRA
TAL1
CCNT2
KLF4
TCF7
PAX5
HIC1
SP1
GATA
NANOG
PLAG1
FOXA
E2F2
HBP1
ETS
HNF4
WT1
NR3C1
PAX5
RUNX1
STAT
JASPAR predictions
Motif count
NM_000298.5

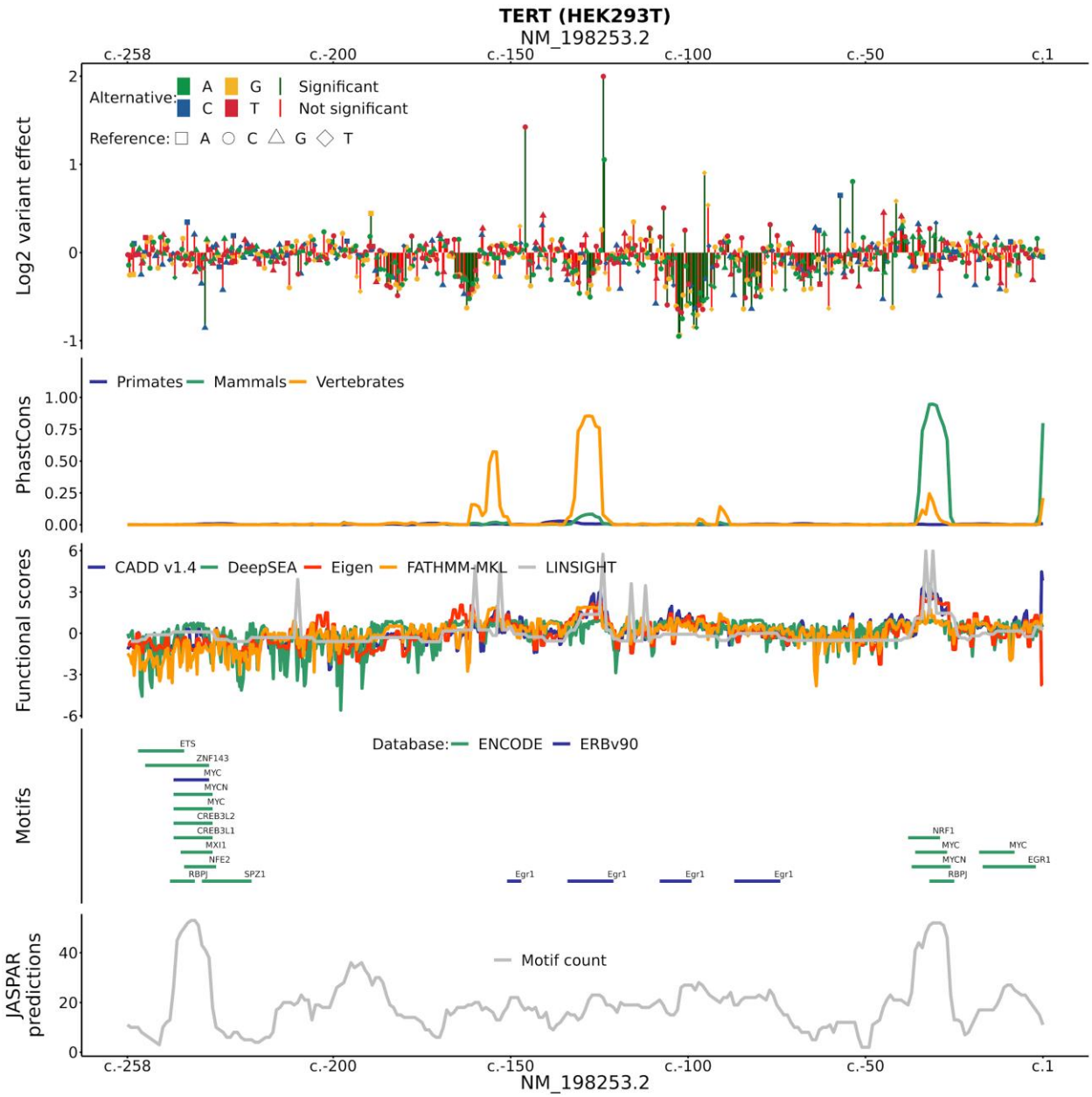
TERT (HEK293T)
NM_198253.2
c.-258
c.-200
c.-150
c.-100
c.-50
c.1
Alternative: A C G T Significant Not significant
Reference: A C G T
Log2 variant effect
2
1
0
-1
Primates Mammals Vertebrates
PhastCons
1.00
0.75
0.50
0.25
0.00
CADD v1.4 DeepSEA Eigen FATHMM-MKL LINSIGHT
Functional scores
6
3
0
-3
-6
Database: ENCODE ERBv90
Motifs
ETS
ZNF143
MYC
MYCN
MYC
CREB3L2
CREB3L1
MXI1
NFE2
RBPJ
SPZ1
Egr1
Egr1
Egr1
Egr1
NRF1
MYC
MYC
MYCN
EGR1
RBPJ
Motif count
JASPAR predictions
40
20
0
c.-258
c.-200
c.-150
c.-100
c.-50
c.1
NM_198253.2

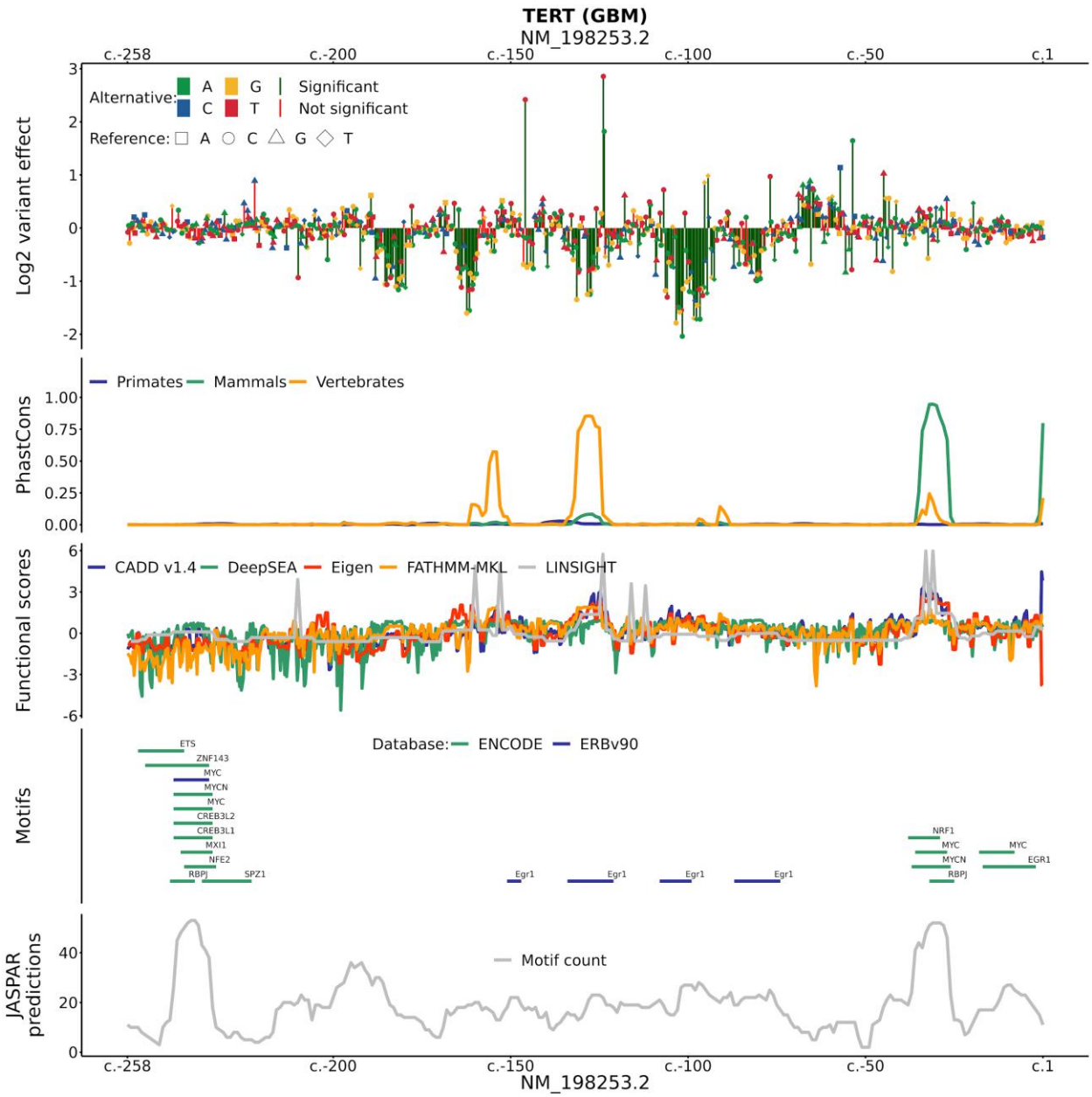
TERT (GBM)
NM_198253.2
c.-258
c.-200
c.-150
c.-100
c.-50
c.1
Alternative: A C G T Significant Not significant
Reference: A C G T
Log2 variant effect
PhastCons
Primates Mammals Vertebrates
Functional scores
CADD v1.4 DeepSEA Eigen FATHMM-MKL LINSIGHT
Motifs
Database: ENCODE ERBv90
ETS
ZNF143
MYC
MYCN
MYC
CREB3L2
CREB3L1
MXI1
NFE2
RBPJ
SPZ1
Egr1
Egr1
Egr1
Egr1
NRF1
MYC
MYC
MYCN
EGR1
RBPJ
JASPAR predictions
Motif count
NM_198253.2

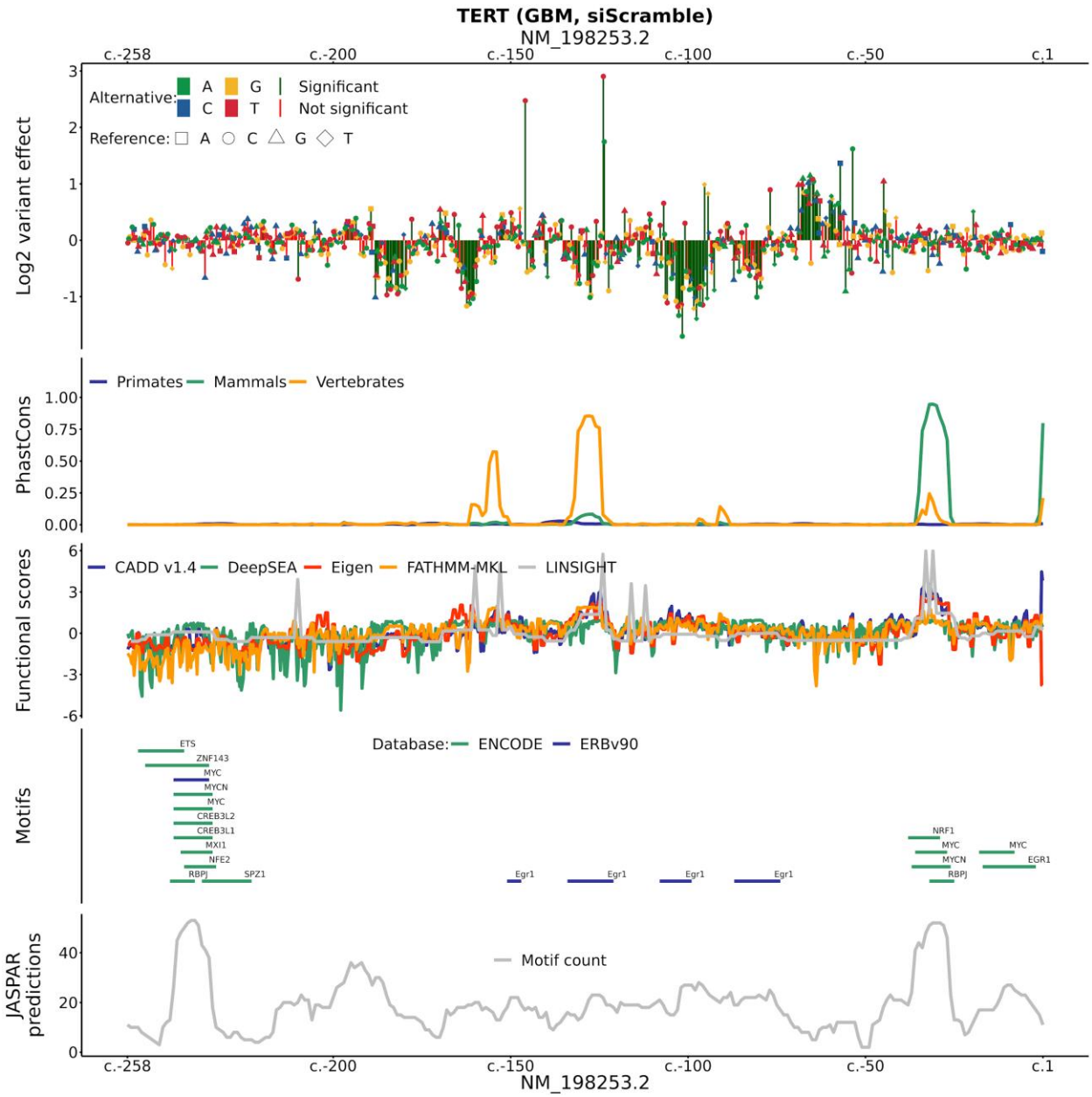
TERT (GBM, siScramble)
NM_198253.2
c.-258
c.-200
c.-150
c.-100
c.-50
c.1
Alternative: A C G T Significant Not significant
Reference: A C G T
Log2 variant effect
PhastCons
Primates Mammals Vertebrates
Functional scores
CADD v1.4 DeepSEA Eigen FATHMM-MKL LINSIGHT
Motifs
Database: ENCODE ERBv90
ETS
ZNF143
MYC
MYCN
MYC
CREB3L2
CREB3L1
MXI1
NFE2
RBPJ
SPZ1
Egr1
Egr1
Egr1
Egr1
NRF1
MYC
MYC
MYCN
EGR1
RBPJ
JASPAR predictions
Motif count
NM_198253.2

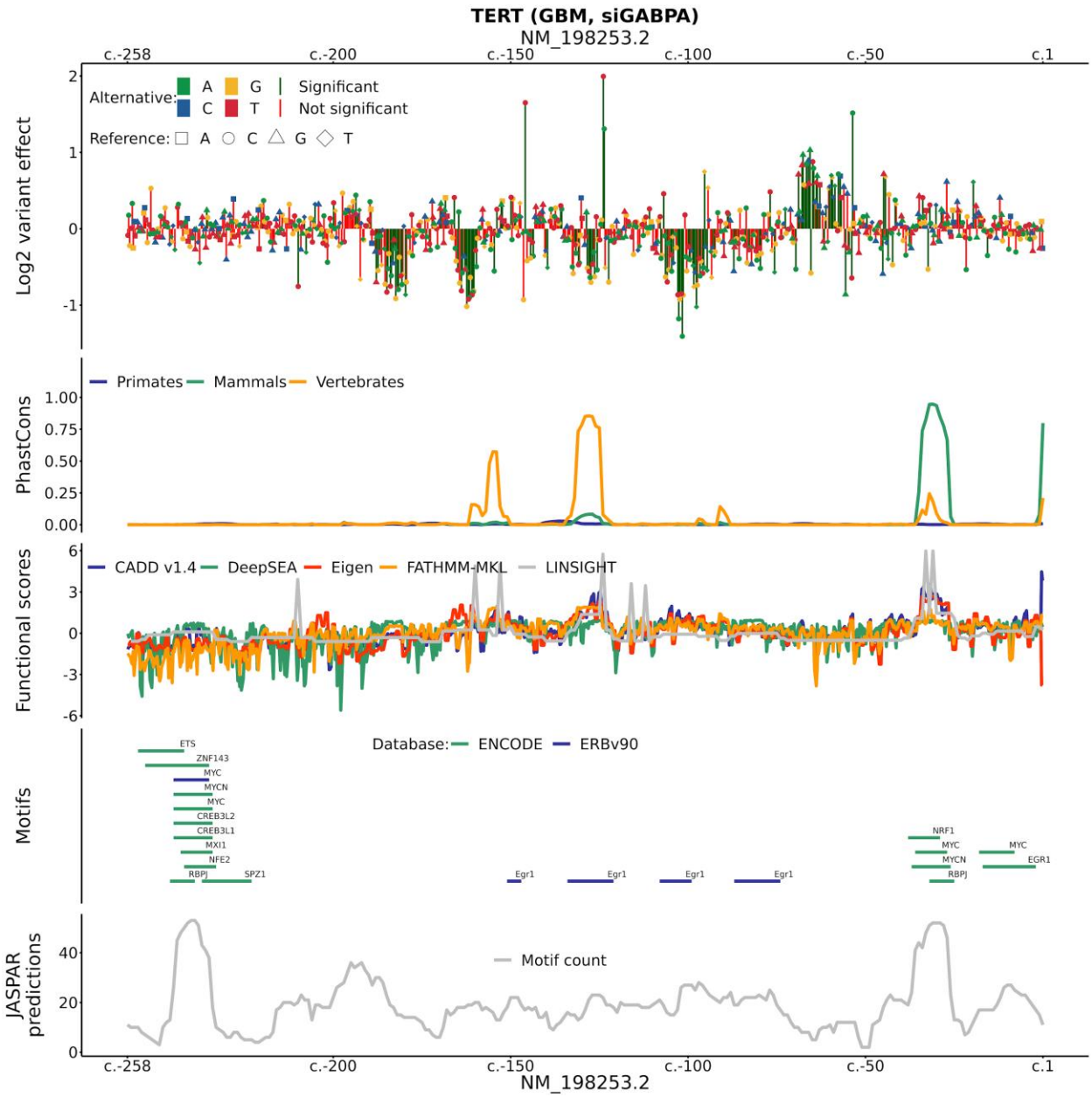

Overlay of inferred variant effects for SNVs from promoter elements with available annotation data. Motif predictions overlayed with biochemical evidence from ChIP-seq experiments were obtained from Ensembl Regulatory Build (ERB)[33] and ENCODE[3] annotations. JASPAR motif predictions were obtained from the JASPAR 2018[6] release.

Supplementary Figure 9

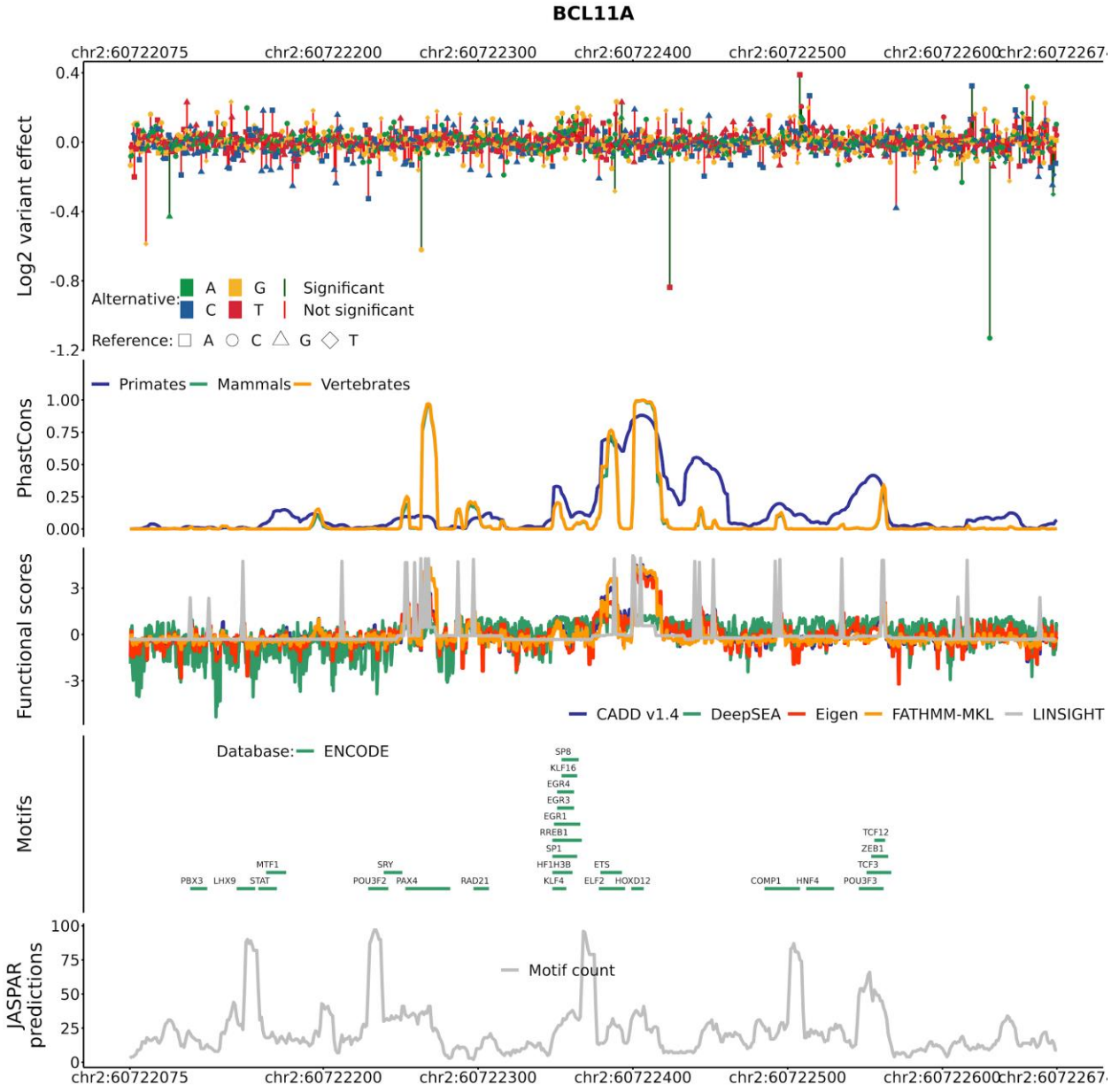

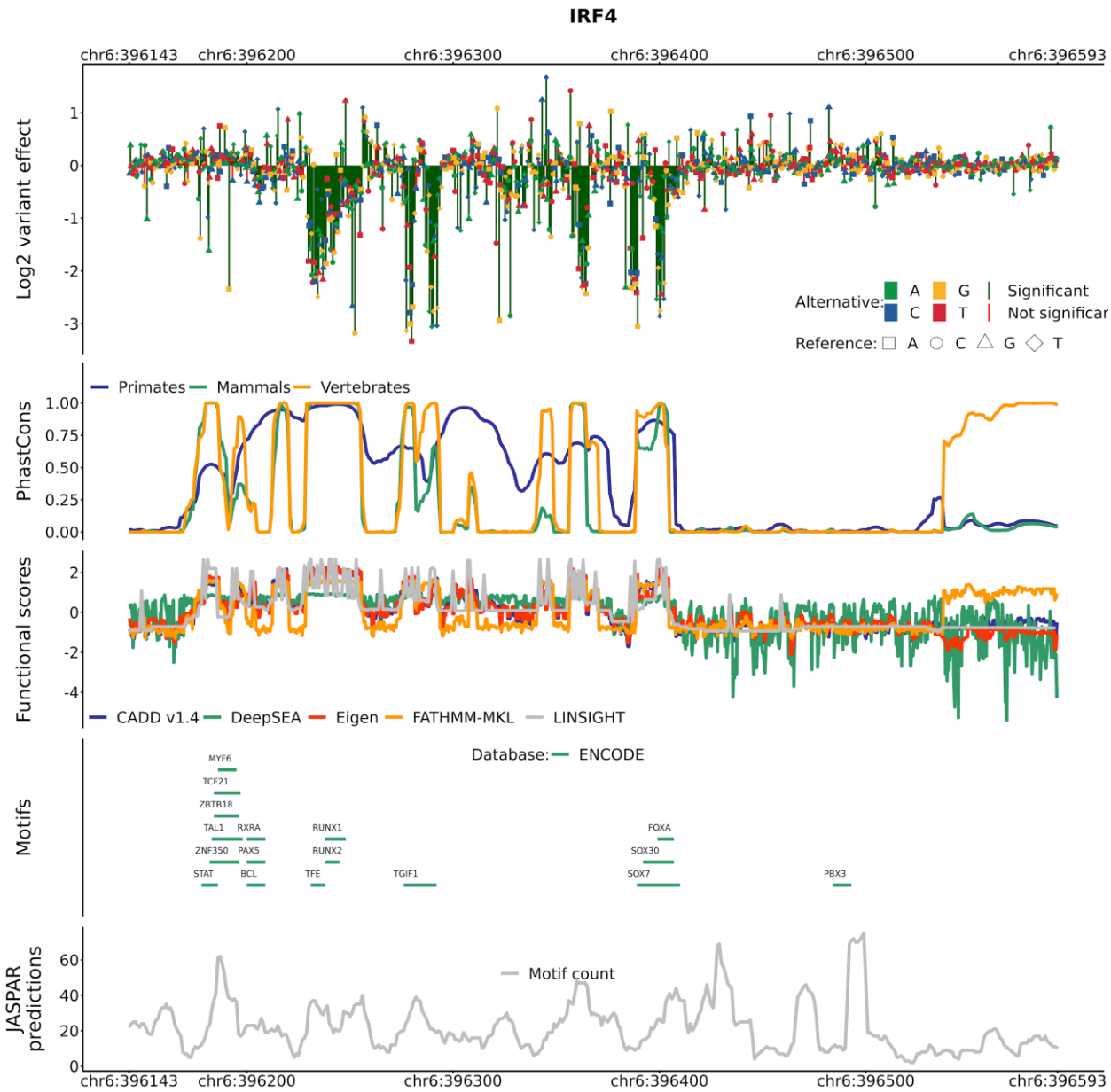
IRF4
chr6:396143
chr6:396200
chr6:396300
chr6:396400
chr6:396500
chr6:396593
Log2 variant effect
1
0
-1
-2
-3
Alternative: A G C T
Significant
Not significar
Reference: A C G T
PhastCons
Primates
Mammals
Vertebrates
1.00
0.75
0.50
0.25
0.00
Functional scores
2
0
-2
-4
CADD v1.4
DeepSEA
Eigen
FATHMM-MKL
LINSIGHT
Motifs
Database: ENCODE
MYF6
TCF21
ZBTB18
TAL1
RXRA
RUNX1
FOXA
ZNF350
PAX5
RUNX2
SOX30
STAT
BCL
TFE
TGIF1
SOX7
PBX3
JASPAR predictions
Motif count
60
40
20
0

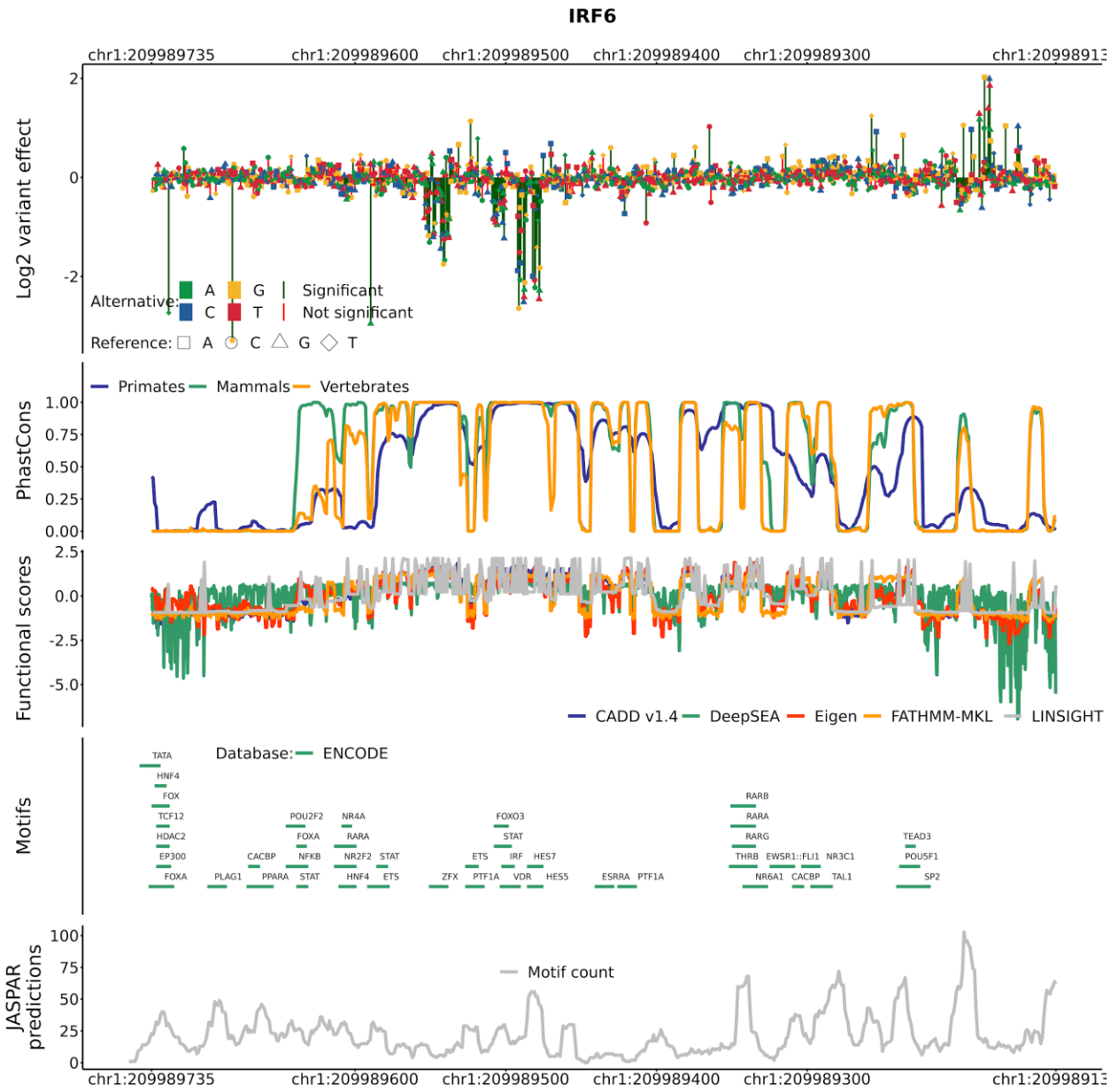
IRF6
chr1:209989735
chr1:209989600
chr1:209989500
chr1:209989400
chr1:209989300
Log2 variant effect
Alternative: A C G T Significant Not significant
Reference: A C G T
Primates Mammals Vertebrates
PhastCons
Functional scores
CADD v1.4 DeepSEA Eigen FATHMM-MKL LINSIGHT
Motifs
Database: ENCODE
TATA HNF4 FOX TCF12 HDAC2 EP300 FOXA
PLAG1 CACBP PPARA POU2F2 FOXA NFKB STAT NR4A RARA NR2F2 STAT HNF4 ETS
ZFX ETS PTF1A FOXO3 STAT IRF VDR HES7 HES5
ESRRA PTF1A
RARB RARA RARG THRB NR6A1 EWSR1::FLI1 CACBP NR3C1 TAL1
TEAD3 POU5F1 SP2
JASPAR predictions
Motif count

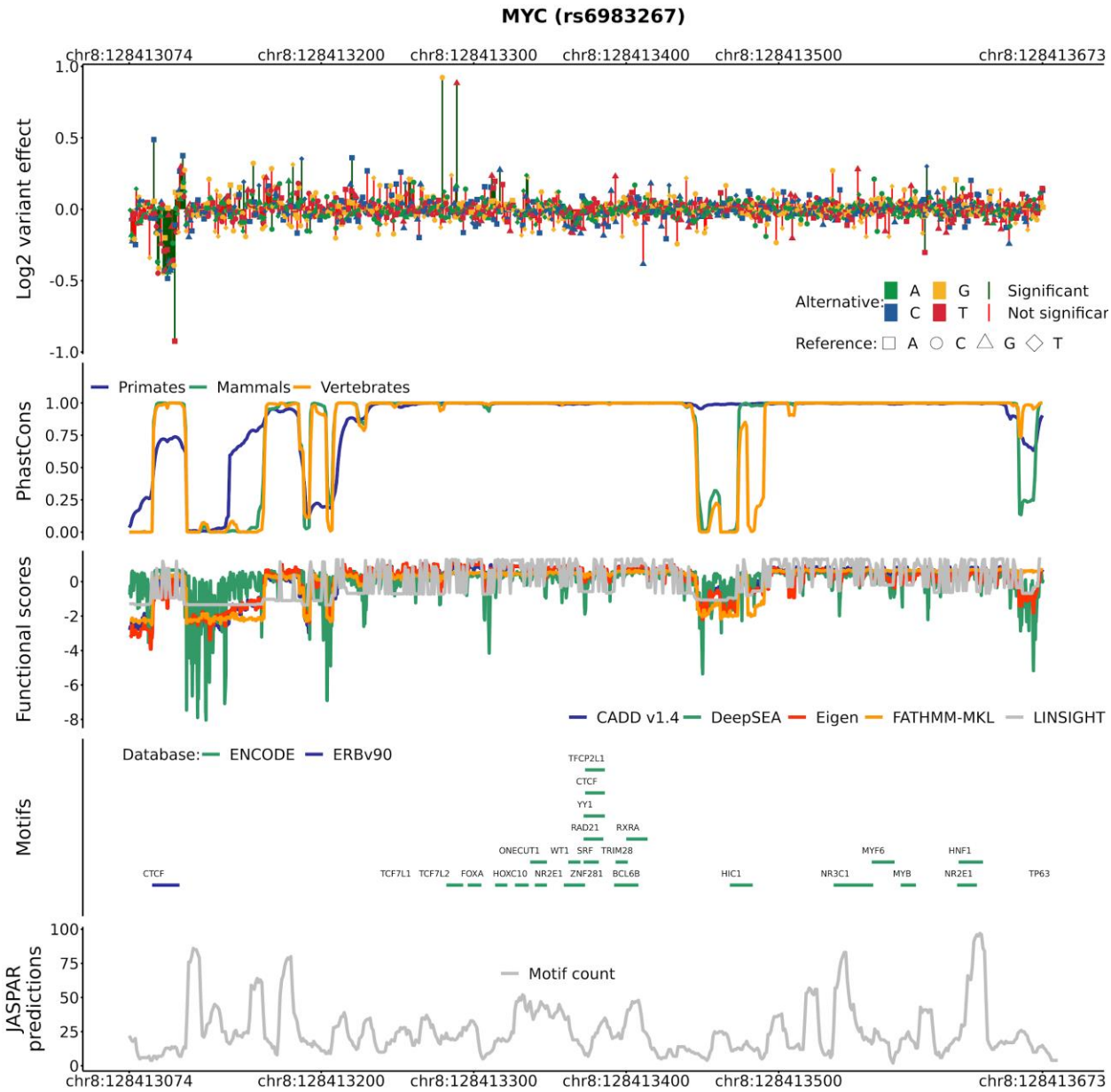
MYC (rs6983267)
chr8:128413074
chr8:128413200
chr8:128413300
chr8:128413400
chr8:128413500
chr8:128413673
Log2 variant effect
1.0
0.5
0.0
-0.5
-1.0
Alternative: A G C T
Significant
Not significar
Reference: A C G T
PhastCons
Primates
Mammals
Vertebrates
1.00
0.75
0.50
0.25
0.00
Functional scores
0
-2
-4
-6
-8
CADD v1.4
DeepSEA
Eigen
FATHMM-MKL
LINSIGHT
Motifs
Database: ENCODE ERBv90
TFCP2L1
CTCF
YY1
RAD21
RXRA
ONECUT1
WT1
SRF
TRIM28
MYF6
HNF1
CTCF
TCF7L1
TCF7L2
FOXA
HOXC10
NR2E1
ZNF281
BCL6B
HIC1
NR3C1
MYB
NR2E1
TP63
JASPAR predictions
100
75
50
25
0
Motif count
chr8:128413074
chr8:128413200
chr8:128413300
chr8:128413400
chr8:128413500
chr8:128413673

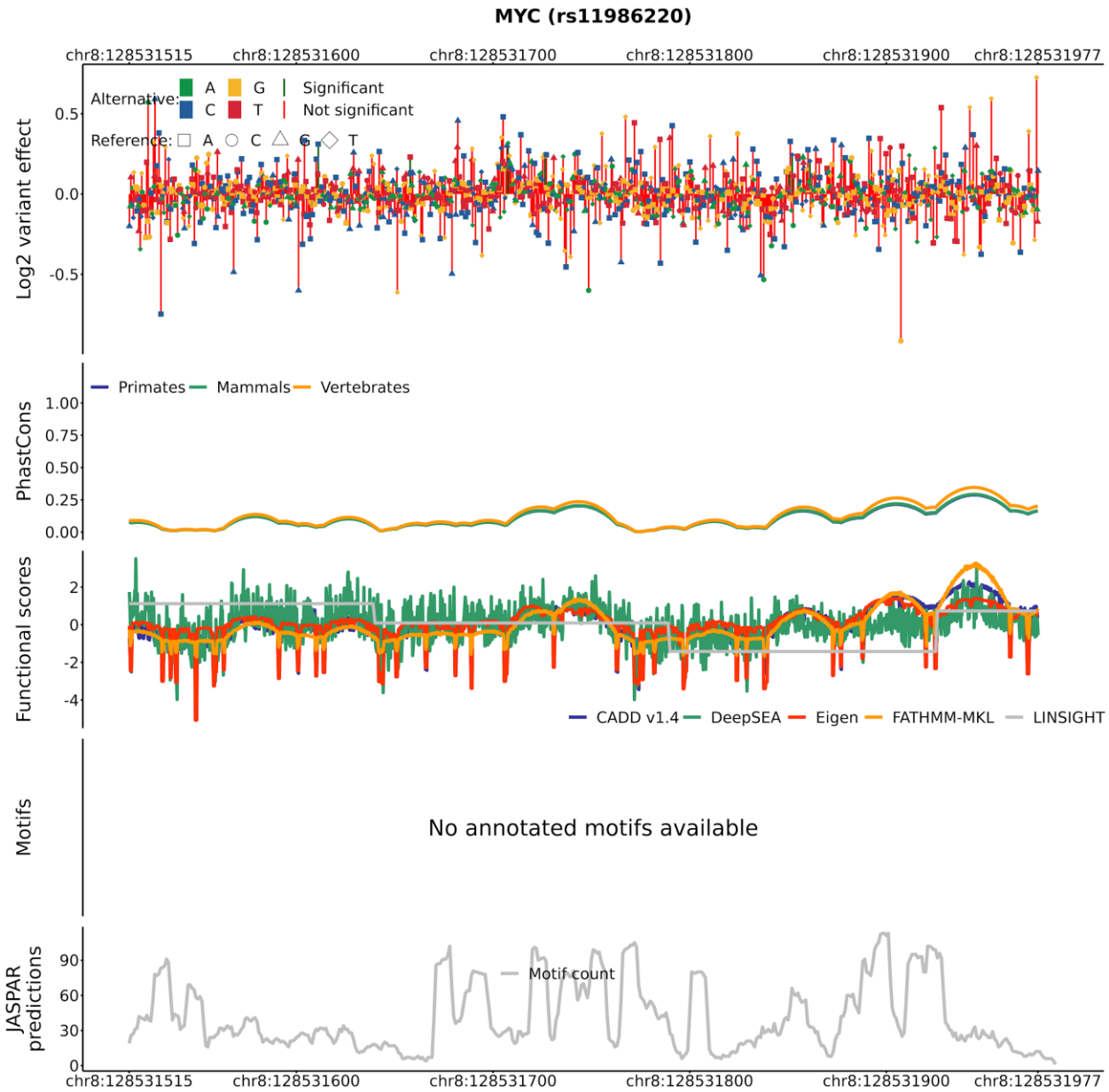
MYC (rs11986220)
chr8:128531515
chr8:128531600
chr8:128531700
chr8:128531800
chr8:128531900
chr8:128531977
Alternative: A C G T
Significant
Not significant
Reference: A C G T
Log2 variant effect
0.5
0.0
-0.5
Primates
Mammals
Vertebrates
PhastCons
1.00
0.75
0.50
0.25
0.00
Functional scores
2
0
-2
-4
CADD v1.4
DeepSEA
Eigen
FATHMM-MKL
LINSIGHT
Motifs
No annotated motifs available
JASPAR predictions
Motif count
90
60
30
0

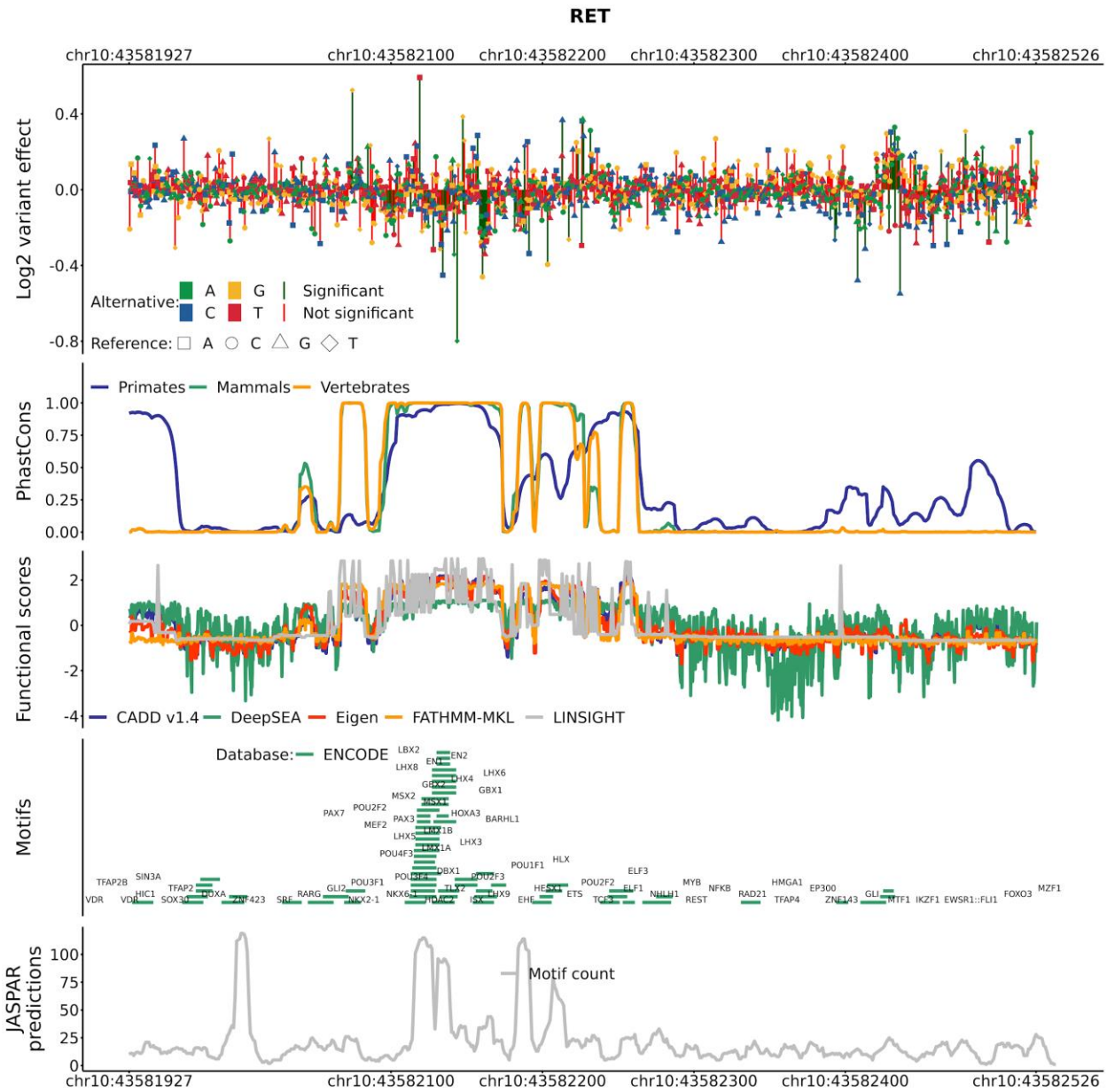
RET
chr10:43581927
chr10:43582100
chr10:43582200
chr10:43582300
chr10:43582400
chr10:43582526
Log2 variant effect
Alternative: A C G T
Significant
Not significant
Reference: A C G T
PhastCons
Primates
Mammals
Vertebrates
Functional scores
CADD v1.4
DeepSEA
Eigen
FATHMM-MKL
LINSIGHT
Motifs
Database: ENCODE
JASPAR predictions
Motif count

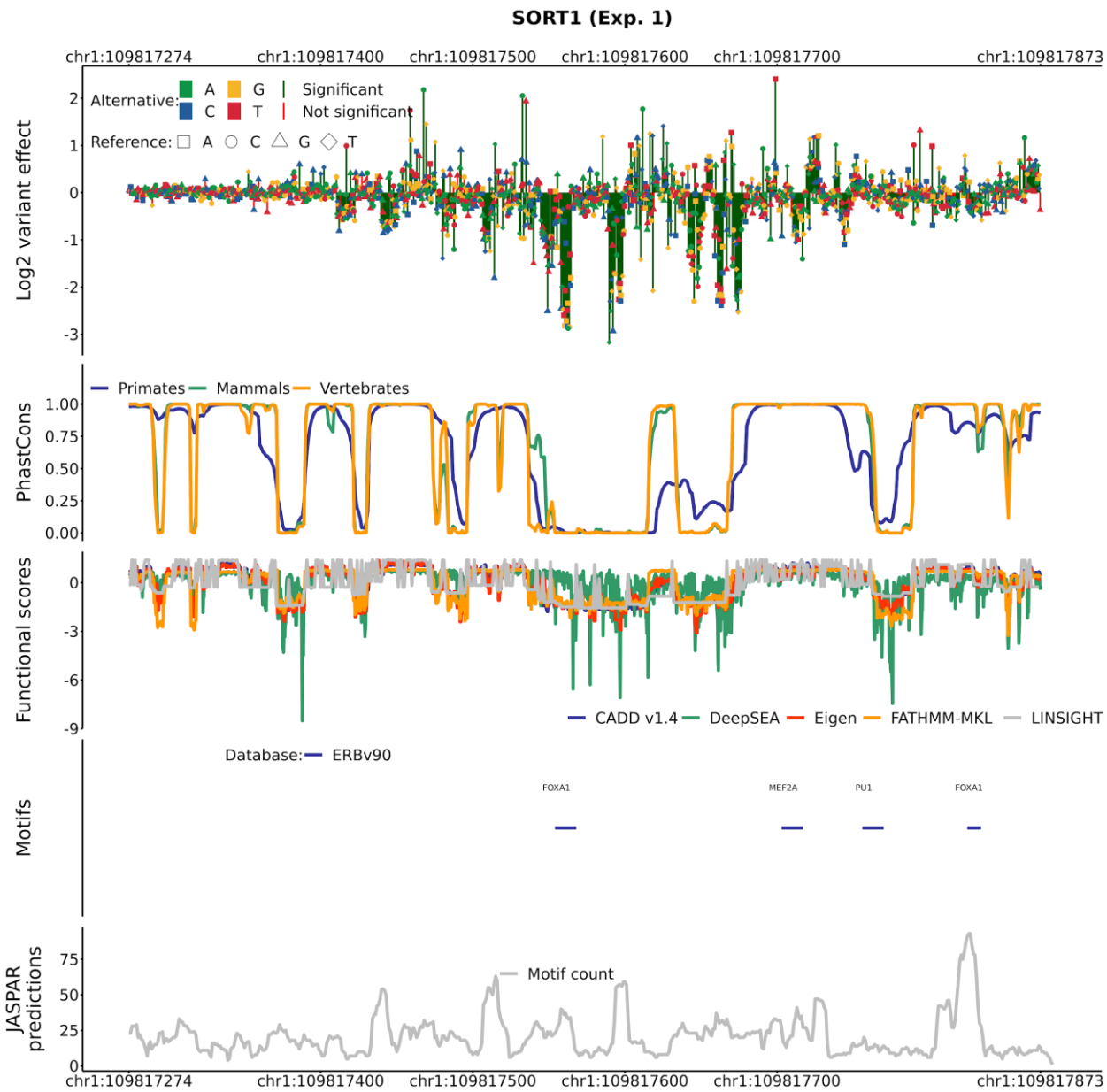
SORT1 (Exp. 1)
chr1:109817274
chr1:109817400
chr1:109817500
chr1:109817600
chr1:109817700
chr1:109817873
Alternative: A C G T
Significant
Not significant
Reference: A C G T
Log2 variant effect
PhastCons
Primates
Mammals
Vertebrates
Functional scores
CADD v1.4
DeepSEA
Eigen
FATHMM-MKL
LINSIGHT
Database: ERBv90
Motifs
FOXA1
MEF2A
PU1
FOXA1
JASPAR predictions
Motif count

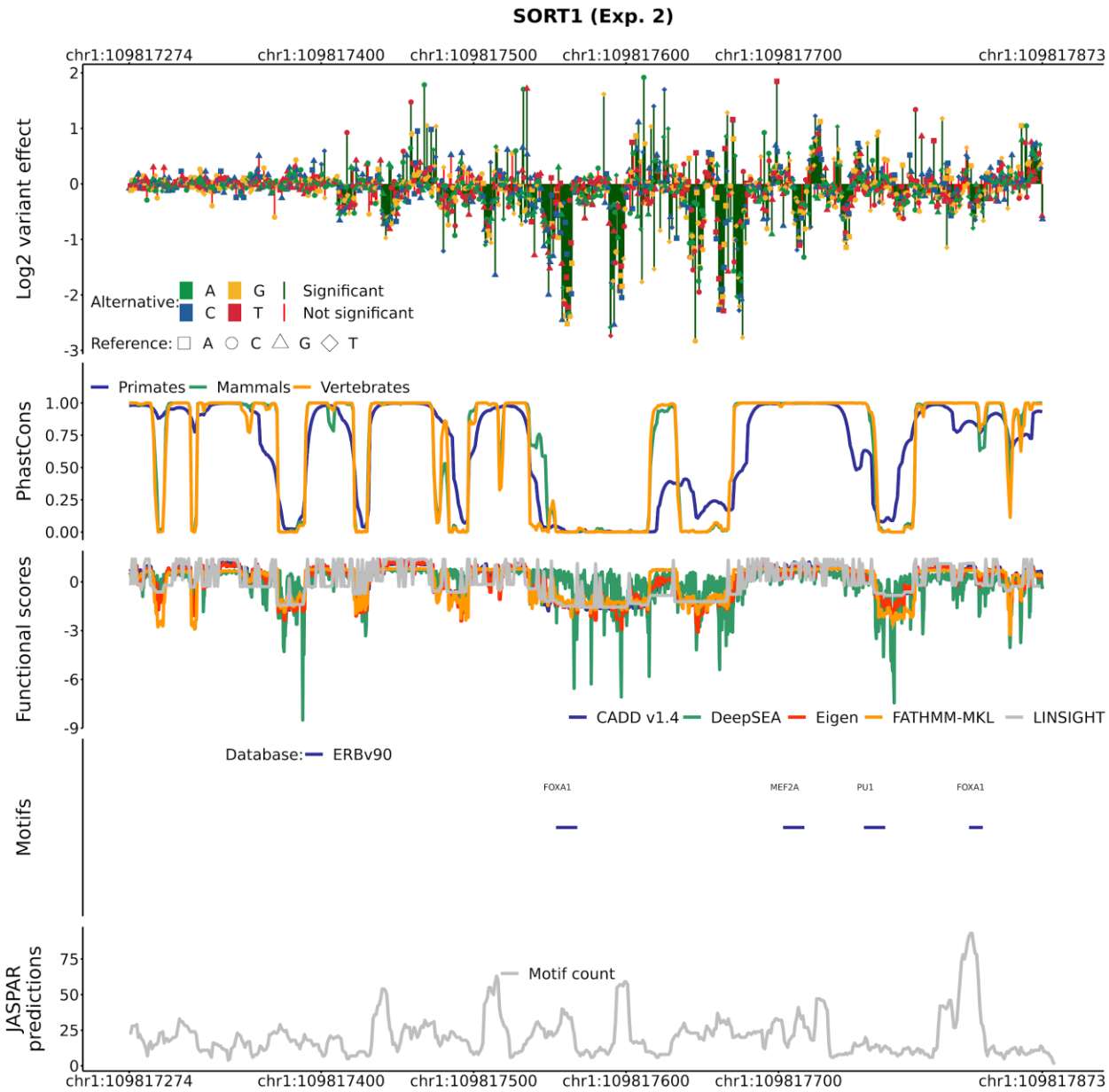
SORT1 (Exp. 2)
chr1:109817274
chr1:109817400
chr1:109817500
chr1:109817600
chr1:109817700
chr1:109817873
Log2 variant effect
Alternative: A C G T
Significant
Not significant
Reference: A C G T
PhastCons
Primates
Mammals
Vertebrates
Functional scores
CADD v1.4
DeepSEA
Eigen
FATHMM-MKL
LINSIGHT
Database: ERBv90
Motifs
FOXA1
MEF2A
PU1
FOXA1
JASPAR predictions
Motif count

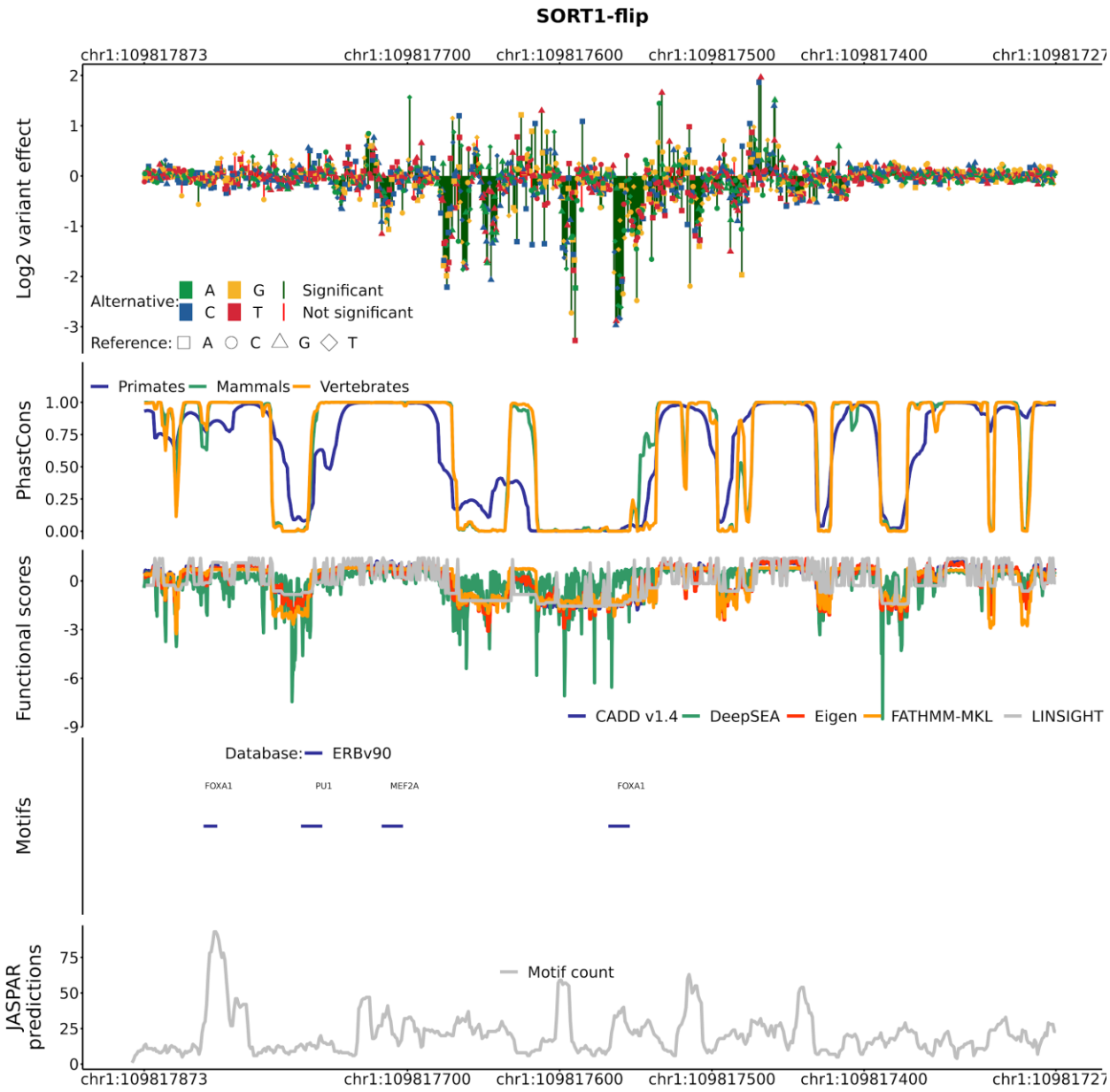
SORT1-flip
chr1:109817873
chr1:109817700
chr1:109817600
chr1:109817500
chr1:109817400
chr1:10981727
Log2 variant effect
Alternative: A C G T
Significant
Not significant
Reference: A C G T
Primates
Mammals
Vertebrates
PhastCons
Functional scores
CADD v1.4
DeepSEA
Eigen
FATHMM-MKL
LINSIGHT
Database: ERBv90
Motifs
FOXA1
PU1
MEF2A
FOXA1
JASPAR predictions
Motif count

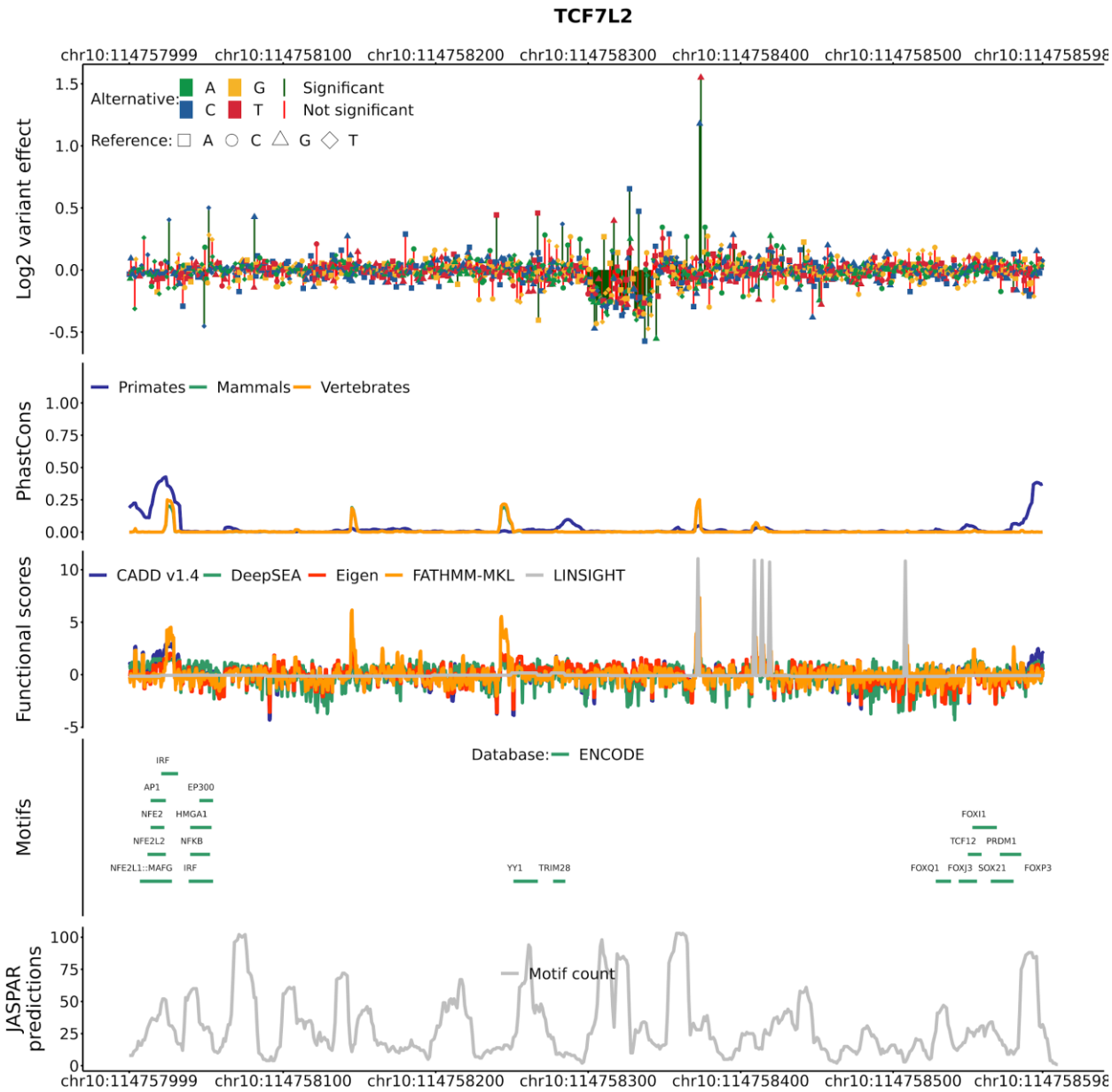
TCF7L2
chr10:114757999
chr10:114758100
chr10:114758200
chr10:114758300
chr10:114758400
chr10:114758500
Log2 variant effect
Alternative: A C G T
Significant
Not significant
Reference: A C G T
PhastCons
Primates
Mammals
Vertebrates
Functional scores
CADD v1.4
DeepSEA
Eigen
FATHMM-MKL
LINSIGHT
Motifs
Database: ENCODE
IRF
AP1
EP300
NFE2
HMGA1
NFE2L2
NFKB
NFE2L1::MAFG
IRF
YY1
TRIM28
FOXI1
TCF12
PRDM1
FOXQ1
FOXJ3
SOX21
FOXP3
JASPAR predictions
Motif count

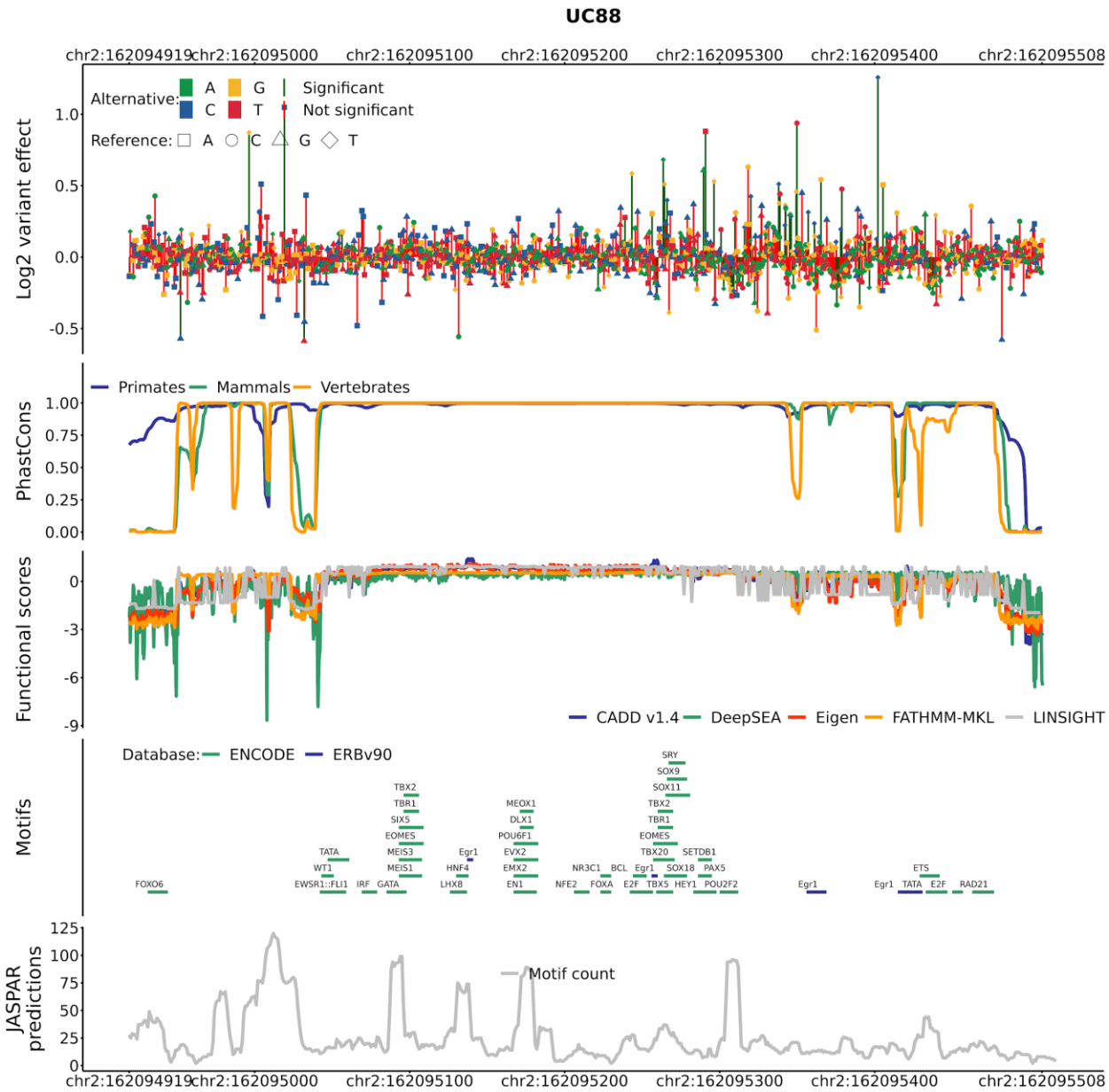
UC88
chr2:162094919
chr2:162095000
chr2:162095100
chr2:162095200
chr2:162095300
chr2:162095400
chr2:162095508
Alternative: A C G T
Significant
Not significant
Reference: A C G T
Log2 variant effect
1.0
0.5
0.0
-0.5
Primates
Mammals
Vertebrates
PhastCons
1.00
0.75
0.50
0.25
0.00
Functional scores
0
-3
-6
-9
CADD v1.4
DeepSEA
Eigen
FATHMM-MKL
LINSIGHT
Database: ENCODE ERBv90
Motifs
FOXO6
TATA
WT1
EWSR1::FLI1
IRF
GATA
TBX2
TBR1
SIX5
EOMES
MEIS3
MEIS1
Egr1
HNF4
LHX8
MEOX1
DLX1
POU6F1
EVX2
EMX2
EN1
NFE2
NR3C1
FOXA
BCL
E2F
Egr1
TBX5
SRY
SOX9
SOX11
TBX2
TBR1
EOMES
TBX20
HEY1
SETDB1
SOX18
PAX5
POU2F2
Egr1
ETS
Egr1
TATA
E2F
RAD21
JASPAR predictions
125
100
75
50
25
0
Motif count

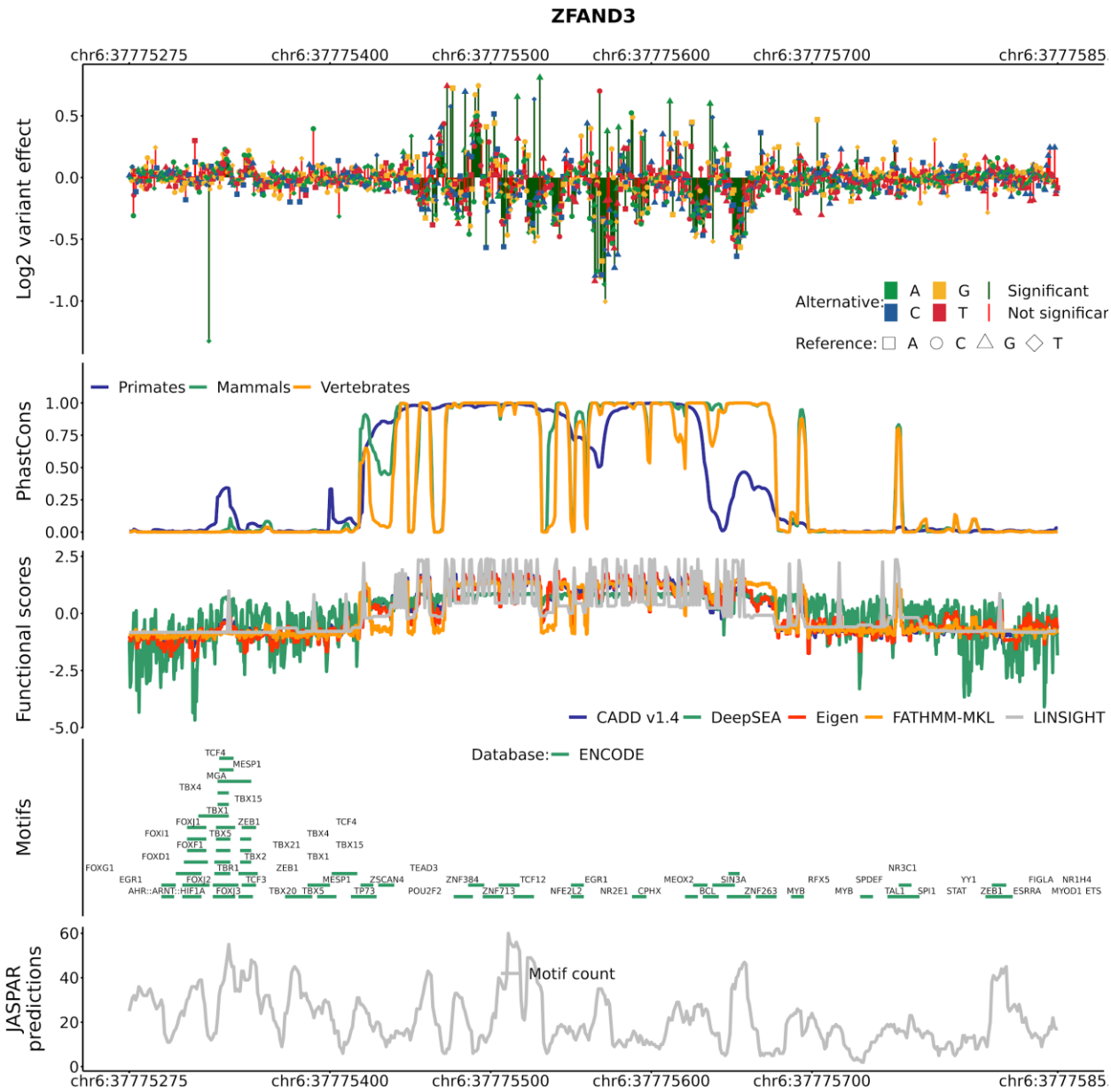
ZFAND3
chr6:37775275
chr6:37775400
chr6:37775500
chr6:37775600
chr6:37775700
chr6:3777585
Log2 variant effect
0.5
0.0
-0.5
-1.0
Alternative: A G C T
Significant
Not significar
Reference: A C G T
PhastCons
Primates
Mammals
Vertebrates
1.00
0.75
0.50
0.25
0.00
Functional scores
2.5
0.0
-2.5
-5.0
CADD v1.4
DeepSEA
Eigen
FATHMM-MKL
LINSIGHT
Motifs
Database: ENCODE
JASPAR predictions
Motif count
60
40
20
0

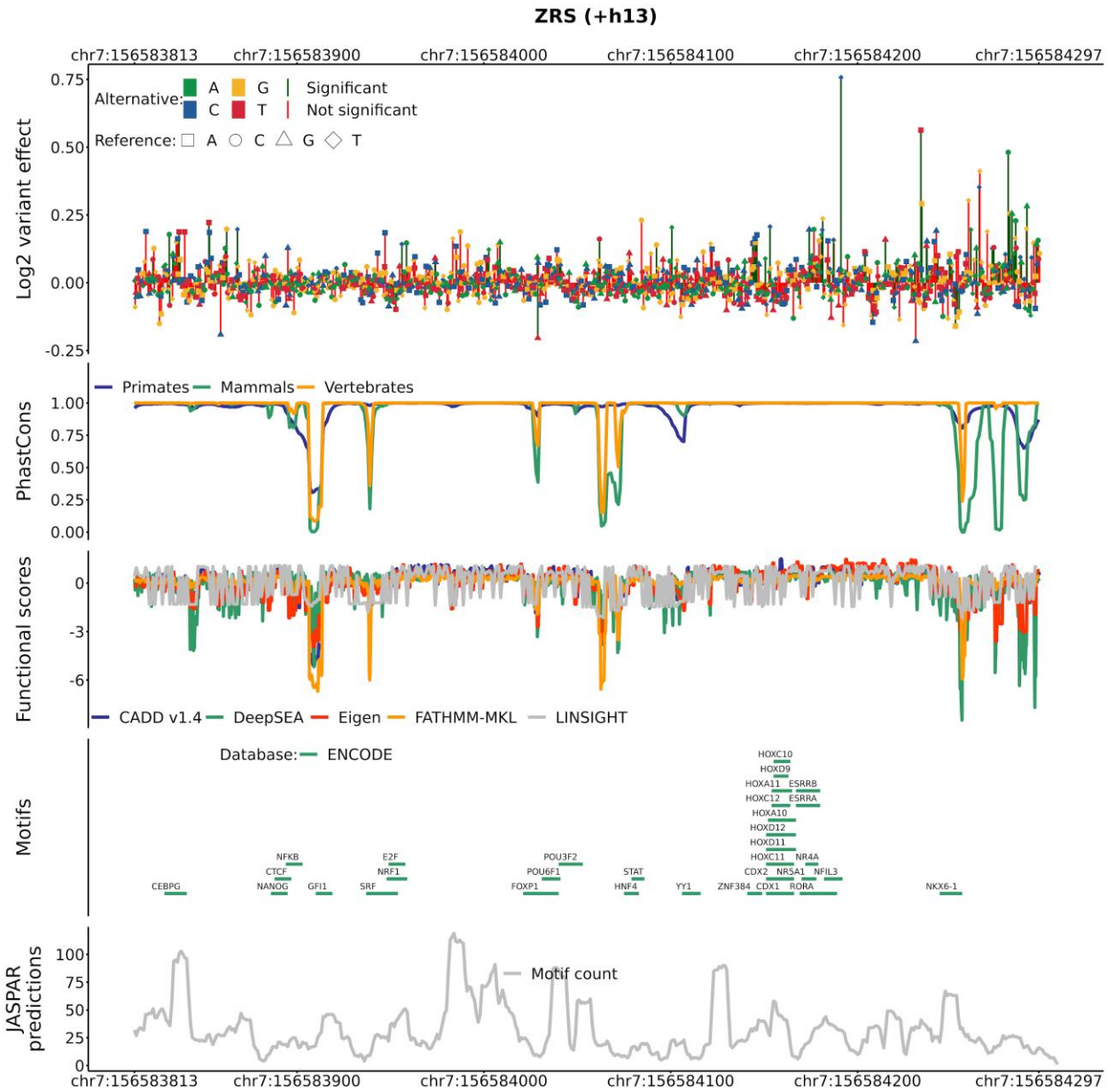
ZRS (+h13)
chr7:156583813
chr7:156583900
chr7:156584000
chr7:156584100
chr7:156584200
chr7:156584297
Log2 variant effect
Alternative: A C G T
Significant
Not significant
Reference: A C G T
PhastCons
Primates
Mammals
Vertebrates
Functional scores
CADD v1.4
DeepSEA
Eigen
FATHMM-MKL
LINSIGHT
Motifs
Database: ENCODE
HOXC10
HOXD9
HOXA11
ESRRB
HOXC12
ESRRA
HOXA10
HOXD12
HOXD11
HOXC11
NR4A
CDX2
NR5A1
NFIL3
ZNF384
CDX1
RORA
NFKB
CTCF
NANOG
GFI1
E2F
NRF1
SRF
POU3F2
POU6F1
FOXP1
STAT
HNF4
YY1
CEBPG
NKX6-1
JASPAR predictions
Motif count

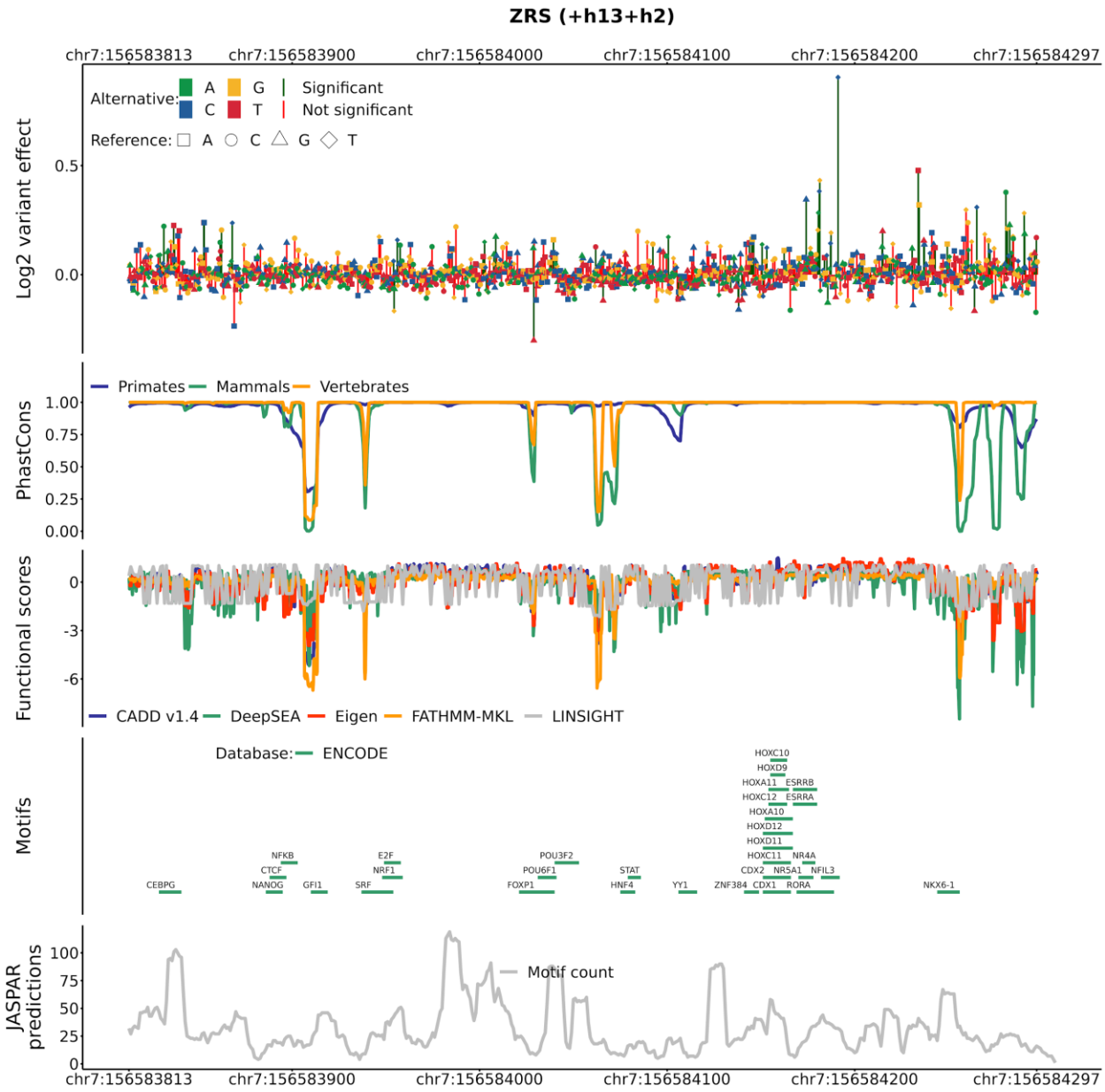

Overlay of inferred variant effects for SNVs with available annotation data for all enhancer elements. Motif predictions overlayed with biochemical evidence from ChIP-seq experiments were obtained from Ensembl Regulatory Build (ERB)[33] and ENCODE[3] annotations. JASPAR motif predictions were obtained from the JASPAR 2018[6] release.

Supplementary Figure 10

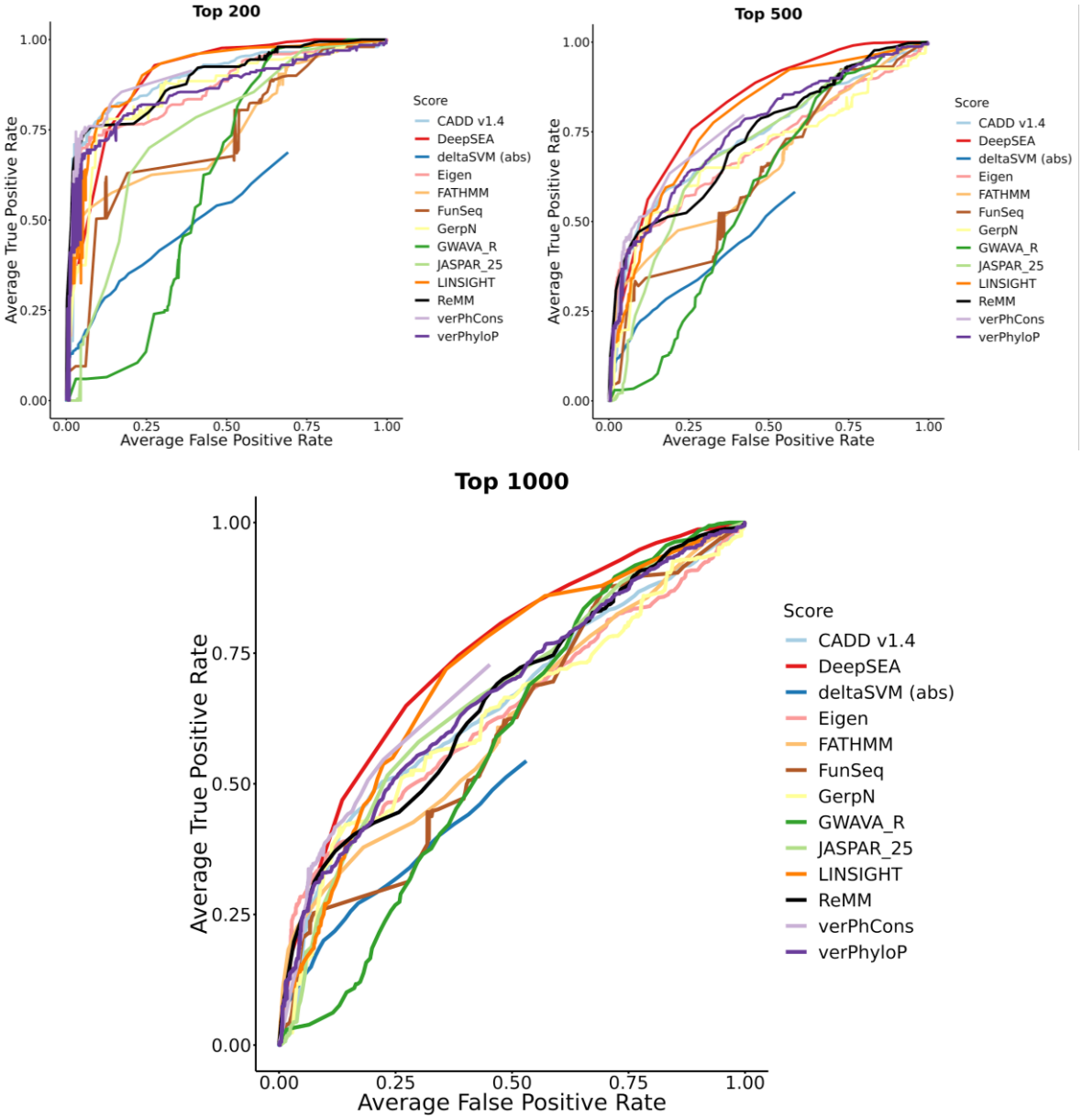

Receiver operating characteristic curves of computational scores used for the binary classification of promoter variants. Plots are divided into the classification of the top 200, 500 and 1000 high-effect promoter variants (p-value < 10^{-5}, min tags 10) versus the same number of random variants (per element) with no expression effect (log_2 value < 0.05, min tags 10). Curves show the average performance across 100 classification rounds (see Methods). If multiple scores exist per method, only the best score is plotted (see Supplementary Table 16).

Supplementary Figure 11

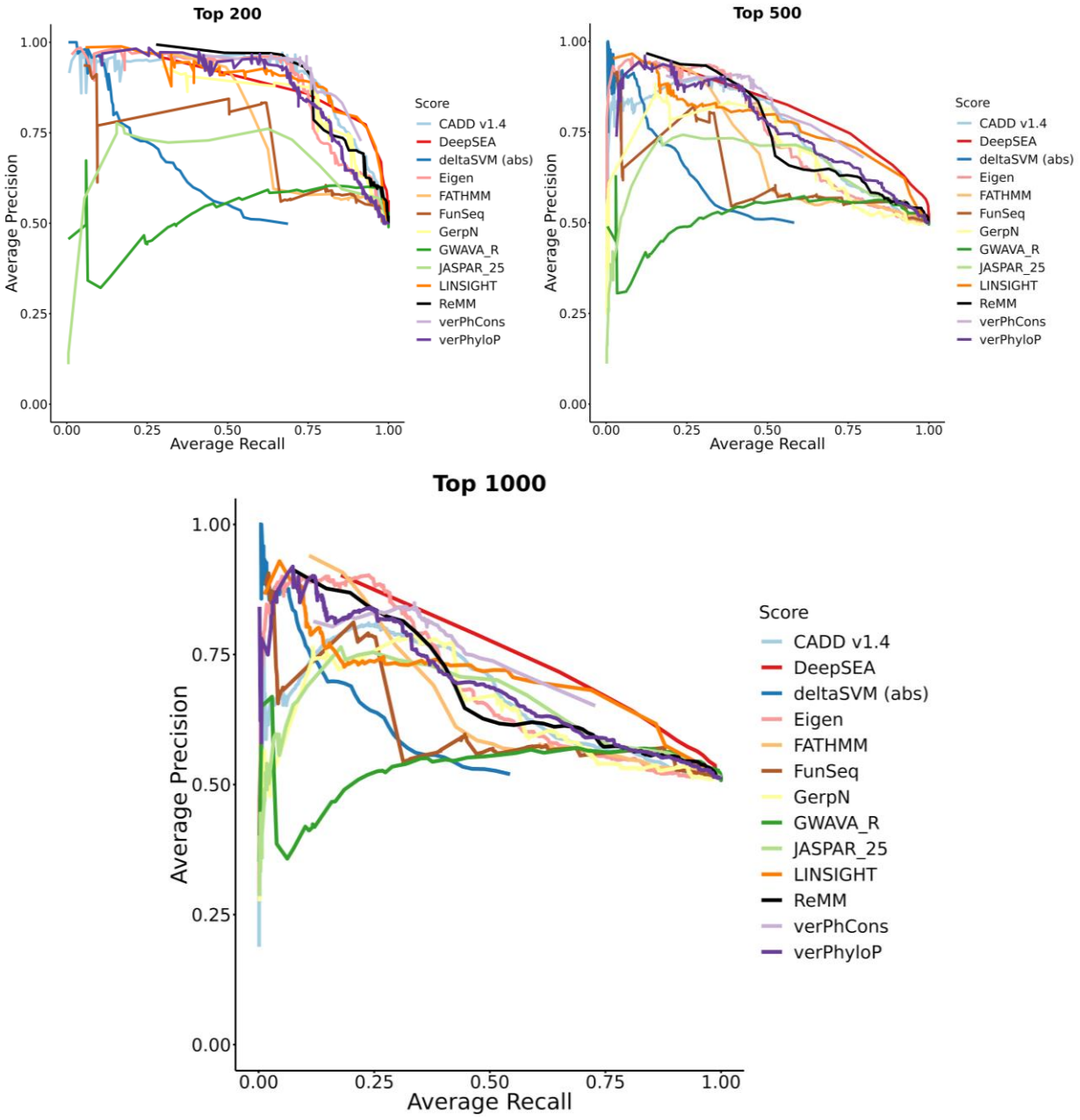

Precision-recall curves of computational scores used for the binary classification of promoter variants. Plots are divided into the classification of the top 200, 500 and 1000 high-effect promoter variants (p-value < 10^{-5}, min tags 10) versus the same number of random variants (per element) with no expression effect (log_2 value < 0.05, min tags 10). Curves show the average across 100 classification rounds (see Methods). If multiple scores exist per method, only the best score is plotted (see Supplementary Table 16).

Supplementary Figure 12

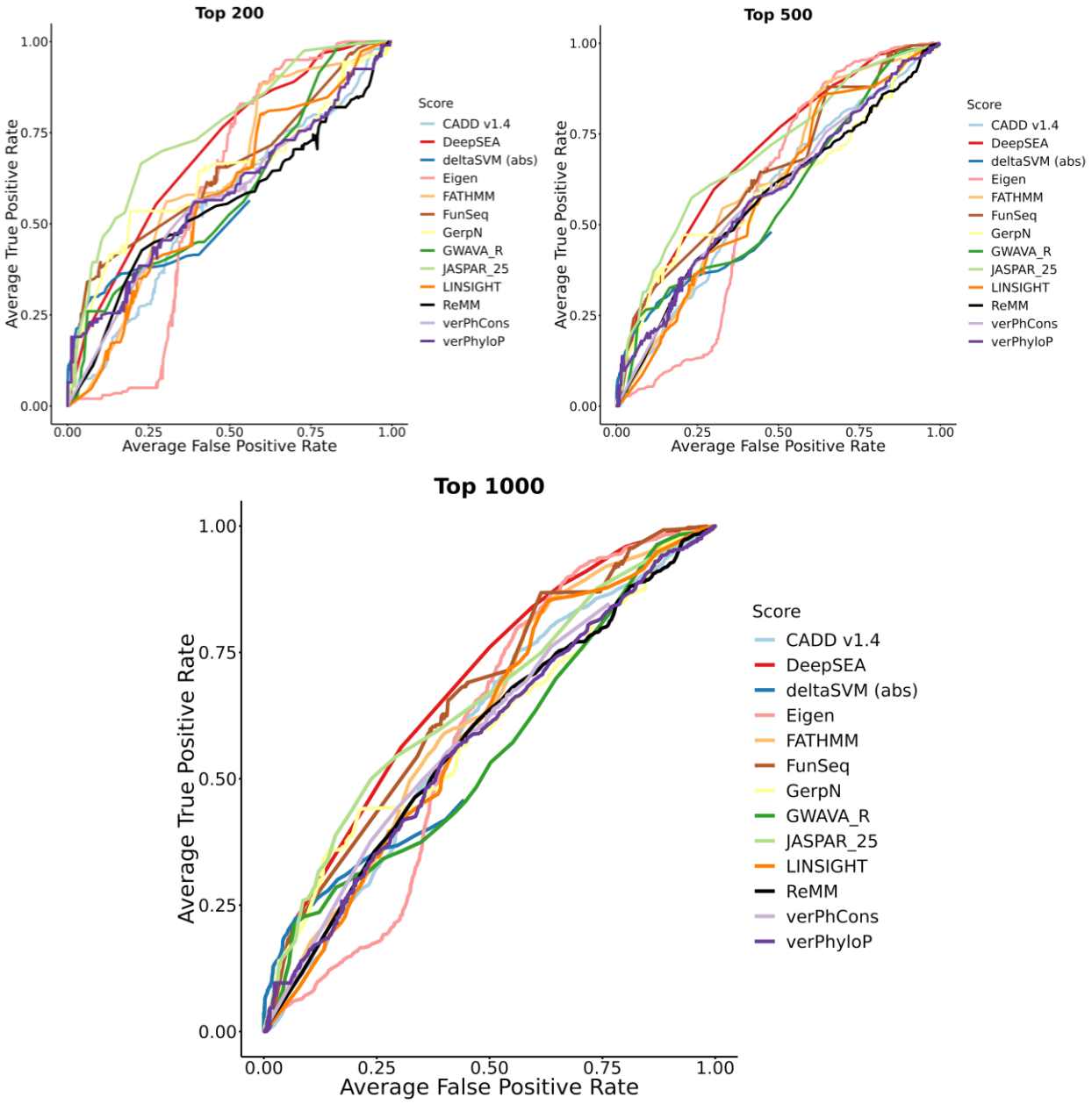

Receiver operating characteristic curves of computational scores used for the binary classification of enhancer variants. Plots are divided into the classification of the top 200, 500 and 1000 high-effect enhancer variants (p-value < 10^{-5}, min tags 10) versus the same number of random variants (per element) with no expression effect (log_2 expression effect < 0.05, min tags 10). Curves show the average across 100 classification rounds (see Methods). If multiple scores exist per method, only the best score is plotted (see Supplementary Table 17).

Supplementary Figure 13

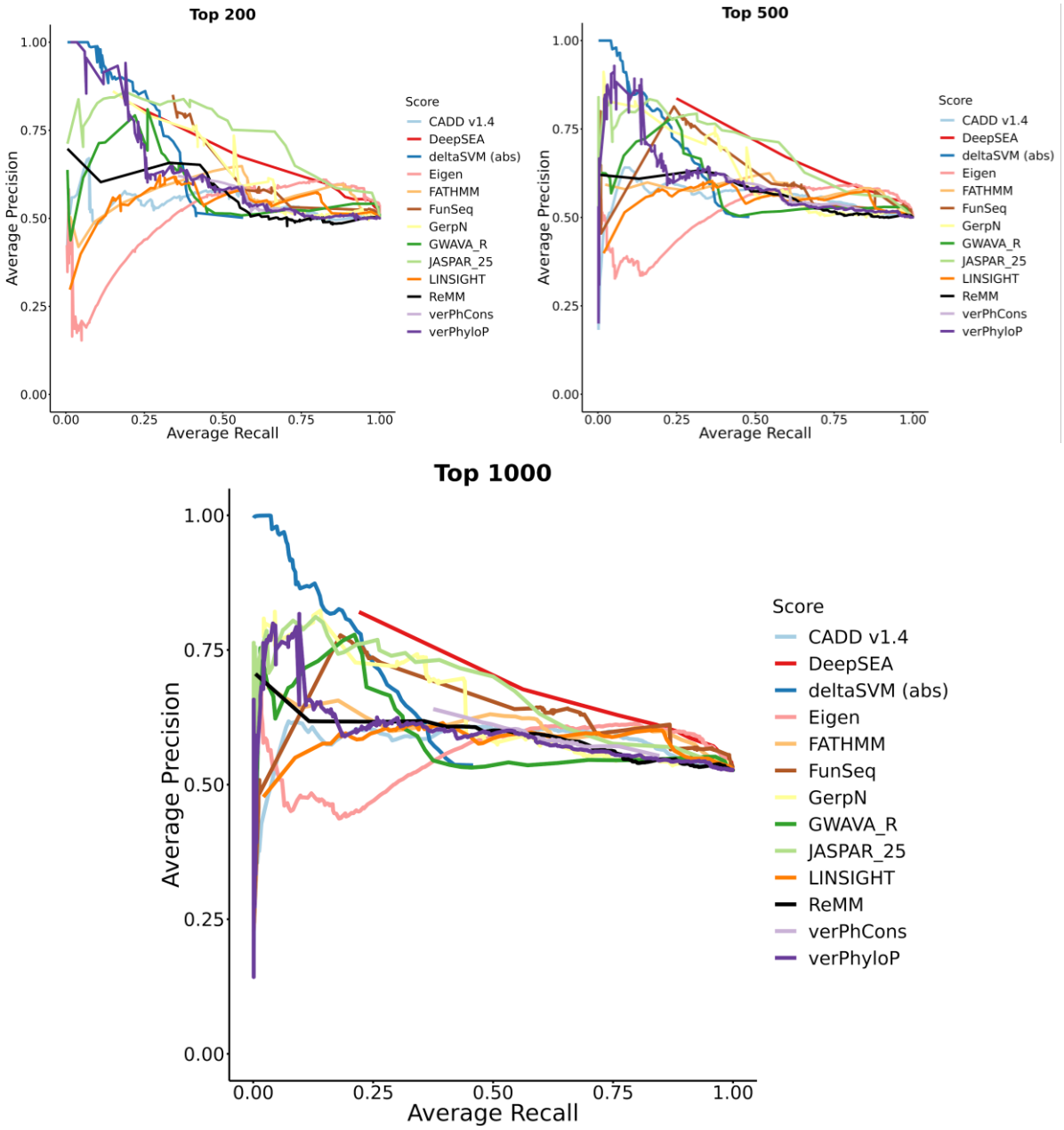

Precision-recall curves of computational scores used for the binary classification of enhancer variants. Plots are divided into the classification of the top 200, 500, and 1000 high-effect enhancer variants (p-value < 10^{-5}, min tags 10) versus the same number of random variants (per element) with no expression effect (log_2 expression effect < 0.05, min tags 10). Curves show the average across 100 classification rounds (see Methods). If multiple scores exist per method only the best score is plotted (see Supplementary Table 17).

Supplementary Tables

Supplementary Table 1

Tested promoter sequences. Note that the construct length of MSMB is 2 bp longer than the described reference genome coordinate range, due to an insertion polymorphism present in the construct. Vector sequences for pGL4.11b and pGL4.11c are available for download from NCBI GenBank (accessions MK484103 and MK484104, respectively) and from our OSF project 75B2M.

Name	Genomic coordinates (GRCh37/GRCh38)	Transcript	Associated Phenotype	Luciferase vector	MPRA vector	Cell line	Transf. time (hr)	Fold Ch. (Wild type)	Fold Ch. (MPRA)	Construct size (bp)
F9	X:138,612,622-138,612,924 X:139,530,463-139,530,765	NM_000133.3	Hemophilia B	pGL4.11b	pGL4.11c	HepG2	24	2.6	2.1	303
FOXE1	9:100,615,537-100,616,136 9:97,853,255-97,853,854	NM_004473.3	Thyroid cancer	pGL4.11b	pGL4.11c	HeLa	24	4.2	2.5	600
GP1BB	22:19,710,789-19,711,173 22:19,723,266-19,723,650	NM_000407.4	Bernard-Soulier Syndrome	pGL4.11b	pGL4.11c	HEL 92.1.7	24	22.1	12.3	385
HBB	11:5,248,252-5,248,438 11:5,227,022-5,227,208	NM_000518.4	Thalassemia	pGL4.11b	pGL4.11c	HEL 92.1.7	24	14.3	8.4	187
HBG1	11:5,271,035-5,271,308 11:5,249,805-5,250,078	NM_000559.2	Hereditary persistence of fetal hemoglobin	pGL4.11b	pGL4.11c	HEL 92.1.7	24	118.1	41.8	274
HNF4A (P2)	20:42,984,160-42,984,444 20:44,355,520-44,355,804	NM_175914.4	Maturity-onset diabetes of the young (MODY)	pGL4.11b	pGL4.11c	HEK293T	24	2.8	1.3	285
LDLR	19:11,199,907-11,200,224 19:11,089,231-11,089,548	NM_000527.4	Familial hypercholesterolemia	pGL4.11b	pGL4.11b	HepG2	24	110.7	76.6	318
MSMB	10:51,548,988-51,549,578 10:46,046,244-46,046,834	NM_002443.3	Prostate cancer	pGL4.11b	pGL4.11c	HEK293T	24	8.4	3.4	593
PKLR	1:155,271,186-155,271,655 1:155,301,395-155,301,864	NM_000298.5	Pyruvate kinase deficiency	pGL4.11b	pGL4.11c	K562	48	29.4	9.6	470
TERT	5:1,295,104-1,295,362 5:1,294,989-1,295,247	NM_198253.2	Various types of cancer	pGL4.11b	pGL4.11b	HEK293T, SF7996	24	231.8,5.2	148.2, 2.7	259

Supplementary Table 2

Tested enhancer sequences. Note that the construct length of MYC (rs11986220) is 1 bp longer than the described reference genome coordinate range, due to an insertion polymorphism present in the construct. Human ZRS (hZRS, a limb-specific enhancer of the Sonic hedgehog gene) was co-transfected with HOXD13 and HOXD13+HAND2. UC88 is an ultraconserved element, which has not been previously associated with a phenotype. Vector sequences for pGL3c, pGL4.23c/d, and pGL4Zc are available for download from NCBI GenBank (accessions MK484107, MK484105/MK484106, and MK484108, respectively) and our OSF project 75B2M.

Name	Genomic coordinates (GRCh37/GRCh38)	Associated Phenotype	Luciferase vector	MPRA vector	Cell line	Transf. time (hr)	Fold Ch. (Wild type)	Fold Ch. (MPRA)	Construct (bp)
BCL11A +58	2:60,722,075-60,722,674 2:60,494,940-60,495,539	Sickle cell disease	pGL4.23	pGL4.23d	HEL 92.1.7	24	2.5	1.7	600
IRF4	6:396,143-396,593 6:396,143-396,593	Human pigmentation	pGL4.23	pGL4.23d	SK-MEL-28	24	44.5	16.3	451
IRF6	1:209,989,135-209,989,735 1:209,815,790-209,816,390	Cleft lip	pGL4.23	pGL4.23c	HaCaT	24	17.0	16.7	600
MYC (rs 6983267)	8:128,413,074-128,413,673 8:127,400,829-127,401,428	Various types of cancer	pGL4.23	pGL4.23c	HEK293T	32, 20nM LiCl added after 24hr	2.8	0.7	600
MYC (rs 11986220)	8:128,531,515-128,531,977 8:127,519,270-127,519,732	Various types of cancer	pGL4.23	pGL4.23d	LNCaP + 100nM DHT	24	5.5	3.2	464
RET	10:43,581,927-43,582,526 10:43,086,479-43,087,078	Hirschsprung	pGL3	pGL3c	Neuro-2a	24	2.0	0.9	600
SORT1	1:109,817,274-109,817,873 1:109,274,652-109,275,251	Plasma low-density lipoprotein cholesterol & myocardial infarction	pGL4.23	pGL4.23c	HepG2	24	235.3	202.2	600
TCF7L2	10:114,757,999-114,758,598 10:112,998,240-112,998,839	Type 2 diabetes	pGL4.23	pGL4.23d	MIN6	24	9.0	2.7	600
UC88	2:162,094,919-162,095,508 2:161,238,408-161,238,997	-	pGL4.23	pGL4.23c	Neuro-2a	24	9.3	5.4	590
ZFAND3	6:37,775,275-37,775,853 6:37,807,499-37,808,077	Type 2 diabetes	pGL4.23	pGL4.23c	MIN6	24	14.3	7.3	579
ZRS	7:156,583,813-156,584,297 7:156,791,119-156,791,603	Limb malformations	TATA-pGL4m (EV087)*	pGL4Zc	NIH/3T3 (with HOXD13/ HOXD13+HAND2)	24	4.2/ 2.0	3.7/ 2.6	485

Supplementary Table 3

Saturation mutagenesis statistic. Twenty-four tag assignments obtained by saturation mutagenesis. A minimum read coverage of three was required for reads aligning across the construct length before a tag was considered in analysis.

Assignment	Construct length	Associated tags	Fraction WT inserts	Variants called per insert	Mutation rate	SNV cov.	1bp-del cov	Ave #tags per SNV	Ave #tags per 1bp-del
BCL11A	600	263,000	0.03%	6.00	1.00%	100.00%	61.00%	809.1	40.9
F9	303	134,665	43.22%	0.96	0.32%	99.56%	54.13%	132.7	20.7
FOXE1	600	148,459	19.61%	2.00	0.33%	100.00%	56.50%	154.9	21.2
GP1BB	385	485,856	31.82%	1.25	0.33%	99.91%	66.23%	488.4	89.8
HBB	187	2,010,638	55.62%	0.62	0.33%	100.00%	71.12%	2064.4	414.5
HBG1	274	150,499	43.36%	0.92	0.34%	100.00%	55.11%	155.7	31.4
HNF4A	285	555,705	40.47%	0.98	0.35%	100.00%	63.16%	595.0	105.5
IRF4	451	342,770	25.43%	1.66	0.37%	100.00%	63.64%	396.8	57.7
IRF6	601	33,174	14.03%	2.33	0.39%	99.45%	31.45%	41.6	2.9
LDLR.2	318	159,867	39.27%	1.04	0.33%	100.00%	56.92%	154.5	45.6
LDLR	318	96,145	17.78%	1.99	0.62%	100.00%	58.80%	185.3	35.6
MSMB	593	738,972	15.72%	2.07	0.35%	100.00%	67.12%	817.3	109.3
MYC (rs11986220)	464	541,564	2.45%	2.52	0.54%	100.00%	55.39%	884.1	73.7
MYC (rs6983267)	600	70,234	16.34%	2.05	0.34%	99.67%	43.33%	75.4	8.8
PKLR	470	119,675	22.88%	1.75	0.37%	99.93%	45.74%	125.5	12.7
RET	600	257,630	29.19%	1.51	0.25%	99.94%	55.50%	199.6	41.5
SORT1.2	600	132,222	15.78%	2.07	0.34%	99.94%	49.83%	139.5	27.3
SORT1-flip	600	192,602	21.12%	1.73	0.29%	99.61%	50.83%	169.8	31.7
SORT1	600	45,509	12.78%	2.29	0.38%	99.72%	41.67%	53.9	9.0
TCF7L2	600	120,996	19.03%	1.85	0.31%	99.06%	42.33%	119.8	9.9
TERT	259	276,048	19.22%	1.76	0.68%	100.00%	57.53%	549.3	103.9
UC88	590	87,948	11.16%	2.44	0.41%	99.77%	52.71%	111.1	17.2
ZFAND3	579	183,352	6.52%	3.00	0.52%	99.94%	63.21%	297.5	38.4
ZRS	485	850,422	16.94%	2.07	0.43%	100.00%	66.19%	1130.2	192.9

Supplementary Table 4

Obtained RNA and DNA tag counts across 29 experiments with each 3 transfection replicates. MYC (rs11986220) was abbreviated to MYCs1. MYC (rs6983267) was abbreviated to MYCs2. TERT-GBM-SiGABPA and TERT-GBM-SiScramble were abbreviated to TERT-GAa and TERT-GSc, respectively.

Exp.	Tags	DNA	RNA	Assign. tags	[%]	DNA assigned	[%]	RNA assigned	[%]	WT tags	[%]	Variants	Var/ tag
BCL11A-1	298,966	5,639,266	12,078,937	219,172	73.3	4,782,063	84.8	10,265,384	85.0	63	0.0	1,295,570	5.6
BCL11A-2	285,273	5,482,187	7,401,487	218,289	76.5	4,660,218	85.0	6,302,212	85.1	64	0.0	1,290,502	5.9
BCL11A-3	298,554	4,098,878	18,055,670	218,565	73.2	3,466,623	84.6	15,372,758	85.1	65	0.0	1,291,930	5.9
F9-1	342,802	4,373,175	2,377,127	110,714	32.3	2,941,983	67.3	1,532,333	64.5	48,303	43.6	104,215	0.9
F9-2	393,783	5,913,265	3,343,343	114,478	29.1	3,895,338	65.9	2,142,187	64.1	50,414	44.0	106,735	0.9
F9-3	399,823	5,288,624	3,885,413	114,669	28.7	3,467,454	65.6	2,489,575	64.1	50,479	44.0	106,929	0.9
FOXE1-1	371,106	5,844,884	12,244,334	104,919	28.3	5,071,439	86.8	10,307,674	84.2	21,761	20.7	202,298	1.9
FOXE1-2	403,744	6,652,522	14,494,525	107,339	26.6	5,746,967	86.4	12,188,942	84.1	22,141	20.6	207,434	1.9
FOXE1-3	343,043	5,769,389	9,841,232	101,484	29.6	5,048,490	87.5	8,271,983	84.1	21,082	20.8	195,486	1.9
GP1BB-1	486,707	6,643,587	43,000,079	355,564	73.1	6,072,911	91.4	39,803,462	92.6	119,228	33.5	424,334	1.2
GP1BB-2	578,012	6,367,523	83,229,576	380,180	65.8	5,752,248	90.3	77,001,869	92.5	126,862	33.4	455,869	1.2
GP1BB-3	523,517	6,606,471	54,650,491	366,222	70.0	6,013,969	91.0	50,533,028	92.5	122,381	33.4	438,316	1.2
HBB-1	695,586	2,525,201	6,773,900	472,421	67.9	1,900,539	75.3	4,963,191	73.3	262,233	55.5	294,795	0.6
HBB-2	791,164	3,308,597	9,589,115	528,865	66.8	2,472,343	74.7	6,979,796	72.8	293,299	55.5	330,805	0.6
HBB-3	762,560	3,072,583	9,994,200	511,302	67.1	2,299,623	74.8	7,295,451	73.0	283,360	55.4	319,728	0.6
HBG1-1	185,967	5,162,824	14,791,792	120,433	64.8	4,949,744	95.9	14,271,858	96.5	53,434	44.4	107,176	0.9
HBG1-2	175,408	5,018,528	12,030,988	120,273	68.6	4,820,630	96.1	11,613,726	96.5	53,323	44.3	107,094	0.9
HBG1-3	184,771	4,015,818	16,150,944	120,736	65.3	3,837,946	95.6	15,589,891	96.5	53,489	44.3	107,672	0.9
HNF4A-1	543,584	10,113,379	13,852,568	463,549	85.3	9,618,823	95.1	13,191,109	95.2	190,726	41.1	446,023	1.0
HNF4A-2	542,733	8,186,687	14,864,839	462,195	85.2	7,774,829	95.0	14,159,802	95.3	190,130	41.1	444,659	1.0
HNF4A-3	561,090	9,046,256	19,619,664	464,283	82.7	8,580,599	94.9	18,684,171	95.2	191,001	41.1	446,731	1.0
IRF4-1	728,932	32,932,153	27,880,905	284,578	39.0	30,206,386	91.7	25,292,566	90.7	75,644	26.6	450,535	1.6
IRF4-2	567,407	29,656,398	15,481,379	277,818	49.0	27,343,569	92.2	14,048,886	90.7	74,623	26.9	435,912	1.6
IRF4-3	740,887	31,370,721	29,406,932	282,446	38.1	28,740,624	91.6	26,627,825	90.5	75,361	26.7	445,782	1.6
IRF6-1	151,722	9,739,620	8,560,920	25,571	16.9	9,387,362	96.4	8,135,409	95.0	3,200	12.5	60,112	2.4
IRF6-2	119,932	7,757,534	5,329,576	25,366	21.2	7,495,059	96.6	5,057,007	94.9	3,175	12.5	59,593	2.3
IRF6-3	172,660	8,680,655	14,173,746	25,715	14.9	8,324,169	95.9	13,503,071	95.3	3,222	12.5	60,449	2.4
LDLR-1	130,525	5,638,805	1,273,404	49,591	38.0	5,105,608	90.5	1,064,829	83.6	9,909	20.0	90,699	1.8
LDLR-2	161,476	4,213,346	2,399,123	54,118	33.5	3,761,940	89.3	2,017,701	84.1	10,524	19.4	100,845	1.9
LDLR-3	161,006	4,749,497	2,363,067	53,263	33.1	4,256,408	89.6	1,986,608	84.1	10,462	19.6	98,735	1.9
LDLR.2-1	191,367	4,867,064	17,645,358	126,173	65.9	4,508,376	92.6	16,491,468	93.5	51,876	41.1	122,565	1.0
LDLR.2-2	190,807	4,788,780	18,280,817	126,106	66.1	4,435,204	92.6	17,086,851	93.5	51,828	41.1	122,517	1.0
LDLR.2-3	193,991	5,181,072	17,957,299	126,228	65.1	4,800,137	92.6	16,776,656	93.4	51,907	41.1	122,565	1.0
MSMB-1	685,961	6,701,186	17,507,026	601,035	87.6	6,224,222	92.9	16,299,420	93.1	97,346	16.2	1,221,342	2.0
MSMB-2	682,883	7,320,007	13,849,695	601,313	88.1	6,805,746	93.0	12,888,944	93.1	97,407	16.2	1,221,803	2.0
MSMB-3	670,037	6,390,696	11,781,755	594,914	88.8	5,944,966	93.0	10,973,851	93.1	96,308	16.2	1,208,546	2.0
MYCs1-1	553,764	6,429,193	6,814,583	113,598	20.5	1,731,164	26.9	1,545,201	22.7	2,878	2.5	268,226	2.4

MYCs1-2	687,851	8,899,471	6,461,177	140,778	20.5	2,369,217	26.6	1,463,349	22.6	3,683	2.6	331,779	2.4
MYCs1-3	657,970	8,930,292	26,961,629	113,323	17.2	2,363,234	26.5	6,025,793	22.3	2,933	2.6	266,889	2.4
MYCs2-1	242,405	10,383,834	25,278,391	47,311	19.5	9,761,909	94.0	23,938,321	94.7	7,589	16.0	94,555	2.0
MYCs2-2	238,102	10,450,639	24,253,590	47,256	19.8	9,828,501	94.0	22,978,218	94.7	7,569	16.0	94,471	2.0
MYCs2-3	230,792	10,097,657	22,738,159	47,230	20.5	9,500,218	94.1	21,544,683	94.8	7,565	16.0	94,496	2.0
PKLR-24h-1	173,084	60,070,760	2,163,171	46,646	26.9	58,491,803	97.4	1,955,698	90.4	11,769	25.2	71,122	1.5
PKLR-24h-2	138,614	60,223,777	1,429,279	45,523	32.8	58,768,966	97.6	1,288,776	90.2	11,463	25.2	69,411	1.5
PKLR-24h-3	149,197	63,764,262	1,519,080	44,389	29.8	62,203,474	97.6	1,359,753	89.5	11,326	25.5	67,361	1.5
PKLR-48h-1	136,270	7,455,307	4,969,789	49,614	36.4	7,208,398	96.7	4,723,095	95.0	12,465	25.1	75,773	1.5
PKLR-48h-2	154,324	8,986,733	6,822,420	50,683	32.8	8,680,506	96.6	6,504,490	95.3	12,624	24.9	77,809	1.5
PKLR-48h-3	191,654	8,862,707	7,912,466	53,256	27.8	8,510,594	96.0	7,457,785	94.3	13,132	24.7	82,482	1.5
RET-1	212,407	6,490,718	5,332,490	162,442	76.5	5,777,363	89.0	4,740,932	88.9	46,024	28.3	247,543	1.5
RET-2	209,619	5,497,713	9,949,970	163,221	77.9	4,891,505	89.0	8,864,017	89.1	46,268	28.3	248,715	1.5
RET-3	228,711	7,153,233	9,256,893	163,304	71.4	6,351,594	88.8	8,224,281	88.8	46,292	28.3	248,789	1.5
SORT1.2-1	361,601	18,633,183	6,148,782	103,019	28.5	14,099,010	75.7	4,443,731	72.3	17,317	16.8	204,598	2.0
SORT1.2-2	377,463	15,970,828	7,364,456	103,869	27.5	12,028,676	75.3	5,314,027	72.2	17,426	16.8	206,638	2.0
SORT1.2-3	268,226	10,332,218	5,286,779	102,015	38.0	7,838,126	75.9	3,903,519	73.8	17,227	16.9	202,268	2.0
SORT1-1	746,577	16,673,908	31,367,939	39,578	5.3	14,474,306	86.8	24,750,248	78.9	5,307	13.4	88,124	2.2
SORT1-2	723,742	18,962,383	19,747,191	39,511	5.5	16,517,700	87.1	15,807,222	80.0	5,300	13.4	87,955	2.2
SORT1-3	748,314	20,320,267	17,953,683	39,516	5.3	17,683,609	87.0	14,046,965	78.2	5,309	13.4	87,964	2.2
SORT1-flip-1	331,589	12,166,621	29,066,644	140,787	42.5	9,953,413	81.8	24,014,577	82.6	31,099	22.1	235,726	1.7
SORT1-flip-2	313,075	11,542,062	25,124,427	140,650	44.9	9,455,478	81.9	20,763,311	82.6	31,109	22.1	235,379	1.7
SORT1-flip-3	317,684	11,916,102	25,362,908	140,795	44.3	9,759,092	81.9	20,955,947	82.6	31,113	22.1	235,724	1.7
TCF7L2-1	374,223	15,108,800	23,655,355	100,157	26.8	14,202,439	94.0	22,260,177	94.1	18,273	18.2	185,613	1.9
TCF7L2-2	417,767	14,956,164	32,468,628	100,350	24.0	14,006,822	93.7	30,546,904	94.1	18,328	18.3	185,912	1.9
TCF7L2-3	368,615	14,520,864	23,374,207	100,134	27.2	13,646,053	94.0	21,988,603	94.1	18,278	18.3	185,497	1.9
TERT-HEK-1	335,270	11,248,490	11,378,602	58,565	17.5	7,294,186	64.8	7,127,589	62.6	13,188	22.5	94,368	1.6
TERT-HEK-2	171,124	2,560,571	3,994,303	54,373	31.8	1,678,719	65.6	2,574,708	64.5	12,301	22.6	87,278	1.6
TERT-HEK-3	183,808	3,252,096	3,789,458	55,035	29.9	2,132,221	65.6	2,403,315	63.4	12,438	22.6	88,395	1.6
TERT-GBM-1	355,220	13,418,248	19,211,451	58,007	16.3	8,720,079	65.0	12,333,250	64.2	13,065	22.5	93,285	1.6
TERT-GBM-2	267,946	11,585,462	8,259,377	56,500	21.1	7,598,877	65.6	5,308,817	64.3	12,796	22.6	90,455	1.6
TERT-GBM-3	321,270	10,799,638	15,808,970	57,477	17.9	7,012,582	64.9	10,147,049	64.2	12,968	22.6	92,378	1.6
TERT-GAa-1	330,418	13,997,031	12,720,466	54,526	16.5	9,157,350	65.4	8,074,884	63.5	12,293	22.5	87,683	1.6
TERT-GAa-2	273,034	13,438,634	7,480,710	52,841	19.4	8,872,520	66.0	4,759,939	63.6	11,896	22.5	84,944	1.6
TERT-GAa-3	330,409	13,973,219	11,210,584	54,503	16.5	9,142,186	65.4	7,061,935	63.0	12,263	22.5	87,683	1.6
TERT-GSc-1	274,950	15,911,173	6,513,278	54,440	19.8	10,480,550	65.9	4,149,292	63.7	12,280	22.6	87,358	1.6
TERT-GSc-2	313,078	15,921,742	9,269,517	55,079	17.6	10,438,703	65.6	5,878,186	63.4	12,447	22.6	88,329	1.6
TERT-GSc-3	319,046	16,567,050	9,177,995	54,956	17.2	10,870,900	65.6	5,814,748	63.4	12,434	22.6	88,139	1.6
UC88-1	189,033	10,320,132	12,162,659	58,087	30.7	8,982,208	87.0	10,610,535	87.2	6,939	11.9	135,643	2.3
UC88-2	282,779	13,218,404	25,762,258	58,905	20.8	11,430,470	86.5	22,389,889	86.9	7,019	11.9	137,570	2.3
UC88-3	130,950	6,816,894	6,412,974	57,784	44.1	5,958,971	87.4	5,621,456	87.7	6,883	11.9	134,912	2.3
ZFAND3-1	762,485	13,009,004	9,895,152	146,235	19.2	5,678,835	43.7	4,176,057	42.2	10,071	6.9	427,345	2.9
ZFAND3-2	730,676	15,242,143	8,146,864	144,184	19.7	6,739,354	44.2	3,433,906	42.2	9,927	6.9	421,275	2.9
ZFAND3-3	739,848	15,163,717	7,536,228	145,076	19.6	6,669,983	44.0	3,179,378	42.2	9,994	6.9	423,932	2.9
ZRS-h13-1	753,735	5,879,814	15,487,602	614,082	81.5	5,123,141	87.1	13,538,056	87.4	106,980	17.4	1,247,544	2.0

ZRS-h13-2	697,780	5,652,278	5,038,577	581,126	83.3	4,948,648	87.6	4,404,719	87.4	101,040	17.4	1,181,566	2.0
ZRS-h13-3	764,586	6,731,343	15,815,800	620,257	81.1	5,866,656	87.2	13,817,121	87.4	108,107	17.4	1,259,238	2.0
ZRS-h13h2-1	714,593	4,064,366	13,354,202	590,306	82.6	3,544,054	87.2	11,695,065	87.6	102,860	17.4	1,199,781	2.0
ZRS-h13h2-2	719,151	4,510,062	11,064,121	594,407	82.7	3,935,117	87.3	9,680,563	87.5	103,505	17.4	1,208,072	2.0
ZRS-h13h2-3	736,156	4,822,109	15,527,744	604,186	82.1	4,203,127	87.2	13,583,482	87.5	105,191	17.4	1,228,001	2.0

Supplementary Table 5

Correlation of SORT1 and LDLR with different minimum required tags. Pearson and Spearman correlation coefficients between LDLR and SORT1 replicate experiments requiring different minimum number of tags readouts per substitution or 1 bp deletion variant included.

LDLR	Pearson	Spearman	SORT1	Pearson	Spearman
All	0.93292	0.81082	*All*	0.93912	0.83928
Min 10	0.97144	0.86273	*Min 10*	0.96099	0.86436
Min 20	0.97484	0.86045	*Min 20*	0.96796	0.87945
Min 30	0.97664	0.86358	*Min 30*	0.97311	0.89615
Min 40	0.97827	0.87610	*Min 40*	0.97626	0.90280
Min 50	0.98004	0.87905	*Min 50*	0.97793	0.90508

Supplementary Table 6

Variant coverage with different thresholds of required tags. Single nucleotide coverage and 1 bp deletion coverage obtained after combining transfection replicates, tabulated for different minimum numbers of tags. MYC (rs11986220) is abbreviated to MYCs1 and MYC (rs6983267) abbreviated to MYCs2. TERT-GBM-SiGABPA and TERT-GBM-SiScramble-2 are abbreviated to TERT-GAa and TERT-GSc, respectively.

Combined Exp.	Len.	All				Min 10 Obs				Min 20 Obs			
		SNVs		1bpDel		SNVs		1bpDel		SNVs		1bpDel	
BCL11A	600	1799	99.94%	263	43.83%	1798	99.89%	187	31.17%	1794	99.67%	167	27.83%
F9	303	904	99.45%	80	26.40%	888	97.69%	64	21.12%	852	93.73%	52	17.16%
FOXE1	600	1800	100.00%	248	41.33%	1793	99.61%	130	21.67%	1768	98.22%	111	18.50%
GP1BB	385	1154	99.91%	114	29.61%	1154	99.91%	85	22.08%	1154	99.91%	79	20.52%
HBB	187	561	100.00%	62	33.16%	561	100.00%	35	18.72%	561	100.00%	34	18.18%
HBG1	274	822	100.00%	85	31.02%	820	99.76%	68	24.82%	811	98.66%	61	22.26%
HNF4A	285	855	100.00%	122	42.81%	854	99.88%	77	27.02%	854	99.88%	69	24.21%
IRF4	451	1353	100.00%	157	34.81%	1353	100.00%	105	23.28%	1353	100.00%	91	20.18%
IRF6	601	1785	99.00%	121	20.13%	1676	92.96%	63	10.48%	1497	83.03%	41	6.82%
LDLR	318	954	100.00%	129	40.57%	945	99.06%	59	18.55%	924	96.86%	49	15.41%
LDLR.2	318	954	100.00%	139	43.71%	950	99.58%	74	23.27%	941	98.64%	57	17.92%
MSMB	593	1779	100.00%	247	41.65%	1778	99.94%	140	23.61%	1777	99.89%	124	20.91%
MYCs1	464	1392	100.00%	293	63.15%	1375	98.78%	183	39.44%	1339	96.19%	159	34.27%
MYCs2	600	1792	99.56%	158	26.33%	1715	95.28%	94	15.67%	1578	87.67%	77	12.83%
PKLR-24h	470	1407	99.79%	369	78.51%	1369	97.09%	134	28.51%	1279	90.71%	83	17.66%
PKLR-48h	470	1407	99.79%	387	82.34%	1379	97.80%	154	32.77%	1307	92.70%	94	20.00%
RET	600	1797	99.83%	165	27.50%	1776	98.67%	135	22.50%	1752	97.33%	127	21.17%
SORT1	600	1790	99.44%	137	22.83%	1710	95.00%	96	16.00%	1572	87.33%	76	12.67%
SORT1.2	600	1798	99.89%	200	33.33%	1787	99.28%	131	21.83%	1760	97.78%	114	19.00%
SORT1-flip	600	1791	99.50%	183	30.50%	1755	97.50%	129	21.50%	1709	94.94%	116	19.33%
TCF7L2	600	1770	98.33%	140	23.33%	1700	94.44%	101	16.83%	1650	91.67%	87	14.50%
TERT-GAa	259	777	100.00%	197	76.06%	769	98.97%	100	38.61%	747	96.14%	77	29.73%
TERT-GBM	259	777	100.00%	196	75.68%	770	99.10%	108	41.70%	751	96.65%	78	30.12%
TERT-GSc	259	777	100.00%	197	76.06%	769	98.97%	97	37.45%	750	96.53%	76	29.34%
TERT-HEK	259	777	100.00%	198	76.45%	770	99.10%	95	36.68%	753	96.91%	72	27.80%
UC88	590	1761	99.49%	203	34.41%	1706	96.38%	134	22.71%	1642	92.77%	112	18.98%
ZFAND3	579	1736	99.94%	276	47.67%	1735	99.88%	158	27.29%	1725	99.31%	140	24.18%
ZRS-h13	485	1455	100.00%	206	42.47%	1455	100.00%	116	23.92%	1455	100.00%	106	21.86%
ZRS-h13h2	485	1455	100.00%	207	42.68%	1455	100.00%	117	24.12%	1455	100.00%	106	21.86%
Average			99.79%		44.43%		98.43%		25.29%		95.97%		20.87%
Minimum			98.33%		20.13%		92.96%		10.48%		83.03%		6.82%
Maximum			100.00%		82.34%		100.00%		41.70%		100.00%		34.27%

Comb. Exp.	Len.	Min 30 Obs				Min 40 Obs				Min 50 Obs			
		SNVs		1bpDel		SNVs		1bpDel		SNVs		1bpDel	
BCL11A	600	1784	99.11%	153	25.50%	1772	98.44%	145	24.17%	1750	97.22%	141	23.50%
F9	303	821	90.32%	43	14.19%	790	86.91%	41	13.53%	768	84.49%	36	11.88%
FOXE1	600	1729	96.06%	101	16.83%	1685	93.61%	93	15.50%	1621	90.06%	86	14.33%
GP1BB	385	1153	99.83%	74	19.22%	1152	99.74%	72	18.70%	1145	99.13%	70	18.18%
HBB	187	561	100.00%	33	17.65%	561	100.00%	33	17.65%	559	99.64%	33	17.65%

HBG1	274	802	97.57%	55	20.07%	783	95.26%	47	17.15%	760	92.46%	46	16.79%
HNF4A	285	853	99.77%	69	24.21%	853	99.77%	67	23.51%	853	99.77%	66	23.16%
IRF4	451	1353	100.00%	84	18.63%	1344	99.33%	81	17.96%	1337	98.82%	80	17.74%
IRF6	601	1317	73.04%	32	5.32%	1158	64.23%	23	3.83%	1054	58.46%	13	2.16%
LDLR	318	892	93.50%	45	14.15%	843	88.36%	43	13.52%	787	82.49%	40	12.58%
LDLR.2	318	929	97.38%	50	15.72%	906	94.97%	47	14.78%	879	92.14%	44	13.84%
MSMB	593	1777	99.89%	117	19.73%	1776	99.83%	114	19.22%	1774	99.72%	113	19.06%
MYCs1	464	1267	91.02%	142	30.60%	1204	86.49%	126	27.16%	1132	81.32%	117	25.22%
MYCs2	600	1462	81.22%	67	11.17%	1330	73.89%	51	8.50%	1227	68.17%	48	8.00%
PKLR-24h	470	1170	82.98%	59	12.55%	1082	76.74%	48	10.21%	1007	71.42%	36	7.66%
PKLR-48h	470	1205	85.46%	66	14.04%	1126	79.86%	53	11.28%	1049	74.40%	48	10.21%
RET	600	1726	95.89%	119	19.83%	1665	92.50%	110	18.33%	1612	89.56%	101	16.83%
SORT1	600	1416	78.67%	66	11.00%	1280	71.11%	58	9.67%	1178	65.44%	54	9.00%
SORT1.2	600	1712	95.11%	103	17.17%	1665	92.50%	94	15.67%	1617	89.83%	83	13.83%
SORT1-flip	600	1661	92.28%	102	17.00%	1593	88.50%	95	15.83%	1539	85.50%	90	15.00%
TCF7L2	600	1605	89.17%	76	12.67%	1527	84.83%	64	10.67%	1458	81.00%	58	9.67%
TERT-GAa	259	714	91.89%	61	23.55%	676	87.00%	57	22.01%	631	81.21%	50	19.31%
TERT-GBM	259	721	92.79%	63	24.32%	682	87.77%	59	22.78%	646	83.14%	52	20.08%
TERT-GSc	259	716	92.15%	62	23.94%	675	86.87%	58	22.39%	636	81.85%	48	18.53%
TERT-HEK	259	718	92.41%	62	23.94%	682	87.77%	56	21.62%	639	82.24%	49	18.92%
UC88	590	1562	88.25%	98	16.61%	1453	82.09%	82	13.90%	1357	76.67%	75	12.71%
ZFAND3	579	1715	98.73%	129	22.28%	1689	97.24%	117	20.21%	1664	95.80%	101	17.44%
ZRS-h13	485	1454	99.93%	100	20.62%	1452	99.79%	97	20.00%	1451	99.73%	94	19.38%
ZRS-h13h2	485	1454	99.93%	99	20.41%	1453	99.86%	97	20.00%	1450	99.66%	95	19.59%
Average			92.91%		18.38%		89.49%		16.89%		86.25%		15.59%
Minimum			73.04%		5.32%		64.23%		3.83%		58.46%		2.16%
Maximum			100.00%		30.60%		100.00%		27.16%		99.77%		25.22%

Supplementary Table 7

Pearson correlation across different transfection replicates. Correlation from the three transfection replicates of fitted SNV and 1 bp deletion variant effects divided by their standard deviation (requiring at least 10 tags in each replicate). MYC (rs11986220) is abbreviated to MYCs1 and MYC (rs6983267) abbreviated to MYCs2. TERT-HEK293T, TER-GBM, TERT-GBM-SiGABPA and TERT-GBM-SiScramble-2 are abbreviated to TERT-H, TERT-G, TERT-GAa and TERT-GSc, respectively. The left side considers all estimates obtained, the right side tries to exclude nonsignificant allele effects by requiring a lenient p-value threshold (<0.01) in at least one of the replicates. We use the reduction in included alleles as a proxy for the proportion of alleles with regulatory activity for each element (Frac.). We note that this estimate is confounded by other factors of experimental reproducibility, as can be seen from the variance observed for elements with multiple experiments (LDLR, PKLR, SORT1, TERT).

	Min. 10 tags				**Min. 10 tags, excl. non-significant effects**				
Name	**Rep 1 v. 2**	**Rep 1 v. 3**	**Rep 2 v. 3**	**Mean**	**Rep 1 v. 2**	**Rep 1 v. 3**	**Rep 2 v. 3**	**Mean**	**Frac.**
BCL11A	0.38 (1937)	0.42 (1938)	0.35 (1938)	0.38	0.70 (107)	0.69 (108)	0.66 (95)	0.68	5%
F9	0.88 (863)	0.87 (861)	0.90 (865)	0.88	0.95 (196)	0.95 (215)	0.96 (210)	0.95	21%
FOXE1	0.17 (1827)	0.12 (1823)	0.18 (1827)	0.16	0.46 (65)	0.23 (63)	0.38 (52)	0.36	3%
GP1BB	0.88 (1226)	0.89 (1225)	0.88 (1227)	0.88	0.94 (268)	0.95 (249)	0.94 (276)	0.94	21%
HBB	0.78 (594)	0.75 (594)	0.77 (594)	0.77	0.89 (119)	0.89 (115)	0.89 (119)	0.89	19%
HBG1	0.92 (856)	0.92 (856)	0.91 (858)	0.92	0.96 (239)	0.95 (244)	0.94 (246)	0.95	27%
HNF4A	0.88 (922)	0.89 (922)	0.88 (922)	0.89	0.95 (192)	0.96 (182)	0.96 (171)	0.96	19%
IRF4	0.99 (1437)	0.99 (1438)	0.99 (1437)	0.99	0.99 (789)	0.99 (793)	0.99 (777)	0.99	52%
IRF6	0.96 (1347)	0.97 (1351)	0.96 (1347)	0.96	0.98 (340)	0.98 (390)	0.98 (371)	0.98	19%
LDLR	0.97 (930)	0.97 (928)	0.98 (936)	0.98	0.98 (354)	0.98 (352)	0.99 (369)	0.98	34%
LDLR.2	0.99 (979)	0.99 (979)	0.99 (979)	0.99	1.00 (455)	1.00 (454)	1.00 (448)	1.00	42%
MSMB	0.89 (1893)	0.88 (1894)	0.88 (1893)	0.88	0.96 (477)	0.95 (466)	0.95 (469)	0.95	23%
MYCs1	0.33 (1385)	0.26 (1355)	0.35 (1376)	0.31	0.58 (83)	0.61 (64)	0.69 (77)	0.63	5%
MYCs2	0.75 (1529)	0.76 (1529)	0.76 (1529)	0.75	0.92 (136)	0.93 (133)	0.93 (138)	0.93	7%
PKLR 24h	0.87 (1220)	0.85 (1208)	0.86 (1209)	0.86	0.94 (328)	0.93 (326)	0.93 (322)	0.93	20%
PKLR 48h	0.91 (1246)	0.91 (1255)	0.92 (1267)	0.91	0.95 (366)	0.95 (383)	0.96 (386)	0.95	22%
RET	0.70 (1845)	0.68 (1845)	0.75 (1845)	0.71	0.87 (306)	0.85 (308)	0.89 (325)	0.87	16%
SORT1	0.99 (1483)	0.99 (1482)	0.99 (1483)	0.99	1.00 (753)	1.00 (756)	1.00 (756)	1.00	39%
SORT1.2	0.98 (1815)	0.97 (1812)	0.98 (1815)	0.98	0.99 (793)	0.98 (773)	0.98 (790)	0.99	39%
SORT1-flip	0.99 (1763)	0.99 (1763)	0.99 (1763)	0.99	1.00 (780)	0.99 (754)	0.99 (778)	0.99	39%
TCF7L2	0.75 (1680)	0.77 (1681)	0.75 (1682)	0.76	0.91 (221)	0.92 (230)	0.91 (215)	0.91	12%
TERT-G	0.97 (778)	0.97 (785)	0.96 (780)	0.97	0.98 (341)	0.98 (343)	0.98 (341)	0.98	35%
TERT-GAa	0.91 (769)	0.93 (779)	0.91 (771)	0.92	0.96 (239)	0.96 (247)	0.96 (244)	0.96	25%
TERT-GSc	0.95 (778)	0.95 (777)	0.95 (780)	0.95	0.97 (281)	0.97 (279)	0.97 (273)	0.97	29%
TERT-H	0.87 (777)	0.87 (781)	0.81 (775)	0.85	0.93 (216)	0.93 (228)	0.92 (164)	0.93	21%
UC88	0.67 (1660)	0.59 (1659)	0.66 (1661)	0.64	0.91 (140)	0.88 (113)	0.92 (134)	0.90	7%
ZFAND3	0.89 (1842)	0.90 (1841)	0.89 (1841)	0.89	0.96 (429)	0.96 (474)	0.96 (440)	0.96	22%
ZRSh13	0.73 (1553)	0.80 (1554)	0.75 (1553)	0.76	0.90 (194)	0.93 (199)	0.91 (190)	0.91	12%
ZRSh13h2	0.74 (1553)	0.77 (1552)	0.78 (1552)	0.76	0.90 (164)	0.92 (180)	0.93 (178)	0.92	11%

Supplementary Table 8

Number of mutations (Mut.) and sites studied for a representative experiment of each element. The number of mutations with a significant p-value (< 10^{-5}) is reported from the model combining transfection replicates. Counts are provided for reporter expression increasing (↑) and decreasing (↓) mutations. The overlap with single nucleotide variants present in the gnomAD r2.1 database is reported including singleton variants (gnAD columns) and excluding singleton variants (no sgl columns). Of the 31,243 mutations, 28,937 are single nucleotide variants. MYC (rs11986220) is abbreviated to MYCs1 and MYC (rs6983267) abbreviated to MYCs2.

Experiment	**Mut.**	**Sites**	**Sig. (10^{-5})**	↑	↓	**2-fold**	↑	↓	**gnAD**	**Sig. (10^{-5})**	↑	↓	**gnAD (no sgl)**	**Sig. (10^{-5})**	↑	↓
BCL11A	1985	600	66	35	31	2	0	2	47	3	2	1	14	0	0	0
F9	952	303	142	76	66	2	1	1	11	2	1	1	4	0	0	0
FOXE1	1923	600	6	3	3	0	0	0	38	0	0	0	20	0	0	0
GP1BB	1239	385	184	33	151	11	0	11	43	5	3	2	11	2	1	1
HBB	596	187	90	33	57	1	1	0	18	7	0	7	8	4	0	4
HBG1	888	274	181	24	157	26	0	26	13	3	0	3	5	2	0	2
HNF4a	931	285	119	63	56	1	1	0	22	3	1	2	11	1	0	1
IRF4	1458	451	678	267	411	135	9	126	39	20	7	13	20	9	4	5
IRF6	1739	599	306	112	194	51	13	38	38	8	0	8	18	5	0	5
LDLR.2	1024	318	411	103	308	136	9	127	17	5	2	3	5	1	1	0
MSMB	1912	591	369	177	192	1	0	1	34	12	8	4	17	6	6	0
MYCs1	1554	463	11	11	0	0	0	0	20	0	0	0	10	0	0	0
MYCs2	1809	600	85	47	38	0	0	0	41	2	1	1	13	2	1	1
PKLR (48h)	1533	470	277	88	189	78	10	68	28	9	4	5	13	3	3	0
RET	1911	600	165	67	98	0	0	0	57	9	4	5	25	6	4	2
SORT1.1	1806	600	789	267	522	143	29	114	54	26	7	19	26	10	2	8
TCF7L2	1801	595	130	43	87	2	2	0	42	3	3	0	19	1	1	0
TERT (GBM)	878	259	293	99	194	48	6	42	24	13	6	7	10	4	3	1
UC88	1840	590	69	41	28	2	2	0	39	2	2	0	11	0	0	0
ZFAND3	1893	579	328	104	224	3	0	3	40	12	2	10	22	6	1	5
ZRS (+h13)	1571	485	131	96	35	0	0	0	24	0	0	0	12	0	0	0
Sum	**31243**	**9834**	**4830**	**1789**	**3041**	**642**	**83**	**559**	**689**	**144**	**53**	**91**	**294**	**62**	**27**	**35**

Supplementary Table 9

Effects of specific substitution or transition (ts) vs. transversion (tv) effects for significant readouts across a representative experiment of each element. The number of mutations with a significant p-value (< 10^{-5}) is reported from models combining transfection replicates. The overlap with single nucleotide variants present in the gnomAD r2.1 is reported. Elements from Supplementary Table 8 were used.

Subst	Type	All	Sig.	Sig.20%	Sig. 2-fold	Var.	Var.Sig.	Var.Sig.20%	Var.Sig.2-fold
A>-	Del	571	54	35	13	n.a.			
A>C	Tv	2291	208	177	43	18	1	1	4
A>G	Ts	2371	534	223	42	70	21	10	0
A>T	Tv	2372	374	194	47	10	3	1	1
C>-	Del	635	69	44	12	n.a.			
C>A	Tv	2673	372	281	68	47	10	6	1
C>G	Tv	2584	283	236	73	48	4	4	0
C>T	Ts	2704	575	287	60	159	46	20	2
G>-	Del	576	61	46	7	n.a.			
G>A	Ts	2456	488	226	33	150	32	15	2
G>C	Tv	2334	201	180	44	54	3	3	1
G>T	Tv	2443	320	235	46	39	6	5	1
T>-	Del	524	45	31	8	n.a.			
T>A	Tv	2289	422	248	47	9	2	1	0
T>C	Ts	2293	593	265	48	66	15	9	1
T>G	Tv	2127	231	204	51	19	1	0	0
Total	**Dels**	**2306**	**229**	**156**	**40**	**n.a.**			
Total	**SNVs**	**28937**	**4601**	**2756**	**602**	**689**	**144**	**75**	**13**
Total	**Tv**	**19113**	**2411**	**1755**	**419**	**244**	**30**	**21**	**8**
Total	**Ts**	**9824**	**2190**	**1001**	**183**	**445**	**114**	**54**	**5**

Supplementary Table 10

Previously described variants of promoters. Clinical variants of promoters (HBB, HBG1, PKLR, F9, GP1BB, TERT, HNF4A, MSMB, and FOXE1) measured in this MPRA study, as well as additional described variants in Supplementary Note 1. Corresponding RefSeq transcripts of the HGVS annotation are listed in Supplementary Table 1. Fold changes are reported as "non significant" (n.s), if the associated p-value is higher than 10^{-5}. Variants that were not available from our experiments are marked as “not covered” (n.c.). We are including effects for the PKLR_24h and PKLR_48h (PKLR_24h/PKLR_48h) as well as TERT-GBM and TERT-HEK experiments (TERT-GBM/TERT-HEK). Previous reported phenotypes in literature are summarized in the Phenotype column.

Coordinates [GRCh37, GRCh38]	Variants	Expression effect [log_2]	Promoter activity (ratio of WT)	Phenotype
X:138612869 X:139530710	F9:c.-55G>C	n.s.	(0.84)	Hemophilia B Leyden
X:138612874 X:139530715	F9:c.-50T>G	n.s.	(0.94)	Hemophilia B Leyden
X:138612875 X:139530716	F9:c.-49T>A	-0.14	0.91	Hemophilia B Leyden
X:138612889 X:139530730	F9:c.-35G>A	n.s.	(0.8)	Hemophilia B Leyden
X:138612889 X:139530730	F9:c.-35G>C	n.c.	n.c	Hemophilia B Leyden
X:138612890 X:139530731	F9:c.-34A>T	n.s.	(1.00)	Hemophilia B Leyden
X:138612902 X:139530743	F9:c.-22T>C	-0.15	0.9	Hemophilia B Leyden
X:138612907 X:139530748	F9:c.-17A>G	n.s.	(0.91)	Hemophilia B Leyden
X:138612907 X:139530748	F9:c.-17A>C	n.s.	(0.89)	Hemophilia B Leyden
9:100615914 9:97853632	FOXE1:c.-283G>A, rs1867277	n.s.	0.94	thyroid cancer-associated
22:19710933 22:19723410	GP1BB:c.-160C>G	-0.93	0.52	Bernard-Soulier Syndrome
11:5248402 11:5227172	HBB:c.-151C>T	-0.28	0.82	beta+ thal
11:5248394 11:5227164	HBB:c.-143C>G	n.s.	(0.90)	beta+ thal
11:5248393 11:5227163	HBB:c.-142C>T	-0.23	0.85	beta+ thal
11:5248391 11:5227161	HBB:c.-140C>T	-0.31	0.81	beta+ thal

11:5248389 11:5227159	HBB:c.-138C>A	n.s.	(0.86)	beta+ thal
11:5248389 11:5227159	HBB:c.-138C>T	-0.29	0.82	beta+ thal
11:5248389 11:5227159	HBB:c.-138C>G	n.s.	(0.89)	beta0 thal
11:5248388 11:5227158	HBB:c.-137C>A	-0.22	0.86	beta+ thal
11:5248388 11:5227158	HBB:c.-137C>G	-0.25	0.84	beta+ thal
11:5248388 11:5227158	HBB:c.-137C>T	-0.28	0.82	beta+ thal
11:5248387 11:5227157	HBB:c.-136C>A	-0.18	0.88	beta+ thal
11:5248387 11:5227157	HBB:c.-136C>G	n.s.	(0.85)	beta+ thal
11:5248378 11:5227148	HBB:c.-127G>C	n.s.	(0.89)	beta+ thal
11:5248373 11:5227143	HBB:c.-122T>A	-0.29	0.82	beta+ thal
11:5248372 11:5227142	HBB:c.-121C>T	-0.25	0.84	beta0 thal
11:5248351 11:5227121	HBB:c.-100G>A	-0.22	0.86	beta+ thal
11:5248350 11:5227120	HBB:c.-99C>G	1.19	2.28	no previously reported phenotype
11:5248333 11:5227103	HBB:c.-82C>T	n.s.	(0.96)	beta0 thal
11:5248333 11:5227103	HBB:c.-82C>A	n.s.	(0.97)	beta+ thal
11:5248332 11:5227102	HBB:c.-81A>C	n.s.	(0.89)	beta+ thal
11:5248332 11:5227102	HBB:c.-81A>G	-0.15	0.90	beta+ thal
11:5248331 11:5227101	HBB:c.-80T>C	-0.23	0.85	beta0 thal
11:5248331 11:5227101	HBB:c.-80T>G	n.s.	(0.84)	beta0 thal
11:5248331 11:5227101	HBB:c.-80T>A	-0.28	0.82	beta+ thal
11:5248330 11:5227100	HBB:c.-79A>G	-0.38	0.77	beta+ thal
11:5248329 11:5227099	HBB:c.-78A>C	-0.38	0.77	beta+ thal
11:5248329 11:5227099	HBB:c.-78A>G	-0.34	0.79	beta+ thal
11:5248327 11:5227097	HBB:c.-76A>C	n.s.	(0.88)	beta0 thal
11:5248326	HBB:c.-75G>C	n.s.	(0.97)	beta0 thal

11:5227096				
11:5248301 11:5227071	HBB:c.-50A>C	n.s.	(0.94)	beta+ thal
11:5248280 11:5227050	HBB:c.-29G>A	n.s.	(0.91)	beta+ thal
11:5248269 11:5227039	HBB:c.-18C>G	n.s.	(1.01)	beta+ thal
11:5271298 11:5250068	HBG1:c.-264C>T	n.s.	(0.98)	HPFH
11:5271289 11:5250059	HBG1:c.-255C>T	-0.20	0.87	HPFH
11:5271289 11:5250059	HBG1:c.-255C>G	n.s.	(1.05)	HPFH
11:5271285 11:5250055	HBG1:c.-251T>C	0.31	1.24	HPFH
11:5271284 11:5250054	HBG1:c.-250C>T	n.s.	(0.88)	HPFH
11:5271283 11:5250053	HBG1:c.-249C>T	n.s.	(0.98)	HPFH
11:5271282 11:5250052	HBG1:c.-248C>G	n.s.	(0.97)	HPFH
11:5271262 11:5250032	HBG1:c.-228T>C	0.61	1.53	HPFH
11:5271245 11:5250015	HBG1:c.-211C>T	0.25	1.19	HPFH
11:5271204 11:5249974	HBG1:c.-170G>A	n.s.	(1.09)	HPFH
11:5271201 11:5249971	HBG1:c.-167C>T	-0.63	0.65	HPFH
11:5271201 11:5249971	HBG1:c.-167C>G	n.s.	(1.00)	HPFH
11:5271201 11:5249971	HBG1:c.-167C>A	-0.30	0.81	HPFH
11:5271197 11:5249967	HBG1:c.-163A>C	n.s.	(1.12)	HPFH
20:42984253 20:44355613	HNF4A:c.-192C>G	0.20	1.15	monogenic B cell diabetes
20:42984264 20:44355624	HNF4A:c.-181G>A	n.s.	(0.98)	monogenic B cell diabetes
20:42984276 20:44355636	HNF4A:c.-169C>T	n.s.	(0.99)	monogenic B cell diabetes
20:42984299 20:44355659	HNF4A:c.-146T>C	-0.06	0.96	monogenic B cell diabetes

20:42984307 20:44355667	HNF4A:c.-138T>C	1.04	2.06	no previous reported phenotype
20:42984309 20:44355669	HNF4A:c.-136A>G	n.s.	(0.02)	monogenic B cell diabetes
20:42984439 20:44355799	HNF4A:c.-6T>G	0.96	1.95	no previous reported phenotype
10:51549496 10:46046326	MSMB:c.-89C>T, rs10993994	0.20	1.15	prostate cancer-associated
1:155271510 1:155301719	PKLR:c.-324T>A	n.s./n.s.	(1.29)/(1.23)	nonfunctional polymorphisms
1:155271434 1:155301643	PKLR:c.-248delT	n.s./n.s.	(1.57)/(0.75)	nonfunctional polymorphisms
1:155271269 1:155301478	PKLR:c.-83G>C	n.s./-2.19	(0.42)/0.22	PK deficiency
1:155271258 1:155301467	PKLR:c.-72A>G	-1.77/-2.40	0.29/0.19	PK deficiency
5:1295349 5:1295234	TERT:c.-245T>C, rs2853669	n.s./n.s.	(0.95)/(0.99)	melanoma
5:1295250 5:1295135	TERT:c.-146C>T	2.42/1.42	5.35/2.68	glioblastoma
5:1295242 - 1295243 5:1295127- 1295128	TERT:c.[-138C>T;-139C>T], rs35550267	[0.20;n.s.]/ [n.s.;n.s.]	[1.15;(0.99)]/ [(1.04);(0.95)]	melanoma
5:1295228- 1295229 5:1295113- 1295112	TERT:c.[-124C>T;-125C>T]	[n.s.;2.86]/ [n.s.;2.00]	[(0.91);7.26]/ [(0.93);4.00]	bladder carcinoma, melanoma and glioma
5:1295161 5:1295046	TERT:c.-57A>C	1.14/0.65	2.2/1.57	melanoma, bladder cancer
5:1295158 5:1295043	TERT:c.-54C>A	1.65/0.81	3.14/1.75	Bladder cancer
5:1295149 5:1295034	TERTc.-45:G>T	1.03/n.s.	2.04/(1.37)	Bladder cancer

Supplementary Table 11

Previously described variants of enhancers. Clinical variants of enhancers (IRF4, IRF6, MYC, RET, TCF7L2, ZFAND3, SORT1, and ZRS) characterized in this MPRA study, as well as some additional described variants in the Supplementary Note 1. Fold changes are reported as "non significant" (n.s), if the associated p-value is higher than 10^{-5}. Results from multiple experiments are separated by a dash and refer to SORT1/SORT1.2/SORT1-flip and ZRS+HOXD13/ZRS+HOXD13+HAND2, respectively. Phenotypes previously reported in literature are summarized in the Phenotype column.

Coordinates [GRCh37, GRCh38]	**Variants**	**Expression effect [log_2]**	**Enhancer activity (ratio of WT)**	**Phenotype**
6:396321 6:396321	IRF4:C>T, rs12203592	-1.47	0.36	pigmentation associated
1:209989232 1:209815887	IRF6:T>C, rs76145088	-0.28	0.82	no annotation
1:209989270 1:209815925	IRF6:C>T, rs642961	n.s.	(1.06)	isolated cleft lip associated
1:209989281 1:209815936	IRF6:C>T, rs77542756	n.s.	(1.00)	no annotation
8:128413279 8:127401034	MYCrs6983267:C>G	0.92	1.86	no previous reported phenotype
8:128413289 8:127401044	MYCrs6983267:G>T	0.88	1.84	no previous reported phenotype
8:128413305 8:127401060	MYCrs6983267:G>T, rs6983267	n.s.	(0.95)	cancer related
8:128531689 8:127519444	MYC:T>A, rs11986220	n.s.	(0.86)	cancer related
10:43582056 10:43086608	RET:T>C, rs2435357	n.s.	(0.99)	Hirschsprung disease
1:109817590 1:109274968	SORT1:G>T, rs12740374	2.92/2.74	7.57/6.68	Associated with plasma low-density lipoprotein cholesterol and myocardial infarctio.
10:114758349 10:112998590	TCF7L2:C>T, rs7903146	0.25	1.19	Diabetes associated
10:114758373 10:112998614	TCF7L2:G>C	1.18	2.27	no previous reported phenotype
6:37775652 6:37807876	ZFAND3:C>T, rs58692659	-0.51	0.7	Diabetes associated
7:156583831 7:156791137	ZRS:T>C	n.s./n.s.	(1.04/1.04)	Preaxial polydactyly & TPT
7:156583949 7:156791255	ZRS:G>C	n.s./n.s.	(0.94/0.94)	Preaxial polydactyly & TPT

7:156583951 7:156791257	ZRS:G>A	-0.07/n.s.	0.95/(0.97)	Townes Brocks syndrome
7:156584006 7:156791312	ZRS:A>G	n.s./n.s.	(0.99/1.00)	No phenotype
7:156584015 7:156791321	ZRS:C>T	n.s./ n.s.	(0.99/0.98)	Polydactyly（mouse）
7:156584093 7:156791399	ZRS:T>C	n.s./n.s.	(1.01/0.99)	Polydactyly (cat)
7:156584095 7:156791401	ZRS:T>C	n.s. /n.s.	(1.01/1.00)	Polydactyly (cat)
7:156584107 7:156791413	ZRS:A>C	n.s./n.s.	(1.04/0.99)	Preaxial polydactyly & TPT
7:156584153 7:156791459	ZRS:T>C	0.21 /0.12	1.16 /1.09	Polydactyly of the four extremities and bilateral tibial deficiency
7:156584163 7:156791469	ZRS:A>T	n.s./n.s.	(1.01/0.98)	Polydactyly (mouse)
7:156584164 7:156791470	ZRS:T>C	0.06/n.s.	1.04/(1.03)	Polydactyly (mouse)
7:156584166 7:156791472	ZRS:C>A	n.s./n.s.	(0.91/0.9)	Polydactyly
7:156584166 7:156791472	ZRS:C>G	n.s./n.s.	(0.99/0.99)	Werner mesomelic syndrome
7:156584166 7:156791472	ZRS:C>T	n.s./n.s	(0.99/1.01)	Werner mesomelic syndrome
7:156584168 7:156791474	ZRS:G>A	n.s./-0.06	(0.99)/0.96	Werner mesomelic syndrome
7:156584174 7:156791480	ZRS:G>A	n.s. /n.s.	(1.02/1.01)	Polydactyly & TPT
7:156584236 7:156791542	ZRS:A>C	n.s./n.s.	(0.97/0.99)	Polydactyly
7:156584241 7:156791547	ZRS:A>G	0.08/n.s.	1.06 /(1.04)	Polydactyly
7:156584265 7:156791571	ZRS:T>A	n.s./n.s.	(0.99/0.99)	Polydactyly
7:156584273 7:156791579	ZRS:C>T	0.13/n.s.	1.09 /(1.04)	Polydactyly
7:156584275 7:156791581	ZRS:A>G	n.s./n.s.	(0.99/1.01)	TPT
7:156584283 7:156791589	ZRS:G>T	n.s./n.s.	(1.00/1.01)	Polydactyly & TPT & syndactyly
7:156584285 7:156791591	ZRS:C>A	0.23/0.17	1.17/1.13	Polydactyly (chicken)

Supplementary Table 12

Comparison with previously described LDLR mutations showing effect on promoter activity or being implicated in disease. This table has been modified from Khamis *et al.* 2015[48]. We are reporting $\log_2$ fold changes as well as percentages for our LDLR and LDLR.2 experiments. A reported fold change is considered "no effect" (noEff), if the associated p-Value is higher than 10^{-5}. In all other cases, we report a variant as enhancing (Enh) or repressing (Repr), depending on the sign of the $\log_2$ fold change. Familial hypercholesterolemia is abbreviated with FH. FP1 stands for Footprint. SP1 refers to a binding site of the transcription factor SP1. SRE stands for sterol-dependent regulatory element. SREBP1 and SREBP1 are SRE repeat 1 and 2, respectively.

Coordinates [GRCh37, GRCh38]	Variant in NM_000527.4 [Khamis A et al. 2015]	Location	Promoter activity (% of WT)	This experiment (Exp 1/2)	Reference (PMID)
19:11199957 19:11089281	c.-268G>T	1 bp from FP1	In FH and normal (polymorphism)	0.06 (104%, noEff) -0.07 (95%, noEff)	10484771
19:11200008 19:11089332	c.-217C>T	2 bp from FP1	160% Luciferase	1.45 (273%, Enh) 1.40 (263%, Enh)	10484771
19:11200010 19:11089334	c.-215A>G	4 bp from FP1	100% Luciferase [results depending on Serum level]	-0.78 (58%, Repr) - 0.81 (57%, Repr)	22881376
19:11200017 19:11089341	c.-208A>T	Between SREBP1 and FP1	100% Luciferase	-1.28 (41%, Repr) - 1.06 (47%, Repr)	21538688
19:11200019 19:11089343	c.-206C>T	Between SREBP1 and FP1	Not tested	-0.84 (55%, Repr) - 0.81 (57%, Repr)	12052488
19:11200037 19:11089361	c.-188C>T	SREBP1	Not tested	-2.41 (18%, Repr) - 2.84 (13%, Repr)	16250003
19:11200069 19:11089393	c.-156C>T	SREBP2	Not tested	-2.52 (17%, Repr) - 2.67 (15%, Repr)	14974088
19:11200072 19:11089396	c.-153C>T	SREBP2	Not tested, considered pathogenic by location in conserved region (SREBP2)	-1.22 (42%, Repr) - 1.36 (38%, Repr)	15303010, 3030558, 10484771
19:11200073 19:11089397	c.-152C>T	SREBP2	40% Luciferase	-1.33 (39%, Repr) - 1.60 (32%, Repr)	10484771
19:11200079 19:11089403	c.-146C>A	Between SREBP2 and SP1	Not tested	-0.48 (71%, noEff) - 0.33 (79%, Repr)	9259195
19:11200083 19:11089407	c.-142C>T	SP1	20% Luciferase	-2.28 (20%, Repr) - 3.09 (11%, Repr)	11792717
19:11200085 19:11089409	c.-140C>G	SP1	7% Luciferase	-2.15 (22%, Repr) - 3.29 (10%, Repr)	21538688

19:11200085 19:11089409	c.-140C>T	SP1	6% Luciferase	-2.87 (13%, Repr) - 3.55 (8%, Repr)	21538688
19:11200086 19:11089410	c.-139C>A	SP1	Not tested	-2.70 (15%, Repr) - 3.24 (10%, Repr)	16250003
19:11200086 19:11089410	c.-139C>G	SP1	26% Luciferase	-2.70 (15%, Repr) - 3.31 (10%, Repr)	17625505
19:11200087 19:11089411	c.-138T>C	SP1	24% LDLR activity	-2.36 (19%, Repr) - 2.75 (14%, Repr)	8589690
19:11200087 19:11089411	c.-138delT	SP1	25% Luciferase	- -	14616764
19:11200088 19:11089412	c.-137C>T	SP1	Not tested	-2.59 (16%, Repr) - 3.52 (8%, Repr)	1301956
19:11200089 19:11089413	c.-136C>G	SP1	12% Luciferase	-2.57 (16%, Repr) - 3.06 (11%, Repr)	21538688
19:11200089 19:11089413	c.-136C>T	SP1	5% CAT assay	-2.62 (16%, Repr) - 3.51 (8%, Repr)	7937987
19:11200090 19:11089414	c.-135C>G	SP1	Pathogenic, LIPOchip assay	-2.70 (15%, Repr) - 3.01 (12%, Repr)	1301956
19:11200104 19:11089428	c.-121T>C	Between TATA box and SP1	72% Luciferase	-0.56 (67%, Repr) - 0.63 (64%, Repr)	20236128
19:11200105 19:11089429	c.-120C>T	Between TATA box and SP1	3% Luciferase / 10% Luciferase	-0.14 (90%, noEff) - 0.17 (88%, Repr)	15303010
19:11200124 19:11089448	c.-101T>C	TATA BOX	64% Luciferase	-0.32 (80%, Repr) - 0.31 (80%, Repr)	22881376
19:11200137 19:11089461	c.-88G>A	5′UTR	100% Luciferase	-0.23 (85%, Repr) - 0.05 (96%, noEff)	21538688
19:11200157 19:11089481	c.-68A>C	5′UTR	Not tested	-0.16 (89%, noEff) - 0.04 (97%, noEff)	15556094
19:11200189 19:11089513	c.-36T>G	5′UTR	100% Luciferase	0.10 (107%, noEff) 0.18 (113%, noEff)	21538688
19:11200202 19:11089526	c.-23A>C	5′UTR	Not tested	- 0.09 (106%, noEff)	15241806
19:11200211 19:11089535	c.-14C>A	5′UTR	Not tested	0.18 (113%, noEff) -0.05 (96%, noEff)	9259195
19:11200212 19:11089536	c.-13A>G	5′UTR	100% Luciferase	-0.03 (97%, noEff) 0.09 (106%, noEff)	20828696
19:11200220 19:11089544	c.-5C>T	5′UTR	Not tested	0.01 (100%, noEff) -0.07 (95%, noEff)	16250003

Supplementary Table 13

Variants that are significantly different between the knockdown of the scrambled siRNA and siGABPA (non-overlapping 95% confidence intervals). In addition the motif of the Ets-family with the highest change in the position weight matrix (PWM) is reported where available. For the majority of significantly different variants, a member of the Ets-family transcription factors is annotated or matched using PWMs in JASPAR 2018[6]. The variants NM_198253.2:c.-146C>A and c.-124C>A create similar ETV/GABPA binding motifs to the previously known variants at the same positions, as observed in previous studies[49]. A new ETV motif is created by c.-79C>A, c.-78delT and c.-77C>T, and a novel GABPA/ETS1 motif is created by c.-189A>G, c.-189A>T or c.-126C>T. Finally, two of the three less common activating variants identified in cancer studies[50–52], c.-45G>A and c.-57A>C, create an ETS motif. Following Jaspar IDs (including motif name) of the Ets-family are used: MA0062.1 (GABPA), MA0098.3 (ETS1), MA0764.1 (ETV4), MA0765.1 (ETV5), MA0645.1 (ETV6), MA0076.2 (ELK4).

Coordinates [GRCh37, GRCh38]	Variants (NM_198253.2)	Log_2 variant effect scramble siRNA	Log_2 variant effect siGABPA	Motif	PWM score change
5:1295293 5:1295178	c.-189A>G	0.56	0.25	GABPA	4.95
5:1295293 5:1295178	c.-189A>T	0.25	-0.06	GABPA	2.95
5:1295292 5:1295177	c.-188G>C	-1.01	-0.30	GABPA	-2.11
5:1295267 5:1295152	c.-163G>A	-0.71	-0.53		
5:1295264 5:1295149	c.-160C>T	-0.46	-0.28		
5:1295250 5:1295135	c.-146C>T	2.47	1.65	GABPA	5.17
5:1295248 5:1295133	c.-144C>T	-0.36	-0.18	GABPA	-5.17
5:1295245 5:1295130	c.-141G>A	0.33	0.10	GABPA	-2.59
5:1295238 5:1295123	c.-134G>A	-0.32	-0.15		
5:1295237 5:1295122	c.-133C>T	0.24	0.02		
5:1295232 5:1295117	c.-128C>A	-1.01	-0.64		
5:1295232 5:1295117	c.-128C>T	-0.75	-0.56		
5:1295231 5:1295116	c.-127C>T	-0.63	-0.46	GABPA	-4.39

5:1295230 51295115	c.-126C>T	0.35	0.16	GABPA	1.42
5:1295228 5:1295113	c.-124C>A	1.75	1.31	ETV4	5.86
5:1295228 5:1295113	c.-124C>T	2.9	1.99	ETV6	7.70
5:1295225 5:1295110	c.-121C>G	-0.21	0.03	ETV6	-15.03
5:1295224 5:1295109	c.-120G>A	-0.23	-0.04	ETS1	-13.71
5:1295215 5:1295100	c.-111C>T	0.46	0.26		
5:1295211 5:1295096	c.-107C>T	0.65	0.46		
5:1295210 5:1295095	c.-106C>T	-1.11	-0.7		
5:1295207 5:1295092	c.-103delC	-0.8	-0.51	ELK4	-0.89
5:1295207 5:1295092	c.-103C>T	-1.18	-0.86	ELK4	0.00
5:1295206 5:1295091	c.-102C>A	-1.7	-1.41	ELK4	-8.70
5:1295206 5:1295091	c.-102C>T	-1.14	-0.85	ETV6	-0.65
5:1295204 5:1295089	c.-100C>A	-0.87	-0.4	ETV6	-15.03
5:1295204 5:1295089	c.-100C>T	-0.56	-0.23	ELK4	-14.06
5:1295203 5:1295088	c.-99T>A	-0.86	-0.48	ELK4	-14.06
5:1295203 5:1295088	c.-99T>C	-0.69	-0.29	ETV6	-7.70
5:1295202 5:1295087	c.-98T>A	-1.39	-1.02	ETV6	-15.03
5:1295202 5:1295087	c.-98T>C	-1.02	-0.57	ELK4	-14.06
5:1295201 5:1295086	c.-97delC	-0.98	-0.39	ELK4	-2.00
5:1295201 5:1295086	c.-97C>A	-1.13	-0.62	ELK4	-11.29
5:1295201 5:1295086	c.-97C>T	-0.85	-0.39	ETV5	-14.40
5:1295200 5:1295085	c.-96C>T	-1.15	-0.58	ETV5	-14.40
5:1295199 5:1295084	c.-95T>A	-1.03	-0.55	ELK4	-14.06

5:1295199 5:1295084	c.-95T>C	-0.49	-0.24	ETV4	-3.83
5:1295197 5:1295082	c.-93T>A	-0.88	-0.36	ETV6	-15.03
5:1295191 5:1295076	c.-87G>A	-0.32	-0.17		
5:1295188 5:1295073	c.-84C>T	-0.47	-0.22		
5:1295187 5:1295072	c.-83C>T	-0.51	-0.28		
5:1295187 5:1295072	c.-83C>A	-0.63	-0.25		
5:1295185 5:1295070	c.-81C>A	-1.01	-0,41		
5:1295185 5:1295070	c.-81C>T	-0.66	-0.29		
5:1295184 5:1295069	c.-80C>T	-0.6	-0.25	ETV6	-0.65
5:1295183 5:1295068	c.-79C>A	-0.17	0.19	ETV6	4.84
5:1295182 5:1295067	c.-78delT	0.36	-1.19	ETV6	1.29
5:1295181 5:1295066	c.-77C>T	0.89	0.48	ETV6	7.70
5:1295171 5:1295056	c.-67C>T	0.82	0.56		
5:1295169 5:1295054	c.-65C>T	1.08	0.88		
5:1295164 5:1295049	c.-60T>C	0.68	0.55	GABPA	-5.17
5:1295161 5:1295046	c.-57A>C	1.37	0.69	ETS1	13.71
5:1295159 5:1295044	c.-55G>A	-0.52	-0.31	ETS1	-6.92
5:1295149 5:1295034	c.-45G>A	0.03	-0.13	ETV5	0.83
5:1295146 5:1295031	c.-42C>A	-0.09	0.38	ETV5	-5.72
5:1295140 5:1295025	c.-36C>G	-0.22	0.01		
5:1295138 5:1295023	c.-34C>T	0.12	0.41		
5:1295137 5:1295022	c.-33A>G	-0.05	0.08		
5:1295136 5:1295021	c.-32C>T	0.18	0.31		

5:1295134 5:1295019	c.-30T>C	0.14	0.31		
5:1295133 5:1295018	c.-29G>A	0.03	0.25		
5:1295111 5:1294996	c.-7C>A	-0.17	0.01		
5:1295104 5:1294989	c.1delA	0.55	0.21		

Supplementary Table 14

Pearson correlation of computational scores with measured expression effects of all SNVs with at least 10 tags. The table reports Pearson correlation coefficients of the absolute expression effect for each element with various measures agnostic to the cell-type. If the wild-type allele at a position did not match the human reference genome, the position was excluded. The measures include conservation (PhyloP, PhastCons, GERP++), overlapping TFBS as predicted in JASPAR 2018 (exploring different score thresholds or factors predicted most frequently across the region; for details see Methods) and computational tools that integrate large sets of functional genomics data in combined scores (CADD, DeepSEA, Eigen, FATHMM-MKL, FunSeq2, GWAVA, LINSIGHT, ReMM). Eigen scores are not defined on the X chromosome (F9). In addition, we compared a subset of experiments (10/21) to sequence-based models (deltaSVM) publically available only for specific cell-types (HEK293T, HeLa S3, HepG2, K562, and LNCaP). The table lists correlations with absolute expression effects in all rows other than "deltaSVM", where directionality of the expression alteration was considered. In cases where an annotation is based on positions rather than alleles, we assumed the same value for all substitutions at each position. MYC (rs11986220) is abbreviated to MYCs1 and MYC (rs6983267) abbreviated to MYCs2. TERT-GBM is abbreviated as TERT-G. Blue bars denote positive and red bars negative correlation.

Name	BCL11A	F9	FOXE1	GP1BB	HBB	HBG1	HNF4a	IRF4	IRF6	LDLR.2	MSMB	MYCs1	MYCs2	PKLR_48h	RET	SORT1.1	TCF7L2	TERT-G	UC88	ZFAND3	ZRSh13
Type	enh.	prom.	prom.	prom.	prom.	prom.	prom.	enh.	enh.	prom.	prom.	enh.	enh.	prom.	enh.	enh.	enh.	prom.	UC	enh.	enh.
CADD v1.0	-0.03	0.07	-0.01	-0.05	0.02	0.17	0.14	0.40	0.21	0.41	0.07	-0.01	-0.06	0.24	0.13	-0.26	0.03	0.13	-0.02	0.36	0.20
CADD v1.3	-0.04	0.09	-0.07	-0.09	0.00	0.10	0.10	0.42	0.18	0.57	0.01	-0.06	-0.06	0.39	0.14	-0.28	-0.01	-0.02	-0.02	0.40	0.15
CADD v1.4	-0.05	0.07	-0.03	0.04	0.07	0.25	0.14	0.49	0.20	0.64	0.06	-0.03	-0.03	0.51	0.17	-0.23	0.03	0.10	0.00	0.43	0.04
FunSeq	0.00	0.03	0.05	0.19	0.13	0.13	0.08	0.35	0.12	0.36	0.23	0.02	0.01	0.47	0.10	0.07	0.09	0.15	0.06	0.25	-0.08
Eigen	-0.03		0.00	0.03	0.15	0.27	0.14	0.52	0.18	0.63	0.11	-0.04	-0.05	0.51	0.18	-0.23	0.09	0.23	-0.01	0.44	0.06
FATHMM	0.00	0.01	0.01	0.11	0.09	0.40	0.10	0.37	0.18	0.55	0.12	0.04	-0.01	0.54	0.17	-0.13	0.06	0.20	0.01	0.44	0.07
DeepSEA	0.02	0.17	0.01	0.19	0.21	0.25	0.13	0.32	0.12	0.31	0.16	0.02	0.09	0.33	0.11	-0.05	0.09	0.31	0.04	0.33	0.04
LINSIGHT	-0.01	0.08	-0.02	0.10	0.13	0.09	0.14	0.46	0.14	0.51	0.02	-0.06	-0.10	0.57	0.19	-0.20	-0.03	0.11	-0.02	0.38	0.04
ReMM	-0.01	0.04	-0.01	0.09	0.10	0.05	0.07	0.23	0.09	0.37	-0.05	-0.03	-0.01	0.20	0.11	-0.21	-0.02	0.11	0.02	0.24	-0.01
GWAVA_U	0.02	0.05	-0.03	0.22	0.10	-0.01	0.01	-0.18	-0.02	0.11	0.04	-0.03	-0.15	0.32	0.01	-0.12	-0.02	-0.22	0.05	0.16	-0.19
GWAVA_T	-0.04	0.14	-0.03	0.23	-0.03	0.03	0.11	0.25	-0.03	0.11	0.07	0.06	-0.13	0.18	0.04	0.03	0.14	-0.23	-0.05	0.22	-0.02
GWAVA_R	0.02	0.10	-0.06	0.24	-0.11	0.04	0.08	0.15	-0.06	0.07	0.24	-0.03	-0.01	0.26	0.10	0.16	0.04	-0.03	0.05	0.07	-0.15
deltaSVM		0.44	0.05				0.07			0.26	0.23	0.12	0.23	0.48		0.54		0.27			
deltaSVM (abs)		0.25	0.01				0.03			0.28	0.14	0.07	0.20	0.42		0.39		0.21			
JASPAR_All	0.00	0.05	0.02	0.20	0.12	0.02	0.14	0.22	0.07	-0.01	0.15	0.05	-0.06	0.07	0.11	0.17	0.08	0.14	0.07	0.12	0.04
JASPAR_90	0.02	0.05	0.02	0.19	0.14	0.03	0.14	0.23	0.08	-0.04	0.15	0.05	-0.05	0.09	0.11	0.17	0.07	0.14	0.08	0.11	0.04
JASPAR_75	0.02	0.08	0.01	0.21	0.14	0.03	0.16	0.24	0.08	-0.07	0.14	0.06	-0.04	0.14	0.11	0.17	0.08	0.15	0.09	0.11	0.04
JASPAR_50	0.04	0.11	0.01	0.18	0.16	0.08	0.12	0.25	0.10	0.02	0.14	0.06	-0.03	0.21	0.11	0.18	0.08	0.18	0.11	0.12	0.04
JASPAR_25	0.05	0.17	-0.01	0.18	0.08	0.03	0.12	0.24	0.10	0.16	0.17	0.07	0.00	0.27	0.08	0.20	0.06	0.11	0.14	0.13	0.03
JASPAR_10	0.05	0.18	-0.02	0.18	0.08	0.04	0.13	0.28	0.06	0.32	0.14	0.05	0.08	0.22	0.06	0.13	0.08	0.14	0.12	0.07	0.08
JASPAR_freqTF	-0.03	0.23	0.02	-0.14	0.13	0.00	0.00	0.00	-0.05	0.04	-0.02	0.03	-0.05	0.21	-0.02	-0.02	0.13	0.15	0.11	0.08	0.00
priPhCons	-0.02	0.13	0.02	-0.14	0.05	0.11	0.12	0.37	0.17	0.51	0.03	0.03	-0.09	0.30	0.14	-0.27	-0.02	0.01	0.03	0.39	0.00
mamPhCons	-0.01	0.05	-0.01	0.10	0.11	0.34	0.10	0.51	0.16	0.64	0.11	0.03	0.02	0.56	0.18	-0.20	0.04	-0.05	0.02	0.44	0.00
verPhCons	-0.01	0.01	-0.01	0.09	0.09	0.39	0.10	0.34	0.18	0.62	0.12	0.03	0.02	0.54	0.18	-0.20	0.04	0.12	0.01	0.45	0.06
priPhyloP	-0.06	0.00	-0.01	0.08	0.11	0.00	0.04	0.14	0.07	0.28	0.00	-0.04	0.00	0.11	0.05	-0.13	0.01	0.16	0.04	0.12	0.01
mamPhyloP	-0.01	0.00	0.01	0.13	0.18	0.18	0.11	0.35	0.17	0.45	0.02	-0.04	0.02	0.36	0.11	-0.14	0.04	0.10	-0.01	0.27	0.06
verPhyloP	-0.01	0.02	-0.01	0.10	0.14	0.20	0.11	0.37	0.21	0.51	0.02	-0.04	-0.02	0.38	0.12	-0.15	0.04	0.11	-0.05	0.26	0.07
GerpN	-0.01	0.13	0.02	0.03	0.09	-0.12	0.11	0.29	0.04	0.46	0.26	0.00	-0.04	0.26	0.13	-0.31	0.14	0.17	-0.03	0.32	0.09

Supplementary Table 15

Spearman correlation of computational scores with measured expression effects of all SNVs with at least 10 tags. The table reports Spearman correlation coefficients of the absolute expression effect for each element with various measures agnostic to the cell-type. If the wild-type allele at a position did not match the human reference genome, the position was excluded. The measures include conservation (PhyloP, PhastCons, GERP++), overlapping TFBS as predicted in JASPAR 2018 (exploring different score thresholds or factors predicted most frequently across the region; for details see Methods) and computational tools that integrate large sets of functional genomics data in combined scores (CADD, DeepSEA, Eigen, FATHMM-MKL, FunSeq2, GWAVA, LINSIGHT, ReMM). Eigen scores are not defined on the X chromosome (F9). In addition, we compared a subset of experiments (10/21) to sequence-based models (deltaSVM) publically available only for specific cell-types (HEK293T, HeLa S3, HepG2, K562, and LNCaP). The table lists correlations with absolute expression effects in all rows other than "deltaSVM", where directionality of the expression alteration was considered. In cases where an annotation is based on positions rather than alleles, we assumed the same value for all substitutions at each position. MYC (rs11986220) is abbreviated to MYCs1 and MYC (rs6983267) abbreviated to MYCs2. TERT-GBM is abbreviated as TERT-G. Blue bars denote positive and red bars negative correlation.

Name	BCL11A	F9	FOXE1	GP1BB	HBB	HBG1	HNF4a	IRF4	IRF6	LDLR.2	MSMB	MYCs1	MYCs2	PKLR_48h	RET	SORT1.1	TCF7L2	TERT-G	UC88	ZFAND3	ZRSh13
Type	enh.	prom.	prom.	prom.	prom.	prom.	prom.	enh.	enh.	prom.	prom.	enh.	enh.	prom.	enh.	enh.	enh.	prom.	UC	enh.	enh.
CADD v1.0	-0.05	0.03	-0.01	-0.06	0.00	0.03	0.20	0.42	0.15	0.24	0.06	-0.03	-0.12	0.17	0.11	-0.18	0.03	0.15	-0.07	0.35	0.13
CADD v1.3	-0.07	0.05	-0.06	-0.05	0.03	0.00	0.15	0.43	0.14	0.41	-0.01	-0.07	-0.10	0.17	0.10	-0.21	-0.01	0.02	-0.04	0.37	0.12
CADD v1.4	-0.07	0.03	-0.03	0.05	0.08	0.10	0.20	0.41	0.19	0.51	0.03	-0.05	-0.09	0.20	0.12	-0.15	0.01	0.16	-0.05	0.40	0.02
FunSeq	0.00	0.02	0.04	0.13	0.11	0.11	0.10	0.40	0.12	0.40	0.23	0.02	0.02	0.39	0.07	0.28	0.12	0.21	0.06	0.23	0.00
Eigen	-0.03		0.02	0.00	0.15	0.16	0.22	0.48	0.19	0.58	0.10	-0.01	-0.04	0.25	0.13	-0.13	0.09	0.20	-0.04	0.40	0.07
FATHMM	0.02	0.03	0.04	0.10	0.11	0.15	0.18	0.29	0.23	0.59	0.14	0.01	-0.09	0.26	0.11	0.02	0.04	0.20	-0.03	0.40	0.07
DeepSEA	0.03	0.23	0.05	0.25	0.29	0.26	0.25	0.47	0.28	0.56	0.20	0.04	0.12	0.34	0.14	0.06	0.06	0.37	0.11	0.44	0.07
LINSIGHT	-0.09	0.02	0.03	0.09	0.12	0.13	0.22	0.44	0.15	0.56	0.15	-0.09	-0.11	0.41	0.05	-0.16	0.05	0.11	-0.03	0.38	0.03
ReMM	-0.02	0.04	-0.01	0.07	0.11	0.00	0.14	0.30	0.19	0.52	-0.09	-0.03	-0.01	0.19	0.14	-0.16	-0.06	0.00	-0.07	0.30	0.05
GWAVA_U	0.00	0.10	-0.04	0.28	0.03	-0.09	-0.04	-0.07	0.06	0.06	0.01	-0.03	-0.11	0.32	0.01	-0.20	-0.03	-0.23	0.07	0.16	-0.15
GWAVA_T	-0.01	0.14	-0.03	0.23	0.09	-0.08	0.18	0.23	0.03	0.00	0.08	0.06	-0.10	0.18	0.02	0.09	0.16	-0.28	-0.05	0.24	0.02
GWAVA_R	-0.02	0.04	-0.09	0.28	0.05	-0.03	0.09	0.24	-0.01	0.04	0.27	-0.02	0.02	0.32	0.10	0.15	0.05	-0.04	0.04	0.09	-0.15
deltaSVM		0.43	0.04				0.09			0.21	0.19	0.12	0.12	0.39		0.53		0.26			
deltaSVM (abs)		0.20	0.01				0.03			0.15	0.11	0.06	0.08	0.21		0.28		0.12			
JASPAR_A	-0.01	0.11	0.01	0.28	0.01	-0.02	0.11	0.14	0.06	-0.02	0.22	0.06	-0.09	0.03	0.13	0.21	0.13	0.05	0.04	0.15	0.00
JASPAR_90	0.00	0.12	0.01	0.27	0.02	-0.01	0.10	0.13	0.05	-0.05	0.22	0.06	-0.08	0.05	0.13	0.21	0.12	0.05	0.04	0.14	0.00
JASPAR_75	0.00	0.17	0.00	0.30	0.01	-0.01	0.11	0.13	0.07	-0.04	0.21	0.06	-0.09	0.11	0.15	0.23	0.13	0.06	0.05	0.13	0.00
JASPAR_50	0.01	0.23	0.00	0.28	0.04	0.03	0.09	0.18	0.06	0.06	0.20	0.06	-0.07	0.14	0.15	0.28	0.13	0.08	0.05	0.13	0.00
JASPAR_25	0.01	0.39	0.00	0.29	0.05	0.00	0.08	0.24	0.06	0.18	0.21	0.05	-0.02	0.21	0.16	0.33	0.15	-0.02	0.04	0.11	-0.01
JASPAR_10	0.01	0.52	0.00	0.33	0.05	0.01	0.10	0.26	0.02	0.39	0.17	0.02	0.07	0.15	0.17	0.29	0.15	0.07	0.01	0.04	0.05
JASPAR_TF	0.00	0.24	0.01	-0.14	0.10	-0.08	-0.02	0.01	0.01	-0.04	-0.02	0.03	-0.04	0.08	-0.02	-0.03	0.15	0.14	0.10	0.14	-0.02
priPhCons	-0.02	0.07	-0.01	-0.11	0.00	-0.03	0.23	0.40	0.15	0.54	0.01	0.00	-0.13	0.18	0.15	-0.19	-0.02	0.09	-0.03	0.37	0.01
mamPhCons	-0.01	0.04	-0.01	0.04	0.10	0.21	0.20	0.31	0.21	0.57	0.06	0.00	-0.04	0.23	0.13	-0.12	0.00	0.16	-0.02	0.41	0.01
verPhCons	-0.01	-0.01	-0.02	0.04	0.08	0.23	0.20	0.24	0.23	0.58	0.06	0.00	-0.05	0.20	0.13	-0.11	0.00	0.18	-0.01	0.40	0.06
priPhyloP	-0.01	0.01	0.02	0.13	0.11	0.03	0.02	0.23	0.07	0.35	0.05	0.00	0.05	0.06	0.04	-0.12	0.02	0.12	0.03	0.18	0.04
mamPhyloP	-0.01	0.03	0.02	0.05	0.19	0.12	0.15	0.24	0.17	0.44	0.00	0.00	0.01	0.17	0.11	-0.11	0.03	0.14	-0.02	0.27	0.06
verPhyloP	-0.01	0.05	0.00	0.06	0.14	0.13	0.14	0.24	0.20	0.47	0.00	0.00	-0.02	0.16	0.11	-0.11	0.03	0.14	-0.05	0.27	0.07
GerpN	-0.01	0.02	0.01	0.01	0.05	-0.03	0.22	0.47	0.04	0.59	0.31	-0.01	-0.10	0.28	0.11	-0.28	0.17	0.13	-0.10	0.37	0.07

Supplementary Table 16

Performance of computational scores for binary classification of promoter variants with high and low expression effect. The top 200, 500, and 1000 highest expression effect promoter variants (p-value < 10^{-5}, min tags 10) were selected and matched with no effect variants (log_2 expression effect < 0.05: min tags 10). The same number of effect/no effect variants was sampled for each element, without normalizing each elements' contribution to the overall set. In fact, the three elements contributing the most are top 200: IRF4 (44%), SORT1.1 (42%), IRF6 (14%), top 500: SORT1.1 (44%), IRF4 (35%), IRF6 (16%) and top 1000: SORT1.1 (42%), IRF4 (31%), IRF6 (14%). The average of the area under the receiver operating characteristic (AUROC) and precision-recall curves (AUPRC) of 100 sampling rounds is shown with the standard deviation (SD). Computational scores include conservation (PhyloP, PhastCons, GERP++), overlapping TFBS as predicted in JASPAR 2018 (exploring different score thresholds; for details see Methods) and computational tools that integrate functional genomics data in combined scores (CADD, DeepSEA, Eigen, FATHMM-MKL, FunSeq2, GWAVA, LINSIGHT, ReMM). DeltaSVM was only used on a subset of experiments (10/21, see also *Supplementary Table 14*) for which cell-types where publically available (HEK293T, HeLa S3, HepG2, K562, and LNCaP). In cases where an annotation is based on positions rather than alleles, we assumed the same value for all substitutions at each position. Bold text highlights the best performing method.

	Top 200				**Top 500**				**Top 1000**			
Score	**AUROC**	**SD**	**AUPRC**	**SD**	**AUROC**	**SD**	**AUPRC**	**SD**	**AUROC**	**SD**	**AUPRC**	**SD**
CADD v1.0	0.788	±0.014	0.792	±0.019	0.656	±0.008	0.649	±0.011	0.596	±0.004	0.589	±0.007
CADD v1.3	0.828	±0.010	0.845	±0.014	0.665	±0.007	0.680	±0.011	0.603	±0.004	0.607	±0.008
CADD v1.4	0.895	±0.008	0.90	±0.017	0.736	±0.005	0.747	±0.012	0.653	±0.004	0.662	±0.009
FunSeq	0.733	±0.008	0.739	±0.015	0.633	±0.004	0.645	±0.007	0.599	±0.002	0.623	±0.003
Eigen	0.864	±0.007	0.883	±0.014	0.691	±0.004	0.742	±0.010	0.623	±0.003	0.679	±0.007
FATHMM	0.749	±0.006	0.805	±0.009	0.659	±0.003	0.716	±0.005	0.602	±0.002	0.679	±0.001
DeepSEA	**0.910**	**±0.009**	**0.903**	**±0.012**	**0.829**	**±0.005**	**0.826**	**±0.007**	**0.754**	**±0.003**	**0.770**	**±0.005**
LINSIGHT	**0.909**	**±0.008**	**0.907**	**±0.012**	0.789	±0.006	0.781	±0.009	0.716	±0.004	0.709	±0.008
ReMM	0.891	±0.007	0.911	±0.007	0.736	±0.006	0.770	±0.008	0.663	±0.003	0.699	±0.006
GWAVA_U	0.591	±0.016	0.505	±0.011	0.585	±0.008	0.532	±0.006	0.586	±0.004	0.555	±0.002
GWAVA_T	0.559	±0.016	0.489	±0.009	0.547	±0.009	0.497	±0.005	0.531	±0.004	0.503	±0.002
GWAVA_R	0.606	±0.015	0.532	±0.011	0.577	±0.009	0.517	±0.005	0.575	±0.007	0.533	±0.002
DeltaSVM (abs)	0.563	±0.006	0.628	±0.009	0.536	±0.003	0.590	±0.006	0.536	±0.001	0.590	±0.003

JASPAR_A	0.584	±0.020	0.517	±0.016	0.587	±0.010	0.534	±0.009	0.576	±0.005	0.561	±0.005
JASPAR_90	0.566	±0.019	0.513	±0.016	0.592	±0.010	0.541	±0.008	0.589	±0.005	0.569	±0.005
JASPAR_75	0.574	±0.019	0.520	±0.016	0.602	±0.009	0.557	±0.009	0.601	±0.005	0.585	±0.005
JASPAR_50	0.669	±0.018	0.612	±0.020	0.666	±0.008	0.616	±0.010	0.649	±0.004	0.629	±0.005
JASPAR_25	0.747	±0.015	0.678	±0.022	0.706	±0.008	0.651	±0.011	0.668	±0.004	0.649	±0.005
JASPAR_10	0.785	±0.012	0.739	±0.021	0.748	±0.007	0.705	±0.012	0.692	±0.004	0.686	±0.005
JASPAR_TF	0.618	±0.017	0.582	±0.018	0.601	±0.009	0.569	±0.009	0.574	±0.005	0.568	±0.006
priPhCons	0.831	±0.010	0.832	±0.017	0.689	±0.008	0.680	±0.011	0.606	±0.004	0.600	±0.007
mamPhCons	**0.915**	**±0.007**	**0.919**	**±0.012**	0.785	±0.005	0.784	±0.011	0.698	±0.004	0.694	±0.009
verPhCons	**0.901**	**±0.007**	**0.910**	**±0.014**	0.786	±0.005	0.795	±0.009	0.708	±0.004	0.718	±0.008
priPhyloP	0.723	±0.015	0.712	±0.015	0.644	±0.008	0.636	±0.008	0.599	±0.004	0.608	±0.005
mamPhyloP	0.848	±0.008	0.876	±0.009	0.745	±0.006	0.762	±0.007	0.665	±0.004	0.692	±0.006
verPhyloP	0.860	±0.007	0.808	±0.015	0.756	±0.006	0.764	±0.010	0.670	±0.004	0.694	±0.006
GerpN	0.856	±0.010	0.852	±0.017	0.690	±0.005	0.701	±0.013	0.632	±0.003	0.641	±0.007

Supplementary Table 17

Performance of computational scores for binary classification of enhancers variants with high and low expression effect. The top 200, 500, and 1000 highest expression effect enhancer variants (p-value < 10^{-5}, min tags 10) were selected and matched with no effect variants (log_2 expression effect < 0.05: min tags 10). The same number of effect/no effect variants was sampled for each element, without normalizing each elements' contribution to the overall set. In fact, the three elements contributing the most are top 200: LDLR.2 (53%), PKLR-48h (30%), TERT-GBM (13%), top 500: LDLR.2 (32%), PKLR-48h (29%), TERT-GBM (19%) and top 1000: LDLR.2 (26%), PKLR-48h (25%), TERT-GBM (18%). The average of the area under the receiver operating characteristic (AUROC) and precision-recall curves (AUPRC) of 100 sampling rounds is shown with standard deviation (SD). Computational scores include conservation (PhyloP, PhastCons, GERP++), overlapping TFBS as predicted in JASPAR 2018 (exploring different score thresholds; for details see Methods) and computational tools that integrate functional genomics data in combined scores (CADD, DeepSEA, Eigen, FATHMM-MKL, FunSeq2, GWAVA, LINSIGHT, ReMM). DeltaSVM was only used on a subset of experiments (10/21, see also *Supplementary Table 14*) for which cell-types where publically available (HEK293T, HeLa S3, HepG2, K562, and LNCaP). In cases where an annotation is based on positions rather than alleles, we assumed the same value for all substitutions at each position. Bold text marks the best performing method.

	Top 200				Top 500				Top 1000			
Score	**AUROC**	**SD**	**AUPRC**	**SD**	**AUROC**	**SD**	**AUPRC**	**SD**	**AUROC**	**SD**	**AUPRC**	**SD**
CADD v1.0	0.537	±0.009	0.655	±0.018	0.571	±0.005	0.647	±0.010	0.587	±0.003	0.651	±0.008
CADD v1.3	0.548	±0.009	0.664	±0.014	0.575	±0.006	0.658	±0.009	0.592	±0.003	0.667	±0.006
CADD v1.4	0.556	±0.014	0.542	±0.017	0.584	±0.008	0.557	±0.008	0.594	±0.004	0.580	±0.004
FunSeq	0.651	±0.010	0.683	±0.012	0.640	±0.006	0.648	±0.008	0.652	±0.004	0.649	±0.005
Eigen	0.585	±0.013	0.504	±0.010	0.584	±0.007	0.515	±0.005	0.588	±0.003	0.555	±0.002
FATHMM	0.624	±0.016	0.568	±0.018	0.624	±0.007	0.580	±0.007	0.622	±0.004	0.612	±0.002
DeepSEA	0.712	±0.015	0.713	±0.018	**0.716**	**±0.006**	**0.726**	**±0.007**	**0.698**	**±0.004**	**0.718**	**±0.005**
LINSIGHT	0.579	±0.015	0.538	±0.016	0.590	±0.008	0.550	±0.007	0.598	±0.004	0.580	±0.003
ReMM	0.553	±0.015	0.566	±0.018	0.576	±0.007	0.570	±0.007	0.580	±0.004	0.590	±0.004
GWAVA_U	0.444	±0.007	0.441	±0.004	0.456	±0.003	0.451	±0.003	0.482	±0.002	0.494	±0.001
GWAVA_T	0.572	±0.008	0.572	±0.015	0.538	±0.004	0.539	±0.006	0.530	±0.002	0.568	±0.001
GWAVA_R	0.586	±0.011	0.589	±0.017	0.576	±0.006	0.584	±0.008	0.557	±0.003	0.594	±0.002
DeltaSVM (abs)	0.557	±0.003	0.645	±0.009	0.543	±0.002	0.612	±0.004	0.545	±0.000	0.632	±0.001

JASPAR_A	0.718	±0.017	0.657	±0.021	0.664	±0.009	0.625	±0.011	0.631	±0.005	0.632	±0.006
JASPAR_90	0.722	±0.017	0.671	±0.022	0.662	±0.008	0.634	±0.011	0.628	±0.005	0.634	±0.006
JASPAR_75	0.718	±0.017	0.673	±0.022	0.661	±0.008	0.636	±0.011	0.623	±0.005	0.632	±0.006
JASPAR_50	**0.730**	**±0.015**	0.702	±0.022	0.679	±0.008	0.667	±0.011	0.639	±0.005	0.657	±0.007
JASPAR_25	**0.759**	**±0.014**	**0.741**	**±0.022**	0.701	±0.007	0.692	±0.011	0.651	±0.005	0.607	±0.007
JASPAR_10	0.686	±0.012	0.722	±0.019	0.654	±0.007	0.682	±0.010	0.624	±0.005	0.665	±0.007
JASPAR_TF	0.511	±0.019	0.536	±0.015	0.511	±0.008	0.541	±0.008	0.512	±0.005	0.554	±0.006
priPhCons	0.519	±0.014	0.515	±0.015	0.558	±0.008	0.550	±0.007	0.574	±0.004	0.574	±0.005
mamPhCons	0.558	±0.014	0.552	±0.015	0.593	±0.007	0.579	±0.007	0.596	±0.004	0.605	±0.003
verPhCons	0.569	±0.016	0.568	±0.017	0.592	±0.007	0.584	±0.008	0.597	±0.004	0.608	±0.003
priPhyloP	0.504	±0.019	0.513	±0.016	0.526	±0.009	0.525	±0.009	0.542	±0.005	0.555	±0.006
mamPhyloP	0.577	±0.017	0.580	±0.018	0.586	±0.007	0.573	±0.009	0.573	±0.005	0.583	±0.005
verPhyloP	0.586	±0.017	0.642	±0.015	0.591	±0.007	0.609	±0.009	0.578	±0.004	0.597	±0.005
GerpN	0.639	±0.011	0.677	±0.017	0.604	±0.008	0.639	±0.011	0.601	±0.004	0.644	±0.007

Supplementary Table 18

PCR primers for amplification of targeted regions from genomic DNA. Overhanging primers add cloning sites for downstream vector integration. All sequences are provided 5' to 3'.

Element	Primer	Sequence
F9	Forward	CCCGGGCTCGAGATCTCCCACTGATGAACTGTGC
F9	Reverse	CCGGATTGCCAAGCTTAACCTTTGCTAGCAGATTGTG
FOXE1	Forward	CCCGGGCTCGAGATCTCTCGCCAGCGGTCCGCAGG
FOXE1	Reverse	CCGGATTGCCAAGCTTGGCCTGGCGTCCCCGGAACG
GP1BB	Forward	CCCGGGCTCGAGATCTTTGTGAATGCCGCGTCCTG
GP1BB	Reverse	CCGGATTGCCAAGCTTACGACCAGAGCTCCTCTC
HBB	Forward	CCCGGGCTCGAGATCTAAGGACAGGTACGGCTGTC
HBB	Reverse	CCGGATTGCCAAGCTTGGTGTCTGTTTGAGGTTGC
HBG1	Forward	CCCGGGCTCGAGATCTGCAGTATCCTCTTGGGGGCC
HBG1	Reverse	CCGGATTGCCAAGCTTGGCGTCTGGACTAGGAGCTTATTG
HNF4A	Forward	CCCGGGCTCGAGATCCCCCAGAGTGCAGGACTAG
HNF4A	Reverse	CCGGATTGCCAAGCTGGCCAAGCCCACCCAG
LDLR	Forward	CCCGGGCTCGAGATCTAGCTCTTCACCGGAGACCCA
LDLR	Reverse	CCGGATTGCCAAGCTTGCTCGCAGCCTCTGCCAG
MSMB	Forward	CCCGGGCTCGAGATCAAAGGTCCAGCAATTCAGC
MSMB	Reverse	CCGGATTGCCAAGCTAAGCAGGACTCCTTATAGACAGG
PKLR	Forward	CCCGGGCTCGAGATCTAGGTTACAGAGTGGTGAAGGC
PKLR	Reverse	CCGGATTGCCAAGCTTGCTTTCAGTGTGGGCCTGG
TERT	Forward	CCCGGGCTCGAGATCCCAGGACCGCGCTTCCCAC
TERT	Reverse	CCGGATTGCCAAGCTCGCGGGGGTGGCCGGG
SORT1	Forward	GAGGATATCAAGATCTGAACTGGAAAAGCCCTGTCCGG
SORT1	Reverse	TCTAGTGTCTAAGCTTCAGACCCCCGGGACTGGAC
IRF4	Forward	GAGGATATCAAGATCTGGCGTGTCCGCCTGTTGG
IRF4	Reverse	TCTAGTGTCTAAGCTTACGGGGGTAAAGGAGTGC
IRF6	Forward	GAGGATATCAAGATCTTCTGTTTGCTTAGCTTACCTC
IRF6	Reverse	TCTAGTGTCTAAGCTTGTAAATGGTGAGTAGGAAGTTG
MYC (rs6983267)	Forward	GAGGATATCAAGATCTCTGCATCGCTCCATAGAG
MYC (rs6983267)	Reverse	TCTAGTGTCTAAGCTTTGCTGGTAGAACTTACG
MYC (rs11986220)	Forward	GAGGATATCAAGATCTGGTAAGTCAACATGAAATTATAAACC
MYC (rs11986220)	Reverse	TCTAGTGTCTAAGCTTCAAGTACTGTGGGGGTTTTGTTAG
TCF7L2	Forward	GAGGATATCAAGATCTAGGTTCTGTTTCTTGCTTAG
TCF7L2	Reverse	TCTAGTGTCTAAGCTTATTACAAATTATTAGAACTTTC
ZFAND3	Forward	GAGGATATCAAGATCTTTCATGTTTCCCCCGTATGTG
ZFAND3	Reverse	TCTAGTGTCTAAGCTTTCCTGCCCCAAGTTGCACAGC
BCL11A	Forward	GCTCGCTAGCCTCGAGCCTAACACAGTAGCTGGTACCTG
BCL11A	Reverse	CGCCGAGGCCAGATCTGTACTGATGGACCTTGGGTG
UC88	Forward	GAGGATATCAAGATCTTACAGATAAATGCACACATGTATACG
UC88	Reverse	TCTAGTGTCTAAGCTTGGGACTCGGTGGCGGTG
ZRS	Forward	TGGCCTAACTGGCCGGTACCTGAGATATGGCTTCATTTTCTGT
ZRS	Reverse	ATGATCTAAGCTTAAGGCTGAGCAACATGACAGCAC
RET	Forward	CTAGCCCGGGCTCGAGCAGAGGCACCAGGGTCAAAGC
RET	Reverse	TGCAGATCGCAGATCTGAAGCCCAGAATTCCCGCTGC

Supplementary Table 19

PCR primers for amplification from luciferase vectors prior to mutagenesis. Overhanging primers add cloning sites and adaptor sequence for downstream vector integration. All sequences are provided 5' to 3'.

Element	Primer	Sequence
F9	Forward	CCGGGCTCGAGATCTGCGATCTAAGTAAGCGTCCCACTGATGAACTGTGC
F9	Reverse	TCTAGACCTGCAGGGCATGCAAGCTTTAACCTTTGCTAGCAGATTGTG
FOXE1	Forward	CCGGGCTCGAGATCTGCGATCTAAGTAAGCCTCGCCAGCGGTCCGCAGG
FOXE1	Reverse	TCTAGACCTGCAGGGCATGCAAGCTTGGCCTGGCGTCCCCGGAACG
GP1BB	Forward	CCGGGCTCGAGATCTGCGATCTAAGTAAGCGTTGTGAATGCCGCGTCCTG
GP1BB	Reverse	TCTAGACCTGCAGGGCATGCAAGCTTACGACCAGAGCTCCTCTC
HBB	Forward	CCGGGCTCGAGATCTGCGATCTAAGTAAGCAAGGACAGGTACGGCTGTC
HBB	Reverse	TCTAGACCTGCAGGGCATGCAAGCTTGGTGTCTGTTTGAGGTTGC
HBG1	Forward	CCGGGCTCGAGATCTGCGATCTAAGTAAGCGCAGTATCCTCTTGGGGGC
HBG1	Reverse	TCTAGACCTGCAGGGCATGCAAGCTTGGCGTCTGGACTAGGAGCTTATTG
HNF4A	Forward	CCGGGCTCGAGATCTGCGATCTAAGTAAGCCCCCAGAGTGCAGGACTAG
HNF4A	Reverse	TCTAGACCTGCAGGGCATGCAAGCTTGGCCAAGCCCACCCAG
LDLR	Forward	CCGGGCTCGAGATCTGCGATCTAAGTAAGCAGCTCTTCACCGGAGACCCA
LDLR	Reverse	TCTAGACCTGCAGGGCATGCAAGCTTTGCTCGCAGCCTCTGCCAG
MSMB	Forward	CCGGGCTCGAGATCTGCGATCTAAGTAAGCAAAGGTCCAGCAATTCAGC
MSMB	Reverse	TCTAGACCTGCAGGGCATGCAAGCTTAAGCAGGACTCCTTATAGACAGG
PKLR	Forward	CCGGGCTCGAGATCTGCGATCTAAGTAAGCAGGTTACAGAGTGGTGAAGGC
PKLR	Reverse	TCTAGACCTGCAGGGCATGCAAGCTTTGCTTTCAGTGTGGGCCTGG
TERT	Forward	CCGGGCTCGAGATCTGCGATCTAAGTAAGCCCAGGACCGCGCTTCCCAC
TERT	Reverse	TCTAGACCTGCAGGGCATGCAAGCTTCGCGGGGGTGGCCGGG
SORT1	Forward	GATATCAAGATCTGGCCTCGGCGGCCAAGCGAACTGGAAAAGCCCTGTCCGG
SORT1	Reverse	TCTAGACCTGCAGGGCATGCAAGCTTCAGACCCCCGGGACTGGAC
SORT1-flip	Forward	GATATCAAGATCTGGCCTCGGCGGCCAAGCCAGACCCCCGGGACTGGAC
SORT1-flip	Reverse	TCTAGACCTGCAGGGCATGCAAGCTTGAACTGGAAAAGCCCTGTCCGG
IRF4	Forward	GATATCAAGATCTGGCCTCGGCGGCCGAATGGCGTGTCCGCCTGTTGG
IRF4	Reverse	TCTAGACCTGCAGGGCATGCGAATTCACGGGGGTAAAGGAGTGC
IRF6	Forward	GATATCAAGATCTGGCCTCGGCGGCCAAGCCTCTGTTTGCTTAGCTTACCTC
IRF6	Reverse	TCTAGACCTGCAGGGCATGCAAGCTTGTAAATGGTGAGTAGGAAGTTG
MYC (rs6983267)	Forward	GATATCAAGATCTGGCCTCGGCGGCCAAGCCTGCATCGCTCCATAGAG
MYC (rs6983267)	Reverse	TCTAGACCTGCAGGGCATGCAAGCTTTGCTGGTAGAACTTACG
MYC (rs11986220)	Forward	GATATCAAGATCTGGCCTCGGCGGCCGAATGGTAAGTCAACATGAAATTATAAACC
MYC (rs11986220)	Reverse	TCTAGACCTGCAGGGCATGCGAATTCCAAGTACTGTGGGGGTTTTGTTAG
TCF7L2	Forward	GATATCAAGATCTGGCCTCGGCGGCCGAATAGGTTCTGTTTCTTGCTTAG
TCF7L2	Reverse	TCTAGACCTGCAGGGCATGCGAATTCATTACAAATTATTAGAACTTTC
ZFAND3	Forward	GATATCAAGATCTGGCCTCGGCGGCCAAGCGTTCATGTTTCCCCCGTATGTG
ZFAND3	Reverse	TCTAGACCTGCAGGGCATGCAAGCTTTCCTGCCCCAAGTTGCACAGC
BCL11A	Forward	GATATCAAGATCTGGCCTCGGCGGCCGAATCCTAACACAGTAGCTGGTACCTG
BCL11A	Reverse	TCTAGACCTGCAGGGCATGCGAATTCGTACTGATGGACCTTGGGTG
UC88	Forward	GATATCAAGATCTGGCCTCGGCGGCCAAGCATACAGATAAATGCACACATGTATACG
UC88	Reverse	TCTAGACCTGCAGGGCATGCAAGCTTGGGACTCGGTGGCGGTG
ZRS	Forward	AACATTTCTCTGGCCTAACTGGCCGGTACCTGAGATATGGCTTCATTTTCTGT
ZRS	Reverse	TCTAGACCTGCAGGGCATGCAAGCTTGCTGAGCAACATGACAGCAC
RET	Forward	GAGCTCTTACGCGTGCTAGCCCGGGCTCGAGCAGAGGCACCAGGGTCAAAGC
RET	Reverse	TCTAGACCTGCAGGGCATGCAGATCTGAAGCCCAGAATTCCCGCTGC

Supplementary Table 20

Primers for error-prone PCR with Mutazyme II. This PCR adds a 15 or 20 bp random tag (i.e. barcode and marked with N characters below) contained within an overhanging primer oligo to each construct. All sequences are provided 5' to 3'.

Element type	Primer	Sequence
Promoter	Forward	CCGGGCTCGAGATCTGCGATCTAAGTAAGC
Promoter	Reverse	GCTCGAAGCGACTGTCAGCTCAGACTCTAGGNNN...NNNTCTAGACCTGCAGGGC ATGCAAGCTT
Enhancer pGL4.23c, pGL3c, pGL4Zc	Forward	GATATCAAGATCTGGCCTCGGCGGCCAAGC
Enhancer pGL4.23d	Forward	GATATCAAGATCTGGCCTCGGCGGCCGAAT
Enhancer pGL4.23c, pGL4Zc	Reverse	GCTCGAAGCGACTGTCAGCTCAGACTCTAGGNNN...NNNTCTAGACCTGCAGGGC ATGCAAGCTT
Enhancer pGL3c	Reverse	GCTCGAAGCGACTGTCAGCTCAGACTCTAGGNNN...NNNTCTAGACCTGCAGGGC ATGCAGATCT
Enhancer pGL4.23d	Reverse	GCTCGAAGCGACTGTCAGCTCAGACTCTAGGNNN...NNNTCTAGACCTGCAGGGC ATGCGAATTC

Supplementary Table 21

Primers for preparing association libraries for short enhancers/promoters. These primers are also used to amplify longer enhancers and then those products are fragmented for subassembly (Supplementary Table 22). Plasmid DNA libraries are amplified with sequencing adaptor primers capturing the cloned sequence with its tag and adding the P5/P7 Illumina flow cell sequences. All sequences are provided 5' to 3'.

Element	Primer	Sequence
Promoter/ pGL4.11	Forward	AATGATACGGCGACCACCGAGATCTACAC##########CCGGGCTCGAGATCTGC GATCTAAG
Enhancer/ pGL4.23c	Forward	AATGATACGGCGACCACCGAGATCTACAC##########GATATCAAGATCTGGCC TCGGCGGCCAAGC
Enhancer/ pGL4.23d	Forward	AATGATACGGCGACCACCGAGATCTACAC##########GATATCAAGATCTGGCC TCGGCGGCCGAAT
Enhancer/ pGL3	Forward	AATGATACGGCGACCACCGAGATCTACAC##########TCGATAGGTACCGAGCT CTTACGCGTGCTAG
Enhancer/ pGL4Zc	Forward	AATGATACGGCGACCACCGAGATCTACAC##########AACATTTCTCTGGCCTA ACTGGCCGGTACC
All	Reverse	CAAGCAGAAGACGGCATACGAGATGCTCGAAGCGACTGTCAGCTCAGAC

Supplementary Table 22

Amplification of Nextera fragmented molecules for the preparation of fragment association libraries (long enhancers/promoters). Hash characters (#) denote a placeholder for a defined index sequence (i.e. sample barcode), one for each sample/replicate.

Primer	Sequence
Forward	AATGATACGGCGACCACCGAGATCTACAC##########TCGTCGGCAGCGTCAGATGTGTATAAGAGACAG
Reverse	CAAGCAGAAGACGGCATACGAGATGCTCGAAGCGACTGTCAGCTCAGAC

Supplementary Table 23

Sequencing primers used for association libraries. All sequences are provided 5' to 3'.

Primer	Sequence
Promoter/pGL4.11	
Read 1	CCGGGCTCGAGATCTGCGATCTAAGTAAGC
Read 2	TCTAGACCTGCAGGGCATGCAAGCTT
Index Read 1	AAGCTTGCATGCCCTGCAGGTCTAGA
Index Read 2	GCTTACTTAGATCGCAGATCTCGAGCCCGG
Enhancer/pGL4.23c	
Read 1	GATATCAAGATCTGGCCTCGGCGGCCAAGC
Read 2	TCTAGACCTGCAGGGCATGCAAGCTT
Index Read 1	AAGCTTGCATGCCCTGCAGGTCTAGA
Index Read 2	GCTTGGCCGCCGAGGCCAGATCTTGATATC
Enhancer/pGL4.23d	
Read 1	GATATCAAGATCTGGCCTCGGCGGCCGAAT
Read 2	TCTAGACCTGCAGGGCATGCGAATTC
Index Read 1	GAATTCGCATGCCCTGCAGGTCTAGA
Index Read 2	ATTCGGCCGCCGAGGCCAGATCTTGATATC
Enhancer/pGL3c	
Read 1	TCGATAGGTACCGAGCTCTTACGCGTGCTAG
Read 2	TCTAGACCTGCAGGGCATGCAGATCT
Index Read 1	AGATCTGCATGCCCTGCAGGTCTAGA
Index Read 2	CTAGCACGCGTAAGAGCTCGGTACCTATCGA
Enhancer/pGL4Zc	
Read 1	AACATTTCTCTGGCCTAACTGGCCGGTACC
Read 2	TCTAGACCTGCAGGGCATGCAAGCTT
Index Read 1	AAGCTTGCATGCCCTGCAGGTCTAGA
Index Read 2	GGTACCGGCCAGTTAGGCCAGAGAAATGTT
Nextera fragment library	
Read 1	TCGTCGGCAGCGTCAGATGTGTATAAGAGACAG
Read 2 (pGL4.23c/pGL4Zc/pGL4.11c)	TCTAGACCTGCAGGGCATGCAAGCTT
Read 2 (pGL4.23d)	TCTAGACCTGCAGGGCATGCGAATTC
Read 2 (pGL3c)	TCTAGACCTGCAGGGCATGCAGATCT
Index Read 1 (pGL4.23c/pGL4Zc/pGL4.11c)	AAGCTTGCATGCCCTGCAGGTCTAGA
Index Read 1 (pGL4.23d)	GAATTCGCATGCCCTGCAGGTCTAGA
Index Read 1 (pGL3)	AGATCTGCATGCCCTGCAGGTCTAGA
Index Read 2	CTGTCTCTTATACACATCTGACGCTGCCGACGA

Supplementary Table 24

Primers used for measuring siRNA knockdown efficiency using qPCR. All sequences are provided 5' to 3'.

Element	Primer	Sequence
GABPA	Forward	AAGAACGCCTTGGGATACCCT
GABPA	Reverse	GTGAGGTCTATATCGGTCATGCT
TERT	Forward	TCACGGAGACCACGTTTCAAA
TERT	Reverse	TTCAAGTGCTGTCTGATTCCAAT
GUSB	Forward	CTCATTTGGAATTTTGCCGATT
GUSB	Reverse	CCGAGTGAAGATCCCCTTTTTA

Supplementary Table 25

Primers used for preparing RNA and DNA count sequencing libraries. The 1st round reverse primer is also the RT primer. Hash characters (#) denote a placeholder for a defined index sequence (i.e. sample barcode), one for each sample/replicate. Ten N characters ("NNNNNNNNNN") are the UMI positions ordered as random bases. Amplifications were performed in two rounds, a 1st round of three cycles incorporating unique molecular identifiers (UMIs) followed by an Ampure cleanup and 2nd round of 15 cycles with primers matching the Illumina flowcell oligos. Sequences are provided 5' to 3'.

Element	Primer	Sequence
Promoter/ pGL4.11	Forward 1st round	AATGATACGGCGACCACCGAGATCTACACTAGACACCCTGCTGCTTGCGCCAGC
Enhancer/ pGL4	Forward 1st round	AATGATACGGCGACCACCGAGATCTACACGCGAGATTCTCATTAAGGCCAAGAAG
Enhancer/ pGL3	Forward 1st round	AATGATACGGCGACCACCGAGATCTACACGAGAGATCCTCATAAAGGCCAAGAAG
All	Reverse 1st round	CAAGCAGAAGACGGCATACGAGATAC##########CANNNNNNNNNNCTGCTCGA AGCGACTGTCAGCTCAGAC
All	Forward 2nd round	AATGATACGGCGACCACCGAGATCTACAC
All	Reverse 2nd round	CAAGCAGAAGACGGCATACGAGAT

Supplementary Table 26

Sequencing primers used for RNA and DNA count libraries. All sequences are provided 5' to 3'.

Primer	Sequence
Read 1 (Promoter/pGL4.11)	GCCAGGATCAACGTCTAAGGCCGCGACTCTAGA
Read 1 (Enhancer/pGL4)	GAAGGGCGGCAAGATCGCCGTGTAATAATTCTAGA
Read 1 (Enhancer/pGL3)	CAAGAAGGGCGGAAAGATCGCCGTGTAATTCTAGA
Read 2	CTGCTCGAAGCGACTGTCAGCTCAGACTCTAGG
Index Read	CCTAGAGTCTGAGCTGACAGTCGCTTCGAGCAG

Supplementary References

1. Reijnen, M. J., Sladek, F. M., Bertina, R. M. & Reitsma, P. H. Disruption of a binding site for hepatocyte nuclear factor 4 results in hemophilia B Leyden. *Proc. Natl. Acad. Sci. U. S. A.* **89**, 6300–6303 (1992).
2. Reijnen, M. J., Peerlinck, K., Maasdam, D., Bertina, R. M. & Reitsma, P. H. Hemophilia B Leyden: substitution of thymine for guanine at position -21 results in a disruption of a hepatocyte nuclear factor 4 binding site in the factor IX promoter. *Blood* **82**, 151–158 (1993).
3. Kheradpour, P. & Kellis, M. Systematic discovery and characterization of regulatory motifs in ENCODE TF binding experiments. *Nucleic Acids Res.* **42**, 2976–2987 (2014).
4. Landa, I. *et al.* The variant rs1867277 in FOXE1 gene confers thyroid cancer susceptibility through the recruitment of USF1/USF2 transcription factors. *PLoS Genet.* **5**, e1000637 (2009).
5. Ludlow, L. B. *et al.* Identification of a mutation in a GATA binding site of the platelet glycoprotein Ibbeta promoter resulting in the Bernard-Soulier syndrome. *J. Biol. Chem.* **271**, 22076–22080 (1996).
6. Khan, A. *et al.* JASPAR 2018: update of the open-access database of transcription factor binding profiles and its web framework. *Nucleic Acids Res.* **46**, D260–D266 (2018).
7. Giardine, B. *et al.* HbVar database of human hemoglobin variants and thalassemia mutations: 2007 update. *Hum. Mutat.* **28**, 206 (2007).
8. Moi, P. *et al.* A novel silent beta-thalassemia mutation in the distal CACCC box affects the binding and responsiveness to EKLF. *Br. J. Haematol.* **126**, 881–884 (2004).
9. Sgourou, A. *et al.* Thalassaemia mutations within the 5'UTR of the human beta-globin gene disrupt transcription. *Br. J. Haematol.* **124**, 828–835 (2004).
10. Gumucio, D. L. *et al.* Nuclear proteins that bind the human gamma-globin gene promoter: alterations in binding produced by point mutations associated with hereditary persistence of fetal hemoglobin. *Mol. Cell. Biol.* **8**, 5310–5322 (1988).
11. Sykes, K. & Kaufman, R. A naturally occurring gamma globin gene mutation enhances SP1 binding activity. *Mol. Cell. Biol.* **10**, 95–102 (1990).
12. Thomas, H. *et al.* A distant upstream promoter of the HNF-4alpha gene connects the transcription factors involved in maturity-onset diabetes of the young. *Hum. Mol. Genet.* **10**, 2089–2097 (2001).
13. Wirsing, A. *et al.* Novel monogenic diabetes mutations in the P2 promoter of the HNF4A gene are associated with impaired function in vitro. *Diabet. Med.* **27**, 631–635 (2010).

14. Thomas, G. *et al.* Multiple loci identified in a genome-wide association study of prostate cancer. *Nat. Genet.* **40**, 310–315 (2008).
15. Eeles, R. A. *et al.* Multiple newly identified loci associated with prostate cancer susceptibility. *Nat. Genet.* **40**, 316–321 (2008).
16. Kote-Jarai, Z. *et al.* Multiple novel prostate cancer predisposition loci confirmed by an international study: the PRACTICAL Consortium. *Cancer Epidemiol. Biomarkers Prev.* **17**, 2052–2061 (2008).
17. Zheng, S. L. *et al.* Genetic variants and family history predict prostate cancer similar to prostate-specific antigen. *Clin. Cancer Res.* **15**, 1105–1111 (2009).
18. Chang, B.-L. *et al.* Fine mapping association study and functional analysis implicate a SNP in MSMB at 10q11 as a causal variant for prostate cancer risk. *Hum. Mol. Genet.* **18**, 1368–1375 (2009).
19. Buckland, P. R. *et al.* Strong bias in the location of functional promoter polymorphisms. *Hum. Mutat.* **26**, 214–223 (2005).
20. Manco, L. *et al.* A new PKLR gene mutation in the R-type promoter region affects the gene transcription causing pyruvate kinase deficiency. *Br. J. Haematol.* **110**, 993–997 (2000).
21. van Wijk, R. *et al.* Disruption of a novel regulatory element in the erythroid-specific promoter of the human PKLR gene causes severe pyruvate kinase deficiency. *Blood* **101**, 1596–1602 (2003).
22. Bauer, D. E. *et al.* An erythroid enhancer of BCL11A subject to genetic variation determines fetal hemoglobin level. *Science* **342**, 253–257 (2013).
23. Canver, M. C. *et al.* BCL11A enhancer dissection by Cas9-mediated in situ saturating mutagenesis. *Nature* **527**, 192–197 (2015).
24. Vinjamur, D. S. & Bauer, D. E. Growing and Genetically Manipulating Human Umbilical Cord Blood-Derived Erythroid Progenitor (HUDEP) Cell Lines. *Methods Mol. Biol.* **1698**, 275–284 (2018).
25. Praetorius, C. *et al.* A polymorphism in IRF4 affects human pigmentation through a tyrosinase-dependent MITF/TFAP2A pathway. *Cell* **155**, 1022–1033 (2013).
26. Rahimov, F. *et al.* Disruption of an AP-2alpha binding site in an IRF6 enhancer is associated with cleft lip. *Nat. Genet.* **40**, 1341–1347 (2008).
27. Yeager, M. *et al.* Genome-wide association study of prostate cancer identifies a second risk locus at 8q24. *Nat. Genet.* **39**, 645–649 (2007).
28. Haiman, C. A. *et al.* A common genetic risk factor for colorectal and prostate cancer. *Nat. Genet.* **39**, 954–956 (2007).
29. Tomlinson, I. *et al.* A genome-wide association scan of tag SNPs identifies a susceptibility variant for colorectal cancer at 8q24.21. *Nat. Genet.* **39**, 984–988 (2007).
30. Pomerantz, M. M. *et al.* The 8q24 cancer risk variant rs6983267 shows long-range interaction with MYC in colorectal cancer. *Nat. Genet.* **41**, 882–884 (2009).

31. Ahmadiyeh, N. *et al.* 8q24 prostate, breast, and colon cancer risk loci show tissue-specific long-range interaction with MYC. *Proc. Natl. Acad. Sci. U. S. A.* **107**, 9742–9746 (2010).
32. Jia, L. *et al.* Functional enhancers at the gene-poor 8q24 cancer-linked locus. *PLoS Genet.* **5**, e1000597 (2009).
33. Zerbino, D. R., Wilder, S. P., Johnson, N., Juettemann, T. & Flicek, P. R. The ensembl regulatory build. *Genome Biol.* **16**, 56 (2015).
34. Emison, E. S. *et al.* A common sex-dependent mutation in a RET enhancer underlies Hirschsprung disease risk. *Nature* **434**, 857–863 (2005).
35. Lyssenko, V. *et al.* Mechanisms by which common variants in the TCF7L2 gene increase risk of type 2 diabetes. *J. Clin. Invest.* **117**, 2155–2163 (2007).
36. Bejerano, G. *et al.* Ultraconserved elements in the human genome. *Science* **304**, 1321–1325 (2004).
37. Visel, A. *et al.* Ultraconservation identifies a small subset of extremely constrained developmental enhancers. *Nat. Genet.* **40**, 158–160 (2008).
38. Visel, A., Minovitsky, S., Dubchak, I. & Pennacchio, L. A. VISTA Enhancer Browser--a database of tissue-specific human enhancers. *Nucleic Acids Res.* **35**, D88–92 (2007).
39. Pasquali, L. *et al.* Pancreatic islet enhancer clusters enriched in type 2 diabetes risk-associated variants. *Nat. Genet.* **46**, 136–143 (2014).
40. VanderMeer, J. E. & Ahituv, N. cis-regulatory mutations are a genetic cause of human limb malformations. *Dev. Dyn.* **240**, 920–930 (2011).
41. Gurnett, C. A. *et al.* Two novel point mutations in the long-range SHH enhancer in three families with triphalangeal thumb and preaxial polydactyly. *Am. J. Med. Genet. A* **143A**, 27–32 (2007).
42. Al-Qattan, M. M., Al Abdulkareem, I., Al Haidan, Y. & Al Balwi, M. A novel mutation in the SHH long-range regulator (ZRS) is associated with preaxial polydactyly, triphalangeal thumb, and severe radial ray deficiency. *Am. J. Med. Genet. A* **158A**, 2610–2615 (2012).
43. Farooq, M. *et al.* Preaxial polydactyly/triphalangeal thumb is associated with changed transcription factor-binding affinity in a family with a novel point mutation in the long-range cis-regulatory element ZRS. *Eur. J. Hum. Genet.* **18**, 733–736 (2010).
44. Vanlerberghe, C. *et al.* Intrafamilial variability of ZRS-associated syndrome: characterization of a mosaic ZRS mutation by pyrosequencing. *Clin. Genet.* **88**, 479–483 (2015).
45. Wieczorek, D. *et al.* A specific mutation in the distant sonic hedgehog (SHH) cis-regulator (ZRS) causes Werner mesomelic syndrome (WMS) while complete ZRS duplications underlie Haas type polysyndactyly and preaxial polydactyly (PPD) with or without triphalangeal thumb. *Hum. Mutat.* **31**, 81–89 (2010).
46. VanderMeer, J. E. *et al.* A novel ZRS mutation leads to preaxial polydactyly type 2 in

a heterozygous form and Werner mesomelic syndrome in a homozygous form. *Hum. Mutat.* **35**, 945–948 (2014).
47. Maas, S. A., Suzuki, T. & Fallon, J. F. Identification of spontaneous mutations within the long-range limb-specific Sonic hedgehog enhancer (ZRS) that alter Sonic hedgehog expression in the chicken limb mutants oligozeugodactyly and silkie breed. *Dev. Dyn.* **240**, 1212–1222 (2011).
48. Khamis, A. *et al.* Functional analysis of four LDLR 5'UTR and promoter variants in patients with familial hypercholesterolaemia. *Eur. J. Hum. Genet.* **23**, 790–795 (2015).
49. Bell, R. J. A. *et al.* Cancer. The transcription factor GABP selectively binds and activates the mutant TERT promoter in cancer. *Science* **348**, 1036–1039 (2015).
50. Horn, S. *et al.* TERT promoter mutations in familial and sporadic melanoma. *Science* **339**, 959–961 (2013).
51. Hurst, C. D., Platt, F. M. & Knowles, M. A. Comprehensive mutation analysis of the TERT promoter in bladder cancer and detection of mutations in voided urine. *Eur. Urol.* **65**, 367–369 (2014).
52. Huang, D.-S. *et al.* Recurrent TERT promoter mutations identified in a large-scale study of multiple tumour types are associated with increased TERT expression and telomerase activation. *Eur. J. Cancer* **51**, 969–976 (2015).